Title
Global Optimization of Chemical Reactors and Kinetic Optimization

Author
ALHUSSEINI, ZAYNA ISHAQ

Publication Date
2013

Peer reviewed|Thesis/dissertation

UNIVERSITY OF CALIFORNIA

Los Angeles

Global Optimization of Chemical Reactors and Kinetic Optimization

A dissertation submitted in partial satisfaction

of the requirements for the degree

Doctor of Philosophy in Chemical Engineering

by

ZAYNA ISHAQ ALHUSSEINI

2013

ABSTRACT OF THE DISSERTATION

Global Optimization of Chemical Reactors and Kinetic Optimization

by

ZAYNA ISHAQ ALHUSSEINI

Doctor of Philosophy in Chemical Engineering

University of California, Los Angeles, 2013

Professor Vasilios Manousiouthakis, Chair

This work addresses for the first time in chapter 1, the synthesis of globally minimum volume reactor networks featuring SFR/MMR, with the same normalized residence time density function. Global optimality is ascertained by demonstrating that the input-output information maps of SFR and MMR with general RTd/RTD models satisfy all properties required for the application of the IDEAS to the RTd/RTD reactor network problem. The resulting formulation is shown to possess a number of novel properties, which can be used to facilitate its solution. The proposed methodology is demonstrated on three case studies featuring SLFR model in which the Trambouze reaction scheme is carried out.

In chapter 2, the concept of NRT is defined, as a production normalized, capital cost measure for a reactor network. For networks consisting of CSTR's, PFR's, and RTD-SFR/MMR, described within the IDEAS conceptual framework, it is shown that NRT is independent of the network's inlet flowrate. The novel concept of Network Residence Time Constrained Attainable Region for Reactor Networks is then introduced. It is shown to be a convex set, points on the boundary of which are identified through repeated solution of increasingly accurate finite linear program

approximations of infinite linear programs. A case study featuring a network of reactors in which the Trambouze reaction scheme is carried out.

In chapter 3, the optimization of an isothermal monolith reactor is carried out. First, a reaction-diffusion 3-D mathematical model for a monolith reactor is developed. The analytical nature of the obtained solution enables the optimization of a multi-channel 3-D monolith reactor to be carried out. The obtained optimization results are discussed and conclusions are drawn.

Chapter 4 presents a novel method for determining reaction kinetics using the reaction invariant reduction method for any set of complex chemical reactions. An effective way for reducing the dimension of chemical reaction mechanisms and to predict the kinetics from a given set of data. The new method will be developed based on a convex formulation of the associated optimization problem. A case study on the Trambouze reaction scheme carried out in a PFR will be used to illustrate the proposed methodology.

The dissertation of Zayna I. Alhusseini is approved.

Reza Ahmadi

James Davis

Gerassimos Orkoulas

Vasilios Manousiouthakis, Committee Chair

University of California, Los Angeles

2013

TABLE OF CONTENTS

LIST OF FIGURES

LIST OF TABLES

ACKNOWLEDGMENTS

I would like to acknowledge my family for everything they did to make me succeed in every step of my life. I acknowledge Saudi Aramco for the financial support. Also, my special thanks to Dr. Vasilios Manousiouthakis for his mentor and guidance throughout this great experience. I would like to also thank my committee members Prof. Reza Ahmadi, Dr. James Davis, and Prof. Gerassimos Orkoulas. Finally, I would like to thank my group members for the help and friendship and everyone who encouraged and supported me throughout the course of this endeavor.

VITA

2003	B.S in Chemical Engineering,
	Northeastern University, Boston, MA
2006	M.S Engineering Management
	Northeastern University, Boston, MA
2006- 2009	Lab Scientist
	Saudi Aramco R&D Center
	Dhahran, Saudi Arabia

PUBLICATIONS

Al-Husseini, Z, Manousiouthakis, V. I. IDEAS based Synthesis of Minimum Volume Reactor Networks featuring Residence Time Density/Distribution Models. Computers and Chemical Engineering, in press. 2013.

Al-Husseini, Z, Manousiouthakis, V. I. Construction of Attainable Region with Volumetric Constraints. American Institute of Chemical Engineers, 2012. Annual Meeting.

Al-Husseini, Z, Manousiouthakis, V. I. Globally Optimal Control of Nonlinear Process Networks: Easier Than Globally Optimal Control of Nonlinear Processes. . American Institute of Chemical Engineers, 2011 Annual Meeting.

Al-Husseini, Z, Manousiouthakis, V. I. Minimum Volume for a Network of Reactor with a Known RTD. American Institute of Chemical Engineers, 2010 Annual Meeting.

`CHAPTER 1

1 IDEAS based Synthesis of Minimum Volume Reactor Networks featuring Residence Time Density/Distribution Models

Zayna Al-Husseini, Vasilios I. Manousiouthakis

Chemical and Biomolecular Engineering Department

University of California at Los Angeles, Los Angeles, CA 90095, USA

Abstract

This work addresses for the first time, the synthesis of globally minimum volume reactor networks, featuring segregated flow reactors (SFR) and/or maximum mixedness reactors (MMR), with the same normalized residence time density (NRTd) function. Global optimality is ascertained by demonstrating that the input-output information maps of SFR and MMR with general RTd/RTD models satisfy all properties required for the application of the Infinite DimEnsionAl State-space (IDEAS) approach to the RTd/RTD reactor network synthesis problem. The resulting IDEAS formulation is shown to possess a number of novel properties, which can be used to facilitate its solution. The power of the proposed methodology is demonstrated on three case studies featuring segregated laminar flow reactors (SLFR) in which the Trambouze reaction scheme is carried out. In one of the case studies, the identified reactor network is shown to have volume that is as low as half the volume of a single reactor.

Keywords: Reactor; Network; RTD; Volume; Global; Optimum

Abbreviations:

CSTR, continuous stirred tank reactor; DN, distribution network; IDEAS, Infinite DimEnsionAl State-space; ILP, infinite-dimensional linear program; MINLP, mixed-integer nonlinear program;MMR, Maximum Mixedness Reactor; NRTd, normalized residence time density function; OP, operator network; PFR, plug flow reactor; RTd, Residence time density; RTD, residence time distribution;SFR, Segregated Flow Reactor; SLFR, Segregated Laminar Flow Reactors; SR, Segregated Reactor.

Nomenclature:

$C_i : i^{th}$ Component molar concentration $\left(\text{kmol/m}^3\right)$

$C_i^{in} : i^{th}$ Component inlet molar concentration to IDEAS unit model $\left(\text{kmol/m}^3\right)$

$C_i^{out} : i^{th}$ Component outlet molar concentration from IDEAS unit model $\left(\text{kmol/m}^3\right)$

$\left\{C_i^{in}\right\}_{i=1}^{n}$: Inlet molar concentration vector (kmol/m^3)

$\left\{C_i^{out}\right\}_{i=1}^{n}$: Outlet molar concentration vector (kmol/m^3)

E : Residence time density function

$E\left(t'\right)dt'$: The volume fraction of the exit stream that has resided in the system for a time between t' and $t'+dt'$

$\boldsymbol{E}$: Normalized Residence Time density (NRTd) function

$\boldsymbol{E}\left(\theta\right)$: Normalized Residence Time density (NRTd) function value at normalized time θ

F :Volumetric flow rate $\left(\text{m}^3/\text{s}\right)$

F^{in} : Inlet volumetric flow rate $\left(\mathrm{m}^3/\mathrm{s}\right)$

F^{out} : Outlet volumetric flow rate $\left(\mathrm{m}^3/\mathrm{s}\right)$

F : Residence Time Distribution (RTD) function

$F\left(t\right)$: Volume fraction of the exit stream with residence time between 0 and t

$I\left(\alpha\right)$: Internal age density function

$I\left(\alpha'\right)d\alpha'$: The volume fraction of the system contents that has an age between α and $\alpha + d\alpha$

$J\left(\alpha\right)$: Internal age distribution function

$\left\{R_i\right\}_{i=1}^{n}$: i^{th} Component generation rate $\left(\mathrm{kmol}/\left(\mathrm{m}^3 s\right)\right)$ $\forall i = 1, n$

t : The residence time of a fluid element

t_{out} : The time the fluid element exits the system

t_{in} : The time that it entered the system

t_g : Given time

$\bar{t}$: Mean Residence time

V : Volume $\left(m^3\right)$

α : The age of a fluid element

$\bar{\alpha}$: Mean Age

λ : The life expectancy of a fluid element

$\Phi\left(\lambda\right)$: Life expectancy density function

$\Phi\left(\lambda'\right)d\lambda'$: The volume fraction of the system contents that has a life expectancy between λ' and $\lambda' + d\lambda'$

$\Psi(\lambda)$: Life expectancy distribution function

$\Lambda(t)$: Intensity Function

IDEAS Variables:

$C_A(\tau)$: PFR Concentration of A at residence time τ

$\overline{C}_A(\tau)$: SLFR Concentration of A at residence time τ

$C_C(\tau)$: PFR Concentration of C at residence time τ

$\overline{C}_C(\tau)$: SLFR Concentration of C at residence time τ

$C_k^I(j)$: k^{th} Component concentration in the j^{th} network inlet $\forall k = 1, n; \forall j = 1, N_I$

$C_k^{\hat{I}}(i)$: k^{th} Component concentration in the i^{th} OP inlet $\forall k = 1, n; \forall i = 1, \infty$

$C_k^O(i)$: k^{th} Component concentration in the i^{th} network outlet $\forall k = 1, n; \forall i = 1, N_O$

$C_k^{\hat{O}}(i)$: k^{th} Component concentration in the i^{th} OP outlet $\forall k = 1, n; \forall i = 1, \infty$

$F^I(j)$: j^{th} Network inlet flow rate $\forall j = 1, N_I$

$F^O(i)$: i^{th} Network outlet flow rate $\forall i = 1, N_O$

$F^{\hat{I}}(j)$: j^{th} OP inlet flow rate $\forall j = 1, \infty$

$F^{\hat{O}}(i)$: i^{th} OP outlet flow rate $\forall i = 1, \infty$

$F^{OI}(i, j)$: j^{th} Network inlet flow rate to the i^{th} network outlet $\forall j = 1, N_I; \forall i = 1, N_O$

$F^{\hat{I}I}(i, j)$: j^{th} Network outlet flow rate to the i^{th} OP inlet $\forall j = 1, N_I; \forall i = 1, \infty$

$F^{O\hat{O}}(i, j)$: j^{th} OP outlet flow rate to the i^{th} network outlet $\forall j = 1, \infty; \forall i = 1, N_O$

$F^{\hat{I}\hat{O}}(i,j)$: j^{th} OP outlet flow rate to the i^{th} OP network outlet $\forall j = 1,\infty; \forall i = 1,\infty$

$N : u \to y = N(u)$: input output information map

n: component index

N_I: IDEAS Network inlet streams

N_O: IDEAS Network outlets streams

S_{mix}: Index set of the mixing operation's inlet streams

S_{MMR}: Index set indicating units of maximum mixedness reactors

S_{SFR}: Index set indicating units of segregated flow reactors

S_{split}: Index set of the splitting operation's outlet streams

$\tau(i)$: Residence time of the i^{th} OP unit $\forall i = 1,\infty$

τ_c: Critical value of the residence time τ

$u(i)$: Input of the i^{th} OP unit information map $\forall i = 1,\infty$

$u \triangleq [u_1\, u_2]^T$: Input information vector

$y(i)$: Output of the i^{th} OP unit information map $\forall i = 1,\infty$

$y \triangleq [y_1\, y_2]^T$: Output information vector

1.1 Introduction

The goal of this work is to fill the literature gap on the synthesis of reactor networks whose individual reactor units exhibit segregated flow (SFR) and/or maximum mixedness

(MMR), all feature the same normalized residence time density (NRTd) function, and simply possess different mean residence times from one another.

According to Nauman (2008), the RTD approach to reactor modeling and design is carried out under the following assumptions:

(1) The flow system is at steady state.

(2) There is a single inlet and a single outlet.

(3) The inlet and outlet are closed, so that flow across the system boundaries is unidirectional.

(4) The system is homogeneous (i.e., single-phase).

(5) Inert tracer experiments can be performed on the system without disturbing the flow.

(6) When the system is a reactor, it is isothermal.

These assumptions are employed throughout this work.

The concept of RTD was first introduced by MacMullin and Weber (1935) for the analysis of chemical reactor performance. P.V Danckwerts (1953) identified the F-diagrams and age distribution functions of common models including reactors and blenders and calculated efficiency from the use of these diagrams and distribution functions and showed that this can predict the RTD of larger systems. Later on, Danckwerts (1958) addressed the concept of micromixing and developed the idea of the degree of segregation. Zwietering (1959) showed that knowledge of the residence time distribution of a continuous flow system is not sufficient for the description of mixing. Zwietering studied maximum mixedness as an opposite extreme of segregation for a system of a chemical reaction of an arbitrary order and showed that the conversion can be calculated for both cases. L.G. Gilbilaro (1977) showed that the residence time distribution of the flow in the region depends on the internal rate flow but the mean residence time doesn't. He showed that the mean residence time of any material in any region of

the system is equal to its holdup in that region divided by the overall flow rate of the whole system. More recently, Gao et al. (2010) used RTD theory to characterize continuous powder mixing.The RTD's of many common reactor types have now been calculated and are included in reaction engineering textbooks (e.g. Nauman and Buffham (1974), Fogler (2006)). The RTD exhibited by a given reactor however doesn't give enough information on the type of mixing occurring in the reactor. For that reason, models are needed to predict the conversion in non-ideal reactors. These models typically have a number of adjustable parameters. Commonly used models include tanks in series models that have one adjustable parameter per tank employed, and dispersion models which have two adjustable parameters. Two models that have no adjustable parameters, are the Segregated Reactor (SR) and the Maximum Mixedness Reactor (MMR) models shown in figure 1.

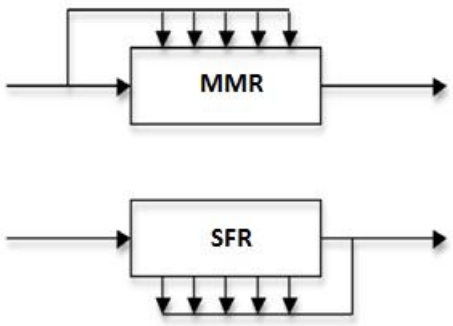

Figure 1-1 Maximum Mixedness Reactor and Segregated Flow Reactor

RTD reactor network related results are scarce in the literature. Glasser et al. (1994) studied the attainable region for segregated reactor (SR) and maximum mixed reactor (MMR) models and showed, for an example, that the conversions attained by these reactor models do not represent conversion bounds for all reactor models. In fact, they showed that the SR and MMR attainable region boundaries lie within the attainable region. Hocine et al. (2008) employed MINLP techniques to locally minimize superstructures consisting of PFR's and CSTR's so as to

create networks whose overall RTD approximates a known residence time distribution. No prior work has considered the optimization of any objective function for a network of reactor units all of which exhibit segregated flow (SFR) and/or maximum mixedness (MMR), have the same NRTd, but each possesses a different mean residence time from one another.

The rest of the paper proceeds as follows. In the next section, the Residence Time Density/Distribution (RTd/RTD) mathematical framework and the Segregated Flow Reactor (SFR) and Maximum Mixedness Reactor (MMR) models are briefly reviewed. Next, the applicability of the IDEAS Conceptual Framework to SFR and MMR networks with the same normalized residence time density (NRTd) function is established. The IDEAS Mathematical Formulation for Minimum Volume RTD Reactor Networks is subsequently presented. A number of novel properties of this formulation are then established, which are subsequently utilized to facilitate its solution. An illustrative case study is then presented, on the IDEAS based globally optimal synthesis of Minimum Volume reactor networks featuring Segregated Laminar Flow Reactors (SLFR) carrying out the Trambouze reaction scheme. The case study demonstrates that RTD networks can exhibit significantly superior performance to that of single RTD reactors. Finally, the presented method is discussed and conclusions are drawn.

1.2 Residence Time Density/Distribution Mathematical Framework

The material in this section are primarily based on Himmelblau and Bischoff (1968); Nauman and Buffham (1974). Consider a system with constant volume $V > 0$, through which fluid flows with a constant flowrate $F > 0$, (Himmelblau and Bischoff, p. 61 (1968)). The residence time t of a fluid element is the difference between the time the fluid element exits the system t_{out} and the

time that it entered the system t_{in}, i.e. $t = t_{out} - t_{in}$. The age α of a fluid element at a given time t_g is the difference between t_g and t_{in}, i.e. $\alpha = t_g - t_{in}$. The life expectancy λ of a fluid element at a given time is the difference between the time that the fluid element will exit the system t_{out} and the given time t_g. Then the following holds $t = \alpha + \lambda$. In relation to this system the following concepts are defined:

Residence time density (RTd) function: $E : \mathbb{R}^+ \to \mathbb{R}^+; E : t \to E(t); \int_0^\infty E(t')dt' = 1$ where $E(t')dt'$ is the volume fraction of the exit stream that has resided in the system for a time between t' and $t' + dt'$. The above implicitly necessitates $\lim_{t \to +\infty} E(t) = 0$

Residence time distribution (RTD) function: $F : \mathbb{R}^+ \to \mathbb{R}^+; F : t \to F(t) \triangleq \int_0^t E(t')dt';$ where $F(t)$ is the volume fraction of the exit stream with residence time between 0 and t. The above implicitly necessitates $F(0) = 0$, $\lim_{t \to +\infty} F(t) = \int_0^\infty E(t')dt' = 1,$ $\int_t^\infty E(t')dt' = 1 - F(t),$ $E(t) = \frac{dF(t)}{dt}$, and $F : \mathbb{R}^+ \to \mathbb{R}^+$ is a nondecreasing function. In addition it must hold $\int_0^\infty (1 - F(t'))dt' < \infty$, which in turn implies $\lim_{t \to +\infty} \left[t \cdot (1 - F(t)) \right] = 0$

Mean Residence time: $\bar{t} \triangleq \int_0^\infty t' E(t')dt'$

Normalized Residence time density (NRTd) function:

Let $E:\mathbb{R}^+\to\mathbb{R}^+; E:t\to E(t)$ be a Residence time density (RTd) function, with Mean Residence time $\bar{t}\triangleq\int_0^\infty t'E(t')dt'$. Then the associated Normalized Residence time density (RTd) function is defined as:

$\boldsymbol{E}:\mathbb{R}^+\to\mathbb{R}^+; \boldsymbol{E}:\theta\triangleq\frac{t}{\bar{t}}\to\boldsymbol{E}(\theta)\triangleq\bar{t}\,E(t)$. It is easy to verify that $\boldsymbol{E}(\cdot)$ possesses the following properties: $\int_0^\infty \boldsymbol{E}(\theta')d\theta'=1$ and $\bar{\theta}\triangleq\int_0^\infty\theta'\boldsymbol{E}(\theta')d\theta'=1.$

Internal age density function: $I:\mathbb{R}^+\to\mathbb{R}^+; I:\alpha\to I(\alpha); \int_0^\infty I(\alpha')d\alpha'=1$ where $I(\alpha')d\alpha'$ is the volume fraction of the system contents that has an age between α and $\alpha+d\alpha$. The above implicitly necessitates $\lim_{\alpha\to+\infty} I(\alpha)=0$.

Internal age distribution function: $J:\mathbb{R}^+\to\mathbb{R}^+; J:\alpha\to J(\alpha)\triangleq\int_0^\alpha I(\alpha')d\alpha'$ where $J(\alpha)$ is the volume fraction of the system contents that has an age between 0 and α. The above implicitly necessitates $J(0)=0,\quad \lim_{\alpha\to+\infty} J(\alpha)=\int_0^\infty I(\alpha')d\alpha'=1,\quad \int_\alpha^\infty I(\alpha')d\alpha'=1-J(\alpha), I(\alpha)=\frac{dJ(\alpha)}{d\alpha}$ and $J:\mathbb{R}^+\to\mathbb{R}^+$ is a nondecreasing function

Mean Age: $\bar{\alpha}\triangleq\int_0^\infty\alpha' I(\alpha')d\alpha'$

The internal age density function $I:\mathbb{R}^+\to\mathbb{R}^+; I:\alpha\to I(\alpha),$ and thus the internal age distribution function $J:\mathbb{R}^+\to\mathbb{R}^+; J:\alpha\to J(\alpha)$ can be evaluated from the residence time distribution through the relations $I(\alpha)=\frac{1}{\bar{t}}\left(1-F(\alpha)\right)$ and $J(\alpha)\triangleq\frac{1}{\bar{t}}\int_0^\alpha\left(1-F(\alpha')\right)d\alpha'$.

Life expectancy density function: $\Phi:\mathbb{R}^+\to\mathbb{R}^+;\Phi:\lambda\to\Phi(\lambda);\int_0^\infty\Phi(\lambda')d\lambda'=1$ where $\Phi(\lambda')d\lambda'$ is the volume fraction of the system contents that has a life expectancy between λ' and $\lambda'+d\lambda'$. The above implicitly necessitates $\lim_{\lambda\to+\infty}\Phi(\lambda)=0$.

Life expectancy distribution function: $\Psi:\mathbb{R}^+\to\mathbb{R}^+;\Psi:\lambda\to\Psi(\lambda)\triangleq\int_0^\lambda\Phi(\lambda')d\lambda'$ where $\Psi(\lambda)$ is the volume fraction of the system contents that has a life expectancy between 0 and λ. The above implicitly necessitates $\Psi(0)=0$, $\lim_{\lambda\to+\infty}\Psi(\lambda)\triangleq\int_0^\infty\Phi(\lambda')d\lambda'=1$, $\int_\lambda^\infty\Phi(\lambda')d\lambda'=1-\Psi(\lambda)$, $\Phi(\lambda)=\frac{d\Psi(\lambda)}{d\lambda}$ and $\Psi:\mathbb{R}^+\to\mathbb{R}^+$ is a nondecreasing function

The life expectancy density function $\Phi:\mathbb{R}^+\to\mathbb{R}^+;\Phi:\lambda\to\Phi(\lambda)$, and thus the life expectancy distribution function $\Psi:\mathbb{R}^+\to\mathbb{R}^+;\Psi:\lambda\to\Psi(\lambda)$, can be evaluated from the residence time distribution through the relations $\Phi(\lambda)=\frac{1}{\bar{t}}\left(1-F(\lambda)\right)$ and $\Psi(\lambda)\triangleq\frac{1}{\bar{t}}\int_0^\lambda\left(1-F(\lambda')\right)d\lambda'$

Intensity Function: $\Lambda:\mathbb{R}^+\to\mathbb{R}^+;\Lambda:t\to\Lambda(t)\triangleq\frac{E(t)}{1-F(t)}$ where $\Lambda(t)$ is the volume fraction of the system contents that has an age $\alpha=t$ and will have a residence time between t and $t+dt$

The intensity and residence time density functions admit a 1:1 equivalence to one another based on the following relations:

$\Lambda(t)=\frac{E(t)}{1-\int_0^t E(t')dt'}$ and $E(t)=\Lambda(t)\cdot\exp\left(-\int_0^t\Lambda(t')dt'\right)$. In addition, the following relations hold among the aforementioned functions in Eq.(1) and Eq.(2):

$$\Lambda(t) \triangleq \frac{E(t)}{1-F(t)} = \frac{1}{\bar{t}} \cdot \frac{E(t)}{I(t)} = -\frac{d}{dt}\left(\ln\left(\bar{t} \cdot I(t)\right)\right) = -\frac{1}{I(t)} \cdot \frac{dI(t)}{dt} \qquad (1)$$

$$E(t) = -\bar{t} \cdot \frac{d\,I(t)}{dt} = \bar{t} \cdot \Lambda(t) \cdot I(t) \qquad (2)$$

Knowledge of a reactor's RTD function and of the species' kinetic generation rates, for any reaction scheme being carried out in the reactor, are not sufficient by themselves to quantify the reactor outlet species concentrations given the reactor's inlet species concentrations. To quantify these outlet concentrations additional information is needed regarding the flow pattern and the quality of mixing inside the reactor. Two models, with no adjustable parameters, that permit quantification of the outlet concentrations are the Segregated Flow Reactor (SFR) Model and the Maximum Mixedness Reactor (MMR) Model.

Segregated Flow Reactor (SFR) Model

Consider a constant density fluid, segregated flow reactor (SFR) with an RTd function $E: \mathbb{R}^+ \to \mathbb{R}^+$, volumetric flowrate $F\left(m^3/s\right)$, reactor volume $V\left(m^3\right)$, mean residence time $\bar{t} \triangleq \int_0^\infty tE(t)\,dt = \frac{V}{F} \triangleq \tau\ (s)$, inlet, outlet component concentrations $\left\{C_i^{in}\right\}_{i=1}^n, \left\{C_i^{out}\right\}_{i=1}^n \left(kmol/m^3\right)$, and ith component generation rate $\{R_i\}_{i=1}^n\ \left(kmol/\left(m^3 s\right)\right)$ respectively. The SFR model considers that there is no mixing among fractions of material that have different residence times in the reactor. As a result, each fraction behaves as a batch reactor with batch time $t(s)$, and inlet and outlet concentrations $\left\{C_i(0)\right\}_{i=1}^n = \left\{C_i^{in}\right\}_{i=1}^n$, $\left\{C_i(t)\right\}_{i=1}^n$ respectively. Then the SFR model is shown in Eq. (3)-(5) with initial condition Eq. (6):

$$\left\{\begin{array}{ll} C_i^{out}(\tau)=\int_0^{\infty} C_i(t)E(t)dt \quad \forall i=1,....,n & (3) \\ \overline{t}\triangleq\int_0^{\infty} tE(t)dt=\frac{V}{F}\triangleq\tau & (4) \\ \frac{dC_i(t')}{dt'}=R_i\left(\left\{C_j(t')\right\}_{j=1}^{n}\right) \quad \forall t'\in[0,t] \ \forall t\in[0,\infty) & (5) \\ C_i(0)=C_i^{in}; \qquad \forall i=1,....,n & (6) \end{array}\right\}$$

Maximum Mixedness Reactor (MMR) Model

Consider a constant density fluid, segregated flow reactor (SFR) with an RTd function $E:\mathbb{R}^+\to\mathbb{R}^+$, volumetric flowrate $F\left(m^3/s\right)$, reactor volume $V\left(m^3\right)$, mean residence time $\overline{t}\triangleq\int_0^{\infty} tE(t)dt=\frac{V}{F}\triangleq\tau\ (s)$, inlet, outlet component concentrations $\left\{C_i^{in}\right\}_{i=1}^{n},\left\{C_i^{out}\right\}_{i=1}^{n}\left(kmol/m^3\right)$, and ith component generation rate $\{R_i\}_{i=1}^{n}\ \left(kmol/\left(m^3s\right)\right)$respectively. The MMR model considers that there is early mixing among fractions of material that have different residence times in the reactor. As a result, each fraction behaves as a batch reactor with batch time t, and inlet and outlet concentrations $\left\{C_i^{in}\right\}_{i=1}^{n}$, $\left\{C_i^{out}\right\}_{i=1}^{n}$ respectively.

Then the MMR model is shown in Eq. (7)-(8):

$$\left\{\begin{array}{ll} \frac{dC_i(\lambda)}{d\lambda}=-R_i\left(\left\{C_j(\lambda)\right\}_1^{n}\right)+\left(C_i(\lambda)-C_i^{in}\right)\frac{E(\lambda)}{1-F(\lambda)} \quad \forall\lambda\in[0,\infty) \ \forall i=1,....,n & (7) \\ C_i(\lambda=0)=C_i^{out} \qquad \forall i=1,....,n; \quad \frac{dC_i}{d\lambda}(\lambda=\infty)=0 \ \forall i=1,....,n & (8) \end{array}\right\}$$

Solution of the MMR model requires that the value of $C_i(\lambda=\infty)$be first identified. This requires that first $\lim_{\lambda\to+\infty}\frac{E(\lambda)}{1-F(\lambda)}$be identified, and then the equations

$$0 = -R_i\left(\left\{C_j(\infty)\right\}_1^n\right) + \left(C_i(\infty) - C_i^{in}\right)\frac{E(\infty)}{1-F(\infty)} \quad \forall i = 1,...,n \text{ be solved for } \left\{C_j(\infty)\right\}_1^n \quad \forall i = 1,...,n$$

Some times this rigorous procedure is abandoned in favor of a solution method that introduces a new independent variable $z \triangleq L - \lambda$ where $L \to +\infty$, and then carries out the solution of the MMR model as an initial value problem whose initial condition is $C_i(z=0) = C_i^{in} \quad \forall i = 1,....,n$.

Figure 1 illustrates the two nonideal reactor models considered. The SFR model is identical to that of a plug flow reactor with one inlet and an infinite number of side outlets. Each of these outlets has a different age α, and all together they are such that the the overall stream that results from the mixing of these outlets corresponds to a residence time distribution equal to the reactor's given residence time distribution. Similarly the MMR model is identical to that of a plug flow reactor with an infinite number of inlets and one outlet. Each of these inlets has a different life expectancy λ, and all together they are such that the overall stream from which these inlets emanate corresponds to a residence time distribution equal to the reactor's given residence time distribution.

1.3 Applicability of IDEAS Conceptual Framework to SFR and MMR networks

The IDEAS conceptual framework has been proposed by Manousiouthakis and coworkers as a globally optimal network synthesis methodology. Its advantage over other process network optimization methodologies is that it guarantees the global optimality of the obtained solution. The reasons are that the underlying mathematical programming formulations have feasible regions defined by linear constraints and that many industrially meaningful optimization objectives (volume, operating cost, area, yield, selectivity, plate area, holdup, etc.) give rise to linear objective functions thus making the underlying mathematical formulations linear programs. The methodology has been demonstrated on a number of applications: by Burri et al.

(2002) they constructed the attainable region through the Infinite Dimensional State-space (IDEAS), in the concentration space a point on the AR boundary is found by solving an Infinite dimensional Linear Programming (ILP). Manousiouthakis and co-workers used IDEAS framework through solutions of a sequence of Linear Programming (LP), to construct increasingly accurate approximations to the true AR, (Burri et al. (2002); Drake and Manousiouthakis (2002a, 2002b); Justanieah and Manousiouthakis (2004); Wilson and Manousiouthakis (2000); Zhou and Manousiouthakis (2008b)). IDEAS, is a general framework that can address most process network synthesis problems. Another alternative IDEAS formulation to extend the AR considering only CSTR's was presented by Kauchali, et al. (2002). Abraham and Feinberg (2004) presented a critical condition for a region to be considered in the true AR. Based on the mathematical formulation of IDEAS to RNS problems, Justanieah et al (2004), presented for the first time necessary and sufficient conditions for a point in the concentration space to belong to the AR, and developed the Shrink-Wrap algorithm to approximate the true AR. Zhou and Manousiouthakis (2006), showed that AR for a non-ideal reactor network synthesis through IDEAS can be larger than an ideal reactor network featuring CSTR's and PFR's. IDEAS research proved that its framework makes no assumptions on the structure of the reactor network and its solution will yield an optimal network.

The main goal of this work, is to demonstrate that the IDEAS Paradigm can be applied to the globally optimal synthesis of reactor networks featuring Non-Ideal RTD Reactor Models and that the Minimum Volume RTD Reactor Network can be identified using an Inifinite Linear Program (ILP).

IDEAS is the first generalized process network synthesis methodology that is capable of delivering globally optimum designs. IDEAS is based on two principles: A vector space is

equivalent to the infinite union of lower dimensional linear varieties, and the projection of the input-output map of a chemical process onto a linear variety, over which only extensive variables vary, is a linear map. To better understand how IDEAS works, consider a flowsheet (See Figure 2) that includes an infinite number of operations classified into two categories, an operator network (OP) and a distribution network (DN). The OP quantifies the actions of the considered process unit operations (reactors, separators, heat exchangers, etc.) and consists of an infinite number of linear input/output maps with extensive and intensive properties for each map. The DN on the other hand quantifies the mixing and splitting processes which can take place among the inlet and outlet streams of the aforementioned unit operations. This unique structure of IDEAS allows all feasible network configurations to be considered, and gives rise to infinite linear programming (ILP) formulations for the synthesis of optimal process networks. The solution of these ILP's is approximated closely by finite dimensional linear programs that are guaranteed to be globally optimal.

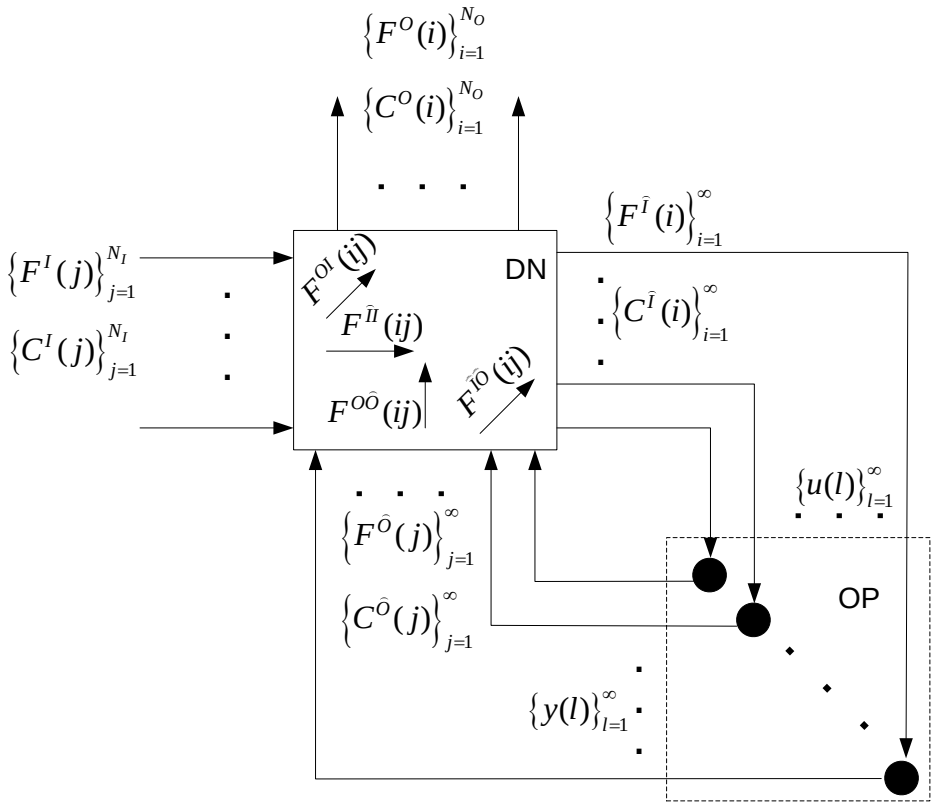

Figure 1-2 IDEAS Representation of a reactor network

Consider a constant density fluid reactor with NRTd function $\boldsymbol{E}:\mathbb{R}^+\to\mathbb{R}^+;\boldsymbol{E}:\theta\to\boldsymbol{E}(\theta)$, volumetric flowrate F (m^3/s), reactor volume V (m^3), mean residence time $\bar{t}$, inlet, outlet component concentrations $\{C_i^{in}\}_{i=1}^n$, $\{C_i^{out}\}_{i=1}^n$ (kmol/m^3), and i^{th}component generation rate $\{R_i\}_{i=1}^n$ (kmol/(m^3 s)) respectively, with input output information map $N:u\to y=N(u)$ where $u\triangleq\left[F\,C_1^{in}\cdots C_n^{in}\,\bar{t}\right]^T;y\triangleq\left[F\,V\,C_1^{out}\cdots C_n^{out}\,\tau\right]^T$

Establishing the applicability of IDEAS to a process network synthesis problem first requires that the input output information map N be shown to possess certain properties, namely that

there exists a decomposition of the input and output vectors $u \triangleq [u_1\, u_2]^T$; $y \triangleq [y_1\, y_2]^T$ such that the input output information map $N: u = [u_1\, u_2]^T \rightarrow y = [y_1\, y_2]^T = N(u) = [N_1(u)\; N_2(u)]^T = [N_1(u_1,u_2)\; N_2(u_1,u_2)]^T$ satisfies the properties

Property 1. $y_2 = N_2(u_1,u_2) = N_2(u_2)$

Property 2. $y_1 = N_1(u_1,u_2) = N_1(u_2)u_1$ where, for fixed u_2, $N_1(u_2)$ is a linear operator.

It can be readily verified that for the input output decomposition $u_1 \triangleq [F]^T$; $u_2 \triangleq [C_1^{in} \cdots C_n^{in}\; \bar{t}]^T$; $y_1 \triangleq [F\; V]^T$; $y_2 \triangleq [C_1^{out} \cdots C_n^{out}\; \tau]^T$, both SFR and MMR models satisfy the above two properties. Indeed,

For the SFR model:

1. $y_2 = N_2(u_1,u_2) = N_2(u_2)$, since knowledge of $\boldsymbol{E}: \theta \rightarrow \boldsymbol{E}(\theta)$ and the mean residence time $\bar{t}$, combined with the equations $\theta \triangleq \frac{t}{\bar{t}}$; $\boldsymbol{E}(\theta) \triangleq \bar{t}\, E(t)$; $\tau \triangleq \frac{V}{F} = \bar{t} \triangleq \int_0^\infty tE(t)dt$ allows calculation of $E(\cdot), \tau$. Knowledge of $R_i\left(\{C_j(\cdot)\}_{j=1}^n\right)$; $C_i^{in}\ \forall i = 1,....,n$ allows first calculation of $C_i(\cdot)\ \forall i = 1,....,n$ based on equations $(5),(6)$, and then calculation of $C_i^{out} = C_i^{out}(\tau)\ \ \forall i = 1,....,n$ based on equation (3).

2. $y_1 = N_1(u_1,u_2) = N_1(u_2)u_1$ where, for fixed u_2, $N_1(u_2)$ is a linear operator , since the output vector $y_1 \triangleq [F\; V]^T$ is related to the input vector $u_1 \triangleq [F]^T$ through the linear relation $y_1 \triangleq [F\; V]^T = [1\; \bar{t}]^T [F]$ since the mean residence time $\bar{t} = \tau$ is constant. The associated operator $N_1(u_2) = [1\; \bar{t}]^T$ is linear for $\bar{t}$ constant.

For the MMR model:

1. $y_2 = N_2(u_1, u_2) = N_2(u_2)$, since again knowledge of $\boldsymbol{E}: \theta \to \boldsymbol{E}(\theta)$ and $\bar{t}$, combined with $\theta \triangleq \frac{t}{\bar{t}}$; $\boldsymbol{E}(\theta) \triangleq \bar{t}\, E(t)$; $\tau \triangleq \frac{V}{F} = \bar{t} \triangleq \int_0^\infty t E(t)\, dt$ allows calculation of $E(\cdot), \tau$. Knowledge of $R_i\left(\{C_j(\cdot)\}_{j=1}^n\right)$; C_i^{in}; $\forall i = 1,....,n$; $E(\cdot)$ allows first calculation of $C_i(\cdot)$ $\forall i = 1,....,n$ based on equations (7), (8), and then calculation of $C_i^{out} = C_i^{out}(\tau)$ $\forall i = 1,....,n$ based on equation (8).

2. $y_1 = N_1(u_1, u_2) = N_1(u_2) u_1$ where, for fixed u_2, $N_1(u_2)$ is a linear operator , since again $y_1 \triangleq [F\ V]^T = [1\ \bar{t}]^T [F] = N_1(u_2) u_1$, where $N_1(u_2) = [1\ \bar{t}]^T$ is a linear operator for $\bar{t}$ constant.

Having established the linearity of the IDEAS OP, it can be ensured that the IDEAS feasible region is linear by proving that the DN defining equations are also linear. The DN contains all the mixing and splitting operations of the overall network. Knowledge of the intensive properties of the inlet and outlet streams for each SFR and MMR unit results in DN overall mass and component balances linear in the DN's flow variables. Thus the linearity of the IDEAS DN is also established.

1.4 IDEAS Mathematical Formulation for Minimum Volume RTD Reactor Networks

The IDEAS representation of a reactor network is illustrated in Figure 1, for a system with N_I network inlet streams, N_O network outlet streams and n components. Under steady-state, homogeneous, isothermal, and constant-density conditions, the infinite-dimensional linear feasible region for the corresponding mathematical formulation of the SFR and MMR reactor network synthesis problems is defined by the following equations and inequalities:

DN total mass balance equations, Eq. (9)-(12)

$$F^{I}(j)=\sum_{i=1}^{N_O}F^{OI}(i,j)+\sum_{i=1}^{\infty}F^{\hat{I}I}(i,j)\quad \forall j=1,...,N_I \tag{9}$$

$$F^{O}(i)=\sum_{j=1}^{N_I}F^{OI}(i,j)+\sum_{j=1}^{\infty}F^{O\hat{O}}(i,j)\quad \forall i=1,...,N_O \tag{10}$$

$$F^{\hat{I}}(i)=\sum_{j=1}^{N_I}F^{\hat{I}I}(i,j)+\sum_{j=1}^{\infty}F^{\hat{I}\hat{O}}(i,j)\quad \forall i=1,...,\infty \tag{11}$$

$$F^{\hat{O}}(j)=\sum_{i=1}^{N_O}F^{O\hat{O}}(i,j)+\sum_{i=1}^{\infty}F^{\hat{I}\hat{O}}(i,j)\quad \forall j=1,...,\infty \tag{12}$$

DN component balance equations, Eq. (13)

$$C_k^{\hat{I}}(i)F^{\hat{I}}(i)=\sum_{j=1}^{N_I}C_k^{I}(j)F^{\hat{I}I}(i,j)+\sum_{j=1}^{\infty}C_k^{\hat{O}}(j)F^{\hat{I}\hat{O}}(i,j)\ \ \forall k=1,...,n\ \ \forall i=1,...,\infty \tag{13}$$

DN outlet specifications, Eq. (14)-(15)

$$\left(F^{O}(i)\right)^{l}\le F^{O}(i)\le\left(F^{O}(i)\right)^{u}\ \ \forall i=1,...,N_O \tag{14}$$

$$\left(C_k^{O}(i)\right)^{l}F^{O}(i)\le\sum_{j=1}^{N_I}C_k^{I}(j)F^{OI}(i,j)+\sum_{j=1}^{\infty}C_k^{\hat{O}}(j)F^{O\hat{O}}(i,j)\le\left(C_k^{O}(i)\right)^{u}F^{O}(i) \tag{15}$$
$$\forall k=1,...,n\ \ \forall i=1,...,N_O$$

OP balance equations, Eq. (16)

$$F^{\hat{O}}(i)=F^{\hat{I}}(i)\qquad\qquad \forall i=1,...,\infty \tag{16}$$

SFR Reactor defining equations, Eq. (17)-(20)

$$C_k^{\hat{O}}(i)=\int_0^{\infty}C_{k,i}(t)E_i(t)dt\quad \forall k=1,....,n\ \forall i\in S_{SFR} \tag{17}$$

$$\tau(i)\triangleq\int_0^{\infty}tE_i(t)dt=\frac{V(i)}{F^{\hat{I}}(i)}\ \ \forall i\in S_{SFR} \tag{18}$$

$$\frac{dC_{k,i}(t')}{dt'} = R_k\left(\left\{C_{j,i}(t')\right\}_{j=1}^{n}\right) \quad \forall k = 1,....,n \;\; \forall t' \in [0,t] \; \forall t \in [0,\infty) \;\; \forall i \in S_{SFR} \tag{19}$$

$$C_{k,i}(0) = C_k^{\hat{I}}(i) \quad \forall i \in S_{SFR} \tag{20}$$

MMR Reactor defining equations, Eq. (21)-(24)

$$\frac{dC_{k,i}(\lambda)}{d\lambda} = -R_i\left(\left\{C_{j,i}(\lambda)\right\}_1^n\right) + \left(C_{k,i}(\lambda) - C_k^{\hat{I}}(i)\right)\frac{E_i(\lambda)}{1-F_i(\lambda)} \tag{21}$$
$$\forall \lambda \in [0,\infty) \;\; \forall k = 1,...,n \;\; \forall i \in S_{MMR}$$

$$\tau(i) \triangleq \int_0^\infty tE_i(t)\,dt = \frac{V(i)}{F^{\hat{I}}(i)} \;\; \forall i \in S_{MMR} \tag{22}$$

$$C_{k,i}(\lambda = 0) = C_k^{\hat{O}}(i) \;\; \forall k = 1,...,n \;\; \forall i \in S_{MMR} \tag{23}$$

$$\frac{dC_{k,i}}{d\lambda}(\lambda = \infty) = 0 \;\forall k = 1,...,n \;\; \forall i \in S_{MMR} \tag{24}$$

where S_{SFR} and S_{MMR} are index sets indicating which units are segregated flow reactors and which units are maximum mixedness reactors respectively, and $S_{SFR} \cup S_{MMR} = \{1,...,\infty\}$

Positivity inequalities, Eq. (25)

$$F^I \geq 0; F^O \geq 0; F^{\hat{I}} \geq 0; F^{\hat{O}} \geq 0; F^{OI} \geq 0; F^{\hat{I}I} \geq 0; F^{\hat{I}\hat{O}} \geq 0; F^{O\hat{O}} \geq 0; V \geq 0 \tag{25}$$

where the upper case on $\left(F^O(i)\right)^l, \left(F^O(i)\right)^u$ and $\left(C_k^O(i)\right)^l, \left(C_k^O(i)\right)^u$ are the lower and upper bounds on the network flowrate and concentration outlets, respectively.

Eq. (26), is the Network Volume Objective function

$$V = \sum_{i=1}^{\infty} \tau(i) F^{\hat{I}}(i) \tag{26}$$

In addition, the following set of nonlinear equations that help define the overall network's outlet compositions hold:

$$C_k^O(i)F^O(i) = \sum_{j=1}^{N_I} C_k^I(j)F^{OI}(i,j) + \sum_{j=1}^{\infty} C_k^{\hat{O}}(j)F^{O\hat{O}}(i,j) \quad (27)$$
$$\forall k = 1,...,n \;\; \forall i = 1,...,N_O$$

1.5 Properties of IDEAS formulation for RTd/RTD SFR-MMR Networks

Proposition 1.

Consider a reaction scheme involving n species whose generation rates are linearly dependent, i.e. $\exists\{\beta_i\}_1^n \in \mathbb{R}^n : \sum_{i=1}^n \beta_i R_i = 0$, and a RTD reactor whose outlet and inlet concentrations are $\{C_i^{out}\}_1^n, \{C_i^{in}\}_1^n$, respectively.

a. Assume that the reactor's Intensity Function satisfies the condition $\Lambda(\infty) > 0$. Then, for the MMR model it holds that $\sum_{i=1}^n \beta_i \left(C_i^{out} - C_i^{in}\right) = 0$

b. The SFR model also satisfies $\sum_{i=1}^n \beta_i \left(C_i^{out} - C_i^{in}\right) = 0$

c. Consider a process network employing MMR / SFR/ Mixing/Splitting unit operations. Then, if each of the streams entering the unit operation satisfies the relation $\sum_{i=1}^n \beta_i \left(C_i^{in} - C_i^0\right) = 0$, the streams exiting this operation satisfy the relation $\sum_{i=1}^n \beta_i \left(C_i^{out} - C_i^0\right) = 0$, where $\{C_i^0\}_1^n$ are reference concentrations.

Proof:

a. Consider the MMR model, Eq. (28)-(29)

$$\left\{\begin{array}{ll} \dfrac{dC_i(\lambda)}{d\lambda} = -R_i + \left(C_i(\lambda) - C_i^{in}\right)\dfrac{E(\lambda)}{1-F(\lambda)} & \forall \lambda \in [0,\infty) \quad (28) \\ C_i(0) = C_i^{out} \quad \forall i = 1,....,n; \quad \dfrac{dC_i}{d\lambda}(\infty) = 0 & \forall i = 1,....,n \quad (29) \end{array}\right\}$$

It is given that $\exists \{\beta_i\}_1^n \in \mathbb{R}^n : \sum_{i=1}^n \beta_i R_i = 0$. Substituting the species generation rate from the MMR model into this equation yields:

$$\sum_{i=1}^n \beta_i \left(-\frac{dC_i(\lambda)}{d\lambda} + \left(C_i(\lambda) - C_i^{in}\right)\frac{E(\lambda)}{1-F(\lambda)} \right) = 0 \Rightarrow \quad (30)$$

$$\left(-\frac{d\left(\sum_{i=1}^n \beta_i C_i(\lambda)\right)}{d\lambda} + \frac{E(\lambda)}{1-F(\lambda)} \cdot \sum_{i=1}^n \beta_i \left(C_i(\lambda) - C_i^{in}\right) \right) = 0 \quad (31)$$

Let us define $z(\lambda) \triangleq \sum_{i=1}^n \beta_i \left(C_i(\lambda) - C_i^{in}\right)$. Then $z(0) = \sum_{i=1}^n \beta_i \left(C_i^{out} - C_i^{in}\right)$, $\frac{dz}{d\lambda}(\infty) = 0$, and the above equation implies $\left(-\frac{dz(\lambda)}{d\lambda} + \frac{E(\lambda)}{1-F(\lambda)} \cdot z(\lambda) \right) = 0$. Combining with the above, Eq. (30)-(31) yields:

$$\int_{z(0)}^{z(\lambda)} \frac{dz}{z} = \int_0^\lambda \frac{E(\lambda')}{1-F(\lambda')} d\lambda' \Rightarrow \ln\left(\frac{z(\lambda)}{z(0)}\right) = \int_0^\lambda \frac{E(\lambda')}{1-F(\lambda')} d\lambda' \Rightarrow \quad (32)$$

$$z(\lambda) = z(0) \cdot \exp\left[\int_0^\lambda \frac{E(\lambda')}{1-F(\lambda')} d\lambda' \right] \Rightarrow \quad (33)$$

$$\frac{dz(\lambda)}{d\lambda} = z(0) \cdot \frac{E(\lambda)}{1-F(\lambda)} \cdot \exp\left[\int_0^\lambda \frac{E(\lambda')}{1-F(\lambda')} d\lambda' \right] \Rightarrow \quad (34)$$

$$\left\{\begin{array}{ll} \dfrac{dz}{d\lambda}(\infty)=z(0)\cdot\dfrac{E(\infty)}{1-F(\infty)}\cdot\exp\left[\int_0^{\infty}\dfrac{E(\lambda')}{1-F(\lambda')}d\lambda'\right] & (35) \\ z(\infty)=z(0)\cdot\exp\left[\int_0^{\infty}\dfrac{E(\lambda')}{1-F(\lambda')}d\lambda'\right] & (36) \end{array}\right\}$$

However, based on the 1:1 equivalence relation given in the previous section between a reactor's intensity function and residence time density function it holds:

$\Lambda(t)\triangleq\dfrac{E(t)}{1-F(t)}=\dfrac{E(t)}{1-\int_0^t E(t')dt'}$ and $E(t)=\Lambda(t)\cdot\exp\left(-\int_0^t\Lambda(t')dt'\right)$. Then

$$\left\{\begin{array}{l} 0=\dfrac{dz}{d\lambda}(\infty)=z(0)\cdot\dfrac{\Lambda^2(\infty)}{E(\infty)} \\ z(\infty)=z(0)\cdot\dfrac{\Lambda(\infty)}{E(\infty)} \end{array}\right\}$$. Based on the proposition's assumption that the reactor's intensity function should be strictly positive at infinity, i.e. that $\Lambda(\infty)>0$, and since $E(\infty)=\lim_{t\to+\infty}E(t)=0$, the conclusion that $z(0)=0$, i.e. $\sum_{i=1}^{n}\beta_i\left(C_i^{out}-C_i^{in}\right)=0$ can be readily reached.

b. Consider the SFR model, Eq. (37)-(40)

$$\left\{\begin{array}{ll} C_i^{out}(\tau)=\int_0^{\infty}C_i(t)E(t)dt \quad \forall i=1,....,n & (37) \\ \tau\triangleq\int_0^{\infty}tE(t)dt=\dfrac{V}{F} & (38) \\ \dfrac{dC_i(t')}{dt'}=R_i\left(\left\{C_j(t')\right\}_{j=1}^{n}\right) \quad \forall t'\in[0,t]\ \forall t\in[0,\infty) & (39) \\ C_i(0)=C_i^{in}; \qquad \forall i=1,....,n & (40) \end{array}\right\}$$

It is given that $\exists\{\beta_i\}_1^n\in\mathbb{R}^n:\sum_{i=1}^{n}\beta_i R_i=0$. Substituting the species generation rate from the SFR model into this equation yields:

$$\sum_{i=1}^{n}\beta_i\left(\frac{dC_i(t')}{dt}\right)=0\ \forall t'\in[0,t]\ \forall t\in[0,\infty)\Rightarrow \tag{41}$$

$$\frac{d\left(\sum_{i=1}^{n}\beta_i C_i(t')\right)}{dt'}=0\ \forall t'\in[0,t]\ \forall t\in[0,\infty)\Rightarrow \tag{42}$$

$$\sum_{i=1}^{n}\beta_i C_i(t)=\sum_{i=1}^{n}\beta_i C_i(0)\ \forall t\in[0,\infty)\Rightarrow \tag{43}$$

$$\sum_{i=1}^{n}\beta_i C_i^{out}(\tau)=\sum_{i=1}^{n}\beta_i\int_0^{\infty}C_i(t)E(t)dt=\int_0^{\infty}\left(\sum_{i=1}^{n}\beta_i C_i(t)\right)E(t)dt\ \forall\tau\in[0,\infty)\Rightarrow \tag{44}$$

$$\begin{aligned}&\sum_{i=1}^{n}\beta_i C_i^{out}(\tau)=\int_0^{\infty}\left(\sum_{i=1}^{n}\beta_i C_i(0)\right)E(t)dt=\\&=\left(\sum_{i=1}^{n}\beta_i C_i(0)\right)\int_0^{\infty}E(t)dt=\left(\sum_{i=1}^{n}\beta_i C_i(0)\right)\ \forall\tau\in[0,\infty)\Rightarrow\end{aligned} \tag{45}$$

$$\sum_{i=1}^{n}\beta_i\left(C_i^{out}(\tau)-C_i^{in}\right)\ \forall\tau\in[0,\infty) \tag{46}$$

c. Consider the MMR / SFR/ Mixing/Splitting unit operations.

We have established above for both the SFR/MMR operations that $\sum_{i=1}^{n}\beta_i\left(C_i^{out}-C_i^{in}\right)$. By assumption, it holds for both the SFR/MMR operations that the streams entering the unit operation satisfy the relation $\sum_{i=1}^{n}\beta_i\left(C_i^{in}-C_i^{0}\right)=0$. Then, summing up the above two equations yields $\sum_{i=1}^{n}\beta_i\left(C_i^{out}-C_i^{0}\right)=0$.

For the Mixing operation it holds $C_i^{out} = \sum_{j \in S_{mix}} F_j C_{i,j}^{in} \Big/ \sum_{j \in S_{mix}} F_j$ where S_{mix} is the index set of the mixing operation's inlet streams. Then $\sum_{i=1}^{n} \beta_i \left(C_i^{out} - C_i^0 \right) = 0 \Leftrightarrow \sum_{i=1}^{n} \beta_i \left(\frac{\sum_{j \in S_{mix}} F_j C_{i,j}^{in}}{\sum_{j \in S_{mix}} F_j} - C_i^0 \right) = 0 \Leftrightarrow$

$$\sum_{i=1}^{n} \beta_i \left(\frac{\sum_{j \in S_{mix}} F_j C_{i,j}^{in}}{\sum_{j \in S_{mix}} F_j} - \frac{\sum_{j \in S_{mix}} F_j C_i^0}{\sum_{j \in S_{mix}} F_j} \right) = 0 \Leftrightarrow \quad (47)$$

$$\sum_{i=1}^{n} \beta_i \frac{\sum_{j \in S_{mix}} F_j \left(C_{i,j}^{in} - C_i^0 \right)}{\sum_{j \in S_{mix}} F_j} = 0 \Leftrightarrow \sum_{i=1}^{n} \sum_{j \in S_{mix}} \frac{F_j \beta_i \left(C_{i,j}^{in} - C_i^0 \right)}{\sum_{j \in S_{mix}} F_j} = 0 \Leftrightarrow \quad (48)$$

$\sum_{j \in S_{mix}} \frac{F_j}{\sum_{j \in S_{mix}} F_j} \sum_{i=1}^{n} \beta_i \left(C_{i,j}^{in} - C_i^0 \right) = 0$, which is true since $\sum_{i=1}^{n} \beta_i \left(C_{i,j}^{in} - C_i^0 \right) = 0 \ \forall j \in S_{mix}$.

For the Splitting operation it holds $C_i^{in} = C_{i,j}^{out} \ \forall i = 1, n \ \forall j \in S_{split}$ where S_{split} is the index set of the splitting operation's outlet streams. Then $\sum_{i=1}^{n} \beta_i \left(C_{i,j}^{out} - C_i^0 \right) = 0 \ \forall j \in S_{split}$,

since $\sum_{i=1}^{n} \beta_i \left(C_i^{in} - C_i^0 \right) = 0$. O.E.Δ.

Proposition 2.

Consider the RTD reactor network illustrated in Figure 1, for a system with N_I network inlet streams, N_O network outlet streams and n components. Under steady-state, homogeneous, isothermal, and constant-density conditions, and under the assumptions that the all network concentrations are bounded and the sum of all network flows is finite, the following holds, Eq. (49):

$$\sum_{i=1}^{N_O} C_k^O(i) F^O(i) - \sum_{i=1}^{N_I} C_k^I(i) F^I(i) = \sum_{i=1}^{\infty} \left(C_k^{\hat{O}}(i) - C_k^{\hat{I}}(i) \right) F^{\hat{I}}(i) \quad \forall k = 1,...,n \tag{49}$$

Proof:

From the governing equations of the aforementioned reactor network, the following holds $\forall k = 1,...,n$:

$$\sum_{i=1}^{N_O} C_k^O(i) F^O(i) = \sum_{i=1}^{N_O} \left(\sum_{j=1}^{N_I} C_k^I(j) F^{OI}(i,j) + \sum_{j=1}^{\infty} C_k^{\hat{O}}(j) F^{O\hat{O}}(i,j) \right) \tag{50}$$

$$\sum_{i=1}^{N_I} C_k^I(i) F^I(i) = \sum_{i=1}^{N_I} C_k^I(i) \left(\sum_{j=1}^{N_O} F^{OI}(j,i) + \sum_{j=1}^{\infty} F^{\hat{I}I}(j,i) \right) \tag{51}$$

$$\begin{aligned} &\sum_{i=1}^{\infty} \left(C_k^{\hat{O}}(i) - C_k^{\hat{I}}(i) \right) F^{\hat{I}}(i) = \sum_{i=1}^{\infty} C_k^{\hat{O}}(i) F^{\hat{I}}(i) - \sum_{i=1}^{\infty} C_k^{\hat{I}}(i) F^{\hat{I}}(i) = \sum_{i=1}^{\infty} C_k^{\hat{O}}(i) F^{\hat{O}}(i) - \sum_{i=1}^{\infty} C_k^{\hat{I}}(i) F^{\hat{I}}(i) = \\ &= \sum_{i=1}^{\infty} C_k^{\hat{O}}(i) \left(\sum_{j=1}^{N_O} F^{O\hat{O}}(j,i) + \sum_{j=1}^{\infty} F^{\hat{I}\hat{O}}(j,i) \right) - \sum_{i=1}^{\infty} \left(\sum_{j=1}^{N_I} C_k^I(j) F^{\hat{I}I}(i,j) + \sum_{j=1}^{\infty} C_k^{\hat{O}}(j) F^{\hat{I}\hat{O}}(i,j) \right) \end{aligned} \tag{52}$$

Then, $\forall k = 1,...,n$ it holds:

$$\sum_{i=1}^{N_O} C_k^O(i) F^O(i) - \sum_{i=1}^{N_I} C_k^I(i) F^I(i) = \sum_{i=1}^{\infty} \left(C_k^{\hat{O}}(i) - C_k^{\hat{I}}(i) \right) F^{\hat{I}}(i) \Leftrightarrow \tag{53}$$

$$\begin{aligned} &\sum_{i=1}^{N_O} \sum_{j=1}^{N_I} C_k^I(j) F^{OI}(i,j) + \sum_{i=1}^{N_O} \sum_{j=1}^{\infty} C_k^{\hat{O}}(j) F^{O\hat{O}}(i,j) - \sum_{i=1}^{N_I} \sum_{j=1}^{N_O} C_k^I(i) F^{OI}(j,i) \\ &- \sum_{i=1}^{N_I} \sum_{j=1}^{\infty} C_k^I(i) F^{\hat{I}I}(j,i) = \sum_{i=1}^{\infty} \sum_{j=1}^{N_O} C_k^{\hat{O}}(i) F^{O\hat{O}}(j,i) + \sum_{i=1}^{\infty} \sum_{j=1}^{\infty} C_k^{\hat{O}}(i) F^{\hat{I}\hat{O}}(j,i) \\ &- \sum_{i=1}^{\infty} \sum_{j=1}^{N_I} C_k^I(j) F^{\hat{I}I}(i,j) - \sum_{i=1}^{\infty} \sum_{j=1}^{\infty} C_k^{\hat{O}}(j) F^{\hat{I}\hat{O}}(i,j) \end{aligned} \tag{54}$$

Since all network concentrations are bounded, and the sum of all network flows is finite, all eight of the above double sums are absolutely convergent. Then, according to Fubini's theorem for infinite sums, the order of summation for each of these sums can be switched, since each one of them is absolutely convergent (see Theorem 8.2.2, p. 217, in Tao (2006)). Following an order switch in the first, second, third and fourth sum, careful examination reveals that the first,

second, fourth, and sixth sum is canceled by the third, fifth, seventh, and eighth sum respectively. O.E.Δ.

Having concluded our theoretical developments we now proceed to illustrate through a case study the power of the proposed approach in synthesizing globally optimal RTD reactor networks

1.6 Case Study: Minimum Volume for a Segregated Laminar Flow Reactor Network featuring a Trambouze Reaction Scheme

The goal of this case study is to illustrate the applicability of the IDEAS conceptual framework to the solution of the minimum volume problem for a RTD reactor network, with known flow pattern and normalized residence time density function (NRTd). The flow regime in each network reactor is considered to be segregated laminar flow, i.e. $S_{SFR} = \{1,...,\infty\};\ S_{MMR} = \varnothing$. Then, the normalized residence time density (NRTd) function of every network unit (SLFR) is

$$\boldsymbol{E}: \theta \to \boldsymbol{E}(\theta) = \begin{Bmatrix} 0 & if\ \ \theta < \frac{1}{2} \\ \frac{1}{2\theta^3}\ if\ \ \theta \geq \frac{1}{2} \end{Bmatrix}, \text{(Fogler, (1999))}.$$

The reactions taking place in each reactor are referred to as the Trambouze reaction scheme shown below, Eq. (55)-(58):

$$A \xrightarrow{k_1} B\ ,\ k_1 = 0.025 \frac{kmol}{m^3 \cdot s} \qquad (55)$$

$$A \xrightarrow{k_2} C\ ,\ k_2 = 0.2 \frac{1}{s} \qquad (56)$$

$$A \xrightarrow{k_3} D\ ,\ k_3 = 0.4 \frac{m^3}{kmol \cdot s} \qquad (57)$$

$$\text{where } k_2{}^2 = 4k_1k_3;\ \ \alpha = \frac{k_2}{2k_3} = 0.25 > 0 \qquad (58)$$

The reactor network inlet is $C_A^I = 1\frac{kmol}{m^3}$, $C_C^I = 0\frac{kmol}{m^3}$ and the reactor network outlet specification for species A is that $C_A^O = 0\frac{kmol}{m^3}$. In regard to the reactor network outlet specification for species C, three cases will be considered:

Case 1: $C_A^O = 0\frac{kmol}{m^3}$, C_C^O *free*

Case 2: $C_A^O = 0\frac{kmol}{m^3}$, $C_C^O \geq 0.45\ \frac{kmol}{m^3}$

Case 3: $C_A^O = 0\frac{kmol}{m^3}$, $C_C^O \leq 0.15\ \frac{kmol}{m^3}$

A model for the plug flow reactor (PFR) is first developed and then employed in deriving a RTd model for the segregated laminar flow reactor (SLFR). $C_A^{in}, C_A(\tau), C_C(\tau)$ denote the inlet concentration of A, and the outlet concentrations of A and C at residence time τ respectively. Species B and D are omitted from the model formulation, since these species' concentrations do not affect the reaction rate laws and there are no network inlet or outlet specifications involving them.

PFR Trambouze reactor model,

$$\left.\begin{cases} \dfrac{dC_A}{d\tau'} = -\left(k_1 + k_2 C_A + k_3 {C_A}^2\right), & C_A(\tau' = 0) = C_A^{in} \\ \dfrac{dC_C}{d\tau'} = k_2 C_A, & C_C(\tau' = 0) = C_C^{in} \end{cases}\right\} \underset{\alpha = \frac{k_2}{2 \cdot k_3}}{\overset{{k_2}^2 = 4k_1k_3}{\Leftrightarrow}} \tag{59}$$

$$\left.\begin{cases} \dfrac{dC_A}{d\tau'} = -k_3\left(\alpha + C_A\right)^2, & C_A(\tau' = 0) = C_A^{in} \\ \displaystyle\int_{C_c^{in}}^{C_c} dC_c' = \int_0^{\tau} k_2 C_A(\tau')\, d\tau', & C_C(\tau' = 0) = C_C^{in} \end{cases}\right\} \Leftrightarrow \tag{60}$$

$$\left\{\begin{array}{ll} \int_{C_A^{in}}^{C_A} \frac{dC_A'}{\left(\alpha + C_A'\right)^2} = -k_3 \int_0^{\tau} d\tau', & C_A\left(\tau' = 0\right) = C_A^{in} \\ C_c = C_c^{in} + \int_0^{\tau} k_2 C_A\left(\tau'\right) d\tau', & C_C\left(\tau' = 0\right) = C_C^{in} \end{array}\right\} \tag{61}$$

Since the rate of one of the reactions ($A \xrightarrow{k_1} B$) for the Trambouze reaction scheme is constant, this implies that there is a finite critical value τ_c of the residence time τ after which the reactor contains no reactant A. This critical value is equal to $\tau_c \triangleq \frac{1}{k_3} \frac{C_A^{in}}{\alpha\left(\alpha + C_A^{in}\right)} > 0$, and is identified by setting $C_A\left(\tau_c\right) = 0$. Then the above PFR model is equivalent to:

$$\left\{\begin{array}{l} C_A(\tau) = \left\{\begin{array}{ll} -\alpha + \dfrac{1}{k_3\tau + \dfrac{1}{C_A^{in} + \alpha}} & if\ \tau \le \tau_c \\ 0 & if\ \tau > \tau_c \end{array}\right\} \\ C_c(\tau) = C_c^{in} + k_2 \int_0^{\tau} C_A(\tau')\, d\tau' \end{array}\right\} \Leftrightarrow \tag{62}$$

$$\left\{\begin{array}{l} C_A(\tau) = \left\{\begin{array}{ll} -\alpha + \dfrac{1}{k_3\tau + \dfrac{1}{C_A^{in} + \alpha}} & if\ \tau \le \tau_c \\ 0 & if\ \tau > \tau_c \end{array}\right\} \\ C_c(\tau) = \left\{\begin{array}{ll} C_c^{in} + k_2 \int_0^{\tau} \left(-\alpha + \dfrac{1}{k_3\tau' + \dfrac{1}{C_A^{in} + \alpha}} \right) d\tau' & if\ \tau \le \tau_c \\ C_c^{in} + k_2 \int_0^{\tau_c} \left(-\alpha + \dfrac{1}{k_3\tau' + \dfrac{1}{C_A^{in} + \alpha}} \right) d\tau' & if\ \tau > \tau_c \end{array}\right\} \end{array}\right\} \Leftrightarrow \tag{63}$$

$$\left\{\begin{array}{l} C_A(\tau)=\left\{\begin{array}{ll} -\alpha+\dfrac{1}{k_3\tau+\dfrac{1}{C_A^{in}+\alpha}} & if\ \tau\le\tau_c \\ 0 & if\ \tau>\tau_c \end{array}\right\} \\ C_C(\tau)=\left\{\begin{array}{l} C_C^{in}-2\alpha^2k_3\tau+2\alpha\ln\left(k_3\tau\left(C_A^{in}+\alpha\right)+1\right)\ if\quad \tau\le\tau_c \\ C_C^{in}-2\alpha^2k_3\tau_c+2\alpha\ln\left(k_3\tau_c\left(C_A^{in}+\alpha\right)+1\right)\ if\ \ \tau>\tau_c \end{array}\right\} \end{array}\right\} \tag{64}$$

$$\left\{\begin{array}{l} C_A(\tau)=\left\{\begin{array}{ll} -\alpha+\dfrac{1}{k_3\tau+\dfrac{1}{C_A^{in}+\alpha}} & if\ \tau\le\tau_c \\ 0 & if\ \tau>\tau_c \end{array}\right\} \\ C_C(\tau)=\left\{\begin{array}{l} C_C^{in}-2\alpha^2k_3\tau+2\alpha\ln\left(k_3\tau\left(C_A^{in}+\alpha\right)+1\right)\ if\quad \tau\le\tau_c \\ C_C^{in}-2\alpha\dfrac{C_A^{in}}{\left(\alpha+C_A^{in}\right)}+2\alpha\ln\left(\dfrac{C_A^{in}+\alpha}{\alpha}\right)\ if\ \ \tau>\tau_c \end{array}\right\} \end{array}\right\} \tag{65}$$

PFR residence times τ less than the critical residence time τ_c, are equal to:

$$\tau=\frac{1}{k_3}\left(\frac{1}{\alpha+C_A}-\frac{1}{\alpha+C_A^{in}}\right)=\frac{1}{k_3}\frac{C_A^{in}-C_A}{\left(\alpha+C_A\right)\left(\alpha+C_A^{in}\right)}\le\tau_c=\frac{1}{k_3}\frac{C_A^{in}}{\alpha\left(\alpha+C_A^{in}\right)}>0 \tag{66}$$

Having developed the model for the PFR model, Eq. (65), the model for the segregated laminar flow reactor (SLFR) is now developed. The exit concentrations $\overline{C}_A(\tau)$ and $\overline{C}_C(\tau)$ of A and C respectively, for a reactor exhibiting segregated flow and possessing a residence time density function $E(\cdot)$ with mean residence time equal to τ is:

$$\left\{\begin{array}{l} \overline{C}_A(\tau)\triangleq\int_0^\infty C_A(t)E(t)dt \\ \overline{C}_C(\tau)\triangleq\int_0^\infty C_C(t)E(t)dt \end{array}\right\}$$ where $C_A(t)$ and $C_C(t)$ are the exit concentrations of A and C respectively, for a batch reactor with residence time equal to t.

Then for the Trambouze reaction scheme the segregated flow reactor's exit concentrations are:

$$\left\{\begin{array}{l}\overline{C}_A(\tau) \triangleq \int_0^{\tau_c}\left(-\alpha+\dfrac{1}{k_3 t+\dfrac{1}{C_A^{in}+\alpha}}\right)E(t)dt+\int_{\tau_c}^{\infty}(0)E(t)dt \\ \overline{C}_C(\tau) \triangleq \int_0^{\tau_c}\left(C_C^{in}-2\alpha^2 k_3 t+2\alpha\ln\left(k_3 t\left(C_A^{in}+\alpha\right)+1\right)\right)E(t)\,dt+ \\ +\int_{\tau_c}^{\infty}\left(C_C^{in}-2\alpha^2 k_3\tau_c+2\alpha\ln\left(k_3\tau_c\left(C_A^{in}+\alpha\right)+1\right)\right)E(t)\,dt\end{array}\right\} \quad (67)$$

The residence time density function for each segregated laminar flow reactor (SLFR) unit can be calculated from the aforementioned NRTd shared by all units and the mean residence time $\overline{t}=\tau$ of each unit which then becomes

$$E(t)=\left\{\begin{array}{l}0 \quad if\ \ t<\dfrac{\tau}{2} \\ \dfrac{\tau^2}{2t^3}\ if\ \ t\geq\dfrac{\tau}{2}\end{array}\right\}. \quad (68)$$

Then, as shown in Appendix A, the SLFR exit concentrations $\overline{C}_A(\tau)$ and $\overline{C}_C(\tau)$ are:

$$\left\{\begin{array}{l}\overline{C}_A(\tau)=\left\{\begin{array}{ll}C_A^{in}\left(1-\dfrac{\tau^2}{4\tau_c^2}\right)+k_3\dfrac{\tau}{2}\left(\dfrac{\tau}{\tau_c}-2\right)\left(C_A^{in}+\alpha\right)^2+ & \\ +k_3^2\dfrac{\tau^2}{2}\left(C_A^{in}+\alpha\right)^3\ln\left(\dfrac{\tau_c\left(k_3\left(C_A^{in}+\alpha\right)\dfrac{\tau}{2}+1\right)}{\dfrac{\tau}{2}\left(k_3\left(C_A^{in}+\alpha\right)\tau_c+1\right)}\right) & \text{if } \tau<2\tau_c \\ 0 & \text{if } \tau\geq 2\tau_c\end{array}\right\} \\ \overline{C}_C(\tau)=\left\{\begin{array}{ll}C_C^{in}+k_3\alpha\tau\left(C_A^{in}\left(1-\dfrac{\tau}{2\tau_c}\right)-\alpha\right)+2\alpha\ln\left(k_3\left(C_A^{in}+\alpha\right)\dfrac{\tau}{2}+1\right)+ & \\ +\dfrac{1}{2}\alpha\tau^2k_3^2\left(C_A^{in}+\alpha\right)^2\ln\left(\dfrac{\dfrac{\tau}{2}\left(k_3\left(C_A^{in}+\alpha\right)\tau_c+1\right)}{\tau_c\left(k_3\left(C_A^{in}+\alpha\right)\dfrac{\tau}{2}+1\right)}\right) & \text{if } \tau<2\tau_c \\ C_C^{in}-2\alpha\dfrac{C_A^{in}}{\left(\alpha+C_A^{in}\right)}+2\alpha\ln\left(\dfrac{C_A^{in}+\alpha}{\alpha}\right) & \text{if } \tau\geq 2\tau_c\end{array}\right\}\end{array}\right\} \quad (69)$$

In carrying out the IDEAS methodology, the inlet and outlet concentrations of A for an SLFR are specified, rather than the inlet concentration of A and the residence time. It is established, in Appendix B, that for given values of $C_A^{in}\geq\overline{C}_A(\tau)\geq 0$, there exists only one value of τ in the interval $(0,2\tau_c)$, that satisfies the mass balance on A in equation (69). Having developed the PFR, Eq. (65) and SLFR, Eq. (69) models for the considered case study, the IDEAS solutions for the minimum network volume problem are presented for the three aforementioned cases:

Case 1: $C_A^O=0\dfrac{kmol}{m^3}$, C_C^O *free*

A single SLFR with inlet concentration of A, $C_A^{in}=1\,kmol/m^3$, and outlet concentration of A, $C_A^{out}=0\,kmol/m^3$, has a residence time equal to $\tau=2\cdot\tau_c=\dfrac{2}{k_3}\dfrac{C_A^{in}}{\alpha\left(\alpha+C_A^{in}\right)}=16\,s$. Thus, for a

network inlet volumetric flowrate of $F^I = 1\frac{m^3}{s}$, the SLFR volume is $V = 16m^3$. This implies that the IDEAS identified minimum network volume should be at or below $16m^3$. For comparison purposes, a PFR with inlet concentration of A, $C_A^{in} = 1 kmol/m^3$, and outlet concentration of A, $C_A^{out} = 0 kmol/m^3$, has a residence time equal to $\tau = \tau_c = 8s$, and for a network inlet volumetric flowrate of $F^I = 1\frac{m^3}{s}$, the PFR volume is $V = 8m^3$. It is thus clear that the nonideal nature of the flow pattern of the SLFR leads to a doubling of the required reactor volume over the PFR, from $8m^3$ to $16m^3$, for reaction completion to occur. In fact, when the outlet concentration of A is $C_A^{out} = 0 kmol/m^3$, both the PFR and the SLFR have the same outlet concentration of C, namely $C_C^{out} = 0.4047 kmol/m^3$. The important difference is that the PFR only requires half the residence time to attain the same outlet concentration as the SLFR. The question that naturally arises then is whether a network of SLFR's with total volume lower than that of the above SLFR can yield reaction completion?(i.e. $C_A^{out} = 0 kmol/m^3$). The answer is affirmative. In fact, the obtained IDEAS solution for the minimum network volume problem, is a sequence of SLFR's whose total volume approaches that of the PFR as their number increases. The PFR and optimal SLFR sequence trajectories are close to each other in C_A, C_C space (see Figure 3). Figure 4 illustrates the IDEAS convergence characteristics as the employed concentration grid is refined.

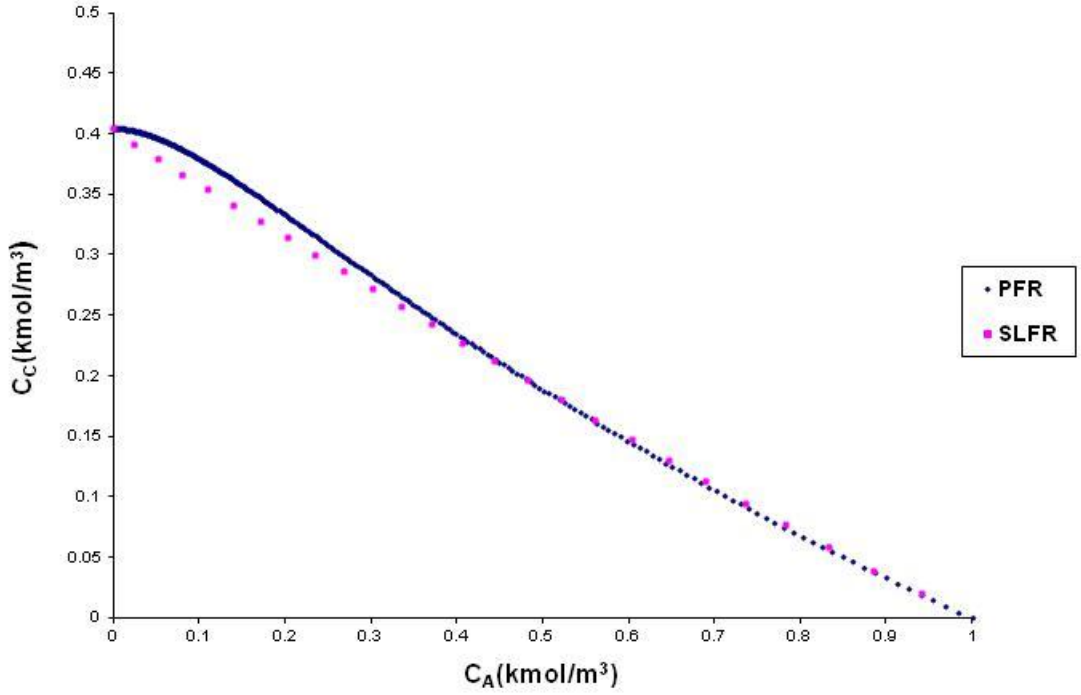

Figure 1-3 PFR and optimal SLFR sequence trajectories in space

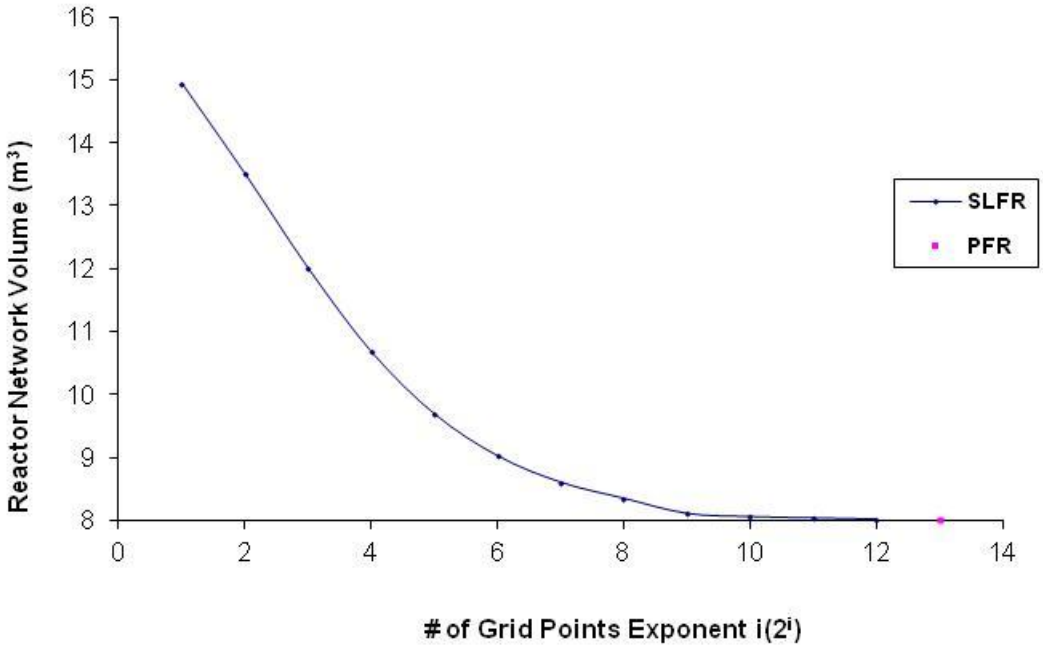

Figure 1-4 Case 1: IDEAS Optimal Sequence Convergence Behavior

Case 2: $C_A^O = 0 \frac{kmol}{m^3}$, $C_C^O \geq 0.45 \frac{kmol}{m^3}$

In this case, the obtained IDEAS minimum volume network has a different structure. For a grid size of $1/2^5 \frac{kmol}{m^3} = 1/32 \frac{kmol}{m^3}$ the obtained optimum network solution is shown in Figure 5, and the network details are summarized in Table 1.

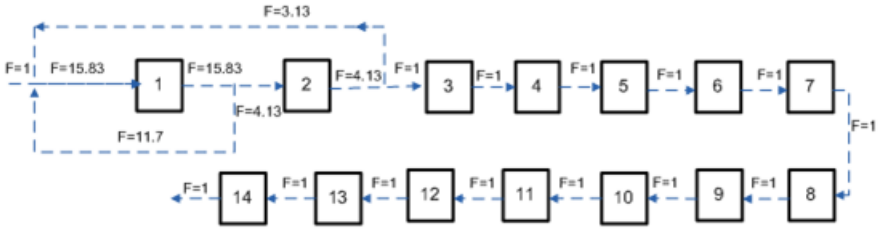

Figure 1-5 Case 2: Optimum network

Reactor #	$C_A^{in}\left(\frac{kmol}{m^3}\right)$	$C_C^{in}\left(\frac{kmol}{m^3}\right)$	$C_A^{out}\left(\frac{kmol}{m^3}\right)$	$C_C^{out}\left(\frac{kmol}{m^3}\right)$	$\tau(s)$	$V(m^3)$	$F\left(\frac{m^3}{s}\right)$
1	0.4375	0.2647	0.4063	0.2794	0.1823	2.8863	15.8300
2	0.4063	0.2794	0.3750	0.2943	0.2009	0.8304	4.1330
3	0.3750	0.2943	0.3438	0.3094	0.2225	0.2225	1.0000
4	0.3438	0.3094	0.3125	0.3248	0.2477	0.2477	1.0000
5	0.3125	0.3248	0.2813	0.3402	0.2775	0.2775	1.0000
6	0.2813	0.3402	0.2500	0.3558	0.3131	0.3131	1.0000
7	0.2500	0.3558	0.2188	0.3712	0.3559	0.3559	1.0000
8	0.2188	0.3712	0.1875	0.3865	0.4083	0.4083	1.0000
9	0.1875	0.3865	0.1563	0.4013	0.4735	0.4735	1.0000
10	0.1563	0.4013	0.1250	0.4153	0.5561	0.5561	1.0000
11	0.1250	0.4153	0.0938	0.4281	0.6642	0.6642	1.0000
12	0.0938	0.4281	0.0625	0.4389	0.8127	0.8127	1.0000
13	0.0625	0.4389	0.0313	0.4467	1.0442	1.0442	1.0000
14	0.0313	0.4467	0.0000	0.4500	2.2220	2.2220	1.0000

Table 1-1Case 2: IDEAS network information

It features a total network volume of $V = 11.1 m^3$, $C_A^{out} = 0\, kmol/m^3$, and $C_C^{out} = 0.45\, kmol/m^3$. It consists of 14 SLFR's, 12 of which are configured in a sequential manner. The network feed is mixed with some of the outlets of both the first SLFR and the second SLFR to constitute the inlet to the first SLFR. The second SLFR's inlet is simply part of the first SLFR's outlet. The remaining network is a sequence of SLFR's. Some insight into the obtained optimal design can be obtained as follows. As discussed earlier, a PFR or a SLFR whose inlet is the network feed can only deliver a

concentration of C equal to $C_C^{out} = 0.4047\, kmol/m^3$, which does not meet the specification $C_C^O \geq 0.45\ \frac{kmol}{m^3}$. Thus, IDEAS constructs a network that emulates a CSTR like behavior near the network entrance, and then a PFR like behavior near the network exit. This is consistent with the experience from the literature (Zhou and Manousiouthakis, 2008a), which suggests that the highest concentration of C is obtained by a network consisting of a CSTR followed by a PFR.

Case 3: $C_A^O = 0 \frac{kmol}{m^3}$, $C_C^O \leq 0.15\ \frac{kmol}{m^3}$

In this case, the obtained IDEAS minimum volume network has yet a different structure. For a grid size of $1/2^5 \frac{kmol}{m^3} = 1/32 \frac{kmol}{m^3}$ the obtained optimum network solution is shown in Figure 6, and the network details are summarized in Table 2.

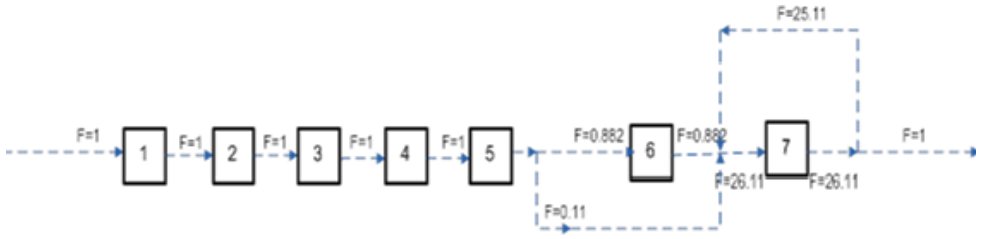

Figure 1-6 Case 3: Optimum network

Reactor #	$C_A^{in}\left(\frac{kmol}{m^3}\right)$	$C_C^{in}\left(\frac{kmol}{m^3}\right)$	$C_A^{out}\left(\frac{kmol}{m^3}\right)$	$C_C^{out}\left(\frac{kmol}{m^3}\right)$	$\tau(s)$	$V(m^3)$	$F\left(\frac{m^3}{s}\right)$
1	1.000	0.000	0.969	0.010	0.053	0.053	1.000
2	0.969	0.010	0.938	0.021	0.056	0.056	1.000
3	0.938	0.021	0.906	0.031	0.059	0.059	1.000
4	0.906	0.031	0.875	0.042	0.062	0.062	1.000
5	0.875	0.042	0.844	0.053	0.066	0.066	1.000
6	0.844	0.053	0.813	0.064	0.070	0.062	0.882
7	0.031	0.146	0.000	0.150	2.222	58.034	26.118

Table 1-2 : Case 3: IDEAS network information

It features a total network volume of $V = 58.39\,m^3$, $C_A^{out} = 0\,kmol/m^3$, and $C_C^{out} = 0.15\,kmol/m^3$. It consists of 7 SLFR's, 5 of which are configured in a sequential manner. The network feed is now processed first through a sequence of SLFR's. Then a stream bypass and a large self-recycle is employed to emulate a CSTR like behavior near the network exit. This again is consistent with the experience from the literature (Zhou and Manousiouthakis, 2008a), which suggests that the lowest concentration of C ($C_C^{out} = 0\ kmol/m^3$) can be obtained by a single large residence time ($\tau = 40\ s$) CSTR. IDEAS creates first a PFR like structure to reduce A without using too high a network volume, and then a CSTR like structure that avoids generating C, albeit at the cost of increased residence time.

1.7 Discussion-Conclusions

The synthesis of globally minimum volume reactor networks, featuring segregated flow reactor (SFR) and/or maximum mixedness reactor (MMR) units, with the same normalized residence time density (NRTd) function, was considered for the first time in this work. It was shown that the input-output information maps of SFR and MMR units with general RTd/RTD models satisfy all properties required for the application of the Infinite DimEnsionAl State-space (IDEAS) approach to the aforementioned synthesis problem. The resulting mathematical formulation is linear, thus guaranteeing the optimality of the obtained solution. The formulation was shown to possess two properties that facilitate the problem's solution. The first property suggests that if the reaction scheme possesses a reaction invariant Waller et al. (1981), then the inlet and outlet concentrations of SFR and MMR units with general RTd/RTD models, and of their networks, exhibit the same linear relation as that defined by the reaction invariant. It is important also to note that for MMR units this property is only established under the assumption that the reactor's Intensity Function satisfies the condition $\Lambda(\infty) > 0$. The second property suggests that the difference between the outlet and inlet component flowrates for a reactor network featuring general RTd/RTD units, is equal to the sum, over all network reactors, of the difference between the outlet and inlet flowrates of that same component for each reactor. This property again allows network outlet performance specifications imposed on various component concentrations to be expressed in terms of concentration differences of that same component in all units of the reactor network.

The power of the proposed globally optimal network synthesis methodology was demonstrated on three case studies featuring segregated laminar flow reactors in which the Trambouze reaction scheme is carried out. What is remarkable is that depending on a single component outlet specification, the structure of the optimal network is completely altered. Indeed, when the exit

concentration is free, then the optimum network is a sequence of SLFR units. The minimum volume of the SLFR sequence approaches the volume of a single PFR ($V = 8m^3$), which in turn is half of the volume of a single SLFR ($V = 16m^3$), that has the same exit concentrations for both components A and C as the single PFR. When the specification on the outlet concentration of C is that it be high, then IDEAS identifies a SLFR network structure that attempts to emulate a network of ideal reactors (CSTR followed by PFR) that is known from the literature to attain high concentrations of C. Finally, when the specification on the outlet concentration of C is that it be low, then IDEAS identifies a completely different SLFR network structure. The identified network consists of a sequence of SLFR's followed by two reactors that exhibit by passing and significant recycling. This optimal network structure can be understood as follows: A single PFR (CSTR) with inlet concentrations of A and C, $C_A^{in} = 1 kmol/m^3$, $C_C^{in} = 0 kmol/m^3$, and $V = 8m^3$ ($V = 40m^3$)has outlet concentrations $C_A^{out} = 0 kmol/m^3$, $C_C^{out} = 0.4047 kmol/m^3$ ($C_A^{out} = 0 kmol/m^3$, $C_C^{out} = 0.4047 kmol/m^3$). This suggests that low C concentrations require CSTR use, while low reactor volumes for a given A concentration change require PFR use. As discussed earlier a sequence of SLFR's approximates the behavior of a PFR as well as the volume of a PFR, and closely follows the PFR trajectory in concentration space. On the other hand a SLFR with significant recycling approximates the behavior of CSTR. Since only SLFR units are available, IDEAS creates first a PFR like structure (SLFR sequence) to reduce A without using too high a network volume and without raising the concentration of C excessively. It then creates a CSTR like structure (SLFR's with recycling) that avoids generating C, albeit at the cost of increased residence time.

1.8 Appendix A.1

The exit concentrations $\overline{C}_A(\tau)$ and $\overline{C}_C(\tau)$ of an SLFR, in which the Trambouze reaction scheme is carried out, are:

$$\left\{\begin{array}{l}\overline{C}_A(\tau)=\left\{\begin{array}{ll}\displaystyle\int_{\frac{\tau}{2}}^{\tau_c}\left(-\alpha+\frac{C_A^{in}+\alpha}{k_3\left(C_A^{in}+\alpha\right)t+1}\right)\frac{\tau^2}{2t^3}dt & if\ \ \tau<2\tau_c\\ 0 & if\ \ \tau\geq 2\tau_c\end{array}\right\}\\ \overline{C}_C(\tau)=\left\{\begin{array}{l}\dfrac{\tau^2}{2}\displaystyle\int_{\frac{\tau}{2}}^{\tau_c}\left[C_C^{in}-2\alpha^2k_3t+2\alpha\ln\left(k_3t\left(C_A^{in}+\alpha\right)+1\right)\right]t^{-3}dt+\\ +\dfrac{\tau^2}{2}\left[C_C^{in}-2\alpha^2k_3\tau_c+2\alpha\ln\left(k_3\tau_c\left(C_A^{in}+\alpha\right)+1\right)\right]\displaystyle\int_{\tau_c}^{\infty}t^{-3}dt \quad if\ \ \dfrac{\tau}{2}<\tau_c\\ \dfrac{\tau^2}{2}\left[C_C^{in}-2\alpha^2k_3\tau_c+2\alpha\ln\left(k_3\tau_c\left(C_A^{in}+\alpha\right)+1\right)\right]\displaystyle\int_{\frac{\tau}{2}}^{\infty}t^{-3}dt \quad if\ \ \dfrac{\tau}{2}\geq\tau_c\end{array}\right\}\end{array}\right\}\Leftrightarrow \text{Eq. (A.1)}$$

$$\left\{\begin{array}{l}\overline{C}_A(\tau)=\left\{\begin{array}{ll}-\dfrac{\alpha\tau^2}{2}\cdot\dfrac{t^{-2}}{-2}\Big|_{\frac{\tau}{2}}^{\tau_c}+\dfrac{\tau^2}{2}\cdot\left(C_A^{in}+\alpha\right)\displaystyle\int_{\frac{\tau}{2}}^{\tau_c}\frac{1}{\left(k_3(C_A^{in}+\alpha)t+1\right)t^3}dt & if\ \ \tau<2\tau_c\\ 0 & if\ \ \tau\geq 2\tau_c\end{array}\right\}\\ \overline{C}_C(\tau)=\left\{\begin{array}{l}\dfrac{\tau^2}{2}C_C^{in}\dfrac{t^{-2}}{-2}\Big|_{\frac{\tau}{2}}^{\tau_c}+\dfrac{\tau^2}{2}\left(-2\alpha^2k_3\right)\dfrac{1}{-t}\Big|_{\frac{\tau}{2}}^{\tau_c}+\dfrac{\tau^2}{2}\left(2\alpha\right)\displaystyle\int_{\frac{\tau}{2}}^{\tau_c}\ln\left(k_3t\left(C_A^{in}+\alpha\right)+1\right)t^{-3}dt+\\ +\dfrac{\tau^2}{2}\left[C_C^{in}-2\alpha^2k_3\tau_c+2\alpha\ln\left(k_3\tau_c\left(C_A^{in}+\alpha\right)+1\right)\right]\dfrac{1}{-2t^2}\Big|_{\tau_c}^{\infty} \quad if\ \ \dfrac{\tau}{2}<\tau_c\\ \dfrac{\tau^2}{2}\left[C_C^{in}-2\alpha^2k_3\tau_c+2\alpha\ln\left(k_3\tau_c\left(C_A^{in}+\alpha\right)+1\right)\right]\dfrac{1}{-2t^2}\Big|_{\frac{\tau}{2}}^{\infty} \quad if\ \ \dfrac{\tau}{2}\geq\tau_c\end{array}\right\}\end{array}\right\}\ \text{Eq. (A.2)}$$

Let $A\triangleq k_3(C_A^{in}+\alpha)$. Then

$$\frac{1}{\left(At+1\right)t^3}=\frac{-A^3}{\left(At+1\right)}+\frac{1}{t^3}+\frac{-A}{t^2}+\frac{A^2}{t}\Rightarrow \qquad \text{Eq. (A.3)}$$

$$\int_{\frac{\tau}{2}}^{\tau_c} \frac{1}{(At+1)t^3}\,dt = A^2 \ln\left(\frac{\tau_c\left(A\frac{\tau}{2}+1\right)}{\frac{\tau}{2}(A\tau_c+1)}\right) - \frac{1}{2}\left(\frac{1}{\tau_c^2}-\frac{4}{\tau^2}\right) + A\left(\frac{1}{\tau_c}-\frac{2}{\tau}\right) \qquad \text{Eq. (A.4)}$$

Similarly,

$$\int_{\frac{\tau}{2}}^{\tau_c} \ln\left(k_3\left(C_A^{in}+\alpha\right)t+1\right)t^{-3}dt =$$

$$\int_{\frac{\tau}{2}}^{\tau_c} \ln(At+1)t^{-3}dt = \left[\frac{1}{2}A^2\ln\left(\frac{At+1}{t}\right) - \frac{1}{2t^2}\ln(At+1) - \frac{A}{2t}\right]_{\frac{\tau}{2}}^{\tau_c} \qquad \text{Eq. (A.5)}$$

Then

$$\left\{\begin{array}{l} \overline{C}_A(\tau) = \left\{\begin{array}{l} -\alpha + \frac{\alpha\tau^2}{4\tau_c^{\,2}} - \frac{\tau^2}{4}\cdot\left(C_A^{in}+\alpha\right)\left(\frac{1}{\tau_c^2}-\frac{4}{\tau^2}\right) \\ +\frac{\tau^2}{2}\cdot\left(C_A^{in}+\alpha\right)\left[A^2\ln\left(\frac{\tau_c\left(A\frac{\tau}{2}+1\right)}{\frac{\tau}{2}(A\tau_c+1)}\right) + A\left(\frac{1}{\tau_c}-\frac{2}{\tau}\right)\right] \quad if\ \ \tau < 2\tau_c \\ 0 \qquad\qquad if\ \ \tau \geq 2\tau_c \end{array}\right\} \\ \overline{C}_C(\tau) = \left\{\begin{array}{l} \frac{\tau^2}{2}C_c^{in}\left(\frac{1}{-2\tau_c^{\,2}}-\frac{2}{-\tau^2}\right) - \alpha^2 k_3\tau^2\left(\frac{1}{-\tau_c}-\frac{2}{-\tau}\right) - \alpha\tau^2\left(\frac{A}{2\tau_c}-\frac{A}{\tau}\right) + \\ +\alpha\tau^2\left[\frac{1}{2}A^2\ln\left(\frac{\frac{\tau}{2}(A\tau_c+1)}{\tau_c\left(A\frac{\tau}{2}+1\right)}\right) - \left(\frac{1}{2\tau_c^{\,2}}\ln(A\tau_c+1) - \frac{2}{\tau^2}\ln\left(A\frac{\tau}{2}+1\right)\right)\right] + \\ +\frac{\tau^2}{4\tau_c^{\,2}}\left[C_C^{in} - 2\alpha^2 k_3\tau_c + 2\alpha\ln\left(k_3\tau_c\left(C_A^{in}+\alpha\right)+1\right)\right] \quad if\ \ \frac{\tau}{2} < \tau_c \\ C_C^{in} - 2\alpha^2 k_3\tau_c + 2\alpha\ln\left(k_3\tau_c\left(C_A^{in}+\alpha\right)+1\right) \quad if\ \ \frac{\tau}{2} \geq \tau_c \end{array}\right\} \end{array}\right\} \Leftrightarrow$$

$$\left\{ \begin{array}{l} \overline{C}_A(\tau) = \left\{ \begin{array}{ll} C_A^{in}\left(1-\dfrac{\tau^2}{4\tau_c^2}\right)+k_3\dfrac{\tau}{2}\left(\dfrac{\tau}{\tau_c}-2\right)\left(C_A^{in}+\alpha\right)^2+ & \\ +k_3^2\dfrac{\tau^2}{2}\left(C_A^{in}+\alpha\right)^3\ln\left(\dfrac{\tau_c\left(k_3\left(C_A^{in}+\alpha\right)\dfrac{\tau}{2}+1\right)}{\dfrac{\tau}{2}\left(k_3\left(C_A^{in}+\alpha\right)\tau_c+1\right)}\right) & if\ \ \tau<2\tau_c \\ 0 & if\ \ \tau\geq 2\tau_c \end{array} \right. \\ \overline{C}_C(\tau) = \left\{ \begin{array}{ll} C_C^{in}+k_3\alpha\tau\left(C_A^{in}\left(1-\dfrac{\tau}{2\tau_c}\right)-\alpha\right)+2\alpha\ln\left(k_3\left(C_A^{in}+\alpha\right)\dfrac{\tau}{2}+1\right)+ & \\ +\dfrac{1}{2}\alpha\tau^2k_3^2\left(C_A^{in}+\alpha\right)^2\ln\left(\dfrac{\dfrac{\tau}{2}\left(k_3\left(C_A^{in}+\alpha\right)\tau_c+1\right)}{\tau_c\left(k_3\left(C_A^{in}+\alpha\right)\dfrac{\tau}{2}+1\right)}\right) & if\ \ \tau<2\tau_c \\ C_C^{in}-2\alpha\dfrac{C_A^{in}}{\left(\alpha+C_A^{in}\right)}+2\alpha\ln\left(\dfrac{C_A^{in}+\alpha}{\alpha}\right) & if\ \ \tau\geq 2\tau_c \end{array} \right. \end{array} \right\} \text{Ο.Ε.Δ.}$$

1.9 Appendix B.1

In carrying out the IDEAS methodology, the inlet and outlet concentrations of A for an SLFR are specified, rather than the inlet concentration of A and the residence time. It is established below that for given values of $C_A^{in} \geq \overline{C}_A(\tau) \geq 0$, there exists only one value of τ in the interval $(0, 2\tau_c)$, that satisfies the mass balance equation below.

$$\overline{C}_A(\tau) = C_A^{in}\left(1-\frac{\tau^2}{4\tau_c^2}\right) + k_3\frac{\tau}{2}\left(\frac{\tau}{\tau_c}-2\right)\left(C_A^{in}+\alpha\right)^2 + k_3^2\frac{\tau^2}{2}\left(C_A^{in}+\alpha\right)^3 \ln\left(\frac{\tau_c\left(k_3\left(C_A^{in}+\alpha\right)\frac{\tau}{2}+1\right)}{\frac{\tau}{2}\left(k_3\left(C_A^{in}+\alpha\right)\tau_c+1\right)}\right) \text{ and}$$

$\tau_c \triangleq \dfrac{C_A^{in}}{k_3\alpha\left(C_A^{in}+\alpha\right)}$. Define

$$\begin{aligned}
A &\triangleq -\frac{C_A^{in}}{4\tau_c^2} + \frac{k_3}{2\tau_c}\left(C_A^{in}+\alpha\right)^2 = \frac{k_3^{\,2}\alpha\left(C_A^{in}+\alpha\right)^2}{4C_A^{in}}\left(2C_A^{in}+\alpha\right) > 0 \\
B &\triangleq -k_3\left(C_A^{in}+\alpha\right)^2 < 0 \\
C &\triangleq \frac{k_3^{\,2}}{2}\left(C_A^{in}+\alpha\right)^3 > 0 \\
D &\triangleq \frac{k_3\left(C_A^{in}+\alpha\right)\tau_c}{k_3\left(C_A^{in}+\alpha\right)\tau_c+1} = \frac{C_A^{in}}{C_A^{in}+\alpha} \in (0,1) \\
E &\triangleq \frac{2\tau_c}{k_3\left(C_A^{in}+\alpha\right)\tau_c+1} = \frac{2C_A^{in}}{k_3\left(C_A^{in}+\alpha\right)^2} > 0 \\
F &\triangleq C_A^{in} - \overline{C}_A(\tau) > 0
\end{aligned} \qquad \text{Eq. (B.1)}$$

The quantities $E^2C^2 + BECD$, and $D + \dfrac{E}{2\tau_c}$ needed later can then be calculated as:

$$E^2C^2 + BECD = \left(\frac{2\tau_c}{k_3\left(C_A^{in}+\alpha\right)\tau_c+1}\right)^2\left(\frac{{k_3}^2}{2}\left(C_A^{in}+\alpha\right)^3\right)^2 +$$

$$+\left(-k_3\left(C_A^{in}+\alpha\right)^2\left(\frac{2\tau_c}{k_3\left(C_A^{in}+\alpha\right)\tau_c+1}\right)\right)\left(\frac{{k_3}^2}{2}\left(C_A^{in}+\alpha\right)^3\right)\left(\frac{k_3\left(C_A^{in}+\alpha\right)\tau_c}{k_3\left(C_A^{in}+\alpha\right)\tau_c+1}\right)=0 \qquad \text{Eq. (B.2)}$$

$$D+\frac{E}{2\tau_c}=\frac{k_3\left(C_A^{in}+\alpha\right)\tau_c}{k_3\left(C_A^{in}+\alpha\right)\tau_c+1}+\frac{\overline{2\tau_c}}{\overline{k_3\left(C_A^{in}+\alpha\right)\tau_c+1}}=1 \qquad \text{Eq. (B.3)}$$

Then the above equation can be written as $f(\tau)=0$, where

$f:\mathbb{R}^+\to\mathbb{R},\quad f:\tau\to f(\tau)\triangleq A\tau^2+B\tau+C\tau^2\ln\left[D+\frac{E}{\tau}\right]+F$ However, it holds:

$$\lim_{\tau\to0^+} f(\tau)\triangleq\lim_{\tau\to0^+}\left(A\tau^2+B\tau+C\tau^2\ln\left[D+\frac{E}{\tau}\right]+F\right)=$$

$$=F+C\frac{\lim_{\tau\to0^+}\ln\left[D+\frac{E}{\tau}\right]}{\lim_{\tau\to0^+}\frac{1}{\tau^2}}=F+C\frac{\lim_{\tau\to0^+}\left[D+\frac{E}{\tau}\right]^{-1}\left(-\frac{E}{\tau^2}\right)}{\lim_{\tau\to0^+}\frac{(-2)}{\tau^3}}=F+C\lim_{\tau\to0^+}\frac{E\tau^2}{2\left[D\tau+E\right]}=CE\cdot\infty>0$$

$$f(2\tau_c)\triangleq A(2\tau_c)^2+B2\tau_c+C(2\tau_c)^2\ln\left[D+\frac{E}{2\tau_c}\right]+F=$$

$$=4\frac{{k_3}^2\alpha\left(C_A^{in}+\alpha\right)^2}{4C_A^{in}}\left(2C_A^{in}+\alpha\right)\left(\frac{C_A^{in}}{k_3\alpha\left(C_A^{in}+\alpha\right)}\right)^2-2k_3\left(C_A^{in}+\alpha\right)^2\frac{C_A^{in}}{k_3\alpha\left(C_A^{in}+\alpha\right)}+C_A^{in}-\overline{C}_A(\tau)=\text{Thus,}$$

$$=-\overline{C}_A(\tau)<0$$

to show that the equation $f(\tau)=0$ has only one real root in the interval $(0,2\tau_c)$, it is necessary and sufficient to show that $\dot{f}(\tau)\le0\ \forall\tau\in(0,2\tau_c)$.

However

$$\dot{f}(\tau) \le 0 \ \forall \tau \in (0, 2\tau_c) \Leftrightarrow 2A\tau + B + 2C\tau \ln\left[D + \frac{E}{\tau}\right] + C\tau^2 \left[D + \frac{E}{\tau}\right]^{-1} \left(\frac{-E}{\tau^2}\right) \le 0$$

$\forall \tau \in (0, 2\tau_c) \Leftrightarrow$ Define

$$\Leftrightarrow 2A\tau + B + 2C\tau \ln\left[D + \frac{E}{\tau}\right] - \frac{EC}{\left[D + \frac{E}{\tau}\right]} \le 0 \ \forall \tau \in (0, 2\tau_c)$$

$$y \triangleq D + \frac{E}{\tau} > D + \frac{E}{2\tau_c} > D > 0 \ \forall \tau \in (0, 2\tau_c) \Leftrightarrow$$ Then

$$2\tau_c > \tau = \frac{E}{y - D} > 0 \ \forall y > D + \frac{E}{2\tau_c} > D > 0$$

$$\dot{f}(\tau) \le 0 \ \forall \tau \in (0, 2\tau_c) \overset{y \triangleq D + \frac{E}{\tau} > D > 0}{\Leftrightarrow}$$ and

$$2A\frac{E}{y - D} + B + 2C\left(\frac{E}{y - D}\right) \ln y - \frac{EC}{y} \le 0 \ \forall y > D + \frac{E}{2\tau_c} > D > 0 \overset{y - D > 0}{\Leftrightarrow}$$

$$2AE - BD - EC + By + 2CE \ln y + \frac{ECD}{y} \le 0 \ \forall y > D + \frac{E}{2\tau_c} > D > 0 \text{. Then,}$$

define $$g : \left\{ y \in \mathbb{R} : y > D + \frac{E}{2\tau_c} > D > 0 \right\} \to \mathbb{R},$$

$$g : y \to g(y) \triangleq (2AE - EC - BD) + By + 2EC \ln y + \frac{ECD}{y}$$

Then $\dot{f}(\tau) \le 0 \ \forall \tau \in (0, 2\tau_c)$ $\overset{y \triangleq D + \frac{E}{\tau} > D + \frac{E}{2\tau_c} > D > 0}{\Leftrightarrow}$ $g(y) \le 0 \ \forall y > D + \frac{E}{2\tau_c} > D > 0$

$$\dot{g}(y) = B + \frac{2EC}{y} - \frac{ECD}{y^2}$$

And

$$\ddot{g}(y) = -\frac{2EC}{y^2} + \frac{2ECD}{y^3} = -\frac{2EC}{y^2}\left(1 - \frac{D}{y}\right) < 0 \ \forall y > D + \frac{E}{2\tau_c} > D > 0$$

Therefore g is a concave function in the set $\left\{ y \in \mathbb{R} : y > D + \frac{E}{2\tau_c} > D > 0 \right\}$. The supremum of g in $\left\{ y \in \mathbb{R} : y > D + \frac{E}{2\tau_c} > D > 0 \right\}$ is either at $y = D + \frac{E}{2\tau_c}$ or at a point $y = y^*$ which satisfies: $\dot{g}\left(y^*\right) = 0 \overset{y>D>0}{\Leftrightarrow} By^{*2} + 2ECy^* - ECD = 0 \Leftrightarrow$

$$y^* = \frac{-EC \pm \sqrt{E^2C^2 + BECD}}{B} \overset{E^2C^2+BECD=0}{\Leftrightarrow} y^* = \frac{-EC}{B} = \frac{k_3\left(C_A^{in} + \alpha\right)\tau_c}{k_3\left(C_A^{in} + \alpha\right)\tau_c + 1} = D \notin \left(D + \frac{E}{2\tau_c}, \infty \right).$$ Thus the supremum of g in $\left\{ y \in \mathbb{R} : y > D + \frac{E}{2\tau_c} > D > 0 \right\}$ is at $y = D + \frac{E}{2\tau_c}$ and its value is equal to

$$g\left(D + \frac{E}{2\tau_c} \right) = \left(2AE - EC - BD\right) + B\left(D + \frac{E}{2\tau_c} \right) + 2EC \ln\left(D + \frac{E}{2\tau_c} \right) + \frac{ECD}{\left(D + \frac{E}{2\tau_c} \right)} =$$

$$\left(2AE - EC - BD\right) + B + ECD = \left[\begin{array}{l} 2\frac{k_3{}^2\alpha\left(C_A^{in} + \alpha\right)^2}{4C_A^{in}}\left(2C_A^{in} + \alpha\right)\frac{2C_A^{in}}{k_3\left(C_A^{in} + \alpha\right)^2} - \\ \frac{2C_A^{in}}{k_3\left(C_A^{in} + \alpha\right)^2}\frac{k_3{}^2}{2}\left(C_A^{in} + \alpha\right)^3 - \\ \left(-k_3\left(C_A^{in} + \alpha\right)^2\right)\frac{C_A^{in}}{C_A^{in} + \alpha} \end{array} \right] - k_3\left(C_A^{in} + \alpha\right)^2 +$$

$$+ \frac{2C_A^{in}}{k_3\left(C_A^{in} + \alpha\right)^2}\frac{k_3{}^2}{2}\left(C_A^{in} + \alpha\right)^3\frac{C_A^{in}}{C_A^{in} + \alpha} = k_3\alpha\left(2C_A^{in} + \alpha\right) - k_3\left(C_A^{in} + \alpha\right)^2 + k_3\left(C_A^{in}\right)^2 = 0$$ In turn this implies $g\left(y\right) \le 0 \ \forall y > D + \frac{E}{2\tau_c} > D > 0$ which, under the condition $y \triangleq D + \frac{E}{\tau} > D + \frac{E}{2\tau_c} > D > 0$, is equivalent to $\dot{f}\left(\tau\right) \le 0 \ \forall \tau \in \left(0, 2\tau_c\right)$. Therefore, the equation $f\left(\tau\right) = 0$ has only one real root in the interval $\left(0, 2\tau_c\right)$. O.E.Δ.

Acknowledgments

Financial support from the U.S. National Science Foundation under grant #CTS-0829211 and Aramco Oil Company R&D is gratefully acknowledged.

1.10 References

Abraham TK, Feinberg M. Kinetic bounds on attainability in the reactor synthesis problem. Industrial & engineering chemistry 2004; 43(2): 449-457.

Burri JF, Wilson SD, Manousiouthakis V. Infinite DimEnsionAl State-Space approach to reactor network synthesis: Application to attainable region construction. Computers & Chemical Engineering 2002; 16(6): 849-862.

Danckwerts PV. Continuous flow systems distribution of residence times. Chemical Engineering Science 1953; 2(1): 1-13.

Danckwerts PV. Local residence times in continuous flow systems. Chemical Engineering Science 1958; 9(1): 78-79.

Drake JE, Manousiouthakis V. IDEAS approach to process network synthesis: minimum plate area for complex distillation networks with fixed utility cost. Industrial & Engineering Chemistry Research 2002a; 41(20): 4984-4992.

Drake JE, Manousiouthakis V. IDEAS approach to process network synthesis: minimum utility cost for complex distillation networks. Chemical Engineering Science 2002b; 57(15): 3095-3106.

Fogler HS. Elements of Chemical Reaction Engineering. 3rd ed. Prentice Hall; 1999.

Fogler HS. Elements of Chemical Reaction Engineering. 4th ed. Prentice Hall; 2006.

Gao Y, Vanarase A, Muzzio F, Ierapetritou M. Characterizing continuous powder mixing using residence time distribution. Chemical Engineering Science 2010; 66: 417-425.

Gilbilaro, LG. Residence time distributions in regions of continuous flow systems. Chemical Engineering Science 1977; 34(5): 697–702.

Glasser D, Hildebrandt D, Godorr S. The attainable region for segregated, maximum mixed, and other reactor models. Industrial & Engineering Chemistry 1994; 33(5): 1136-1144.

Himmelblau DM, Bischoff KB. Process analysis and simulation. New York; 1968.

Hocine S, Pibouleau L, Azzaro-Pantel C, Domenech S. Modelling systems defined by RTD Curves. Computers & Chemical Engineering 2008; 32(12): 3112-3120.

Justanieah A, Manousiouthakis V, Taylor L. The Shrink–Wrap algorithm for the construction of the attainable region: an application of the IDEAS framework. Computers & Chemical Engineering 2004; 28(9):1563–1575.

Kauchali S, Rooney WC, Biegler LT, Glasser D, Hildebrandt D. Linear programming formulations for attainable region analysis. Chemical Engineering Science 2002; 57(11):2015-2028

MacMullin RB, Weber M. The theory of short-circuiting in continuous-flow mixing vessels in series and kinetics of chemical reactions in such systems. Transactions of The American Institute of Chemical Engineers 1935; 31(2): 409-458

Nauman EB, Buffham BA. Mixing in Continuous Flow Systems. New York: Wiley; 1974.

Nauman EB. Residence time theory, Ind. Eng. Chem. Res. 2008; 47: 3752-3766.

Tao T. Analysis I. Hindustan Book Agency. New Delhi: India; 2006.

Waller KV, Makila PM. Chemical reaction invariants and variants and their use in reactor modeling, simulation, and control. Industrial & Engineering Chemistry Process Design and Development. 1981; 20.1: 1-11.

Wilson S, Manousiouthakis V. IDEAS approach to process network synthesis: application to multicomponent (MEN). AIChE J, 2000; 46: 2408-2416.

Zhou W, Manousiouthakis V. Global capital/total annualized cost minimization of homogeneous and isothermal reactor networks. Industrial & Engineering Chemistry Research 2008a; 47(10): 3771-3782.

Zhou W, Manousiouthakis V. On dimensionality of attainable region construction for isothermal reactor networks. Computers & Chemical Engineering 2008b; 32(3): 439-450.

Zhou W, Manousiouthakis V. Non-ideal reactor network synthesis through IDEAS: Attainable region construcion. Chemical Engineering Science 2006; 61(21): 6936-6945.

Zwitering TN. The Degree of mixing continuous flow systems. Chemical Engineering Science 1959; 11(1):1-15.

Chapter 2

2 Network Residence Time Constrained Attainable Region (TRT-C-AR)

Zayna Al-Husseini, Vasilios I. Manousiouthakis*
Chemical and Biomolecular Engineering Department
University of California at Los Angeles, Los Angeles, CA 90095, USA

*To whom all correspondence should be addressed

Abstract

In this work, the concept of Network Residence Time (NRT) is first defined, as a production normalized, capital cost measure for a reactor network. For networks consisting of CSTR's, PFR's, and RTD-Segregated Flow/Maximum Mixedness Reactors, described within the Infinite DimEnsionAl State-space (IDEAS) conceptual framework, it is shown that NRT is independent of the network's inlet flowrate. The novel concept of Network Residence Time Constrained Attainable Region (NRT-C-AR) for Reactor Networks is then introduced. NRT-C-AR is shown to be a convex set, points on the boundary of which are identified through repeated solution of increasingly accurate finite linear program (FLP) approximations of infinite linear programs (ILP). The proposed NRT-C-AR construction methodology is demonstrated on a case study featuring a network of reactors in which the Trambouze reaction scheme is carried out. Three NRT-C-AR's are created: one for CSTR's, one for PFR's, and one for SLFR's. Important differences between the NRT-C-AR and the AR are pointed out. A network of SLFR's whose outlet composition is on the SLFR NRT-C-AR boundary is provided to help emphasize some of these differences.

Keywords: Reactor Network; Attainable Region; Network Residence Time; Network Volume; IDEAS

Abbreviations:

CSTR, continuous stirred tank reactor; NRT, Network Residence Time; NRT-C-AR, Network Residence Time Constrained Attainable Region; DN, distribution network; IDEAS, Infinite DimEnsionAl State-space; ILP, infinite-dimensional linear program; FLP, finite linear program; MINLP, mixed-integer nonlinear program; MMR, Maximum Mixedness Reactor; NRTd, normalized residence time density function; OP, operator network; PFR, plug flow reactor; RTd, Residence time density; RTD, residence time distribution; SFR, Segregated Flow Reactor; SLFR, Segregated Laminar Flow Reactors; SR, Segregated Reactor.

2.1 Introduction

Horn (1964) was the first to propose the concept of AR. He defined it as: "the attainable region corresponds to the totality of physically possible reactors" (Horn, pg. 123). Later, Shinnar and Feng (1985) defined the AR as, "the set of composition reachable from a specified initial condition given a set of overall reactions" (Shinnar and Feng, pg. 154). Glasser et al. defined the AR stating: "For a given system of reactions with given reaction kinetics, find all possible concentrations that can be achieved by using any system of steady-flow chemical reactors, that is, by using the processes of mixing and reaction only" Glasser, et al. (1987). Manousiouthakis et al, (2004) defined the AR by stating: "For a specified feed and specified set of reactions, the attainable region is the set of all reactor network outlet concentrations that can be attained by means of all feasible reactor networks".

The aforementioned work of Glasser et al. (1987) established four necessary conditions that the AR must satisfy:

"(a) It is convex.

(b) No rate vector in the boundary of A (∂A) points outward from A; that is, all rate vectors in ∂A points inward, are tangent to ∂A, or are zero.

(c) There is no plug-flow trajectory in the complement of A (within the stoichiometric subspace), which has two points such that the line joining the later to the earlier point can be extended to intersect A.

(d) No negative of a rate vector in the complement of A (within the stoichiometric subspace), when extended, can intersect a point of ∂A or (A)."

The aforementioned work also presented a geometrically based construction algorithm to produce two and three-dimensional candidate AR's, through the use of PFR trajectories and CSTR loci. This geometric method was adopted by numerous researchers for reactor, reactive separation, and reactive distillation network synthesis (Feinberg, 1991, 1999, 2000a, b; Feinberg and Hildebrant, 1997; Glasser, et al. 1994; Hildebrant, Glasser, et al. 1999; Hoply et al. 1996; Nisoli, Malone and Doherty, 1997; Smith and Melone, 1997; Rooney and Biegler, 2000; Mahajani et al (most recent) and references therein). However, the geometric approach method does not guarantee to identify the true AR.

Burri et al. (2002) proposed an alternative approach to the construction of the AR for reactor networks, through the "Infinite Dimensional State-space (IDEAS)". They formulated an "Infinite dimensional Linear Program (ILP)" whose solution would identify a point in concentration space belonging to the AR boundary. They then proposed the solution of a sequence of "Finite dimensional Linear Programs (FLP)" to construct increasingly accurate approximations of the

true AR. Subsequently, Manousiouthakis et al. (2004) presented necessary and sufficient conditions for a point in concentration space to belong to the true AR, and then proposed a so-called shrink-wrap algorithm that also delivered increasingly accurate approximations of the true AR, without requiring the solution of a sequence of FLP. This method also overcame the difficulty of graphical visualization of the AR, by identifying the vertices of increasingly accurate AR approximants, a task that can be accomplished in dimensions higher than three. Kauchali et al. (2002) presented another alternative IDEAS formulation to extend the AR using CSTR's only. Abraham and Feinberg (2004) presented a critical condition for a region to be part of the true AR. Posada and Manousiouthakis (2008) implemented the Shrink–Wrap algorithm for multi-feed AR construction in mass fraction space.

The above AR studies employed ideal reactor models (PFR/CSTR). However, commonly used non-ideal models were also investigated for finding the AR. Glasser et al. (1994) studied the attainable region for segregated flow reactor (SFR) and maximum mixed reactor (MMR) models and showed, for an example, that the conversions attained by these reactor models do not represent conversion bounds for all reactor models. In fact, they showed that the SR and MMR attainable region boundaries lie within the attainable region. Zhou and Manousiouthakis (2006) showed that the AR for a reactor network whose nonideal reactor units admit 1-dimensional convection-axial dispersion-reaction models is larger than the AR for an ideal reactor network featuring CSTR's and PFR's. Alhusseini and Manousiouthakis (2013) carried out the global minimization of network volume for a network of reactor units all of which exhibit segregated flow (SFR) and/or maximum mixedness (MMR), have the same Normalized Residence Time density (NRTd), but each possesses a different mean residence time from one another.

Other researchers have investigated the AR concept in relation to reactive distillation and other applications. The work of Amte et al. (2011) on reactive distillation is an example. They suggest that reactive distillation is useful in enhancing reactor selection. This is because it facilitates the delineation of components and alters their composition profiles to generate the anticipated reaction. The researchers adopt a geometric method to determine the AR, for networks that include some RD (reactive distillation) configurations. They define novel RD models together with their corresponding components to highlight the need to link RD with reactors and expand the set of attainable compositions. For a case study involving the Van de Vusse reaction scheme, they establish that the RD unit networks are more effective than the traditional reactor networks. Katubilwa et al. (2011) present, using a theoretical perspective, an analysis of the ball diameter impact on milling kinetics with the aid of the AR technique. Zhou and Manousiouthakis (2007) employ the AR concept in carrying out pollution prevention studies. In addition, Okonye, et al. (2012) investigate the interplay between the AR and enthalpy/free energy concepts. More resently, Ghougassian and Manousiouthakis (2013) established conditions under which entropy generation and energy consumption isoclines can be depicted within a reactor network's AR without prior commitment to a reactor network structure.

Since reactor design is never carried out in a bubble, cost must be a crucial factor in the reactor design process. Reactor network capital cost is typically correlated to the volume of all the reactors present in the network. Research efforts in the direction of incorporating capital cost considerations in reactor network design have focused on the global minimization of capital cost/total annualized cost for CSTR/PFR networks (Zhou and Manousiouthakis, 2008) and the global minimization of total reactor volume for networks of RTD-SFR/RTD-MMR non-ideal reactors (Alhusseini and Manousiouthakis , 2013). Since the AR is a significant tool in reactor

network design studies, it is desirable that capital cost (volume) be incorporated in AR construction. Since a reactor network's volume is inlet flowrate dependent, while the AR is inlet flowrate independent, the novel concept of "Network Residence Time" is next introduced to allow for the incorporation of capital cost considerations in AR construction. Peter et al. (2003).

Definition

The concept of "Network Residence Time" (NRT) for a reactor network is defined as the ratio of the sum of the volumes of all reactors participating in the reactor network over the total volumetric flowrate entering the network.

Having introduced the NRT concept, the remainder of this work proceeds as follows: The applicability of IDEAS to synthesis problems for reactor networks featuring CSTR/PFR/RTD-SFR/RTD-MMR reactor units is briefly reviewed. Subsequently, the Network Residence Time Constrained Attainable Region (NRT-C-AR) concept is introduced, and the Infinite Dimensional State-space (IDEAS) framework is employed to develop a general mathematical formulation for the construction of NRT-C-AR. Properties of NRT-C-AR are then theoretically established. A case study is used to illustrate NRT-C-AR construction for CSTR/PFR/RTD-SFR networks. Finally, the obtained results are discussed and conclusions are drawn.

2.2 Applicability of IDEAS to CSTR, PFR, RTD-SFR, RTD-MMR Reactor Networks

The IDEAS conceptual framework has been proposed by Manousiouthakis and coworkers as a globally optimal network synthesis methodology. Its advantage over other process network optimization methodologies is that it guarantees the global optimality of the obtained solution. The reasons are that the underlying mathematical programming formulations have feasible regions defined by linear constraints and that many industrially meaningful optimization objectives (volume, operating cost, area, yield, selectivity, plate area, holdup, etc.) give rise to

linear objective functions, thus making the underlying mathematical formulations linear programs. The methodology has been demonstrated on a number of applications, such as mass exchange network synthesis, Wilson and Manousiouthakis (2000); distillation network synthesis, Drake and Manousiouthakis (2002a, 2002b); reactor network synthesis featuring ideal reactor units, namely PFR and CSTR,(Burri et al. (2002); Justanieah and Manousiouthakis (2004); Zhou and Manousiouthakis (2008b)) and non-ideal RTD SFR/MMR reactor units by Al-Husseini and Manousiouthakis (2013). IDEAS, is a general framework that can address most process network synthesis problems.

IDEAS is the first generalized process network synthesis methodology that is capable of delivering globally optimum designs. IDEAS is based on two principles: A vector space is equivalent to the infinite union of lower dimensional linear varieties, and the projection of the input-output map of a chemical process onto a linear variety, over which only extensive variables vary, is a linear map. To better understand how IDEAS works, consider a flowsheet (See Figure 1) that includes an infinite number of operations classified into two categories, an operator network (OP) and a distribution network (DN). The OP quantifies the actions of the considered process unit operations (in this case reactors) and consists of an infinite number of linear input/output maps with extensive and intensive properties for each map. The DN on the other hand quantifies the mixing and splitting processes which can take place among the inlet and outlet streams of the aforementioned unit operations. This unique structure of IDEAS allows all feasible network configurations to be considered, and gives rise to infinite linear programming (ILP) formulations for the synthesis of optimal process networks. The solution of these ILP's is approximated with increasing accuracy by a sequence of finite dimensional linear programs whose solutions are guaranteed to be globally optimal.

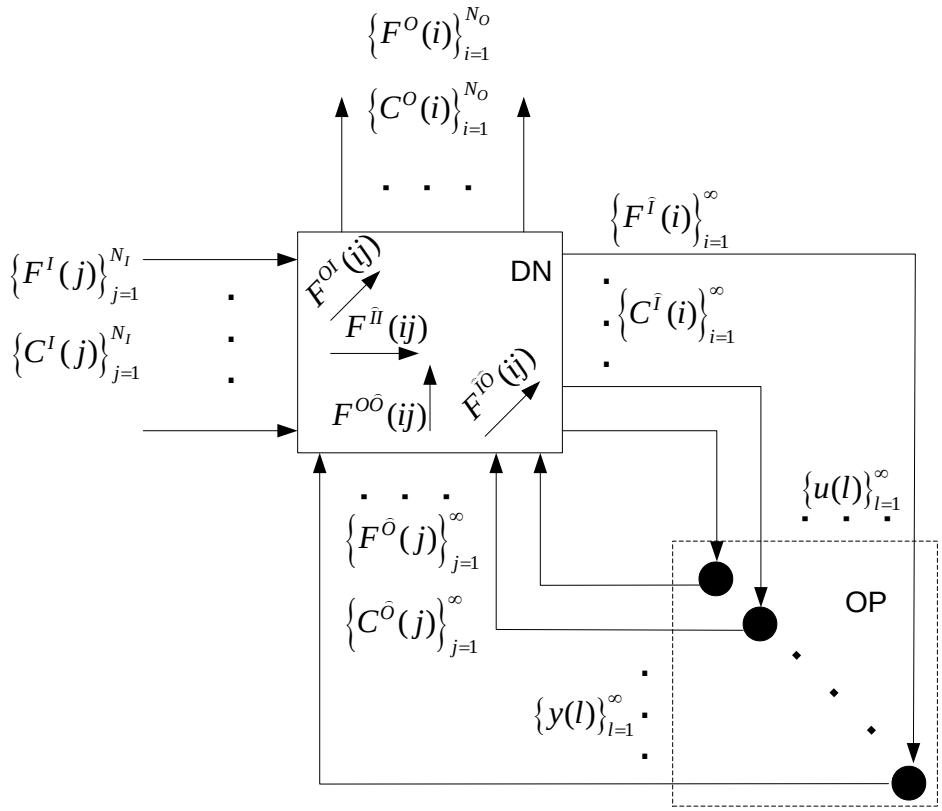

Figure 2-1. IDEAS Representation of a reactor network

Establishing the applicability of IDEAS to a process network synthesis problem requires that the process input output information map N be shown to possess certain properties, namely that there exists a decomposition of the input and output vectors $u \triangleq [u_1\, u_2]^T$; $y \triangleq [y_1\, y_2]^T$ such that the input output information map $N : u = [u_1\, u_2]^T \rightarrow y = [y_1\, y_2]^T = N(u) = [N_1(u)\; N_2(u)]^T = [N_1(u_1,u_2)\; N_2(u_1,u_2)]^T$ satisfies the properties

Property 1. $y_2 = N_2(u_1,u_2) = N_2(u_2)$

Property 2. $y_1 = N_1(u_1,u_2) = N_1(u_2)u_1$ where, for fixed u_2, $N_1(u_2)$ is a linear operator.

In this work, networks consisting of constant density fluid, isothermal, CSTR's, PFR's, RTD-Segregated Flow Reactors (RTD-SFR), and RTD-Maximum Mixedness Reactors (RTD-MMR) are considered. Below, the governing equations for each reactor model are defined, and the input and output vectors $u \triangleq \left[u_1\, u_2\right]^T ; y \triangleq \left[y_1\, y_2\right]^T$ for the reactor's input-output information map are identified.

1. CSTR model and information map defined in equations (1&2) respectively,

$$\left\{ C_k^{in} - C_k^{out} = \tau R_k\left(\left\{C_j^{out}\right\}_{j=1}^{n}\right) \quad \forall k = 1,...,n \right\} \quad (1)$$

$$u_1 \triangleq \left[F\right]^T ;\; u_2 \triangleq \left[C_1^{in} \cdots C_n^{in}\; \tau\right]^T ;\; y_1 \triangleq \left[F\; V\right]^T ;\; y_2 \triangleq \left[C_1^{out} \cdots C_n^{out}\; \tau\right]^T \quad (2)$$

2. PFR model and information map defined in equations (3&4) respectively,

$$\left\{ \begin{array}{ll} \dfrac{dC_k}{d\bar{\tau}} = R_k\left(\left\{C_j\right\}_{j=1}^{n}\right) & \forall k = 1,...,n \\ C_k\big|_{\bar{\tau}=0} = C_k^{in}, \quad C_k\big|_{\bar{\tau}=\tau} = C_k^{out} & \forall k = 1,...,n \end{array} \right\} \quad (3)$$

$$u_1 \triangleq \left[F\right]^T ;\; u_2 \triangleq \left[C_1^{in} \cdots C_n^{in}\; \tau\right]^T ;\; y_1 \triangleq \left[F\; V\right]^T ;\; y_2 \triangleq \left[C_1^{out} \cdots C_n^{out}\; \tau\right]^T \quad (4)$$

3. Segregated RTD model and information map defined in equations (5&6) respectively,

$$\left\{ \begin{array}{ll} C_k^{out}\left(\tau\right) = \displaystyle\int_0^{\infty} C_k\left(t\right) E\left(t\right) dt & \forall k = 1,....,n \\ \tau \triangleq \displaystyle\int_0^{\infty} tE\left(t\right) dt = \dfrac{V}{F} & \\ \dfrac{dC_k\left(t'\right)}{dt'} = R_k\left(\left\{C_j\left(t'\right)\right\}_{j=1}^{n}\right) & \forall t' \in \left[0,t\right] \quad \forall t \in \left[0,\infty\right) \\ C_k\left(0\right) = C_k^{in}; & \forall k = 1,....,n \end{array} \right\} \quad (5)$$

$$u_1 \triangleq \left[F\right]^T ;\; u_2 \triangleq \left[C_1^{in} \cdots C_n^{in}\; \tau E\left(\cdot\right)\right]^T ;\; y_1 \triangleq \left[F\; V\right]^T ;\; y_2 \triangleq \left[C_1^{out} \cdots C_n^{out}\; \tau E\left(\cdot\right)\right]^T \quad (6)$$

4. MMR model and information map defined in equations (7&8) respectively,

$$\left\{\begin{array}{l} \dfrac{dC_k(\lambda)}{d\lambda} = -R_k\left(\left\{C_j(\lambda)\right\}_{j=1}^{n}\right) + \left(C_k(\lambda) - C_k^{in}\right)\dfrac{E(\lambda)}{1-F(\lambda)} \qquad \forall \lambda \in [0,\infty) \\ \tau \triangleq \int_0^{\infty} tE(t)\,dt = \dfrac{V}{F} \\ C_k(0) = C_k^{out} \quad \forall k = 1,....,n; \quad \dfrac{dC_k}{d\lambda}(\infty) = 0 \quad \forall k = 1,....,n \\ 0 = -R_k\left(\left\{\lim\limits_{\lambda\to+\infty} C_j(\lambda)\right\}_1^n\right) + \left(\lim\limits_{\lambda\to+\infty} C_k(\lambda) - C_i^{in}\right)\lim\limits_{\lambda\to+\infty}\dfrac{E(\lambda)}{1-F(\lambda)} \quad \forall i = 1,...,n \end{array}\right\} (7)$$

$$u_1 \triangleq [F]^T;\ u_2 \triangleq \left[C_1^{in}\cdots C_n^{in}\ \tau\ E(\cdot)\right]^T;\ y_1 \triangleq [F\ V]^T;\ y_2 \triangleq \left[C_1^{out}\cdots C_n^{out}\ \tau\ E(\cdot)\right]^T \quad (8)$$

As shown in Burri et al. (2002); Justanieah and Manousiouthakis (2004); Zhou and Manousiouthakis (2008b) for the CSTR and PFR ideal reactor units, and in Al-Husseini and Manousiouthakis (2013) for the non-ideal RTD-SFR/RTD-MMR reactor units, the identified input and output vectors $u \triangleq [u_1\, u_2]^T$; $y \triangleq [y_1\, y_2]^T$ and associated input-output information maps satisfy properties 1, 2 listed above

2.3 IDEAS Formulation for CSTR, PFR, RTD-SFR, RTD-MMR Reactor Networks

The IDEAS representation of a reactor network is illustrated in Figure 1, for a system with N_I network inlet streams, N_O network outlet streams and *n* components. Under steady-state, homogeneous, isothermal, and constant-density conditions, the infinite-dimensional linear feasible region for the corresponding mathematical formulation of the CSTR, PFR, RTD-SFR and RTD-MMR reactor network synthesis problems is defined by the following equations and inequalities:

DN total mass balance equations, Eq. (9)-(12)

$$F^I(j) = \sum_{i=1}^{N_O} F^{OI}(i,j) + \sum_{i=1}^{\infty} F^{\hat{I}I}(i,j) \quad \forall j = 1,...,N_I \qquad (9)$$

$$F^{O}(i)=\sum_{j=1}^{N_I}F^{OI}(i,j)+\sum_{j=1}^{\infty}F^{O\hat{O}}(i,j)\quad \forall i=1,...,N_O \tag{10}$$

$$F^{\hat{I}}(i)=\sum_{j=1}^{N_I}F^{\hat{I}I}(i,j)+\sum_{j=1}^{\infty}F^{\hat{I}\hat{O}}(i,j)\quad \forall i=1,...,\infty \tag{11}$$

$$F^{\hat{O}}(j)=\sum_{i=1}^{N_O}F^{O\hat{O}}(i,j)+\sum_{i=1}^{\infty}F^{\hat{I}\hat{O}}(i,j)\quad \forall j=1,...,\infty \tag{12}$$

DN component balance equations, Eq. (13)

$$C_k^{\hat{I}}(i)F^{\hat{I}}(i)=\sum_{j=1}^{N_I}C_k^{I}(j)F^{\hat{I}I}(i,j)+\sum_{j=1}^{\infty}C_k^{\hat{O}}(j)F^{\hat{I}\hat{O}}(i,j)\ \ \forall k=1,...,n\ \ \forall i=1,...,\infty \tag{13}$$

DN outlet specifications, Eq. (14)-(15)

$$\left(F^{O}(i)\right)^{l}\le F^{O}(i)\le\left(F^{O}(i)\right)^{u}\ \ \forall i=1,...,N_O \tag{14}$$

$$\left(C_k^{O}(i)\right)^{l}F^{O}(i)\le\sum_{j=1}^{N_I}C_k^{I}(j)F^{OI}(i,j)+\sum_{j=1}^{\infty}C_k^{\hat{O}}(j)F^{O\hat{O}}(i,j)\le\left(C_k^{O}(i)\right)^{u}F^{O}(i) \tag{15}$$
$$\forall k=1,...,n\ \ \forall i=1,...,N_O$$

OP balance equations, Eq. (16)

$$F^{\hat{O}}(i)=F^{\hat{I}}(i)\qquad\qquad \forall i=1,...,\infty \tag{16}$$

RTD-SFR Reactor defining equations, Eq. (17)-(20)

$$C_k^{\hat{O}}(i)=\int_0^{\infty}C_{k,i}(t)E_i(t)dt\quad \forall k=1,....,n\ \forall i\in S_{SFR} \tag{17}$$

$$\tau(i)\triangleq\int_0^{\infty}tE_i(t)dt=\frac{V(i)}{F^{\hat{I}}(i)}\ \ \forall i\in S_{SFR} \tag{18}$$

$$\frac{dC_{k,i}(t')}{dt'}=R_k\left(\left\{C_{j,i}(t')\right\}_{j=1}^{n}\right)\ \ \forall k=1,....,n\ \ \forall t'\in[0,t]\ \ \forall t\in[0,\infty)\ \forall i\in S_{SFR} \tag{19}$$

$$C_{k,i}(0)=C_k^{\hat{I}}(i)\quad \forall i\in S_{SFR} \tag{20}$$

RTD-MMR Reactor defining equations, Eq. (21)-(24)

$$\frac{dC_{k,i}(\lambda)}{d\lambda} = -R_k\left(\left\{C_{j,i}(\lambda)\right\}_1^n\right) + \left(C_{k,i}(\lambda) - C_k^{\hat{I}}(i)\right)\frac{E_i(\lambda)}{1-F_i(\lambda)} \quad \forall \lambda \in [0,\infty) \;\; \forall k = 1,...,n \;\; \forall i \in S_{MMR}$$

$$0 = -R_k\left(\left\{\lim_{\lambda\to+\infty} C_{j,i}(\lambda)\right\}_1^n\right) + \left(\lim_{\lambda\to+\infty} C_{k,i}(\lambda) - C_k^{\hat{I}}(i)\right)\lim_{\lambda\to+\infty}\frac{E_i(\lambda)}{1-F_i(\lambda)} \quad \forall k = 1,...,n \;\; \forall i \in S_{MMR}$$

(21)

$$\tau(i) \triangleq \int_0^\infty tE_i(t)\,dt = \frac{V(i)}{F^{\hat{I}}(i)} \;\; \forall i \in S_{MMR} \tag{22}$$

$$C_{k,i}(\lambda = 0) = C_k^{\hat{O}}(i) \;\; \forall k = 1,...,n \;\; \forall i \in S_{MMR} \tag{23}$$

$$\frac{dC_{k,i}}{d\lambda}(\lambda = \infty) = 0 \;\; \forall k = 1,...,n \;\; \forall i \in S_{MMR} \tag{24}$$

PFR Reactor defining equations, eq. 25

$$\left\{\begin{array}{ll} \dfrac{dC_{k,i}(\bar{\tau})}{d\bar{\tau}} = R_k\left(\left\{C_{j,i}(\bar{\tau})\right\}_{j=1}^n\right) & \forall k = 1,...,n \;\; \forall \bar{\tau} \in \left[0,\tau(i)\right] \;\; \forall i \in S_{PFR} \\ \tau(i) \triangleq \dfrac{V(i)}{F^{\hat{I}}(i)} & \forall i \in S_{PFR} \\ C_{k,i}\big|_{\bar{\tau}=0} = C_k^{\hat{I}}(i), \quad C_k\big|_{\bar{\tau}=\tau} = C_k^{\hat{O}}(i) & \forall k = 1,...,n \;\; \forall i \in S_{PFR} \end{array}\right\} \tag{25}$$

CSTR Reactor defining equations, eq. 26

$$\left\{\begin{array}{ll} C_k^{\hat{I}}(i) - C_k^{\hat{O}}(i) = \tau(i)R_k\left(\left\{C_j^{\hat{O}}(i)\right\}_{j=1}^n\right) & \forall k = 1,...,n \;\; \forall i \in S_{CSTR} \\ \tau(i) \triangleq \dfrac{V(i)}{F^{\hat{I}}(i)} & \forall i \in S_{CSTR} \end{array}\right\} \tag{26}$$

where S_{SFR} , S_{MMR}, S_{PFR}, and S_{CSTR} are index sets indicating which units are segregated flow reactors, which units are maximum mixedness reactors, which units are plug flow reactors, and which units are continuous stirred tank reactors respectively, and $S_{SFR} \cup S_{MMR} \cup S_{PFR} \cup S_{CSTR} = \{1,...,\infty\}$

Positivity inequalities, Eq. (27)

$$F^I \geq 0; F^O \geq 0; F^{\hat{I}} \geq 0; F^{\hat{O}} \geq 0; F^{OI} \geq 0; F^{\hat{I}I} \geq 0; F^{\hat{I}\hat{O}} \geq 0; F^{O\hat{O}} \geq 0; V \geq 0 \quad (27)$$

where the upper case on $\left(F^O(i)\right)^l, \left(F^O(i)\right)^u$ and $\left(C_k^O(i)\right)^l, \left(C_k^O(i)\right)^u$ are the lower and upper bounds on the network flowrate and concentration outlets, respectively.

Having defined the infinite-dimensional linear feasible region of the IDEAS formulation, it is then easy to establish that for CSTR/PFR/RTD-SFR/RTD-MMR networks whose inlet and outlet flowrates are fixed percentages of the sum of all inlet flowrates (which is equal to the sum of all outlet flowrates), then the IDEAS network's NRT is independent of the sum of all inlet flowrates. To this end, the following Theorem holds:

Theorem 1:

Consider the IDEAS reactor network described by equations and inequalities 9 through 27. Consider in addition that the following assumption holds:

$$\left\{ \begin{array}{ll} \left(F^O(i)\right)^l = F^O(i) = \left(F^O(i)\right)^u = \alpha^O(i)\left(\sum_{l=1}^{N_O} F^O(l)\right) = \alpha^O(i)\left(\sum_{p=1}^{N_I} F^I(p)\right) & \forall i = 1,...,N_O \\ F^I(j) = \alpha^I(j)\left(\sum_{l=1}^{N_O} F^O(l)\right) = \alpha^I(j)\left(\sum_{p=1}^{N_I} F^I(p)\right) & \forall j = 1,...,N_I \\ \alpha^I(j) = known \;\; \forall j = 1,...,N_I; & \alpha^O(i) = known \;\; \forall i = 1,...,N_O \end{array} \right\} \quad (28)$$

Then, the IDEAS network's Network Residence Time is independent of the inlet flowrate sum $\sum_{p=1}^{N_I} F^I(p)$.

Proof

Consider that(9) through (28) hold for the inlet flowrate sum $\sum_{p=1}^{N_I} F^I(p)$, and for the vectors of variable sequences $F = \left[F^I \; F^O \; F^{\hat{I}} \; F^{\hat{O}} \; V \; F^{OI} \; F^{\hat{I}I} \; F^{\hat{I}\hat{O}} \; F^{O\hat{O}} \right]^T$ and parameter sequences $C = \left[C^I \; C^O \; C^{\hat{I}} \; C^{\hat{O}} \; \tau \; E \; \alpha^O \; \alpha^I \right]^T$. Then the Network Residence Time (NRT) is calculated as

$$NRT \triangleq \frac{\sum_{i=1}^{\infty} V(i)}{\sum_{p=1}^{N_I} F^I(p)} = \frac{\sum_{i=1}^{\infty} \tau(i) F^{\hat{I}}(i)}{\sum_{p=1}^{N_I} F^I(p)}.$$

Now consider that the IDEAS network's inlet flowrate sum is altered to $\lambda \sum_{p=1}^{N_I} F^I(p)$, $\lambda > 0$. Since the parameter sequence $C = \left[C^I \; C^O \; C^{\hat{I}} \; C^{\hat{O}} \; \tau \; E \; \alpha^O \; \alpha^I \right]^T$ remains unaltered, it is then easy to verify , that (9) through (28) hold for the inlet flowrate sum $\lambda \sum_{p=1}^{N_I} F^I(p)$, and for the vector of variable sequences $F^\lambda = \left[\lambda F^I \; \lambda F^O \; \lambda F^{\hat{I}} \; \lambda F^{\hat{O}} \; \lambda V \; \lambda F^{OI} \; \lambda F^{\hat{I}I} \; \lambda F^{\hat{I}\hat{O}} \; \lambda F^{O\hat{O}} \right]^T$, $\forall \lambda > 0$. For each of the networks resulting from a different value of $\lambda > 0$, the corresponding Network Residence Time (NRT) is calculated as:

$$NRT^\lambda \triangleq \frac{\sum_{i=1}^{\infty} \lambda V(i)}{\lambda \sum_{p=1}^{N_I} F^I(p)} = \frac{\sum_{i=1}^{\infty} \lambda \tau(i) F^{\hat{I}}(i)}{\lambda \sum_{p=1}^{N_I} F^I(p)} = \frac{\lambda \sum_{i=1}^{\infty} \tau(i) F^{\hat{I}}(i)}{\lambda \sum_{p=1}^{N_I} F^I(p)} = \frac{\sum_{i=1}^{\infty} \tau(i) F^{\hat{I}}(i)}{\sum_{p=1}^{N_I} F^I(p)} = NRT \qquad \text{O.E.}\Delta.$$

Having established the independence of the Network Residence Time (NRT) from the network's inlet flowrate sum, we are now in the position to introduce the concept of the Network Residence Time Constrained Attainable Region (NRT-C-AR) for a single inlet, single outlet, CSTR/PFR/RTD-SFR/RTD-MMR network.

Definition

For a single inlet, single outlet, CSTR/PFR/RTD-SFR/RTD-MMR network with a known inlet concentration vector, and a set of reactions with known kinetic rates, the Network Residence Time Constrained Attainable Region (NRT-C-AR) is the set of all reactor network outlet concentration vectors that can be attained by means of CSTR/PFR/RTD-SFR/RTD-MMR networks whose NRT is constrained above.

Having defined NRT-C-AR, we next establish that it is a convex set.

Theorem 2.

The Network Residence Time Constrained Attainable Region with NRT upper bound τ^U, $NRTCAR_{\tau^U}$, of a single inlet, single outlet, CSTR/PFR/RTD-SFR/RTD-MMR network with a known inlet concentration vector, and a set of reactions with known kinetic rates, is a convex set.

Proof

Consider two CSTR/PFR/RTD-SFR/RTD-MMR single inlet single outlet networks, whose outlet concentration vectors belong to $NRTCAR_{\tau^U}$. Since the NRT of a CSTR/PFR/RTD-SFR/RTD-MMR network is independent of the inlet flowrate sum, it can be assumed without loss of generality that the inlet flowrate of both networks is the same. Denote the vectors of variable sequences and parameter sequences for each network to be $F_a = \left[F^I \; F^O \; F_a^{\hat{I}} \; F_a^{\hat{O}} \; V_a \; F_a^{OI} \; F_a^{\hat{I}I} \; F_a^{\hat{I}\hat{O}} \; F_a^{O\hat{O}} \right]^T, C_a = \left[C^I \; C_a^O \; C^{\hat{I}} \; C^{\hat{O}} \; \tau \; E \right]^T$ and

$F_b = \left[F^I \; F^O \; F_b^{\hat{I}} \; F_b^{\hat{O}} \; V_b \; F_b^{OI} \; F_b^{\hat{I}I} \; F_b^{\hat{I}\hat{O}} \; F_b^{O\hat{O}} \right]^T, C_b = \left[C^I \; C_b^O \; C^{\hat{I}} \; C^{\hat{O}} \; \tau \; E \right]^T$, and assume that the NRT of each network is bounded above by the same bound, i.e. assume that $NRT^a \triangleq \frac{\sum_{i=1}^{\infty} V_a(i)}{F^I} \leq \tau^U$, and

$NRT^b \triangleq \dfrac{\sum_{i=1}^{\infty} V_b(i)}{F^I} \le \tau^U$, where τ^U is a known fixed upper bound. It is easy to verify that the CSTR/PFR/RTD-SFR/RTD-MMR network with vectors of variable sequences and parameter sequences equal to

$$F_{\lambda a+(1-\lambda)b} = \begin{bmatrix} \left[F^I \; F^O \; \lambda F_a^{\hat{I}} + (1-\lambda) F_b^{\hat{I}} \; \lambda F_a^{\hat{O}} + (1-\lambda) F_b^{\hat{O}} \; \lambda V_a + (1-\lambda) V_b \; \lambda F_a^{OI} + (1-\lambda) F_b^{OI} \right]^T \\ \left[\lambda F_a^{\hat{I}I} + (1-\lambda) F_b^{\hat{I}I} \; \lambda F_a^{\hat{I}\hat{O}} + (1-\lambda) F_b^{\hat{I}\hat{O}} \; \lambda F_a^{O\hat{O}} + (1-\lambda) F_b^{O\hat{O}} \right]^T \end{bmatrix},$$

and $C_{\lambda a+(1-\lambda)b} = \left[C^I \; \lambda C_a^O + (1-\lambda) C_b^O \; C^{\hat{I}} \; C^{\hat{O}} \; \tau \; E \right]^T$ respectively, also satisfies (9) through (28) $\forall \lambda \in [0,1]$. In addition, $NRT^{\lambda a+(1-\lambda)b} \triangleq \dfrac{\sum_{i=1}^{\infty} \left[\lambda V_a(i) + (1-\lambda) V_b(i) \right]}{F^I} = \lambda \dfrac{\sum_{i=1}^{\infty} V_a(i)}{F^I} + (1-\lambda) \dfrac{\sum_{i=1}^{\infty} V_b(i)}{F^I} =$. The above imply $= \lambda NRT^a + (1-\lambda) NRT^b \le \lambda \tau^U + (1-\lambda) \tau^U = \tau^U \quad \forall \lambda \in [0,1]$ that $\left[\lambda C_a^O + (1-\lambda) C_b^O \right] \in NRTCAR_{\tau^U} \quad \forall C_a^O \in NRTCAR_{\tau^U} \quad \forall C_b^O \in NRTCAR_{\tau^U} \quad \forall \lambda \in [0,1]$. In turn this implies that the set $NRTCAR_{\tau^U}$ is convex. O.E.Δ.

Having established the convexity of $NRTCAR_{\tau^U}$, a case study is next carried out for illustrative purposes. Numerical computations are carried out through repeated solution of finite dimensional approximations of the IDEAS ILP, with objective function to be minimized

$$\pm \frac{C_k^I F^{OI}(1,1) + \sum_{j=1}^{\infty} C_k^{\hat{O}}(j) F^{O\hat{O}}(1,j)}{F^I} \quad \forall k = 1,...,n$$

and the following additional constraints incorporated in the IDEAS formulation.

$$C_m^O = \frac{C_m^I F^{OI}(1,1) + \sum_{j=1}^{\infty} C_m^{\hat{O}}(j) F^{O\hat{O}}(1,j)}{F^I} = known \quad \forall m \in \{1,...,n\} - \{k\}$$

$$\frac{\sum_{i=1}^{\infty}\tau(i)F^{\hat{I}}(i)}{F^{I}} \leq \tau^{U}$$

2.4 Case Study: CSTR-NRTCAR, PFR-NRTCAR, and SLFR-NRTCAR Construction

The goal of this case study is to quantify the NRTC-AR for reactor networks featuring three different reactor unit models: Continuous Stirred Tank Reactor (CSTR), Plug Flow Reactor (PFR), and Segregated Laminar Flow Reactor (SLFR). The considered reaction scheme is the Trambouze reaction scheme shown below:

$$\left\{\begin{array}{l} A \xrightarrow{k_1} B\ ,\ k_1 = 0.025\dfrac{kmol}{m^3 \cdot s} \\ A \xrightarrow{k_2} C\ ,\ k_2 = 0.2\dfrac{1}{s} \\ A \xrightarrow{k_3} D\ ,\ k_3 = 0.4\dfrac{m^3}{kmol \cdot s} \end{array}\right\} \tag{29}$$

with

$$\left\{\begin{array}{l} R_A = -\left(k_1 + k_2 C_A + k_3 {C_A}^2\right) \\ R_C = k_2 C_A \end{array}\right\} \tag{30}$$

where ${k_2}^2 = 4k_1k_3$; $\alpha \triangleq \dfrac{k_2}{2k_3} = 0.25 > 0$

The network's inlet concentrations of A and C are: $C_A^{in} = 1 {kmol}/{m^3}$, $C_C^{in} = 0 {kmol}/{m^3}$.

The behavior of the three aforementioned reactor types, when no outlet specifications are imposed on the B and D species' concentrations, are captured by the following model equations:

CSTR:

$$\boxed{\begin{aligned} C_A^{out}(\tau) &= \left\{ \begin{array}{ll} \dfrac{-(k_2\tau+1)+\sqrt{1+4k_3\tau\left(\alpha+C_A^{in}\right)}}{2k_3\tau} & if\ \tau \le \tau_{cCSTR} \\ 0 & if\ \tau > \tau_{cCSTR} \end{array} \right\} \\ C_C^{out}(\tau) &= \left\{ \begin{array}{ll} C_C^{in}+\alpha\left(-(k_2\tau+1)+\sqrt{1+4k_3\tau\left(\alpha+C_A^{in}\right)}\right) & if\ \tau \le \tau_{cCSTR} \\ C_C^{in} & if\ \tau > \tau_{cCSTR} \end{array} \right\} \end{aligned}} \text{ where } \boxed{\tau_{cCSTR} \triangleq \frac{C_A^{in}}{k_1} > 0}$$

PFR:

$$\boxed{\begin{aligned} C_A^{out}(\tau) &= \left\{ \begin{array}{ll} -\alpha + \dfrac{1}{k_3\tau + \dfrac{1}{C_A^{in}+\alpha}} & if\ \tau \le \tau_c \\ 0 & if\ \tau > \tau_c \end{array} \right\} \\ C_C^{out}(\tau) &= \left\{ \begin{array}{ll} C_C^{in} - 2\alpha^2 k_3\tau + 2\alpha\ln\left(k_3\tau\left(C_A^{in}+\alpha\right)+1\right) & if\ \tau \le \tau_{cPFR} \\ C_C^{in} - 2\alpha^2 k_3\tau_c + 2\alpha\ln\left(k_3\tau_c\left(C_A^{in}+\alpha\right)+1\right) & if\ \tau > \tau_{cPFR} \end{array} \right\} \end{aligned}}, \boxed{\tau_{cPFR} \triangleq \frac{C_A^{in}}{k_3\alpha\left(\alpha+C_A^{in}\right)} > 0}$$

SLFR:

The residence time density (RTD) function for a laminar flow reactor, with mean residence time τ, is (Fogler, 3rd, 4th Edition),

$E(t) = \left\{ \begin{array}{ll} 0 & if\ t < \dfrac{\tau}{2} \\ \dfrac{\tau^2}{2t^3} & if\ t \ge \dfrac{\tau}{2} \end{array} \right\}$, while its flow pattern is that of a segregated flow reactor. Then the model equations for a SLFR in which the Trambouze reaction scheme is carried out are (Al-husseini and Manousiouthakis, 2013) :

$$C_A^{out}(\tau)=\begin{cases} C_A^{in}\left(1-\dfrac{\tau^2}{4\tau_c^2}\right)+k_3\dfrac{\tau}{2}\left(\dfrac{\tau}{\tau_c}-2\right)\left(C_A^{in}+\alpha\right)^2+ \\ +k_3^2\dfrac{\tau^2}{2}\left(C_A^{in}+\alpha\right)^3\ln\left(\dfrac{\tau_c\left(k_3\left(C_A^{in}+\alpha\right)\dfrac{\tau}{2}+1\right)}{\dfrac{\tau}{2}\left(k_3\left(C_A^{in}+\alpha\right)\tau_c+1\right)}\right) & if\ \ \tau<\tau_{cSLFR} \\ 0 & if\ \ \tau\geq\tau_{cSLFR} \end{cases}$$

$$C_C^{out}(\tau)=\begin{cases} C_C^{in}+k_3\alpha\tau\left(C_A^{in}\left(1-\dfrac{\tau}{2\tau_c}\right)-\alpha\right)+2\alpha\ln\left(k_3\left(C_A^{in}+\alpha\right)\dfrac{\tau}{2}+1\right)+ \\ +\dfrac{1}{2}\alpha\tau^2k_3^2\left(C_A^{in}+\alpha\right)^2\ln\left(\dfrac{\dfrac{\tau}{2}\left(k_3\left(C_A^{in}+\alpha\right)\tau_c+1\right)}{\tau_c\left(k_3\left(C_A^{in}+\alpha\right)\dfrac{\tau}{2}+1\right)}\right) & if\ \ \tau<\tau_{cSLFR} \\ C_C^{in}-2\alpha\dfrac{C_A^{in}}{\left(\alpha+C_A^{in}\right)}+2\alpha\ln\left(\dfrac{C_A^{in}+\alpha}{\alpha}\right) & if\ \ \tau\geq\tau_{cSLFR} \end{cases}$$

where $\tau_{cSLFR}\triangleq 2\tau_{cPFR}\triangleq 2\dfrac{C_A^{in}}{k_3\alpha\left(\alpha+C_A^{in}\right)}>0$

In carrying out the IDEAS methodology, SLFR inlet and outlet concentrations of A (C_A^{in}, $C_A^{out}(\tau)$) are specified, rather than the inlet concentration of A and the residence time. As shown in Appendix B of (Al-husseini and Manousiouthakis, 2013), for given values of C_A^{in}, $C_A^{out}(\tau)$ there exists only one value of τ in the interval $(0,\tau_{cSLFR})$, that satisfies the SLFR mass balance equation.

The true AR boundary, quantified both analytically and through increasingly accurate IDEAS approximations, is presented in figure 2.

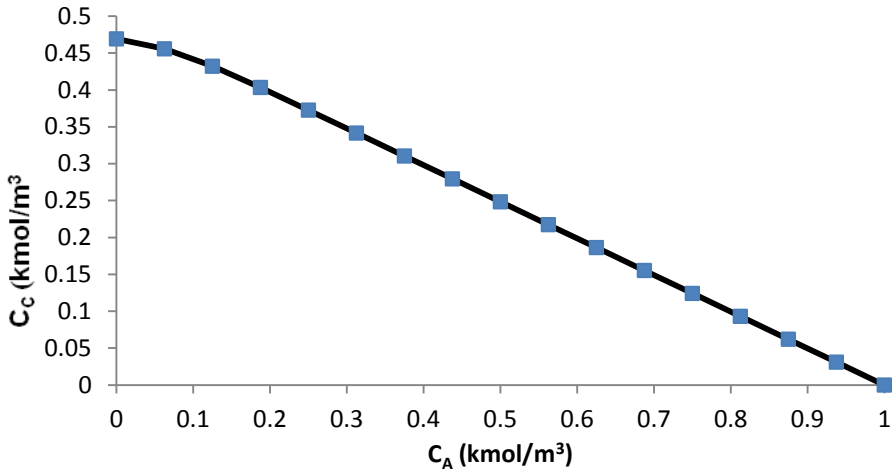

Figure 2-2. True AR Boundary

The IDEAS obtained CSTR NRTC-AR, PFR NRTC-AR, and SLFR NRTC-AR with $NRT \le \tau^U = 2.5s$ are presented in figure 3. Figures 4, 5, and 6 present the IDEAS obtained CSTR NRTC-AR, PFR NRTC-AR, and SLFR NRTC-AR respectively, with $NRT \le \tau^U = 2.5s$, and $NRT \le \tau^U = 10s$.

As can be seen in the above figures, the NRTCAR is always a convex subset of the AR. It is also shown that as the NRT upper bound becomes smaller, the NRTCAR shrinks.

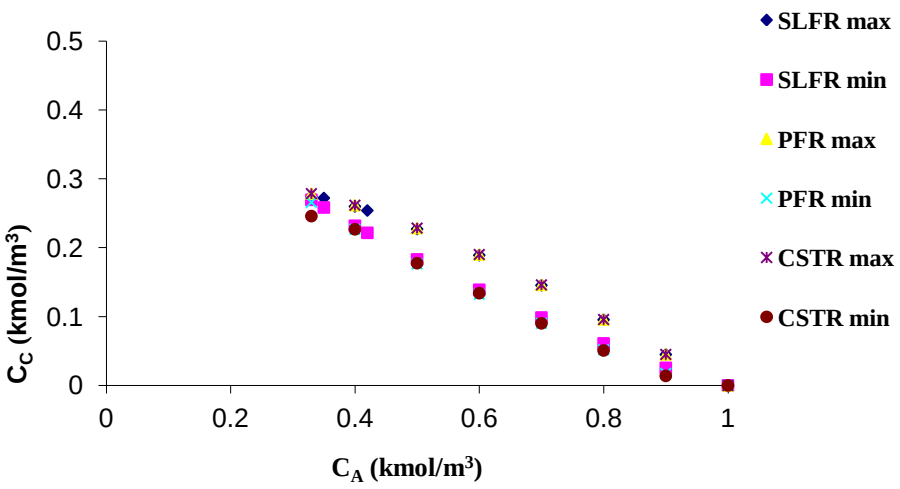

Figure 2-3. IDEAS obtained CSTR NRTC-AR, PFR NRTC-AR, SLFR NRTC-AR with $\tau^U = 2.5\,s$,

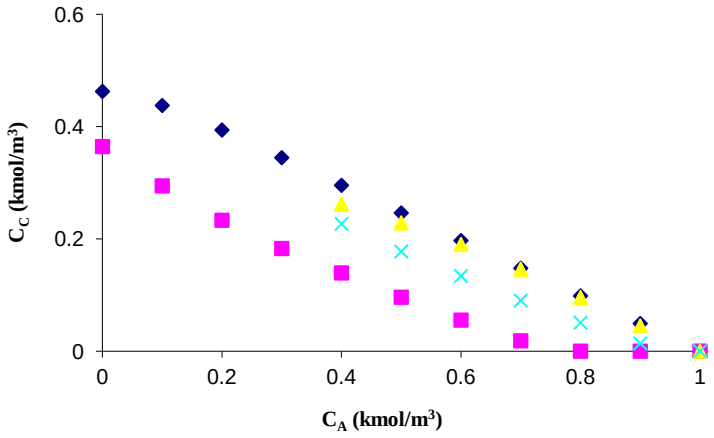

Figure 2-4. IDEAS obtained CSTR NRTC-AR with $\tau^U = 2.5\,s$ *and* $\tau^U = 10\,s$

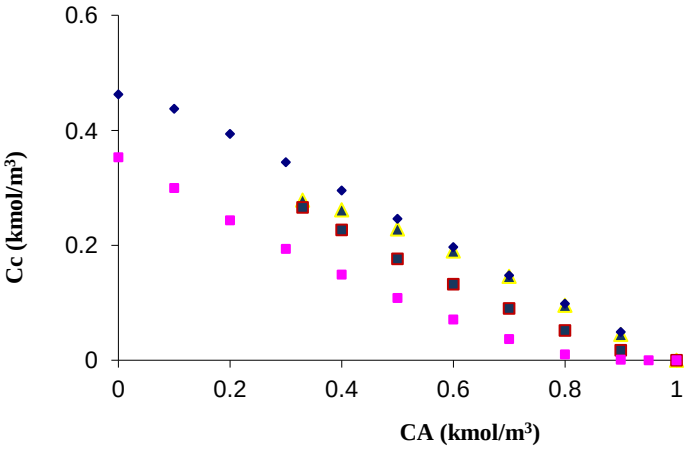

Figure 2-5. IDEAS obtained PFR NRTC-AR with $\tau^U = 2.5s$ *and* $\tau^U = 10s$

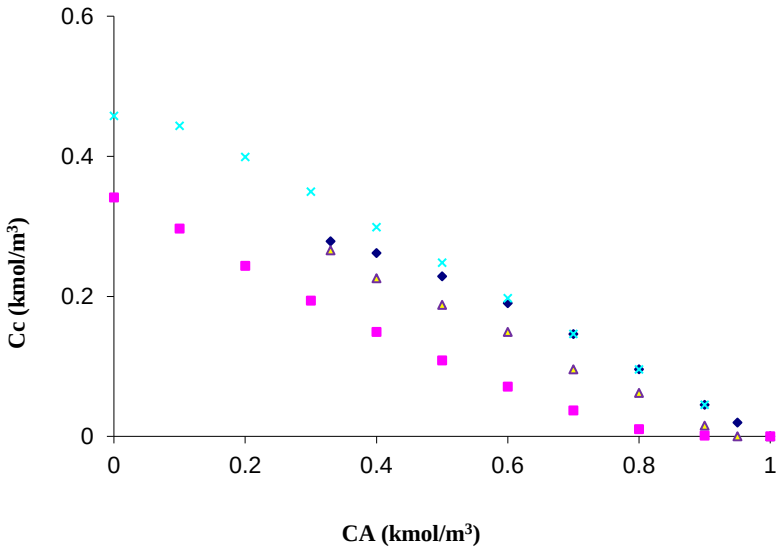

Figure 2-6. IDEAS obtained SLFR NRTC-AR with $\tau^U = 2.5s$ *and* $\tau^U = 10s$

2.5 Discussion-Conclusions

As stated in the introduction section, the AR possesses four properties. They are:

"(a) It is convex.

(b) No rate vector in the boundary of A (∂A) points outward from A; that is, all rate vectors in ∂A points inward, are tangent to ∂A, or are zero.

(c) There is no plug-flow trajectory in the complement of A (within the stoichiometric subspace), which has two points such that the line joining the later to the earlier point can be extended to intersect A.

(d) No negative of a rate vector in the complement of A (within the stoichiometric subspace), when extended, can intersect a point of ∂A or (A)."

Earlier, in Theorem 2, it was established that property (a) also holds true for NRTCAR. As shown however in Figure 8 below, the other three AR properties ((b), (c), (d)) do not hold true for NRTCAR. For example, at the point $(C_A, C_C) = (0.33, 0.266)$ the rate vector $(R_A, R_C) = \left(-\left(k_1 + k_2 C_A + k_3 C_A^{\,2}\right), k_2 C_A\right) = (-0.13456, 0.00825)$ points outward from NRTCAR , thus violating property (b) for NRTCAR. At the points $(C_A, C_C) = (0.1, 0.299)$, $(C_A, C_C) = (0.2, 0.243)$, both of which belong to a PFR trajectory in the complement of NRTCAR, the backward extension of the line connecting the two points intersects the NRTCAR, thus violating property(c), for NRTCAR. At the point $(C_A, C_C) = (0.1, 0.299)$, which belongs to the complement of NRTCAR, the rate vector

$(R_A, R_C) = \left(-\left(k_1 + k_2 C_A + k_3 C_A{}^2\right), k_2 C_A\right) = (-0.0675, 0.4)$, has a backward extension that intersects the NRTCAR, thus violating property(d), for NRTCAR.

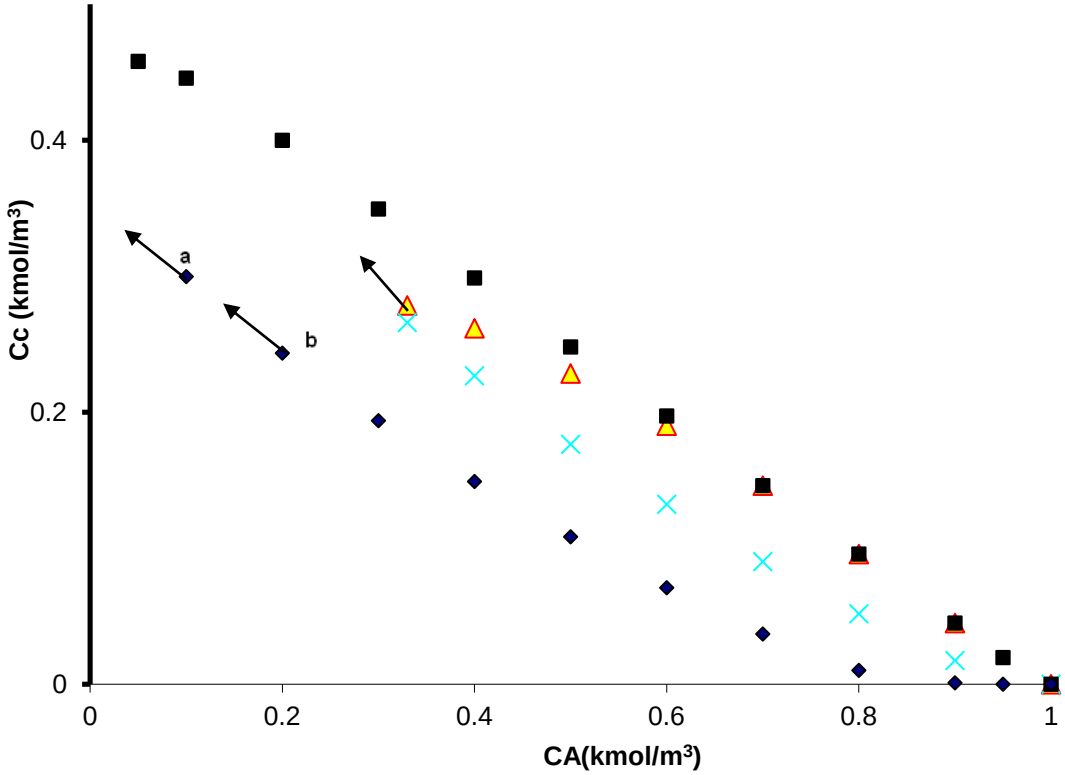

Figure 2-7. Counterexamples demonstrating that three AR properties do not hold for NRTCAR

Another interesting observation, is that one of the SLFR reactors that delivers one of the SLFR NRTCAR vertices has its outlet concentration vector completely outside the SLFR NRTCAR, something not possible for AR.

In this work, the Network Residence Time (NRT) of CSTR/PFR/RTD-SFR/RTD-MMR networks is introduced for the first time. For single inlet, single outlet, CSTR/PFR/RTD-SFR/RTD-MMR networks, the Network Residence Time Constrained Attainable Region (NRTCAR) concept is also introduced for the first time, and is rigorously proved to be a convex

set. The IDEAS conceptual framework is shown to be applicable to the problem of NRT-C-AR construction. The resulting mathematical formulation is linear, thus guaranteeing the optimality of the obtained solution. The introduced concepts are illustrated with a case study on the Trambouze reaction scheme. It is shown that as the NRT upper bound is tightened, the corresponding NRTCAR shrinks in size. Several AR properties are shown, through counterexamples, not to hold for the NRTCAR.

Acknowledgements

Financial support from the U.S. National Science Foundation under grant #CTS-0829211, Jeremy Burri, and Saudi Aramco Oil Company R&D is gratefully acknowledged.

Nomenclature

$C_i : i^{th}$ Component molar concentration $\left(\text{kmol/m}^3\right)$

$C_i^{in} : i^{th}$ Component inlet molar concentration to IDEAS unit model $\left(\text{kmol/m}^3\right)$

$C_i^{out} : i^{th}$ Component outlet molar concentration from IDEAS unit model $\left(\text{kmol/m}^3\right)$

$\left\{C_i^{in}\right\}_{i=1}^{n}$: Inlet molar concentration vector (kmol/m^3)

$\left\{C_i^{out}\right\}_{i=1}^{n}$: Outlet molar concentration vector (kmol/m^3)

F : Volumetric flow rate $\left(\text{m}^3/\text{s}\right)$

F^{in} : Inlet volumetric flow rate $\left(\text{m}^3/\text{s}\right)$

F^{out} : Outlet volumetric flow rate $\left(\text{m}^3/\text{s}\right)$

V : Volume (m^3)

τ_N : Constraint volume m^3

IDEAS Variables:

$C_A(\tau)$: PFR Concentration of A at residence time τ

$\overline{C}_A(\tau)$: SLFR Concentration of A at residence time τ

$C_C(\tau)$: PFR Concentration of C at residence time τ

$\overline{C}_C(\tau)$: SLFR Concentration of C at residence time τ

$C_k^I(j)$: k^{th} Component concentration in the j^{th} network inlet $\forall k = 1, n; \forall j = 1, N_I$

$C_k^{\hat{I}}(i)$: k^{th} Component concentration in the i^{th} OP inlet $\forall k = 1, n; \forall i = 1, \infty$

$C_k^O(i)$: k^{th} Component concentration in the i^{th} network outlet $\forall k = 1, n; \forall i = 1, N_O$

$C_k^{\hat{O}}(i)$: k^{th} Component concentration in the i^{th} OP outlet $\forall k = 1, n; \forall i = 1, \infty$

$F^I(j)$: j^{th} Network inlet flow rate $\forall j = 1, N_I$

$F^O(i)$: i^{th} Network outlet flow rate $\forall i = 1, N_O$

$F^{\hat{I}}(j)$: j^{th} OP inlet flow rate $\forall j = 1, \infty$

$F^{\hat{O}}(i)$: i^{th} OP outlet flow rate $\forall i = 1, \infty$

$F^{OI}(i, j)$: j^{th} Network inlet flow rate to the i^{th} network outlet $\forall j = 1, N_I; \forall i = 1, N_O$

$F^{\hat{I}I}(i, j)$: j^{th} Network outlet flow rate to the i^{th} OP inlet $\forall j = 1, N_I; \forall i = 1, \infty$

$F^{O\hat{O}}(i, j)$: j^{th} OP outlet flow rate to the i^{th} network outlet $\forall j = 1, \infty; \forall i = 1, N_O$

$F^{\hat{I}\hat{O}}(i, j)$: j^{th} OP outlet flow rate to the i^{th} OP network outlet $\forall j = 1, \infty; \forall i = 1, \infty$

$N : u \to y = N(u)$: input output information map

n: component index

N_I : IDEAS Network inlet streams

N_O : IDEAS Network outlets streams

S_{mix} : Index set of the mixing operation's inlet streams

S_{MMR} : Index set indicating units of maximum mixedness reactors

S_{SFR} : Index set indicating units of segregated flow reactors

S_{split} : Index set of the splitting operation's outlet streams

$\tau(i)$: Residence time of the i^{th} OP unit $\forall i = 1, \infty$

τ_c : Critical value of the residence time τ

$u(i)$: Input of the i^{th} OP unit information map $\forall i = 1, \infty$

$u \triangleq [u_1 \, u_2]^T$: Input information vector

$y(i)$: Output of the i^{th} OP unit information map $\forall i = 1, \infty$

$y \triangleq [y_1 \, y_2]^T$: Output information vector

2.6 References

Abraham TK, Feinberg M. Kinetic bounds on attainability in the reactor synthesis problem. Industrial & engineering chemistry 2004; 43(2): 449-457.

Al-husseini, Z, Manousiouthakis, V. I. IDEAS based Synthesis of Minimum Volume Reactor Networks featuring Residence Time Density/Distribution Models. *Computers and Chemical Engineering, in press*. 2013.

Amte, V., Nistala, S., Malik, R., & Mahajani, S. Attainable regions of reactive distillation—Part III. Complex reaction scheme: Van de Vusse reaction. *Chemical Engineering Science*. 2011; *66*, 11: 2285-2297.

Burri JF, Wilson SD, Manousiouthakis V. Infinite DimEnsionAl State-Space approach to reactor network synthesis: Application to attainable region construction. Computers & Chemical Engineering 2002; 16(6): 849-862.

Drake JE, Manousiouthakis V. IDEAS approach to process network synthesis: minimum plate area for complex distillation networks with fixed utility cost. Industrial & Engineering Chemistry Research 2002a; 41(20): 4984-4992.

Drake JE, Manousiouthakis V. IDEAS approach to process network synthesis: minimum utility cost for complex distillation networks. Chemical Engineering Science 2002b; 57(15): 3095-3106.

Feinberg, M. Optimal reactor design from a geometric viewpoint. Part II. Critical sidestream reactors. *Chemical Engineering Science. 2000a; 55*,13: 2455–2479.

Feinberg, M. Optimal reactor design from a geometric viewpoint. Part III. Critical cfstrs. *Chemical Engineering Scienc*e. 2000b; *55*,17: 3553–3565.

Feinberg, M. Personal communication to D. Hildebrandt as referenced in Kauchali et al. 2002.

Feinberg, M. Recent results in optimal reactor synthesis via attainable region theory. *Chemical Engineering Science*.. 1999; *54*: 2535–2543.

Feinberg, M., & Hildebrandt, D. Optimal reactor design from a geometric viewpoint-I. universal properties of the attainable region.*Chemical Engineering Science. 1997; 52*,10: 1637–1665.

Fogler HS. Elements of Chemical Reaction Engineering. 3rd ed. Prentice Hall; 1999.

Fogler HS. Elements of Chemical Reaction Engineering. 4th ed. Prentice Hall; 2006.

Gavalas, G. R. *Nonlinear differential equations of chemically reacting systems*. Berlin, Germany: Springer, 1968.

Ghougassian, P. G., & Manousiouthakis, V. Attainable Composition, Energy Consumption, and Entropy Generation Properties for Isothermal/Isobaric Reactor Networks. *Industrial & Engineering Chemistry Research*. 2013;*52*, 9: 3225-3238.

Glasser D, Hildebrandt D, Godorr S, The Attainable Region for Segregated, Maximum Mixed, and other Reactor Models, Industrial & Engineering Chemistry. 1994; 33, 5: 1136-1144.

Glasser, D., Hildebrandt, D., & Crowe, C. A geometric approach to steady flow reactors: The attainable region and optization in concentration space. *Industrial and Engineering Chemical Research.* 1987; *26*,9:1803–1810.

Glasser, D., Hildebrandt, D., & Godorr, S. The attainable region for segregated maximum mixed and other reactor models. *Industrial and Engineering Chemical Research.* 1990; *33*: 1136.

Godorr, S., Hildebrandt, D., Glasser, D., & McGregor, C. Choosing optimal control policies using the attainable region approach. *Industrial and Engineering Chemical Researc. 1999; 38*,3: 639-651.

Hildebrandt, D., Glasser, D., & Crowe, C. Geometry of the attainable region generated by reaction and mixing: With and without constraints. *Industrial and Engineering Chemical Research.* 1990; *29*,1: 49–58.

Hopley, F., Glasser, D., & Hildebrandt, D. Opimal ractor structures for exothermic reversible reactions with complex kinetics. *Chemical Engineering Science*. 1996; *51*,10: 2399–2407.

Horn, F. Attainable and non-attainable regions in chemical reactor technique.
In *Proceedings of the Third European Symposium on Chemical Reaction Engineering.*
1964 ;(pp. 123–138). London: Pergamon Press.

Horn, F., & Tsai, M. The use of the adjoint variables in the development of improvement criteria for chemical reactors. *Journal of Optimal Theory and Application.*
1967; *1*, 2: 131–145.

Katubilwa, F. M., Moys, M. H., Glasser, D., & Hildebrandt, D. An attainable region analysis of the effect of ball size on milling. *Powder Technology*. 2011; *210*, 1: 36-46.

Kauchali S, Rooney WC, Biegler LT, Glasser D, Hildebrandt D. Linear programming formulations for attainable region analysis. Chemical Engineering Science 2002; 57(11):2015-2028

Manousiouthakis V, Justanieah A, Taylor L, The Shrink-Wrap algorithm for the construction of the attainable region: an application of the IDEAS framework, Computers & Chemical Engineering. *2004*; 28, 9: 1563–1575

Nisoli, A., Malone, M., & Doherty, M. Attainable regions for reaction with separation. *American Institute of Chemical Engineers. 1997;43*,2; 374–387.

Okonye, L. U., Hildebrandt, D., Glasser, D., & Patel, B. Attainable regions for a reactor: Application of Δ< i> H</i>–Δ< i> G</i> plot. *Chemical Engineering Research and Design*. 2012; *90*, 10: 1590-1609.

Peter, M. S., Timmerhaus, K.D. & West, R. E. Plant design and economics for chemical engineers (5th ed.). New York: McGRaw-Hill, 2003.

Posada, A., & Manousiouthakis, V. Multi-feed attainable region construction using shrink-wrap algorithm. *Chemical Engineering Science. 2008; 63*, 5571–5592.

Smith, R. L., & Malone, M. F. Attainable regions for polymerization reaction systems. *Industrial and Engineering Chemical Research. 1997;36*, 4:, 1076–1084.

Wilson S, Manousiouthakis V. IDEAS approach to process network synthesis: application to multicomponent (MEN). AIChE J, 2000; 46: 2408-2416.

Zhou W, Manousiouthakis V. Global capital/total annualized cost minimization of homogeneous and isothermal reactor networks. Industrial & Engineering Chemistry Research 2008a; 47(10): 3771-3782.

Zhou W, Manousiouthakis V. On dimensionality of attainable region construction for isothermal reactor networks. Computers & Chemical Engineering 2008b; 32(3): 439-450.

Zhou, W., & Manousiouthakis, V. I. Non-ideal reactor network synthesis through IDEAS: Attainable region construction. *Chemical engineering science* 2006; *61*, 21: 6936-6945.

Zhou, W., & Manousiouthakis, V. I. Variable density fluid reactor network synthesis—construction of the attainable region through the IDEAS approach. *Chemical Engineering Journal*. 2007;*129*, 1: 91-103.

Chapter 3

3 Optimization of a 3-D Monolith Reactor

Abstract

In this work, the optimization of an isothermal monolith reactor is carried out for the first time. First, a reaction-diffusion 3-D mathematical model for a monolith reactor is developed. An analytical solution of this model is then developed, based on separation of variables. The analytical nature of the obtained solution enables the optimization of a multi-channel 3-D monolith reactor to be carried out. The obtained optimization results are discussed and conclusions are drawn.

Keywords: Model; 3-D; Monolith; Reactor; Optimization

3.1 Introduction

The word monolith derives from the Greek word μονόλιθος (monolithos), which is a composite of two words: μόνος ("one" or "single") and λίθος ("stone "). Monolith reactors are typically multichannel reactors constructed of ceramic material. The shape of the channels varies from rectangular, to square, triangular, hexagonal, or circular. The internal surface of each channel is typically coated with catalytic material that accelerates the reaction rate of the reactions taking place inside the reactor. Monolith reactors possess many attractive features. These include:

(1) Low pressure drop, especially under high fluid throughputs

(2) Elimination of pore diffusion limitations associated with the use of porous catalyst particles

(3) Low axial dispersion and backmixing, and therefore high product selectivity

(4) Large reaction surface

(5) Uniform distribution of flow (gas phase)

(6) Elimination of fouling and plugging, and thus extended catalyst lifetime

(7) Easy scale-up

Monolith reactors became commonplace when the automotive industry used them as engine emission converters, to remove NO_x and CO from vehicle emissions. Their use allowed high selectivity and elimination of hot-spots, and promoted the conversion rate and reactor performance in exhaust gas treatment (Tomasic, 2007) (R.E. Hayes, 2004) (R.M. Heck, 2001) (A. Cybulski, 1998) (I.M. Lachman, 1985) (L.L. Johnson, 1961). The success of monolith reactors as engine emission converters, has led researchers to investigate how they may also improve other gas phase reactions. These include catalytic combustion (P. Marin, 2005) (S. Tischer, 2005) (P. Canu, 2002) (Kolaczkowski, 1999) (R.E. Hayes S. K., 1002) (R.E. Hayes S. K., 1996) (G. Groppi, 1995) (Tucci, 1982) (Parkinson, 1981), catalytic oxidation (T. Boger, 2005) (G. Veser, 2000) (C. Nicolella, 1998) (E. Zabar, 1982), hydrogenation or dehydrogenation (V.A. Sadykov, 2000) (A. Parmaliana, 1984) (A. Parmaliana M. S., 1983), and methanation (E.L. Sughrue, 1982) (G.A. Jarvi, 1980) (E.R. Tucci, 1979).

In recent studies, monoliths have been replacing multiphase (trickle-bed, slurry, etc.) reactors. The applications that have been proposed and explored include hydrodesulphurization of oil (D.S. Soni, 1981), liquefied coal (J. Scinta, 1977/1978), and debenzothiophene (R.K. Edvinsson, 1993). Hydrogenation or dehydrogenation of various aromatic compounds has also been carried out in monolith reactors (M.T. Kreutzer, 2005) (W. Liu, 2002) (T.A Nijhuis, 2002) (T.A Nijhuis, 2001) (X. Xu, 1996) (R.K. Edvinsson A. H., 1995) (V. Hatziantoniou, 1986) (V. Hatziantoniou B. A., 1984), as well as oxidation reactions (R.A. Edvinsson, 2001) (T.A. Patrick, 2000) (A.A. Klinghoffer, 1988) (L.L. Crynes, 1995).

Aside from the aforementioned experimental studies, there has also been a number of detailed modeling and simulation studies of monolith reactors. Young and Finlayson (L.C. Young, 1974), Ferguson and Finlayson (N.B. Ferguson, 1974), and Heck et al. (R.H. Heck, 1976), were among the first to carry out monolith reactor modeling. More recent contributions came from (Tomasic, 2007) (R.E. Hayes L. M., 2004) (G.N. Pontikakis, 2004) (H. Mei, 2006) (R.E. Hayes B. L., 2004) (G. Groppi E. T., 2001) (G.C. Koltsakis, 1997) (R. Jahn, 1997) (G. Groppi E. T., 1997), on both gas-phase and multiphase monolith reactors.

Particular issues related to monolith reactors, such as reactor construction/catalyst preparation, and mass/heat transfer effects, have been discussed by several investigators. Irandoust and Andersson (S. Irandoust, 1988) gave a summary on the use of monolith reactors in non-automobile applications; Kolaczkowski (Kolaczkowski, 1999) discussed challenges in kinetics, intra-phase diffusion effects, and the selection of mass and heat transfer coefficients; Groppi and Tronconi (G. Groppi E. T., 2005) discussed the use of catalysts with large thermal conductivity for gas-solid exothermic processes carried out in monolith reactors.

Another important consideration in monolith reactor modeling is single-channel versus multi-channel modeling. Pontikakis (G.N. Pontikakis, 2004) suggests that every channel in the reactor behaves exactly in the same way as the entire reactor. This remains true even in the presence of mass and heat transfer effects between the catalyst and the fluid. There are however certain conditions under which single channel modeling may not be adequate. These circumstances include non-uniform inlet gas distribution, or blocked/deactivated channels. In these situations the entire reactor should be modeled (A. James, 2003), and such models should be considered at the reactor level (G.N. Pontikakis, 2004). Mei et al, compared simulation results of single-channel and the whole reactor models, and found that the two cases gave valid simulations.

With the exception of (Meiet al. 2006),, none of the aforementioned models is 3-dimensional. In addition, none of the 3d models are solved analytically. This work therefore focuses on single-channel modeling and addresses both of the above literature shortcomings. First, a detailed 3-D mathematical model is developed and solved analytically. This is then followed with the formulation of an optimization problem whose solution identifies the optimal design of a 3-D monolith reactor.

3.2 Mathematical model of a 3-D monolith reactor

Consider a monolithic reactor consisting of an array of N rectangular channels each with length $L(m)$, width $2W(m)$, and height $2H(m)$. The reactor is fed with a stream with flowrate $F\left(\frac{m^3}{s}\right)$ and inlet concentrations of A equal to $C_A^{\,in}\left(\frac{mol}{m^3}\right)$.

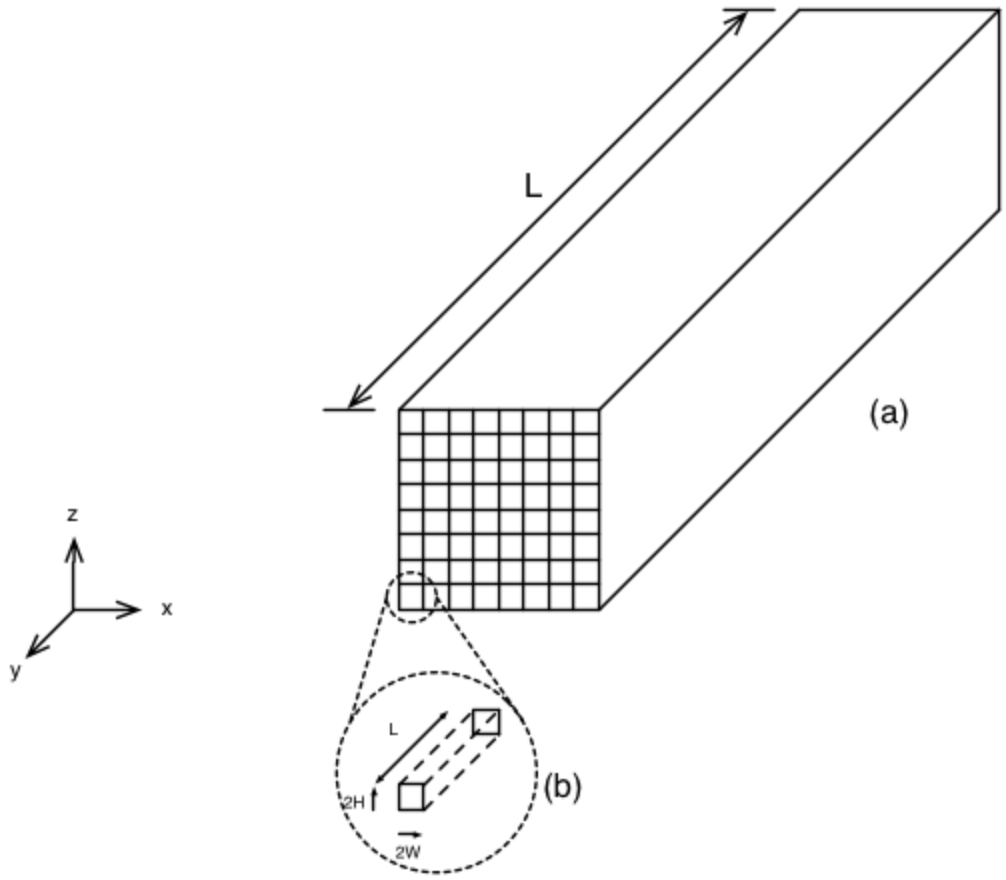

Figure 3-1 3-D Monolith Multi-channel Reactor

The surfaces of each rectangular channel are coated with a catalyst driving the irreversible surface reaction $A \xrightarrow{k} B$. Reaction may or may not occur in the bulk (gas control volume). It is assumed that each channel of the monolith reactor behaves in an identical manner to each other channel.

Normalization parameters:

$$x^* \triangleq \frac{x}{W}, y^* = \frac{y}{H}, z^* = \frac{z}{L}, C_A{}^* = \frac{C_A}{C_A{}^{in}}, S \triangleq \frac{kW}{D_A}, T \triangleq \frac{kH}{D_A}, U \triangleq \frac{kL}{D_A}, V \triangleq \frac{v_z}{k}, K \triangleq \frac{k'D_A}{k^2}, \quad (1)$$

Consider the first order irreversible surface reaction $A \xrightarrow{k} B$ taking place in an isothermal monolith reactor, both on each channel's internal surface and bulk interior. The reactor model consists of a species A balance, as shown below.

$$v_z \frac{\partial C_A(x,y,z)}{\partial z} = D_A \left(\frac{\partial^2 C_A(x,y,z)}{\partial x^2} + \frac{\partial^2 C_A(x,y,z)}{\partial y^2} + \frac{\partial^2 C_A(x,y,z)}{\partial z^2} \right) - k' C_A(x,y,z), \qquad (2)$$

with boundary conditions

$$C_A{}^{in} = C_A(x,y,0) - \frac{D_A}{v_z} \frac{\partial C_A}{\partial z}(x,y,0) \;\; \forall (x,y) \in [0,W] \times [0,H], \qquad (3)$$

$$\frac{\partial C_A}{\partial z}(x,y,L) = 0 \;\; \forall (x,y) \in [0,W] \times [0,H], \qquad (4)$$

$$\frac{\partial C_A}{\partial x}(0,y,z) = 0 \;\; \forall (y,z) \in [0,H] \times [0,L], \qquad (5)$$

$$0 = -kC_A(W,y,z) - D_A \frac{\partial C_A}{\partial x}(W,y,z) \;\; \forall (y,z) \in [0,H] \times [0,L], \qquad (6)$$

$$\frac{\partial C_A}{\partial y}(x,0,z) = 0 \;\; \forall (x,z) \in [0,W] \times [0,L], \qquad (7)$$

$$0 = -kC_A(x,H,z) - D_A \frac{\partial C_A}{\partial y}(x,H,z) \;\; \forall (x,z) \in [0,W] \times [0,L], \qquad (8)$$

Substitution of the above dimensionless variables yields the dimensionless equations:

$$\left\{ \begin{array}{l} \dfrac{v_z C_A{}^{in}}{L} \dfrac{\partial C_A{}^*}{\partial z^*} = \dfrac{D_A C_A{}^{in}}{W^2} \dfrac{\partial^2 C_A{}^*(x^*,y^*,z^*)}{\partial x^{*2}} + \dfrac{D_A C_A{}^{in}}{H^2} \dfrac{\partial^2 C_A{}^*(x^*,y^*,z^*)}{\partial y^{*2}} \\ + \dfrac{D_A C_A{}^{in}}{L^2} \dfrac{\partial^2 C_A{}^*(x^*,y^*,z^*)}{\partial z^{*2}} - k' C_A{}^{in} C_A{}^*(x^*,y^*,z^*) \end{array} \right\} \Leftrightarrow \qquad (9)$$

$$\left\{ \begin{array}{l} \dfrac{\partial C_A{}^*}{\partial z^*} = \dfrac{D_A L}{v_z W^2} \dfrac{\partial^2 C_A{}^*(x^*,y^*,z^*)}{\partial x^{*2}} + \dfrac{D_A L}{v_z H^2} \dfrac{\partial^2 C_A{}^*(x^*,y^*,z^*)}{\partial y^{*2}} + \\ + \dfrac{D_A}{v_z L} \dfrac{\partial^2 C_A{}^*(x^*,y^*,z^*)}{\partial z^{*2}} - \dfrac{k'L}{v_z} C_A{}^*(x^*,y^*,z^*) \end{array} \right\} \Leftrightarrow \qquad (10)$$

$$\boxed{\frac{\partial C_A^*}{\partial z^*}=\frac{1}{UV}\left(\frac{U}{S}\right)^2\frac{\partial^2 C_A^*\left(x^*,y^*,z^*\right)}{\partial x^{*2}}+\frac{1}{UV}\left(\frac{U}{T}\right)^2\frac{\partial^2 C_A^*\left(x^*,y^*,z^*\right)}{\partial y^{*2}}+ +\frac{1}{UV}\frac{\partial^2 C_A^*\left(x^*,y^*,z^*\right)}{\partial z^{*2}}-\frac{UK}{V}C_A^*\left(x^*,y^*,z^*\right)} \quad (11)$$

The boundary conditions for these equations in dimensionless form are:

$$1=C_A^*\left(x^*,y^*,0\right)-\frac{1}{UV}\frac{\partial C_A^*}{\partial z^*}\left(x^*,y^*,0\right)\ \forall\left(x^*,y^*\right)\in[0,1]\times[0,1], \quad (12)$$

$$\frac{\partial C_A^*}{\partial z^*}\left(x^*,y^*,1\right)=0\ \forall\left(x^*,y^*\right)\in[0,1]\times[0,1], \quad (13)$$

$$\frac{\partial C_A^*}{\partial x^*}\left(0,y^*,z^*\right)=0\ \forall\left(y^*,z^*\right)\in[0,1]\times[0,1], \quad (14)$$

$$0=-SC_A^*\left(1,y^*,z^*\right)-\frac{\partial C_A^*}{\partial x^*}\left(1,y^*,z^*\right)\ \forall\left(y^*,z^*\right)\in[0,1]\times[0,1] \quad (15)$$

$$\frac{\partial C_A^*}{\partial y^*}\left(x^*,0,z^*\right)=0\ \forall\left(x^*,z^*\right)\in[0,1]\times[0,1], \quad (16)$$

$$0=-TC_A^*\left(x^*,1,z^*\right)-\frac{\partial C_A^*}{\partial y^*}\left(x^*,1,z^*\right)\ \forall\left(x^*,z^*\right)\in[0,1]\times[0,1] \quad (17)$$

Consider that $C_A^*\left(x^*,y^*,z^*\right)=\bar{C}_A^*\left(x^*\right)\hat{C}_A^*\left(y^*\right)\tilde{C}_A^*\left(z^*\right)$. Then dividing by $\bar{C}_A^*\left(x^*\right)\hat{C}_A^*\left(y^*\right)\tilde{C}_A^*\left(z^*\right)$ and rearranging terms the governing equation becomes

$$\frac{UK}{V}+\frac{d\tilde{C}_A^*\left(z^*\right)}{dz^*}\frac{1}{\tilde{C}_A^*\left(z^*\right)}=\frac{1}{UV}\left(\begin{array}{l}\left(\frac{U}{S}\right)^2\frac{d^2\bar{C}_A^*\left(x^*\right)}{dx^{*2}}\frac{1}{\bar{C}_A^*\left(x^*\right)}+\left(\frac{U}{T}\right)^2\frac{d^2\hat{C}_A^*\left(y^*\right)}{dy^{*2}}\frac{1}{\hat{C}_A^*\left(y^*\right)}+\\ +\frac{d^2\tilde{C}_A^*\left(z^*\right)}{dz^{*2}}\frac{1}{\tilde{C}_A^*\left(z^*\right)}\end{array}\right)\Leftrightarrow$$

$$U^2K+UV\frac{d\tilde{C}_A^*\left(z^*\right)}{dz^*}\frac{1}{\tilde{C}_A^*\left(z^*\right)}-\frac{d^2\tilde{C}_A^*\left(z^*\right)}{dz^{*2}}\frac{1}{\tilde{C}_A^*\left(z^*\right)}= \quad (18)$$

$$\left(\frac{U}{S}\right)^2\frac{d^2\bar{C}_A^*\left(x^*\right)}{dx^{*2}}\frac{1}{\bar{C}_A^*\left(x^*\right)}+\left(\frac{U}{T}\right)^2\frac{d^2\hat{C}_A^*\left(y^*\right)}{dy^{*2}}\frac{1}{\hat{C}_A^*\left(y^*\right)}$$

Since the right hand side is a function of x and y, and the left hand side is a function of z, they must both be equal to a constant. Then

$$\left\{\begin{array}{ll} -\frac{d^2\tilde{C}_A^{\,*}\left(z^*\right)}{dz^{*2}}\frac{1}{\tilde{C}_A^{\,*}\left(z^*\right)}+UV\frac{d\tilde{C}_A^{\,*}\left(z^*\right)}{dz^*}\frac{1}{\tilde{C}_A^{\,*}\left(z^*\right)}+U^2K=-\lambda & (1) \\ \left(\frac{U}{S}\right)^2\frac{d^2\bar{C}_A^{\,*}\left(x^*\right)}{dx^{*2}}\frac{1}{\bar{C}_A^{\,*}\left(x^*\right)}+\left(\frac{U}{T}\right)^2\frac{d^2\hat{C}_A^{\,*}\left(y^*\right)}{dy^{*2}}\frac{1}{\hat{C}_A^{\,*}\left(y^*\right)}=-\lambda & (2) \end{array}\right\}\Leftrightarrow \qquad (19)$$

$$\left\{\begin{array}{ll} -\frac{d^2\tilde{C}_A^{\,*}\left(z^*\right)}{dz^{*2}}\frac{1}{\tilde{C}_A^{\,*}\left(z^*\right)}+UV\frac{d\tilde{C}_A^{\,*}\left(z^*\right)}{dz^*}\frac{1}{\tilde{C}_A^{\,*}\left(z^*\right)}+U^2K=-\lambda & (1^*) \\ \left(\frac{U}{S}\right)^2\frac{d^2\bar{C}_A^{\,*}\left(x^*\right)}{dx^{*2}}\frac{1}{\bar{C}_A^{\,*}\left(x^*\right)}=-\lambda-\left(\frac{U}{T}\right)^2\frac{d^2\hat{C}_A^{\,*}\left(y^*\right)}{dy^{*2}}\frac{1}{\hat{C}_A^{\,*}\left(y^*\right)} & (2^*) \end{array}\right\}\Leftrightarrow$$

Since the left hand side of (2^*) is now only a function of x, and the right hand side is only a function of y, they must also both be equal to a constant. Then

$$\left\{\begin{array}{ll} -\frac{d^2\tilde{C}_A^{\,*}\left(z^*\right)}{dz^{*2}}\frac{1}{\tilde{C}_A^{\,*}\left(z^*\right)}+UV\frac{d\tilde{C}_A^{\,*}\left(z^*\right)}{dz^*}\frac{1}{\tilde{C}_A^{\,*}\left(z^*\right)}+U^2K=-\lambda & (1^*) \\ \left(\frac{U}{S}\right)^2\frac{d^2\bar{C}_A^{\,*}\left(x^*\right)}{dx^{*2}}\frac{1}{\bar{C}_A^{\,*}\left(x^*\right)}=-\mu & (2a) \\ -\lambda-\left(\frac{U}{T}\right)^2\frac{d^2\hat{C}_A^{\,*}\left(y^*\right)}{dy^{*2}}\frac{1}{\hat{C}_A^{\,*}\left(y^*\right)}=-\mu & (2b) \end{array}\right\}\Leftrightarrow \qquad (20)$$

$$\left\{\begin{array}{ll} -\frac{d^2\tilde{C}_A^{\,*}\left(z^*\right)}{dz^{*2}}+UV\frac{d\tilde{C}_A^{\,*}\left(z^*\right)}{dz^*}+\left(U^2K+\lambda\right)\tilde{C}_A^{\,*}\left(z^*\right)=0 & (1^*) \\ \left(\frac{U}{S}\right)^2\frac{d^2\bar{C}_A^{\,*}\left(x^*\right)}{dx^{*2}}+\mu\bar{C}_A^{\,*}\left(x^*\right)=0 & (2a) \\ \left(\frac{U}{T}\right)^2\frac{d^2\hat{C}_A^{\,*}\left(y^*\right)}{dy^{*2}}+\left(\lambda-\mu\right)\hat{C}_A^{\,*}\left(y^*\right)=0 & (2b) \end{array}\right\} \qquad (21)$$

In a similar manner the problem boundary conditions on $C_A^{\,*}$ become:

$$\boxed{1=\bar{C}_A^{\,*}\left(x^*\right)\hat{C}_A^{\,*}\left(y^*\right)\tilde{C}_A^{\,*}(0)-\frac{1}{UV}\bar{C}_A^{\,*}\left(x^*\right)\hat{C}_A^{\,*}\left(y^*\right)\frac{d\tilde{C}_A^{\,*}}{dz^*}(0)\ \ \forall\left(x^*,y^*\right)\in[0,1]\times[0,1]} \qquad (22)$$

$$\bar{C}_A^{\,*}\left(x^*\right)\hat{C}_A^{\,*}\left(y^*\right)\frac{d\tilde{C}_A^{\,*}}{dz^*}(1)=0\ \forall\left(x^*,y^*\right)\in[0,1]\times[0,1]\underset{\hat{C}_A^{\,*}\left(y^*\right)\neq 0\ \forall y^*\in[0,1]}{\overset{\bar{C}_A^{\,*}\left(x^*\right)\neq 0\ \forall x^*\in[0,1]}{\Leftrightarrow}}\boxed{\frac{d\tilde{C}_A^{\,*}}{dz^*}(1)=0}$$

$$\frac{d\bar{C}_A^{\,*}}{dx^*}(0)\hat{C}_A^{\,*}\left(y^*\right)\tilde{C}_A^{\,*}\left(z^*\right)=0\ \ \forall\left(y^*,z^*\right)\in[0,1]\times[0,1]\underset{\hat{C}_A^{\,*}\left(y^*\right)\neq 0\ \forall y^*\in[0,1]}{\overset{\tilde{C}_A^{\,*}\left(z^*\right)\neq 0\ \forall z^*\in[0,1]}{\Leftrightarrow}}\boxed{\frac{d\bar{C}_A^{\,*}}{dx^*}(0)=0}$$

$$0=\left[-S\bar{C}_A^{\,*}(1)-\frac{d\bar{C}_A^{\,*}}{dx^*}(1)\right]\hat{C}_A^{\,*}\left(y^*\right)\tilde{C}_A^{\,*}\left(z^*\right)\ \ \forall\left(y^*,z^*\right)\in[0,1]\times[0,1]\underset{\hat{C}_A^{\,*}\left(y^*\right)\neq 0\ \forall y^*\in[0,1]}{\overset{\tilde{C}_A^{\,*}\left(z^*\right)\neq 0\ \forall z^*\in[0,1]}{\Leftrightarrow}}$$

$$\boxed{-S\bar{C}_A^{\,*}(1)-\frac{d\bar{C}_A^{\,*}}{dx^*}(1)=0}$$

$$\bar{C}_A^{\,*}\left(x^*\right)\frac{d\hat{C}_A^{\,*}}{dy^*}(0)\tilde{C}_A\left(z^*\right)=0\ \ \forall\left(x^*,z^*\right)\in[0,1]\times[0,1]\underset{\bar{C}_A^{\,*}\left(x^*\right)\neq 0\ \forall x^*\in[0,1]}{\overset{\tilde{C}_A^{\,*}\left(z^*\right)\neq 0\ \forall z^*\in[0,1]}{\Leftrightarrow}}\boxed{\frac{d\hat{C}_A^{\,*}}{dy^*}(0)=0}$$

$$0=\left[-T\hat{C}_A^{\,*}(1)-\frac{d\hat{C}_A^{\,*}}{dy^*}(1)=0\right]\bar{C}_A^{\,*}\left(x^*\right)\tilde{C}_A^{\,*}\left(z^*\right)\ \ \forall\left(x^*,z^*\right)\in[0,1]\times[0,1]\underset{\bar{C}_A^{\,*}\left(x^*\right)\neq 0\ \forall x^*\in[0,1]}{\overset{\tilde{C}_A^{\,*}\left(z^*\right)\neq 0\ \forall z^*\in[0,1]}{\Leftrightarrow}}$$

$$\boxed{-T\hat{C}_A^{\,*}(1)-\frac{d\hat{C}_A^{\,*}}{dy^*}(1)=0}$$

Solution of equation $(2a)$ leads us to consider the following three cases regarding the sign of μ :

Case1: $\boxed{\mu=0}$ Then, equation $(2a)$ becomes

$\frac{d^2\bar{C}_A^{\,*}}{dx^{*2}}=0\Rightarrow\bar{C}_A^{\,*}\left(x^*\right)=c_1x^*+c_2$. Application of the boundary conditions $\frac{d\bar{C}_A^{\,*}}{dx^*}(0)=0$,

$-S\bar{C}_A^{\,*}(1)-\frac{d\bar{C}_A^{\,*}}{dx^*}(1)=0$ then yields $c_1=0$, $c_2=0$ which yields a trivial solution $\boxed{\bar{C}_A^{\,*}\left(x^*\right)=0}$.

Case2: $\boxed{\mu\triangleq-\kappa^2<0,\ \kappa>0}$ Then, equation $(2a)$ becomes

$\left(\frac{U}{S}\right)^2 \frac{d^2\bar{C}_A^{\,*}\left(x^*\right)}{dx^{*2}} - \kappa^2 \bar{C}_A^{\,*}\left(x^*\right) = 0 \Leftrightarrow \frac{d^2\bar{C}_A^{\,*}\left(x^*\right)}{dx^{*2}} - \kappa^2 \left(\frac{S}{U}\right)^2 \bar{C}_A^{\,*}\left(x^*\right) = 0 \ (2a)$, which has the general solution $\bar{C}_A^{\,*}\left(x^*\right) = c_1 e^{\kappa\left(\frac{S}{U}\right)x^*} + c_2 e^{-\kappa\left(\frac{S}{U}\right)x^*}$, and first derivative $\frac{d\bar{C}_A^{\,*}}{dx^*}\left(x^*\right) = \kappa\left(\frac{S}{U}\right)c_1 e^{\kappa\left(\frac{S}{U}\right)x^*} - \kappa\left(\frac{S}{U}\right)c_2 e^{-\kappa\left(\frac{S}{U}\right)x^*}$. Application of the boundary conditions $\frac{d\bar{C}_A^{\,*}}{dx^*}(0) = 0, -S\bar{C}_A^{\,*}(1) - \frac{d\bar{C}_A^{\,*}}{dx^*}(1) = 0$ then yields

$$\left\{\begin{array}{l} c_1 = c_2 \\ -S\left(c_1 e^{\kappa\left(\frac{S}{U}\right)} + c_2 e^{-\kappa\left(\frac{S}{U}\right)}\right) - \left(\kappa\left(\frac{S}{U}\right)c_1 e^{\kappa\left(\frac{S}{U}\right)} - \kappa\left(\frac{S}{U}\right)c_2 e^{-\kappa\left(\frac{S}{U}\right)}\right) = 0 \end{array}\right\} \Leftrightarrow$$

$$\left\{\begin{array}{l} c_2 = c_1 \\ c_1 = 0 \vee \dfrac{\kappa\dfrac{S}{U} - S}{\kappa\dfrac{S}{U} + S} = e^{2\kappa\frac{S}{U}} \end{array}\right\} \underset{\frac{\kappa\frac{S}{U} - S}{\kappa\frac{S}{U} + S} < 1}{\overset{e^{2\kappa\frac{S}{U}} > 1}{\Leftrightarrow}} \boxed{c_1 = c_2 = 0}$$ which yields a trivial solution $\boxed{\bar{C}_A^{\,*}\left(x^*\right) = 0}$.

Case3: $\boxed{\mu > 0}$ Define $\boxed{\kappa^2 \triangleq \mu > 0,\ \kappa > 0}$. Then, equation $(2a)$ becomes

$\left(\frac{U}{S}\right)^2 \frac{d^2\bar{C}_A^{\,*}\left(x^*\right)}{dx^{*2}} + \kappa^2 \bar{C}_A^{\,*}\left(x^*\right) = 0 \Leftrightarrow \ \frac{d^2\bar{C}_A^{\,*}\left(x^*\right)}{dx^{*2}} + \kappa^2 \left(\frac{S}{U}\right)^2 \bar{C}_A^{\,*}\left(x^*\right) = 0 \Leftrightarrow$
$\frac{d^2\bar{C}_A^{\,*}\left(x^*\right)}{dx^{*2}} + \left(\kappa\left(\frac{S}{U}\right)\right)^2 \bar{C}_A^{\,*}\left(x^*\right) = 0$, whose general solution is

$$\bar{C}_A^{\,*}\left(x^*\right) = c_1 \cos\left(\kappa\left(\frac{S}{U}\right)x^*\right) + c_2 \sin\left(\kappa\left(\frac{S}{U}\right)x^*\right)$$

Then the boundary conditions $\frac{d\bar{C}_A^{\,*}}{dx^*}(0) = 0, -S\bar{C}_A^{\,*}(1) - \frac{d\bar{C}_A^{\,*}}{dx^*}(1) = 0$ become

$-c_1\kappa\left(\frac{S}{U}\right)\sin(0)+c_2\kappa\left(\frac{S}{U}\right)\cos(0)=0$ and

$$-S\left(c_1\cos\left(\kappa\left(\frac{S}{U}\right)\right)+c_2\sin\left(\kappa\left(\frac{S}{U}\right)\right)\right)-\left(-c_1\kappa\left(\frac{S}{U}\right)\sin\left(\kappa\left(\frac{S}{U}\right)\right)+c_2\kappa\left(\frac{S}{U}\right)\cos\left(\kappa\left(\frac{S}{U}\right)\right)\right)=0$$

respectively. Since $\kappa>0$, the above two equations admit the nontrivial solution:

$$\boxed{\bar{C}_A^{\,*}\left(x^*\right)=\cos\left(\kappa\left(\frac{S}{U}\right)x^*\right)\wedge\kappa\left(\frac{S}{U}\right)\tan\left(\kappa\left(\frac{S}{U}\right)\right)=S} \tag{23}$$

To investigate equation $(2b)$ along with $\boxed{\mu>0}$ we have the following 3 cases:

Case3A: $\boxed{\lambda>\mu>0}$ Define $\boxed{\nu^2\triangleq\lambda-\mu>0,\ \nu>0}$.

Then equation $(2b)$ becomes $\left(\frac{U}{T}\right)^2\frac{d^2\hat{C}_A^{\,*}\left(y^*\right)}{dy^{*2}}+\nu^2\hat{C}_A^{\,*}\left(y^*\right)=0\Leftrightarrow$

$\frac{d^2\hat{C}_A^{\,*}\left(y^*\right)}{dy^{*2}}+\left(\nu\left(\frac{T}{U}\right)\right)^2\hat{C}_A^{\,*}\left(y^*\right)=0$. Its general solution is

$$\hat{C}_A^{\,*}\left(y^*\right)=b_1\cos\left(\nu\left(\frac{T}{U}\right)y^*\right)+b_2\sin\left(\nu\left(\frac{T}{U}\right)y^*\right)\Leftrightarrow$$

$\frac{d\hat{C}_A^{\,*}}{dy^*}\left(y^*\right)=-b_1\nu\left(\frac{T}{U}\right)\sin\left(\nu\left(\frac{T}{U}\right)y^*\right)+b_2\nu\left(\frac{T}{U}\right)\cos\left(\nu\left(\frac{T}{U}\right)y^*\right)$. Application of the boundary conditions $\frac{d\hat{C}_A^{\,*}}{dy^*}(0)=0$, $0=-T\hat{C}_A^{\,*}(1)-\frac{d\hat{C}_A^{\,*}}{dy^*}(1)$ then yields:

$$\left\{\begin{array}{l}-b_1\nu\left(\frac{T}{U}\right)\sin\left(\nu\left(\frac{T}{U}\right)0\right)+b_2\nu\left(\frac{T}{U}\right)\cos\left(\nu\left(\frac{T}{U}\right)0\right)=0\\ -T\left(b_1\cos\left(\nu\left(\frac{T}{U}\right)\right)+b_2\sin\left(\nu\left(\frac{T}{U}\right)\right)\right)-\left(-b_1\nu\left(\frac{T}{U}\right)\sin\left(\nu\left(\frac{T}{U}\right)\right)+b_2\nu\left(\frac{T}{U}\right)\cos\left(\nu\left(\frac{T}{U}\right)\right)\right)=0\end{array}\right\}\Leftrightarrow$$

$$\left\{\left\{\begin{array}{l}b_2=0\\ b_1=0\end{array}\right\}\vee\left\{\begin{array}{l}b_2=0\\ b_1\neq 0\ \wedge -T\cos\left(\nu\left(\frac{T}{U}\right)\right)+\nu\left(\frac{T}{U}\right)\sin\left(\nu\left(\frac{T}{U}\right)\right)=0\end{array}\right\}\right\}. \tag{24}$$

The nontrivial solution of this set of two equations is

$$\boxed{\hat{C}_A^{\,*}\left(y^*\right)=\cos\left(\nu\left(\frac{T}{U}\right)y^*\right)\wedge\nu\left(\frac{T}{U}\right)\tan\left(\nu\left(\frac{T}{U}\right)\right)=T} \tag{25}$$

Case3B: $\boxed{\lambda=\mu>0}$ then equation $(2b)$ becomes:

$\frac{d^2\hat{C}_A^{\,*}\left(y^*\right)}{dy^{*2}}=0\Rightarrow\hat{C}_A^{\,*}\left(y^*\right)=c_1y^*+c_2$. Application of the boundary conditions $\frac{d\hat{C}_A^{\,*}}{dy^*}(0)=0$,

$-T\hat{C}_A^{\,*}(1)-\frac{d\hat{C}_A^{\,*}}{dy^*}(1)=0$ then yields $c_1=0$, $c_2=0$ which yields a trivial solution $\boxed{\hat{C}_A^{\,*}\left(y^*\right)=0}$.

Case3C: $\boxed{\mu>0\wedge\mu>\lambda}$ Define $\boxed{\nu^2\triangleq\mu-\lambda>0,\ \nu>0}$. Then equation $(2b)$ becomes

$$\left(\frac{U}{T}\right)^2\frac{d^2\hat{C}_A^{\,*}\left(y^*\right)}{dy^{*2}}-\nu^2\hat{C}_A^{\,*}\left(y^*\right)=0\Leftrightarrow\frac{d^2\hat{C}_A^{\,*}\left(y^*\right)}{dy^{*2}}-\nu^2\left(\frac{T}{U}\right)^2\hat{C}_A^{\,*}\left(y^*\right)=0\quad(2b).$$

Then the general solution of $(2b)$ can be written as: $\hat{C}_A^{\,*}\left(y^*\right)=c_1e^{\left(\nu\left(\frac{T}{U}\right)y^*\right)}+c_2e^{-\left(\nu\left(\frac{T}{U}\right)y^*\right)}\Rightarrow$

$$\frac{d\hat{C}_A^{\,*}\left(y^*\right)}{dy^*}=\nu\left(\frac{T}{U}\right)c_1e^{\left(\nu\left(\frac{T}{U}\right)y^*\right)}-\nu\left(\frac{T}{U}\right)c_2e^{-\left(\nu\left(\frac{T}{U}\right)y^*\right)}.$$

With the boundary conditions $\frac{d\hat{C}_A^{\,*}}{dy^*}(0)=0$, $-T\hat{C}_A^{\,*}(1)-\frac{d\hat{C}_A^{\,*}}{dy^*}(1)=0$, it then holds

$$\left\{\begin{array}{l}c_1=c_2\\ -T\left(c_1e^{\nu\left(\frac{T}{U}\right)}+c_2e^{-\nu\left(\frac{T}{U}\right)}\right)-\nu\left(\frac{T}{U}\right)\left(c_1e^{\nu\left(\frac{T}{U}\right)}-c_2e^{-\nu\left(\frac{T}{U}\right)}\right)=0\end{array}\right\}\Leftrightarrow$$

$$\left\{\begin{array}{l}c_2=c_1\\ c_1=0\vee\dfrac{\nu\left(\frac{T}{U}\right)-T}{\nu\left(\frac{T}{U}\right)+T}=e^{2\nu\left(\frac{T}{U}\right)}\end{array}\right\}\begin{array}{c}\frac{\nu\left(\frac{T}{U}\right)-T}{\nu\left(\frac{T}{U}\right)+T}<1\\ \Leftrightarrow\\ e^{2\nu\left(\frac{T}{U}\right)}>1\end{array}\ \boxed{c_1=c_2=0}$$ which yields a trivial solution $\boxed{\hat{C}_A^{\,*}\left(y^*\right)=0}$.

Case3A is the only one that yields nontrivial solutions for equations $(2a)$ and $(2b)$. It is thus for only this case that solutions for equation (1) are sought. It then holds $\boxed{\mu \triangleq \kappa^2 > 0,\ \kappa > 0}$, and $\boxed{\nu^2 \triangleq \lambda - \mu > 0,\ \nu > 0}$. Then $\boxed{\lambda \triangleq \nu^2 + \kappa^2,\ \nu > 0, \kappa > 0}$

Equation (1^*) then becomes

$$-\frac{d^2\tilde{C}_A^{\,*}\left(z^*\right)}{dz^{*2}} + UV\frac{d\tilde{C}_A^{\,*}\left(z^*\right)}{dz^*} + \left(U^2K + \nu^2 + \kappa^2\right)\tilde{C}_A^{\,*}\left(z^*\right) = 0 \qquad (1^*)$$

The general solution of equation (1^*) has the form $\tilde{C}_A^{\,*}\left(z^*\right) = A_1 e^{\rho_1 z^*} + A_2 e^{\rho_2 z^*} \Rightarrow$

$\frac{d\tilde{C}_A^{\,*}\left(z^*\right)}{dz^*} = A_1\rho_1 e^{\rho_1 z^*} + A_2\rho_2 e^{\rho_2 z^*}$, where

$$\rho_{1,2} = \frac{-1}{2}\left[-UV \pm \sqrt{(UV)^2 + 4\left(U^2K + \nu^2 + \kappa^2\right)}\right] = \frac{UV}{2} \mp \sqrt{\left(\frac{UV}{2}\right)^2 + \left(U^2K + \nu^2 + \kappa^2\right)}.$$

Application of the boundary condition $\boxed{\frac{d\tilde{C}_A^{\,*}}{dz^*}(1) = 0}$ then yields $A_2 = -A_1\frac{\rho_1}{\rho_2}e^{(\rho_1 - \rho_2)}$. Satisfaction of the last boundary condition at $z = 0$ is then pursued by first taking the superposition of all obtained separable solutions as follows:

$$\boxed{C_A^{\,*}\left(x^*, y^*, z^*\right) = \sum_{n=0}^{\infty}\sum_{m=0}^{\infty} A_{n,m}\left(e^{\rho_{1,n,m}z^*} - \frac{\rho_{1,n,m}}{\rho_{2,n,m}}e^{(\rho_{1,n,m} - \rho_{2,n,m})}e^{\rho_{2,n,m}z^*}\right)\cos\left(\kappa_n\left(\frac{S}{U}\right)x^*\right)\left(\cos\left(\nu_m\left(\frac{T}{U}\right)y^*\right)\right)} \quad (26)$$

where

$$\boxed{\rho_{1,n.m} \triangleq \frac{UV}{2} - \sqrt{\left(\frac{UV}{2}\right)^2 + \left(U^2K + {\nu_m}^2 + {\kappa_n}^2\right)} < \rho_{2,n.m} \triangleq \frac{UV}{2} + \sqrt{\left(\frac{UV}{2}\right)^2 + \left(U^2K + {\nu_m}^2 + {\kappa_n}^2\right)}} \quad (27)$$

$$\boxed{\kappa_n\left(\frac{S}{U}\right)\tan\left(\kappa_n\left(\frac{S}{U}\right)\right) = S \ \ n = 0,1,\cdots\infty}, \ \boxed{\nu_m\left(\frac{T}{U}\right)\tan\left(\nu_m\left(\frac{T}{U}\right)\right) = T \ \ m = 0,1,\cdots\infty} \qquad (28)$$

The boundary condition

$$1 = C_A^{\,*}\left(x^*, y^*, 0\right) - \frac{1}{UV}\frac{\partial C_A^{\,*}}{\partial z^*}\left(x^*, y^*, 0\right) \;\; \forall\left(x^*, y^*\right) \in [0,1]\times[0,1] \tag{29}$$

then requires that

$$1 = \sum_{n=0}^{\infty}\sum_{m=0}^{\infty} A_{n,m}\left(1 - \frac{\rho_{1,n,m}}{\rho_{2,n,m}} e^{\left(\rho_{1,n,m}-\rho_{2,n,m}\right)}\right)\cos\left(\kappa_n\left(\frac{S}{U}\right)x^*\right)\left(\cos\left(\nu_m\left(\frac{T}{U}\right)y^*\right)\right)$$

$$-\frac{1}{UV}\sum_{n=0}^{\infty}\sum_{m=0}^{\infty} A_{n,m}\rho_{1,n,m}\left(1 - e^{\left(\rho_{1,n,m}-\rho_{2,n,m}\right)}\right)\cos\left(\kappa_n\left(\frac{S}{U}\right)x^*\right)\left(\cos\left(\nu_m\left(\frac{T}{U}\right)y^*\right)\right)$$

$$\forall\left(x^*, y^*\right) \in [0,1]\times[0,1] \;\Rightarrow$$

$$\boxed{1 = \left\{\sum_{n=0}^{\infty}\sum_{m=0}^{\infty} A_{n,m}\left[1 - \frac{\rho_{1,n,m}}{UV} + \left(\frac{1}{UV} - \frac{1}{\rho_{2,n,m}}\right)\rho_{1,n,m} e^{\left(\rho_{1,n,m}-\rho_{2,n,m}\right)}\right]\cos\left(\kappa_n\left(\frac{S}{U}\right)x^*\right)\left(\cos\left(\nu_m\left(\frac{T}{U}\right)y^*\right)\right)\right\}} \tag{30}$$

$$\forall\left(x^*, y^*\right) \in [0,1]\times[0,1]$$

However, $\forall q = 0,1,\cdots\infty \quad \forall p = 0,1,\cdots\infty$ it holds

$$\boxed{\kappa_q\left(\frac{S}{U}\right)\tan\left(\kappa_q\left(\frac{S}{U}\right)\right) = S \;\; q = 0,1,\cdots\infty}, \tag{31}$$

$$\boxed{\nu_p\left(\frac{T}{U}\right)\tan\left(\nu_p\left(\frac{T}{U}\right)\right) = T \;\; p = 0,1,\cdots\infty} \tag{32}$$

Then

$$\int_0^1\int_0^1 \cos\left(\kappa_q\left(\frac{S}{U}\right)x^*\right)\cos\left(\nu_p\left(\frac{T}{U}\right)y^*\right)dx^*dy^* =$$

$$\int_0^1\int_0^1 \left[\left[\sum_{n=0}^{\infty}\sum_{m=0}^{\infty} A_{n,m}\left[1 - \frac{\rho_{1,n,m}}{UV} + \left(\frac{1}{UV} - \frac{1}{\rho_{2,n,m}}\right)\rho_{1,n,m} e^{\left(\rho_{1,n,m}-\rho_{2,n,m}\right)}\right]\cos\left(\kappa_n\left(\frac{S}{U}\right)x^*\right)\cos\left(\nu_m\left(\frac{T}{U}\right)y^*\right)\right]\right] dx^*dy^* \Leftrightarrow$$

$$\left[\cos\left(\kappa_q\left(\frac{S}{U}\right)x^*\right)\cos\left(\nu_p\left(\frac{T}{U}\right)y^*\right)\right]$$

$$\int_0^1\int_0^1 \cos\left(\kappa_q\left(\frac{S}{U}\right)x^*\right)\cos\left(\nu_p\left(\frac{T}{U}\right)y^*\right)dx^*dy^* =$$

$$=\sum_{n=0}^{\infty}\sum_{m=0}^{\infty}\left[\begin{array}{l} A_{n,m}\left[1-\frac{\rho_{1,n,m}}{UV}+\left(\frac{1}{UV}-\frac{1}{\rho_{2,n,m}}\right)\rho_{1,n,m}e^{\left(\rho_{1,n,m}-\rho_{2,n,m}\right)}\right] \\ \int_0^1\int_0^1 \cos\left(\kappa_n\left(\frac{S}{U}\right)x^*\right)\cos\left(\nu_m\left(\frac{T}{U}\right)y^*\right)\cos\left(\kappa_q\left(\frac{S}{U}\right)x^*\right)\cos\left(\nu_p\left(\frac{T}{U}\right)y^*\right)dx^*dy^* \end{array}\right]\Leftrightarrow$$

$$\left[\int_0^1 \cos\left(\kappa_q\left(\frac{S}{U}\right)x^*\right)dx^*\right]\left[\int_0^1 \cos\left(\nu_p\left(\frac{T}{U}\right)y^*\right)dy^*\right] =$$

$$=\sum_{n=0}^{\infty}\sum_{m=0}^{\infty}\left[\begin{array}{l} A_{n,m}\left[1-\frac{\rho_{1,n,m}}{UV}+\left(\frac{1}{UV}-\frac{1}{\rho_{2,n,m}}\right)\rho_{1,n,m}e^{\left(\rho_{1,n,m}-\rho_{2,n,m}\right)}\right] \\ \left[\int_0^1 \cos\left(\kappa_n\left(\frac{S}{U}\right)x^*\right)\cos\left(\kappa_q\left(\frac{S}{U}\right)x^*\right)dx^*\right]\left[\int_0^1\left(\cos\left(\nu_m\left(\frac{T}{U}\right)y^*\right)\right)\left(\cos\left(\nu_p\left(\frac{T}{U}\right)y^*\right)\right)dy^*\right] \end{array}\right]\Leftrightarrow$$ It

holds however

$$\int_0^1 \cos\left(\kappa_q\left(\frac{S}{U}\right)x^*\right)dx^* = \frac{1}{\kappa_q\left(\frac{S}{U}\right)}\int_0^1 \cos\left(\kappa_q\left(\frac{S}{U}\right)x^*\right)\kappa_q\left(\frac{S}{U}\right)dx^* = \frac{1}{\kappa_q\left(\frac{S}{U}\right)}\int_0^{\kappa_q\left(\frac{S}{U}\right)} \cos\left(\hat{x}\right)d\hat{x} =$$

$$=\frac{1}{\kappa_q\left(\frac{S}{U}\right)}\left[\sin\left(\hat{x}\right)\right]_0^{\kappa_q\left(\frac{S}{U}\right)} = \frac{\sin\left(\kappa_q\left(\frac{S}{U}\right)\right)}{\kappa_q\left(\frac{S}{U}\right)}$$

Similarly

$$\int_0^1 \cos\left(\nu_p\left(\frac{T}{U}\right)y^*\right)dy^* = \frac{\sin\left(\nu_p\left(\frac{T}{U}\right)\right)}{\nu_p\left(\frac{T}{U}\right)}$$

In addition it holds:

$$\int_0^1 \cos\left(\kappa_n\left(\frac{S}{U}\right)x^*\right)\cos\left(\kappa_q\left(\frac{S}{U}\right)x^*\right)dx^* = \frac{\int_0^1 \cos\left(\kappa_n\left(\frac{S}{U}\right)x^*\right)\cos\left(\frac{\kappa_q}{\kappa_n}\kappa_n\left(\frac{S}{U}\right)x^*\right)\kappa_n\left(\frac{S}{U}\right)d\left(x^*\right)}{\kappa_n\left(\frac{S}{U}\right)} =$$

$$= \frac{\int_0^{\kappa_n\left(\frac{S}{U}\right)} \cos\left(\hat{x}\right)\cos\left(\frac{\kappa_q}{\kappa_n}\hat{x}\right)d\hat{x}}{\kappa_n\left(\frac{S}{U}\right)} = \frac{\left\{\begin{array}{ll} \frac{\frac{\kappa_q}{\kappa_n}\cos\left(\hat{x}\right)\sin\left(\frac{\kappa_q}{\kappa_n}\hat{x}\right)-\sin\left(\hat{x}\right)\cos\left(\frac{\kappa_q}{\kappa_n}\hat{x}\right)}{\left(\frac{\kappa_q}{\kappa_n}\right)^2-1} & if\ \frac{\kappa_q}{\kappa_n}\notin\{-1,1\} \\ \frac{\hat{x}}{2}+\frac{1}{2}\sin\left(\hat{x}\right)\cos\left(\hat{x}\right) & if\ \frac{\kappa_q}{\kappa_n}\in\{-1,1\} \end{array}\right\}\Bigg|_0^{\kappa_n\left(\frac{S}{U}\right)}}{\kappa_n\left(\frac{S}{U}\right)} \underset{\kappa_q>0}{\overset{\kappa_n>0}{=}}$$

$$= \frac{\left\{\begin{array}{ll} \frac{\frac{\kappa_q}{\kappa_n}\cos\left(\kappa_n\left(\frac{S}{U}\right)\right)\sin\left(\frac{\kappa_q}{\kappa_n}\kappa_n\left(\frac{S}{U}\right)\right)-\sin\left(\kappa_n\left(\frac{S}{U}\right)\right)\cos\left(\frac{\kappa_q}{\kappa_n}\kappa_n\left(\frac{S}{U}\right)\right)}{\left(\frac{\kappa_q}{\kappa_n}\right)^2-1} & if\ \frac{\kappa_q}{\kappa_n}\neq 1 \\ \frac{\kappa_n\left(\frac{S}{U}\right)}{2}+\frac{1}{2}\sin\left(\kappa_n\left(\frac{S}{U}\right)\right)\cos\left(\kappa_n\left(\frac{S}{U}\right)\right) & if\ \frac{\kappa_q}{\kappa_n}=1 \end{array}\right\}}{\kappa_n\left(\frac{S}{U}\right)} \underset{\kappa_n\left(\frac{S}{U}\right)\tan\left(\kappa_n\left(\frac{S}{U}\right)\right)=S}{\overset{\kappa_q\left(\frac{S}{U}\right)\tan\left(\kappa_q\left(\frac{S}{U}\right)\right)=S}{=}}$$

$$= \left\{\begin{array}{ll} 0 & if\ \frac{\kappa_q}{\kappa_n}\neq 1 \\ \frac{1}{2}+\frac{1}{2\kappa_n\left(\frac{S}{U}\right)}\sin\left(\kappa_n\left(\frac{S}{U}\right)\right)\cos\left(\kappa_n\left(\frac{S}{U}\right)\right) & if\ \frac{\kappa_q}{\kappa_n}=1 \end{array}\right\}$$

Similarly

$$\int_0^1\left(\cos\left(\nu_m\left(\frac{T}{U}\right)y^*\right)\right)\left(\cos\left(\nu_p\left(\frac{T}{U}\right)y^*\right)\right)dy^* = \left\{\begin{array}{ll} 0 & if\ \frac{\nu_p}{\nu_m}\neq 1 \\ \frac{1}{2}+\frac{1}{2\nu_m\left(\frac{T}{U}\right)}\sin\left(\nu_m\left(\frac{T}{U}\right)\right)\cos\left(\nu_m\left(\frac{T}{U}\right)\right) & if\ \frac{\nu_p}{\nu_m}=1 \end{array}\right\}$$

Then, since $\sin(2\theta)=2\sin(\theta)\cos(\theta)\ \ \forall\theta$, the following must hold:

$$\int_0^1\int_0^1 \cos\left(\kappa_q\left(\frac{S}{U}\right)x^*\right)\cos\left(\nu_p\left(\frac{T}{U}\right)y^*\right)dx^*dy^* =$$

$$= \sum_{n=0}^{\infty}\sum_{m=0}^{\infty}\left[\begin{array}{l} A_{n,m}\left[1-\frac{\rho_{1,n,m}}{UV}+\left(\frac{1}{UV}-\frac{1}{\rho_{2,n,m}}\right)\rho_{1,n,m}e^{\left(\rho_{1,n,m}-\rho_{2,n,m}\right)}\right] \\ \int_0^1\int_0^1 \cos\left(\kappa_n\left(\frac{S}{U}\right)x^*\right)\cos\left(\nu_m\left(\frac{T}{U}\right)y^*\right)\cos\left(\kappa_q\left(\frac{S}{U}\right)x^*\right)\cos\left(\nu_p\left(\frac{T}{U}\right)y^*\right)dx^*dy^* \end{array}\right] \Leftrightarrow$$

$$\frac{\sin\left(\kappa_q\left(\frac{S}{U}\right)\right)}{\kappa_q\left(\frac{S}{U}\right)}\frac{\sin\left(\nu_p\left(\frac{T}{U}\right)\right)}{\nu_p\left(\frac{T}{U}\right)} =$$

$$= \sum_{n=0}^{\infty}\sum_{m=0}^{\infty}\left[\begin{array}{l} A_{n,m}\left[1-\frac{\rho_{1,n,m}}{UV}+\left(\frac{1}{UV}-\frac{1}{\rho_{2,n,m}}\right)\rho_{1,n,m}e^{\left(\rho_{1,n,m}-\rho_{2,n,m}\right)}\right] \\ \left[\begin{array}{ll} 0 & if \quad n\neq q \\ \frac{1}{2}+\frac{\sin\left(2\kappa_q\left(\frac{S}{U}\right)\right)}{4\kappa_q\left(\frac{S}{U}\right)} & if \quad n=q \end{array}\right]\left[\begin{array}{ll} 0 & if \quad m\neq p \\ \frac{1}{2}+\frac{\sin\left(2\nu_p\left(\frac{T}{U}\right)\right)}{4\nu_p\left(\frac{T}{U}\right)} & if \quad m=p \end{array}\right] \end{array}\right] \Leftrightarrow$$

$$A_{q,p} = \frac{\left[\frac{\sin\left(\kappa_q\left(\frac{S}{U}\right)\right)}{\kappa_q\left(\frac{S}{U}\right)}\right]\left[\frac{\sin\left(\nu_p\left(\frac{T}{U}\right)\right)}{\nu_p\left(\frac{T}{U}\right)}\right]}{\left[1-\frac{\rho_{1,q,p}}{UV}+\left(\frac{1}{UV}-\frac{1}{\rho_{2,q,p}}\right)\rho_{1,q,p}e^{\left(\rho_{1,q,p}-\rho_{2,q,p}\right)}\right]\left[\frac{1}{2}+\frac{\sin\left(2\kappa_q\left(\frac{S}{U}\right)\right)}{4\kappa_q\left(\frac{S}{U}\right)}\right]\left[\frac{1}{2}+\frac{\sin\left(2\nu_p\left(\frac{T}{U}\right)\right)}{4\nu_p\left(\frac{T}{U}\right)}\right]} \quad (33)$$

Then the reactor's dimensionless concentration profile is:

$$C_A{}^*\left(x^*,y^*,z^*\right)=\sum_{n=0}^{\infty}\sum_{m=0}^{\infty}A_{n,m}\left(e^{\rho_{1,n,m}z^*}-\frac{\rho_{1,n,m}}{\rho_{2,n,m}}e^{\left(\rho_{1,n,m}-\rho_{2,n,m}\right)}e^{\rho_{2,n,m}z^*}\right)\cos\left(\kappa_n\left(\frac{S}{U}\right)x^*\right)\left(\cos\left(\nu_m\left(\frac{T}{U}\right)y^*\right)\right)$$

$$A_{n,m}=\frac{\left[\frac{\sin\left(\kappa_n\left(\frac{S}{U}\right)\right)}{\kappa_n\left(\frac{S}{U}\right)}\right]\left[\frac{\sin\left(\nu_m\left(\frac{T}{U}\right)\right)}{\nu_m\left(\frac{T}{U}\right)}\right]}{\left[1-\frac{\rho_{1,n,m}}{UV}+\left(\frac{1}{UV}-\frac{1}{\rho_{2,n,m}}\right)\rho_{1,n,m}e^{\left(\rho_{1,n,m}-\rho_{2,n,m}\right)}\right]\left[\frac{1}{2}+\frac{\sin\left(2\kappa_n\left(\frac{S}{U}\right)\right)}{4\kappa_n\left(\frac{S}{U}\right)}\right]\left[\frac{1}{2}+\frac{\sin\left(2\nu_m\left(\frac{T}{U}\right)\right)}{4\nu_m\left(\frac{T}{U}\right)}\right]}$$

$$\rho_{1,n.m}\triangleq\frac{UV}{2}-\sqrt{\left(\frac{UV}{2}\right)^2+\left(U^2K+{\nu_m}^2+{\kappa_n}^2\right)}<\rho_{2,n.m}\triangleq\frac{UV}{2}+\sqrt{\left(\frac{UV}{2}\right)^2+\left(U^2K+{\nu_m}^2+{\kappa_n}^2\right)}$$

$$\kappa_n\left(\frac{S}{U}\right)\tan\left(\kappa_n\left(\frac{S}{U}\right)\right)=S\quad n=0,1,\cdots\infty,\qquad \nu_m\left(\frac{T}{U}\right)\tan\left(\nu_m\left(\frac{T}{U}\right)\right)=T\quad m=0,1,\cdots\infty$$

The dimensionless outlet reactor concentration C_A^{out*} can then be evaluated as:

$$C_A^{out*}\triangleq\int_0^1\int_0^1 C_A{}^*\left(x^*,y^*,1\right)dx^*dy^*$$

$$C_A^{out*}=\sum_{n=0}^{\infty}\sum_{m=0}^{\infty}A_{n,m}\left(e^{\rho_{1,n,m}}-\frac{\rho_{1,n,m}}{\rho_{2,n,m}}e^{\left(\rho_{1,n,m}-\rho_{2,n,m}\right)}e^{\rho_{2,n,m}}\right)\int_0^1\int_0^1\cos\left(\kappa_n\left(\frac{S}{U}\right)x^*\right)\left(\cos\left(\nu_m\left(\frac{T}{U}\right)y^*\right)\right)dx^*dy^*\Leftrightarrow$$

$$C_A^{out*}=\sum_{n=0}^{\infty}\sum_{m=0}^{\infty}A_{n,m}e^{\rho_{1,n,m}}\left(1-\frac{\rho_{1,n,m}}{\rho_{2,n,m}}\right)\int_0^1\cos\left(\kappa_n\left(\frac{S}{U}\right)x^*\right)dx^*\int_0^1\left(\cos\left(\nu_m\left(\frac{T}{U}\right)y^*\right)\right)dy^*\Leftrightarrow$$

$$C_A^{out*}=\sum_{n=0}^{\infty}\sum_{m=0}^{\infty}A_{n,m}e^{\rho_{1,n,m}}\left(1-\frac{\rho_{1,n,m}}{\rho_{2,n,m}}\right)\left(\frac{\sin\left(\kappa_n\left(\frac{S}{U}\right)\right)\sin\left(\nu_m\left(\frac{T}{U}\right)\right)}{\kappa_n\left(\frac{S}{U}\right)\nu_m\left(\frac{T}{U}\right)}\right)\Leftrightarrow$$

$$C_A^{out*} = \sum_{n=0}^{\infty}\sum_{m=0}^{\infty} \frac{e^{\rho_{1,n,m}}\left(1-\frac{\rho_{1,n,m}}{\rho_{2,n,m}}\right)\left[\frac{\sin\left(\kappa_n\left(\frac{S}{U}\right)\right)}{\kappa_n\left(\frac{S}{U}\right)}\right]^2\left[\frac{\sin\left(\nu_m\left(\frac{T}{U}\right)\right)}{\nu_m\left(\frac{T}{U}\right)}\right]^2}{\left[1-\frac{\rho_{1,n,m}}{UV}+\left(\frac{1}{UV}-\frac{1}{\rho_{2,n,m}}\right)\rho_{1,n,m}e^{(\rho_{1,n,m}-\rho_{2,n,m})}\right]\left[\frac{1}{2}+\frac{\sin\left(2\kappa_n\left(\frac{S}{U}\right)\right)}{4\kappa_n\left(\frac{S}{U}\right)}\right]\left[\frac{1}{2}+\frac{\sin\left(2\nu_m\left(\frac{T}{U}\right)\right)}{4\nu_m\left(\frac{T}{U}\right)}\right]} \quad (34)$$

$$\rho_{1,n.m} \triangleq \frac{UV}{2}-\sqrt{\left(\frac{UV}{2}\right)^2+\left(U^2K+\nu_m{}^2+\kappa_n{}^2\right)} < \rho_{2,n.m} \triangleq \frac{UV}{2}+\sqrt{\left(\frac{UV}{2}\right)^2+\left(U^2K+\nu_m{}^2+\kappa_n{}^2\right)}$$

$$\kappa_n\left(\frac{S}{U}\right)\tan\left(\kappa_n\left(\frac{S}{U}\right)\right)=S \quad n=0,1,\cdots\infty, \qquad \nu_m\left(\frac{T}{U}\right)\tan\left(\nu_m\left(\frac{T}{U}\right)\right)=T \quad m=0,1,\cdots\infty$$

Define $\theta_n \triangleq \kappa_n\frac{S}{U}, \phi_m \triangleq \nu_m\frac{T}{U}$. Then

$$\theta_n\tan\theta_n = S, \quad 2n\pi \le \theta_n \le 2n\pi+\frac{\pi}{2} \quad n=0,\infty \quad (35)$$

$$\phi_m\tan\phi_m = T, \quad 2m\pi \le \phi_m \le 2m\pi+\frac{\pi}{2} \quad m=0,\infty \quad (36)$$

$\rho_{1,n.m}$, $\rho_{2,n.m}$ are the roots of $s^2-UVs-U^2\left(K+\left(\frac{\phi_m}{T}\right)^2+\left(\frac{\theta_n}{S}\right)^2\right)=0$. Thus they satisfy:

$$\rho_{1,n.m}+\rho_{2,n.m}=UV\,,\ \rho_{1,n.m}\cdot\rho_{2,n.m}=-U^2\left(K+\left(\frac{\phi_m}{T}\right)^2+\left(\frac{\theta_n}{S}\right)^2\right)$$

$$\rho_{1,n.m} \triangleq U\left[\frac{V}{2}-\sqrt{\left(\frac{V}{2}\right)^2+\left(K+\frac{\phi_m{}^2}{T^2}+\frac{\theta_n{}^2}{S^2}\right)}\right] < 0 < \rho_{2,n.m} \triangleq U\left[\frac{V}{2}+\sqrt{\left(\frac{V}{2}\right)^2+\left(K+\frac{\phi_m{}^2}{T^2}+\frac{\theta_n{}^2}{S^2}\right)}\right] \quad (37)$$

Then the dimensionless outlet reactor concentration C_A^{out*} can be written as:

$$C_A^{out^*} = \sum_{n=0}^{\infty}\sum_{m=0}^{\infty}\left\{\frac{\left(1-\frac{\rho_{1,n,m}}{\rho_{2,n,m}}\right)\left[\frac{\sin(\theta_n)}{\theta_n}\right]^2\left[\frac{\sin(\phi_m)}{\phi_m}\right]^2}{\left[\left(1-\frac{\rho_{1,n,m}}{UV}\right)e^{-\rho_{1,n,m}}+\left(\frac{1}{UV}-\frac{1}{\rho_{2,n,m}}\right)\rho_{1,n,m}e^{-\rho_{2,n,m}}\right]\left[\frac{1}{2}+\frac{\sin(2\theta_n)}{4\theta_n}\right]\left[\frac{1}{2}+\frac{\sin(2\phi_m)}{4\phi_m}\right]}\right\} \quad (38)$$

The above expression can also take a form that avoids trigonometric expressions. Since,

$$\left\{\tan\theta_n = \frac{S}{\theta_n},\quad 2n\pi \le \theta_n \le 2n\pi+\frac{\pi}{2}\ \ n=0,\infty\right\}\Leftrightarrow$$

$$\left\{(\tan\theta_n)^2 = \frac{S^2}{\theta_n{}^2},\quad 2n\pi \le \theta_n \le 2n\pi+\frac{\pi}{2}\ \ n=0,\infty\right\}\Leftrightarrow$$

$$\left\{\frac{(\sin\theta_n)^2}{1-(\sin\theta_n)^2} = \frac{S^2}{\theta_n{}^2},\quad 2n\pi \le \theta_n \le 2n\pi+\frac{\pi}{2}\ \ n=0,\infty\right\}\Leftrightarrow$$

$$\left\{\sin\theta_n = \frac{S}{\sqrt{\theta_n{}^2+S^2}},\ \cos\theta_n = \frac{\theta_n}{\sqrt{\theta_n{}^2+S^2}}\quad 2n\pi \le \theta_n \le 2n\pi+\frac{\pi}{2}\ \ n=0,\infty\right\}.\ \text{Similarly}$$

$$\left\{\sin\phi_m = \frac{T}{\sqrt{\phi_m{}^2+T^2}},\ \cos\phi_m = \frac{\phi_m}{\sqrt{\phi_m{}^2+T^2}}\quad 2m\pi \le \phi_m \le 2m\pi+\frac{\pi}{2}\ \ m=0,\infty\right\}.\ \text{Then}$$

$$C_A^{out^*} = \sum_{n=0}^{\infty}\sum_{m=0}^{\infty}\left\{\frac{\left(1-\frac{\rho_{1,n,m}}{\rho_{2,n,m}}\right)\left[\frac{S^2}{(\theta_n{}^2+S^2)\theta_n{}^2}\right]\left[\frac{T^2}{\phi_m{}^2(\phi_m{}^2+T^2)}\right]}{\left[\frac{\rho_{2,n,m}}{UV}e^{-\rho_{1,n,m}}-\frac{(\rho_{1,n,m})^2}{UV\rho_{2,n,m}}e^{-\rho_{2,n,m}}\right]\left[\frac{\theta_n{}^2+S^2+S}{2(\theta_n{}^2+S^2)}\right]\left[\frac{\phi_m{}^2+T^2+T}{2(\phi_m{}^2+T^2)}\right]}\right\}\Leftrightarrow$$

$$C_A^{out^*} = 4UVS^2T^2\sum_{n=0}^{\infty}\sum_{m=0}^{\infty}\left\{\frac{(\rho_{2,n,m}-\rho_{1,n,m})}{\left[\theta_n{}^2(\theta_n{}^2+S^2+S)\right]\left[\phi_m{}^2(\phi_m{}^2+T^2+T)\right]\left[(\rho_{2,n,m})^2e^{-\rho_{1,n,m}}-(\rho_{1,n,m})^2e^{-\rho_{2,n,m}}\right]}\right\} \quad (39)$$

Expressions for the limiting behavior of $C_A^{out^*}$ with respect to U, V are listed below and are derived in the Appendix.

From the formulas $0 < \rho_{2,n.m} \triangleq UV\left[\frac{1}{2}+\sqrt{\left(\frac{1}{2}\right)^2+\frac{1}{V^2}\left(K+\frac{\phi_m^{\,2}}{T^2}+\frac{\theta_n^{\,2}}{S^2}\right)}\right]$, $\rho_{1,n.m}+\rho_{2,n.m}=UV$ and

$\rho_{1,n.m}\cdot\rho_{2,n.m}=-U^2\left(K+\left(\frac{\phi_m}{T}\right)^2+\left(\frac{\theta_n}{S}\right)^2\right)$ it is easy to see that $\lim_{V\to+\infty}\rho_{2,n.m}=+\infty$, $\lim_{V\to+\infty}\rho_{1,n.m}=0$,

$$\lim_{V\to+\infty}\frac{\left(\rho_{2,n,m}\right)^2 e^{-\rho_{1,n,m}}-\left(\rho_{1,n,m}\right)^2 e^{-\rho_{2,n,m}}}{V\left(\rho_{2,n,m}-\rho_{1,n,m}\right)}=\lim_{V\to+\infty}\frac{\frac{\rho_{2,n,m}}{V}e^{-\rho_{1,n,m}}-\left(\rho_{1,n,m}\right)^2\frac{1}{\rho_{2,n,m}V}e^{-\rho_{2,n,m}}}{\left(1-\rho_{1,n,m}\left(\rho_{2,n,m}\right)^{-1}\right)}=U,$$

$$\boxed{\lim_{V\to+\infty}C_A^{out^*}=4S^2T^2\sum_{n=0}^{\infty}\sum_{m=0}^{\infty}\left\{\left[\frac{1}{\theta_n^{\,2}\left(\theta_n^{\,2}+S^2+S\right)}\right]\left[\frac{1}{\phi_m^{\,2}\left(\phi_m^{\,2}+T^2+T\right)}\right]\right\}} \qquad (40)$$

It is important to notice that the aforementioned limit does not depend on the reactor's dimensionless length U.

From the formulas $0 < \rho_{2,n.m} \triangleq UV\left[\frac{1}{2}+\sqrt{\left(\frac{1}{2}\right)^2+\frac{1}{V^2}\left(K+\frac{\phi_m^{\,2}}{T^2}+\frac{\theta_n^{\,2}}{S^2}\right)}\right]$, $\rho_{1,n.m}+\rho_{2,n.m}=UV$, it is easy to see that

$V\left[\frac{1}{2}-\sqrt{\left(\frac{1}{2}\right)^2+\frac{1}{V^2}\left(K+\frac{\phi_m^{\,2}}{T^2}+\frac{\theta_n^{\,2}}{S^2}\right)}\right]=\frac{\rho_{1,n.m}}{U}<0<\frac{\rho_{2,n.m}}{U}=V\left[\frac{1}{2}+\sqrt{\left(\frac{1}{2}\right)^2+\frac{1}{V^2}\left(K+\frac{\phi_m^{\,2}}{T^2}+\frac{\theta_n^{\,2}}{S^2}\right)}\right]$ do not depend on U. Then

$$\boxed{\lim_{U\to+\infty}C_A^{out^*}=0}$$

$$\boxed{\lim_{U\to0^+}C_A^{out^*}=4S^2T^2\sum_{n=0}^{\infty}\sum_{m=0}^{\infty}\left\{\frac{1}{\left[\theta_n^{\,2}\left(\theta_n^{\,2}+S^2+S\right)\right]\left[\phi_m^{\,2}\left(\phi_m^{\,2}+T^2+T\right)\right]}\right\}}$$

Analytical expressions for the partial derivatives of the dimensionless outlet reactor concentration C_A^{out*} with respect to S, T, U, V. To this end, the derivative expressions listed below are derived in the Appendix.

$$\frac{d\theta_n}{dS} = \frac{\theta_n}{\theta_n^2 + S^2 + S}, \quad n\pi \le \theta_n \le n\pi + \frac{\pi}{2} \quad n = 0, \infty$$

$$\frac{d\phi_m}{dT} = \frac{\phi_m}{\phi_m^2 + T^2 + T}, \quad m\pi \le \phi_m \le m\pi + \frac{\pi}{2} \quad m = 0, \infty$$

$$\frac{d\left[\frac{1}{\theta_n^2\left(\theta_n^2 + S^2 + S\right)}\right]}{dS} = \frac{-\left[\frac{2\theta_n^2}{\theta_n^2 + S^2 + S} + 2S + 3\right]}{\left[\theta_n\left(\theta_n^2 + S^2 + S\right)\right]^2}, \quad n\pi \le \theta_n \le n\pi + \frac{\pi}{2} \quad n = 0, \infty$$

$$\frac{d\left[\frac{1}{\phi_m^2\left(\phi_m^2 + T^2 + T\right)}\right]}{dT} = \frac{-\left[\frac{2\phi_m^2}{\phi_m^2 + T^2 + T} + 2T + 3\right]}{\left[\phi_m\left(\phi_m^2 + T^2 + T\right)\right]^2}, \quad m\pi \le \phi_m \le m\pi + \frac{\pi}{2} \quad m = 0, \infty$$

$$\frac{\partial \rho_{1,n.m}}{\partial U} = \frac{\rho_{1,n.m}}{U}, \frac{\partial\left(\rho_{1,n.m}/U\right)}{\partial U} = 0; \quad \frac{\partial \rho_{2,n.m}}{\partial U} = \frac{\rho_{2,n.m}}{U}, \frac{\partial\left(\rho_{2,n.m}/U\right)}{\partial U} = 0$$

$$\frac{\partial \rho_{1,n.m}}{\partial V} = U\frac{\rho_{1,n.m}}{2\rho_{1,n.m} - UV} = U\frac{\rho_{2,n.m} - VU}{2\rho_{2,n.m} - VU} = -U\frac{\rho_{1,n.m}}{\rho_{2,n.m} - \rho_{1,n.m}}$$

$$\frac{\partial \rho_{2,n.m}}{\partial V} = U\frac{VU - \rho_{1,n.m}}{VU - 2\rho_{1,n.m}} = U\frac{\rho_{2,n.m}}{2\rho_{2,n.m} - VU} = U\frac{\rho_{2,n.m}}{\rho_{2,n.m} - \rho_{1,n.m}}$$

$$\frac{\partial \rho_{1,n.m}}{\partial S} = U \frac{\theta_n{}^2 \left(\left(\frac{\theta_n{}^2 + S^2}{\theta_n{}^2 + S^2 + S} \right) \right)}{S^3 \sqrt{\left(\frac{V}{2}\right)^2 + \left(K + \frac{\phi_m{}^2}{T^2} + \frac{\theta_n{}^2}{S^2} \right)}}$$

$$\frac{\partial \rho_{2,n.m}}{\partial S} = -U \frac{\theta_n{}^2 \left(\left(\frac{\theta_n{}^2 + S^2}{\theta_n{}^2 + S^2 + S} \right) \right)}{S^3 \sqrt{\left(\frac{V}{2}\right)^2 + \left(K + \frac{\phi_m{}^2}{T^2} + \frac{\theta_n{}^2}{S^2} \right)}} = -\frac{\partial \rho_{1,n.m}}{\partial S}$$

$$\frac{\partial \rho_{1,n.m}}{\partial T} = U \frac{\phi_m{}^2 \left(\left(\frac{\phi_m{}^2 + T^2}{\phi_m{}^2 + T^2 + T} \right) \right)}{T^3 \sqrt{\left(\frac{V}{2}\right)^2 + \left(K + \frac{\phi_m{}^2}{T^2} + \frac{\theta_n{}^2}{S^2} \right)}} = -\frac{\partial \rho_{2,n.m}}{\partial T}$$

$$\frac{\partial \left[\frac{\left(\rho_{2,n,m}\right)^2 e^{-\rho_{1,n,m}} - \left(\rho_{1,n,m}\right)^2 e^{-\rho_{2,n,m}}}{\left(\rho_{2,n,m} - \rho_{1,n,m}\right)} \right]}{\partial S} = -U \frac{\theta_n{}^2 \left(\frac{\theta_n{}^2 + S^2}{\theta_n{}^2 + S^2 + S} \right)}{S^3 \sqrt{\left(\frac{V}{2}\right)^2 + \left(K + \frac{\phi_m{}^2}{T^2} + \frac{\theta_n{}^2}{S^2} \right)}} \left[\begin{array}{l} \frac{\left[\left(\rho_{2,n,m}\right)^2 e^{-\rho_{1,n,m}} + \left(\rho_{1,n,m}\right)^2 e^{-\rho_{2,n,m}} \right]}{\left(\rho_{2,n,m} - \rho_{1,n,m}\right)} + \\ +2\rho_{1,n,m}\rho_{2,n,m} \frac{\left[e^{-\rho_{2,n,m}} - e^{-\rho_{1,n,m}} \right]}{\left(\rho_{2,n,m} - \rho_{1,n,m}\right)^2} \end{array} \right].$$

$$\frac{\partial \left[\frac{\left(\rho_{2,n,m}\right)^2 e^{-\rho_{1,n,m}} - \left(\rho_{1,n,m}\right)^2 e^{-\rho_{2,n,m}}}{\left(\rho_{2,n,m} - \rho_{1,n,m}\right)} \right]}{\partial T} = -U \frac{\phi_m{}^2 \left(\left(\frac{\phi_m{}^2 + T^2}{\phi_m{}^2 + T^2 + T} \right) \right)}{T^3 \sqrt{\left(\frac{V}{2}\right)^2 + \left(K + \frac{\phi_m{}^2}{T^2} + \frac{\theta_n{}^2}{S^2} \right)}} \left[\begin{array}{l} \frac{\left[\left(\rho_{2,n,m}\right)^2 e^{-\rho_{1,n,m}} + \left(\rho_{1,n,m}\right)^2 e^{-\rho_{2,n,m}} \right]}{\left(\rho_{2,n,m} - \rho_{1,n,m}\right)} + \\ +2\rho_{1,n,m}\rho_{2,n,m} \frac{\left[e^{-\rho_{2,n,m}} - e^{-\rho_{1,n,m}} \right]}{\left(\rho_{2,n,m} - \rho_{1,n,m}\right)^2} \end{array} \right]$$

$$\frac{\partial\left[\frac{\left(\rho_{2,n,m}\right)^2 e^{-\rho_{1,n,m}}-\left(\rho_{1,n,m}\right)^2 e^{-\rho_{2,n,m}}}{\left(\rho_{2,n,m}-\rho_{1,n,m}\right)}\right]}{\partial U}=\frac{1}{U}\frac{\left[\left(\rho_{2,n,m}\right)^2 e^{-\rho_{1,n,m}}\left(1-\rho_{1,n,m}\right)-\left(\rho_{1,n,m}\right)^2 e^{-\rho_{2,n,m}}\left(1-\rho_{2,n,m}\right)\right]}{\left(\rho_{2,n,m}-\rho_{1,n,m}\right)}$$

$$\frac{\partial\left[\frac{\left(\rho_{2,n,m}\right)^2 e^{-\rho_{1,n,m}}-\left(\rho_{1,n,m}\right)^2 e^{-\rho_{2,n,m}}}{\left(\rho_{2,n,m}-\rho_{1,n,m}\right)}\right]}{\partial V}=U\frac{\left[\begin{array}{l}\left[\left(\rho_{2,n,m}\right)^2 e^{-\rho_{1,n,m}}\left(2+\rho_{1,n.m}\right)+\left(\rho_{1,n,m}\right)^2 e^{-\rho_{2,n,m}}\left(2+\rho_{2,n.m}\right)\right]-\\ \left[\left(\rho_{2,n,m}\right)^2 e^{-\rho_{1,n,m}}-\left(\rho_{1,n,m}\right)^2 e^{-\rho_{2,n,m}}\right]\left(\frac{UV}{\rho_{2,n.m}-\rho_{1,n.m}}\right)\end{array}\right]}{\left(\rho_{2,n,m}-\rho_{1,n,m}\right)^2}$$

$$\frac{\partial C_{A}^{out^{*}}}{\partial S}=\frac{2C_{A}^{out^{*}}}{S}-4UVS^{2}T^{2}\left(\sum_{n=0}^{\infty}\sum_{m=0}^{\infty}\frac{\left[\frac{\left[\frac{2\theta_{n}^{2}}{\theta_{n}^{2}+S^{2}+S}+2S+3\right]}{\left[\theta_{n}^{2}+S^{2}+S\right]}\left[\frac{\left(\rho_{2,n,m}\right)^{2}e^{-\rho_{1,n,m}}-\left(\rho_{1,n,m}\right)^{2}e^{-\rho_{2,n,m}}}{\left(\rho_{2,n,m}-\rho_{1,n,m}\right)}\right]-\right.}{\left[\theta_{n}^{2}\left(\theta_{n}^{2}+S^{2}+S\right)\right]\left[\phi_{m}^{2}\left(\phi_{m}^{2}+T^{2}+T\right)\right]\left[\frac{\left(\rho_{2,n,m}\right)^{2}e^{-\rho_{1,n,m}}-\left(\rho_{1,n,m}\right)^{2}e^{-\rho_{2,n,m}}}{\left(\rho_{2,n,m}-\rho_{1,n,m}\right)}\right]^{2}}\right.$$

$$\left.\left.\frac{U\dfrac{\theta_{n}^{2}\left(\dfrac{\theta_{n}^{2}+S^{2}}{\theta_{n}^{2}+S^{2}+S}\right)}{S^{3}\sqrt{\left(\dfrac{V}{2}\right)^{2}+\left(K+\dfrac{\phi_{m}^{2}}{T^{2}}+\dfrac{\theta_{n}^{2}}{S^{2}}\right)}}\left[\begin{array}{l}\dfrac{\left[\left(\rho_{2,n,m}\right)^{2}e^{-\rho_{1,n,m}}+\left(\rho_{1,n,m}\right)^{2}e^{-\rho_{2,n,m}}\right]}{\left(\rho_{2,n,m}-\rho_{1,n,m}\right)}+\\ +2\rho_{1,n,m}\rho_{2,n,m}\dfrac{\left[e^{-\rho_{2,n,m}}-e^{-\rho_{1,n,m}}\right]}{\left(\rho_{2,n,m}-\rho_{1,n,m}\right)^{2}}\end{array}\right]}{\left[\theta_{n}^{2}\left(\theta_{n}^{2}+S^{2}+S\right)\right]\left[\phi_{m}^{2}\left(\phi_{m}^{2}+T^{2}+T\right)\right]\left[\frac{\left(\rho_{2,n,m}\right)^{2}e^{-\rho_{1,n,m}}-\left(\rho_{1,n,m}\right)^{2}e^{-\rho_{2,n,m}}}{\left(\rho_{2,n,m}-\rho_{1,n,m}\right)}\right]^{2}}\right)$$

$$\frac{\partial C_{A}^{out^{*}}}{\partial T}=\frac{2C_{A}^{out^{*}}}{T}-4UVS^{2}T^{2}\left(\sum_{n=0}^{\infty}\sum_{m=0}^{\infty}\frac{\left[\frac{\left[\frac{2\phi_{m}^{2}}{\phi_{m}^{2}+T^{2}+T}+2T+3\right]}{\left[\phi_{m}^{2}+T^{2}+T\right]}\left[\frac{\left(\rho_{2,n,m}\right)^{2}e^{-\rho_{1,n,m}}-\left(\rho_{1,n,m}\right)^{2}e^{-\rho_{2,n,m}}}{\left(\rho_{2,n,m}-\rho_{1,n,m}\right)}\right]-\right.}{\left[\theta_{n}^{2}\left(\theta_{n}^{2}+S^{2}+S\right)\right]\left[\phi_{m}^{2}\left(\phi_{m}^{2}+T^{2}+T\right)\right]\left[\frac{\left(\rho_{2,n,m}\right)^{2}e^{-\rho_{1,n,m}}-\left(\rho_{1,n,m}\right)^{2}e^{-\rho_{2,n,m}}}{\left(\rho_{2,n,m}-\rho_{1,n,m}\right)}\right]^{2}}\right.$$

$$\left.\left.\frac{U\dfrac{\phi_{m}^{2}\left(\dfrac{\phi_{m}^{2}+T^{2}}{\phi_{m}^{2}+T^{2}+T}\right)}{T^{3}\sqrt{\left(\dfrac{V}{2}\right)^{2}+\left(K+\dfrac{\phi_{m}^{2}}{T^{2}}+\dfrac{\theta_{n}^{2}}{S^{2}}\right)}}\left[\begin{array}{l}\dfrac{\left[\left(\rho_{2,n,m}\right)^{2}e^{-\rho_{1,n,m}}+\left(\rho_{1,n,m}\right)^{2}e^{-\rho_{2,n,m}}\right]}{\left(\rho_{2,n,m}-\rho_{1,n,m}\right)}+\\ +2\rho_{1,n,m}\rho_{2,n,m}\dfrac{\left[e^{-\rho_{2,n,m}}-e^{-\rho_{1,n,m}}\right]}{\left(\rho_{2,n,m}-\rho_{1,n,m}\right)^{2}}\end{array}\right]}{\left[\theta_{n}^{2}\left(\theta_{n}^{2}+S^{2}+S\right)\right]\left[\phi_{m}^{2}\left(\phi_{m}^{2}+T^{2}+T\right)\right]\left[\frac{\left(\rho_{2,n,m}\right)^{2}e^{-\rho_{1,n,m}}-\left(\rho_{1,n,m}\right)^{2}e^{-\rho_{2,n,m}}}{\left(\rho_{2,n,m}-\rho_{1,n,m}\right)}\right]^{2}}\right)$$

$$\frac{\partial C_{A}^{out^{*}}}{\partial U}=\frac{C_{A}^{out^{*}}}{U}-4VS^{2}T^{2}\sum_{n=0}^{\infty}\sum_{m=0}^{\infty}\left\{\frac{\left[\left(\rho_{2,n,m}\right)^{2}e^{-\rho_{1,n,m}}\left(1-\rho_{1,n,m}\right)-\left(\rho_{1,n,m}\right)^{2}e^{-\rho_{2,n,m}}\left(1-\rho_{2,n,m}\right)\right]\left(\rho_{2,n,m}-\rho_{1,n,m}\right)}{\left[\theta_{n}^{2}\left(\theta_{n}^{2}+S^{2}+S\right)\right]\left[\phi_{m}^{2}\left(\phi_{m}^{2}+T^{2}+T\right)\right]\left[\left(\rho_{2,n,m}\right)^{2}e^{-\rho_{1,n,m}}-\left(\rho_{1,n,m}\right)^{2}e^{-\rho_{2,n,m}}\right]^{2}}\right\}$$

$$\frac{\partial C_{A}^{out^*}}{\partial V}=\frac{C_{A}^{out^*}}{V}-4U^2VS^2T^2\sum_{n=0}^{\infty}\sum_{m=0}^{\infty}\left\{\frac{\left[\left[\left(\rho_{2,n,m}\right)^2e^{-\rho_{1,n,m}}\left(2+\rho_{1,n.m}\right)+\left(\rho_{1,n,m}\right)^2e^{-\rho_{2,n,m}}\left(2+\rho_{2,n.m}\right)\right]-\right.}{\left.\left[\left(\rho_{2,n,m}\right)^2e^{-\rho_{1,n,m}}-\left(\rho_{1,n,m}\right)^2e^{-\rho_{2,n,m}}\right]\left(\frac{UV}{\rho_{2,n.m}-\rho_{1,n.m}}\right)\right]}{\left[\theta_n^{\,2}\left(\theta_n^{\,2}+S^2+S\right)\right]\left[\phi_m^{\,2}\left(\phi_m^{\,2}+T^2+T\right)\right]\left[\left(\rho_{2,n,m}\right)^2e^{-\rho_{1,n,m}}-\left(\rho_{1,n,m}\right)^2e^{-\rho_{2,n,m}}\right]^2}\right\}$$

Proposition 1

$$\frac{\partial C_{A}^{out^*}}{\partial U}<0\ \ \forall S>0,\forall T>0,\forall U>0,\forall V>0$$

Proof

$$\frac{\partial C_{A}^{out^*}}{\partial U}<0\Leftrightarrow$$

$$\frac{C_{A}^{out^*}}{U}-4VS^2T^2\sum_{n=0}^{\infty}\sum_{m=0}^{\infty}\left\{\frac{\left[\left(\rho_{2,n,m}\right)^2e^{-\rho_{1,n,m}}\left(1-\rho_{1,n,m}\right)-\left(\rho_{1,n,m}\right)^2e^{-\rho_{2,n,m}}\left(1-\rho_{2,n,m}\right)\right]\left(\rho_{2,n,m}-\rho_{1,n,m}\right)}{\left[\theta_n^{\,2}\left(\theta_n^{\,2}+S^2+S\right)\right]\left[\phi_m^{\,2}\left(\phi_m^{\,2}+T^2+T\right)\right]\left[\left(\rho_{2,n,m}\right)^2e^{-\rho_{1,n,m}}-\left(\rho_{1,n,m}\right)^2e^{-\rho_{2,n,m}}\right]^2}\right\}<0\Leftrightarrow$$

$$4VS^2T^2\sum_{n=0}^{\infty}\sum_{m=0}^{\infty}\left\{\frac{\left[\frac{1}{\theta_n^{\,2}\left(\theta_n^{\,2}+S^2+S\right)}\right]\left[\frac{1}{\phi_m^{\,2}\left(\phi_m^{\,2}+T^2+T\right)}\right]}{\left[\frac{\left(\rho_{2,n,m}\right)^2e^{-\rho_{1,n,m}}-\left(\rho_{1,n,m}\right)^2e^{-\rho_{2,n,m}}}{\left(\rho_{2,n,m}-\rho_{1,n,m}\right)}\right]}\right\}-$$

$$4VS^2T^2\sum_{n=0}^{\infty}\sum_{m=0}^{\infty}\left\{\frac{\left[\left(\rho_{2,n,m}\right)^2e^{-\rho_{1,n,m}}\left(1-\rho_{1,n,m}\right)-\left(\rho_{1,n,m}\right)^2e^{-\rho_{2,n,m}}\left(1-\rho_{2,n,m}\right)\right]\left(\rho_{2,n,m}-\rho_{1,n,m}\right)}{\left[\theta_n^{\,2}\left(\theta_n^{\,2}+S^2+S\right)\right]\left[\phi_m^{\,2}\left(\phi_m^{\,2}+T^2+T\right)\right]\left[\left(\rho_{2,n,m}\right)^2e^{-\rho_{1,n,m}}-\left(\rho_{1,n,m}\right)^2e^{-\rho_{2,n,m}}\right]^2}\right\}<0\overset{V>0}{\Leftrightarrow}$$

$$\sum_{n=0}^{\infty}\sum_{m=0}^{\infty}\left\{\begin{array}{l}\dfrac{\left[\left(\rho_{2,n,m}\right)^2e^{-\rho_{1,n,m}}-\left(\rho_{1,n,m}\right)^2e^{-\rho_{2,n,m}}\right]\left(\rho_{2,n,m}-\rho_{1,n,m}\right)}{\left[\theta_n^{\,2}\left(\theta_n^{\,2}+S^2+S\right)\right]\left[\phi_m^{\,2}\left(\phi_m^{\,2}+T^2+T\right)\right]\left[\left(\rho_{2,n,m}\right)^2e^{-\rho_{1,n,m}}-\left(\rho_{1,n,m}\right)^2e^{-\rho_{2,n,m}}\right]^2}-\\ \dfrac{\left[\left(\rho_{2,n,m}\right)^2e^{-\rho_{1,n,m}}\left(1-\rho_{1,n,m}\right)-\left(\rho_{1,n,m}\right)^2e^{-\rho_{2,n,m}}\left(1-\rho_{2,n,m}\right)\right]\left(\rho_{2,n,m}-\rho_{1,n,m}\right)}{\left[\theta_n^{\,2}\left(\theta_n^{\,2}+S^2+S\right)\right]\left[\phi_m^{\,2}\left(\phi_m^{\,2}+T^2+T\right)\right]\left[\left(\rho_{2,n,m}\right)^2e^{-\rho_{1,n,m}}-\left(\rho_{1,n,m}\right)^2e^{-\rho_{2,n,m}}\right]^2}\end{array}\right\}<0\Leftrightarrow$$

$$\sum_{n=0}^{\infty}\sum_{m=0}^{\infty}\left\{\frac{\left[\rho_{2,n,m}e^{-\rho_{1,n,m}}-\rho_{1,n,m}e^{-\rho_{2,n,m}}\right]\rho_{1,n,m}\rho_{2,n,m}\left(\rho_{2,n,m}-\rho_{1,n,m}\right)}{\left[\theta_n^{\,2}\left(\theta_n^{\,2}+S^2+S\right)\right]\left[\phi_m^{\,2}\left(\phi_m^{\,2}+T^2+T\right)\right]\left[\left(\rho_{2,n,m}\right)^2e^{-\rho_{1,n,m}}-\left(\rho_{1,n,m}\right)^2e^{-\rho_{2,n,m}}\right]^2}\right\}<0$$

It is easy to see that each term of this double sum is negative, and thus the above assertion is true.

O.E.Δ.

3.3 Optimization of a single 3-D monolith reactor

In a traditional reactor, fixing the reactor's inlet concentration vector and conversion level α fixes the reactor's residence time τ, which is equal to the reactor's volume to volumetric flowrate ratio $\tau \triangleq V/F$. Since the capital cost of a traditional reactor is proportional to the reactor's volume, fixing the traditional reactor's conversion (and thus residence time τ) fixes the reactor's capital cost to production ratio.

In the case of a multichannel monolith reactor with known inlet concentration vector, the analytical expression developed earlier for $C_A^{out^*}$ suggests that there is not a single design parameter that will determine the reactor's conversion α. In addition, the capital cost of a monolith reactor with no bulk catalyst loading is proportional to the reactor's surface. It is thus desirable to identify a multichannel monolith reactor with a given conversion level α and a minimum catalyst surface area to volumetric flow rate ratio (and thus a minimum capital cost to production ratio).The aforementioned minimization objective can be written as:

$$\frac{A}{F}\triangleq\frac{4(W+H)LN}{4v_zHWN}=\frac{(W+H)L}{v_zHW}. \qquad (41)$$

This objective will be minimized subject to the constraint that the reactor conversion is fixed at α. To determine the resulting optimization problem then becomes:

$$\left\{\begin{array}{l}\sigma \triangleq \min\limits_{W,H,L,v_z} \dfrac{(W+H)L}{v_z HW} \\ \dfrac{C_A^{out}}{C_A^{in}} = 1-\alpha \\ channel\ model\end{array}\right\} \Leftrightarrow \left\{\begin{array}{l}\sigma \triangleq \min\limits_{W,H,L,v_z} \left(\dfrac{1}{W}+\dfrac{1}{H}\right)\dfrac{L}{v_z} \\ \dfrac{C_A^{out}}{C_A^{in}} = 1-\alpha \\ channel\ model\end{array}\right\} \quad (42)$$

Employing the dimensionless ratios $S \triangleq \frac{kW}{D_A}, T \triangleq \frac{kH}{D_A}, U \triangleq \frac{kL}{D_A}, V \triangleq \frac{v_z}{k}$ and the analytical expression developed earlier for $C_A^{out^*} \triangleq \frac{C_A^{out}}{C_A^{in}}$, a dimensionless $\frac{A}{F}$ ratio can be derived as $k\frac{A}{F} = k\frac{kD_A(W+H)L}{kD_A v_z HW} = k\frac{kD_A D_A(S+T)L}{kkD_A v_z HW} = \frac{(S+T)U}{VST}$. In addition, a dimension less flow rate per channel can be derived as follows $\frac{k}{4D_A^{\,2}}\frac{F}{N} = 4\frac{k}{4D_A^{\,2}} v_z HW = \frac{k}{D_A^{\,2}} k\frac{VD_A SD_A T}{kk} = VST$

Then the optimization problem becomes:

$$\left\{\begin{array}{l}\sigma \triangleq \dfrac{1}{k}\cdot \min\limits_{S,T,U,V} \left(\dfrac{1}{S}+\dfrac{1}{T}\right)\dfrac{U}{V} \\ C_A^{out^*} \triangleq 4UVS^2T^2 \sum\limits_{n=0}^{\infty}\sum\limits_{m=0}^{\infty} \left\{ \dfrac{\left[\dfrac{1}{\theta_n^{\,2}\left(\theta_n^{\,2}+S^2+S\right)}\right]\left[\dfrac{1}{\phi_m^{\,2}\left(\phi_m^{\,2}+T^2+T\right)}\right]}{\left[\dfrac{\left(\rho_{2,n,m}\right)^2 e^{-\rho_{1,n,m}} - \left(\rho_{1,n,m}\right)^2 e^{-\rho_{2,n,m}}}{\left(\rho_{2,n,m}-\rho_{1,n,m}\right)}\right]} \right\} = 1-\alpha\end{array}\right\} \quad (43)$$

Consider a feasible point $\left[\hat{S} \quad \hat{T} \quad \hat{U} \quad \hat{V}\right]$ of the above optimization problem. It is easy to verify that the point $\left[\hat{T} \quad \hat{S} \quad \hat{U} \quad \hat{V}\right]$ is also feasible and has the same objective function value. This implies that the above formulation has many local minima. To avoid this degeneracy we assume without loss of generality that $W \geq H \Leftrightarrow S \geq T$. Numerical stability considerations lead us to solve repeatedly the optimization problem below which considers that V is fixed:

$$\left\{\begin{array}{l}\sigma \triangleq \frac{1}{k}\cdot \min\limits_{S,T,U,V}\ \left(\frac{1}{S}+\frac{1}{T}\right)\frac{U}{V} \\ 4UVS^2T^2\sum\limits_{n=0}^{\infty}\sum\limits_{m=0}^{\infty}\left\{\frac{\left[\frac{1}{\theta_n^{\,2}\left(\theta_n^{\,2}+S^2+S\right)}\right]\left[\frac{1}{\phi_m^{\,2}\left(\phi_m^{\,2}+T^2+T\right)}\right]}{\left[\frac{\left(\rho_{2,n,m}\right)^2 e^{-\rho_{1,n,m}}-\left(\rho_{1,n,m}\right)^2 e^{-\rho_{2,n,m}}}{\left(\rho_{2,n,m}-\rho_{1,n,m}\right)}\right]}\right\}+\alpha-1=0 \\ \theta_n\tan\left(\theta_n\right)=S,\ \ n\pi\le\theta_n\le n\pi+\frac{\pi}{2}\ \ n=0,...,\infty;\ \phi_m\tan\left(\phi_m\right)=T,\ \ m\pi\le\phi_m\le m\pi+\frac{\pi}{2}\ \ m=0,...,\infty \\ \rho_{1,n.m}\triangleq U\left[\frac{V}{2}-\sqrt{\left(\frac{V}{2}\right)^2+\left(K+\frac{\phi_m^{\,2}}{T^2}+\frac{\theta_n^{\,2}}{S^2}\right)}\right]<\rho_{2,n.m}\triangleq U\left[\frac{V}{2}+\sqrt{\left(\frac{V}{2}\right)^2+\left(K+\frac{\phi_m^{\,2}}{T^2}+\frac{\theta_n^{\,2}}{S^2}\right)}\right] \\ V=\beta,\ \ S\ge T\end{array}\right\} \quad (44)$$

3.4 Discussion and Conclusions

The above optimization problem's optimum exhibits equal values of S and T. Its optimum objective function values, optimum $S=T$ values and optimum U values are shown in the graphs below, for five cases when the dimensionless velocity V equals 100, 50, 20, 10 and 5. As seen in figures (2, 6, 10, 14, 18) the optimum objective function values, for a given conversion level, goes up, as the dimensionless velocity V goes down. This implies that the minimum catalyst surface area to volumetric flowrate ratio is a decreasing function of the dimensionless velocity V.

The dimensionless optimum channel dimensions, corresponding to the same conversion level, also exhibit a monotonic dependence on the dimensionless velocity V. The optimum dimensionless reactor length U is a weakly monotonically decreasing function of V, while the dimensionless reactor width/height $S=T$ is also a monotonically decreasing function of V.

Another important realization that needs to be emphasized is that the minimization of the dimensionless surface to flowrate ratio $k\frac{A}{F}=\left(\frac{1}{S}+\frac{1}{T}\right)\frac{U}{V}$ for a fixed value of V, completely determines the optimum dimensions of the monolith channel. This however does not determine the flowrate F that can be processed by the monolith reactor. Indeed, although the dimensionless flowrate to number of channels ratio $\frac{k}{4D_A^{\ 2}}\frac{F}{N}=VST$ is determined by the carried out optimization procedure, the reactor's flowrate F can be increased or decreased at will (albeit in integral increments) by altering the monolith reactor's number of channels N, since $F=\frac{4D_A^{\ 2}}{k}VSTN$. Furthermore the reactor's surface area A can be altered at will and in a manner exactly proportional to F, since (as long as V is fixed) $A=\frac{A}{F}F=\frac{1}{k}\left(\frac{1}{S}+\frac{1}{T}\right)\frac{U}{V}F$. This realization bodes well for the future applicability of the IDEAS conceptual framework to this 3d monolith reactor model.

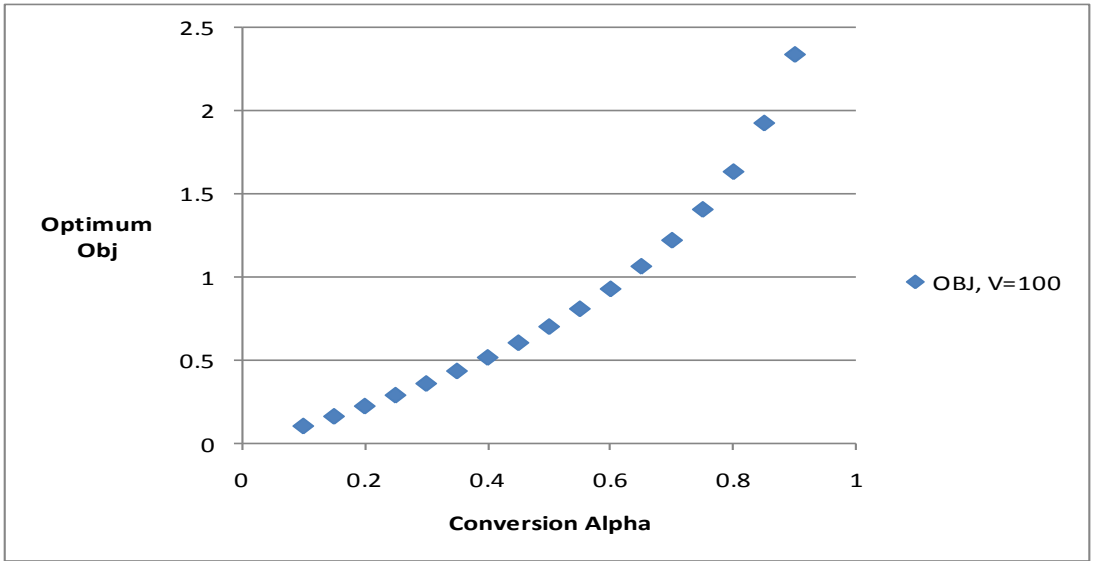

Figure 3-2 Optimum Objective function as a function of Conversion. Case: Velocity =100

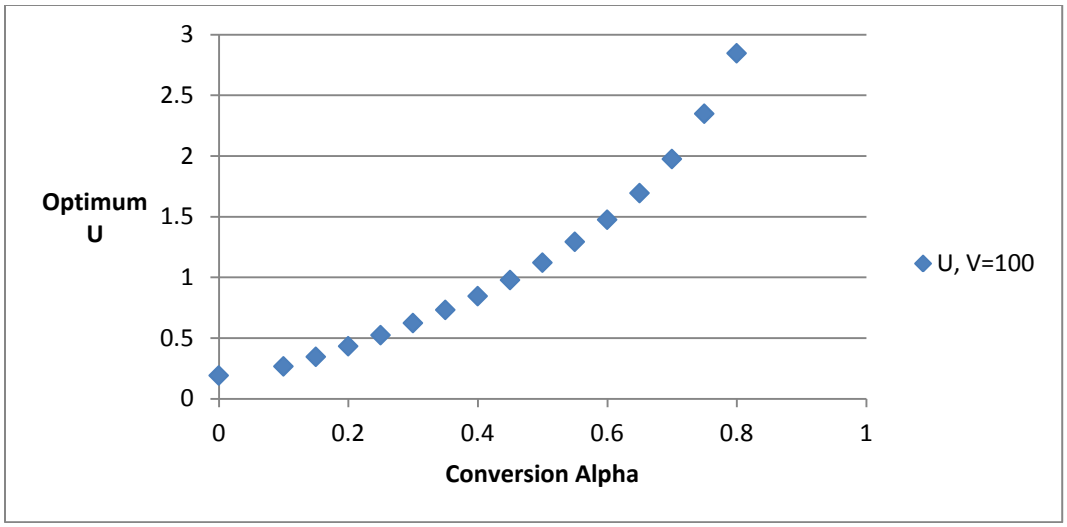

Figure 3-3 Reactor dimensionless length optimum as a function of conversion. Case: Velocity =100

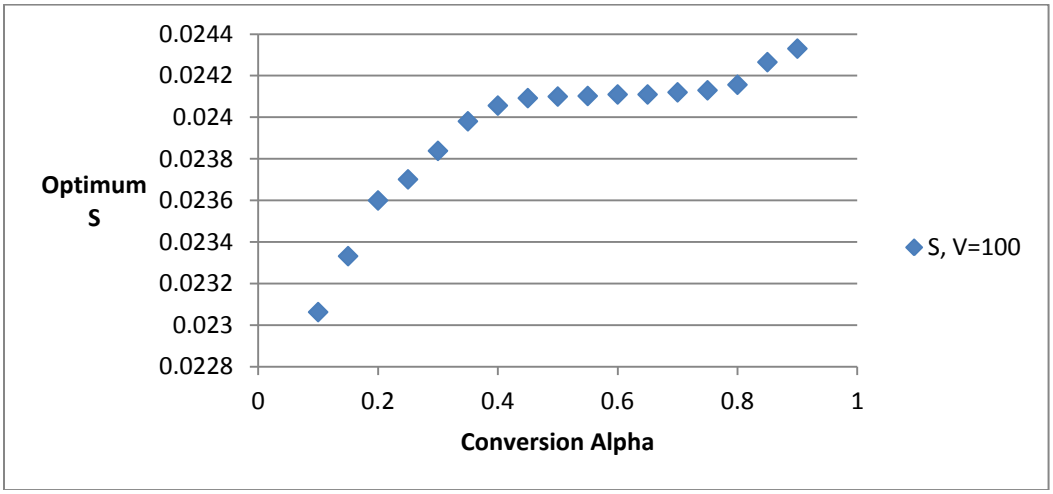

Figure 3-4. Optimum dimensionless height as a function of conversion. Case: Velocity =100

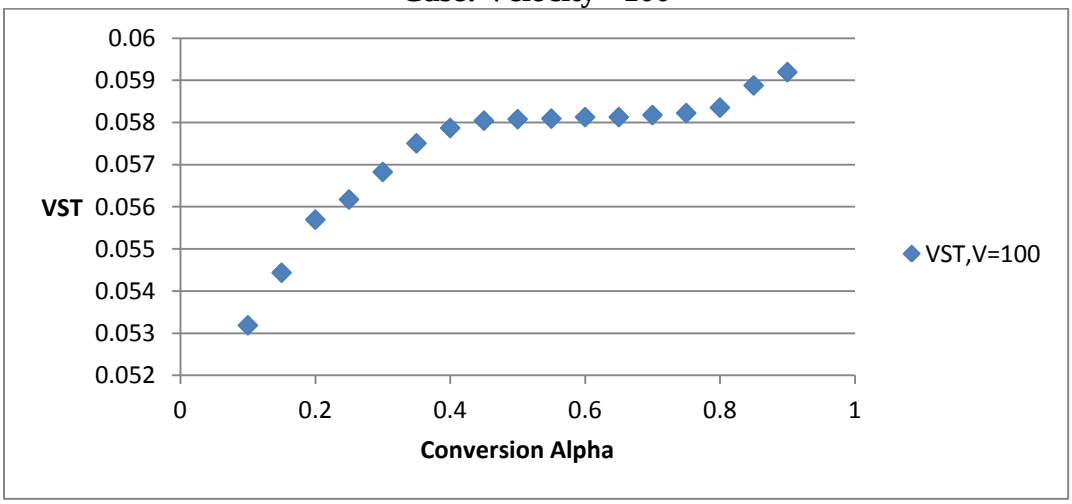

Figure 3-5. Optimum dimensionless VST as a function of conversion. Case: Velocity =100

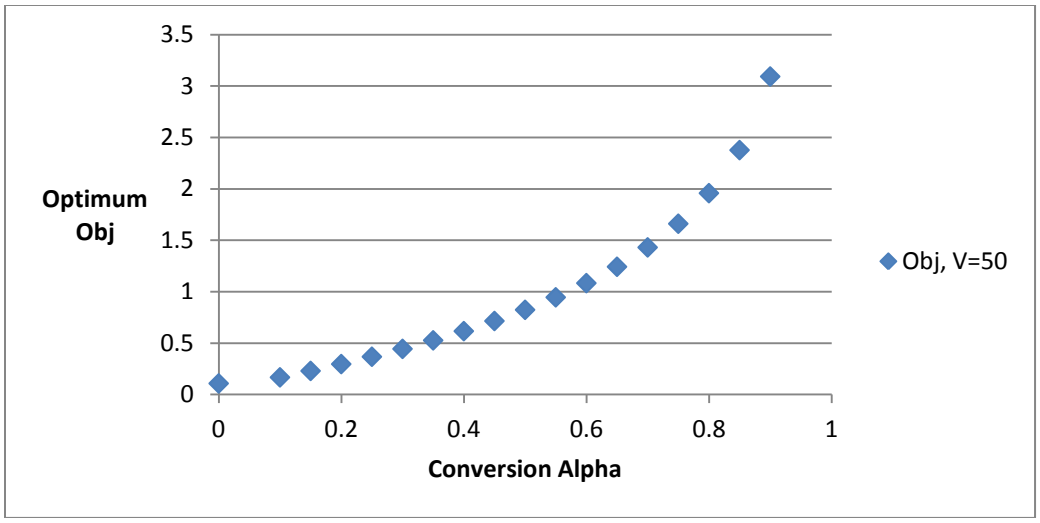

Figure 3-6. Optimum Objective function as a function of Conversion. Case: Velocity =50

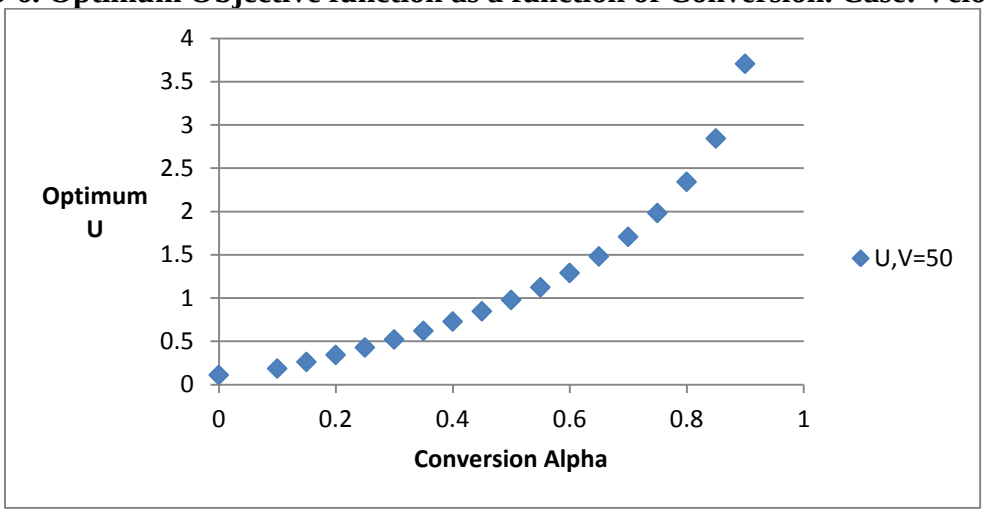

Figure 3-7. Optimum dimensionless length as a function of conversion. Case: Velocity =50

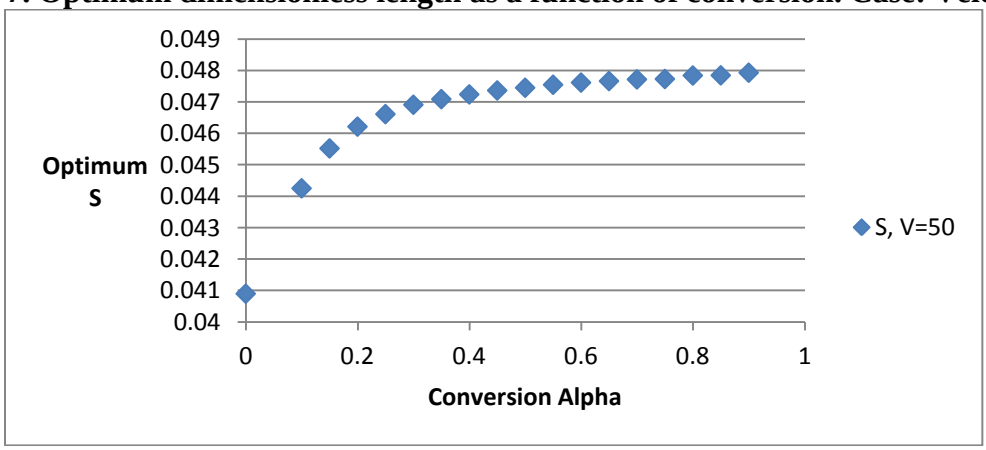

Figure 3-8. Optimum dimensionless height as a function of conversion. Case: Velocity =50

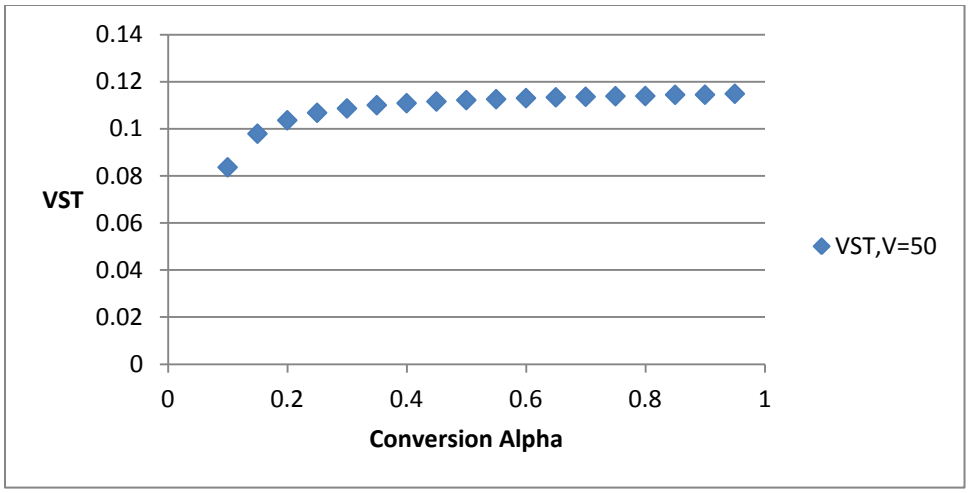

Figure 3-9. Optimum dimensionless VST as a function of conversion. Case: Velocity =50

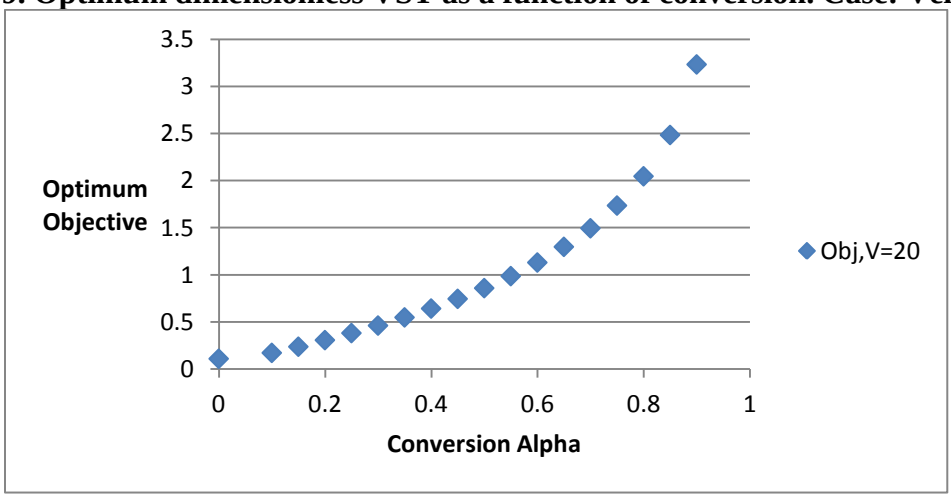

Figure 3-10. Optimum Objective function as a function of Conversion. Case: Velocity =20

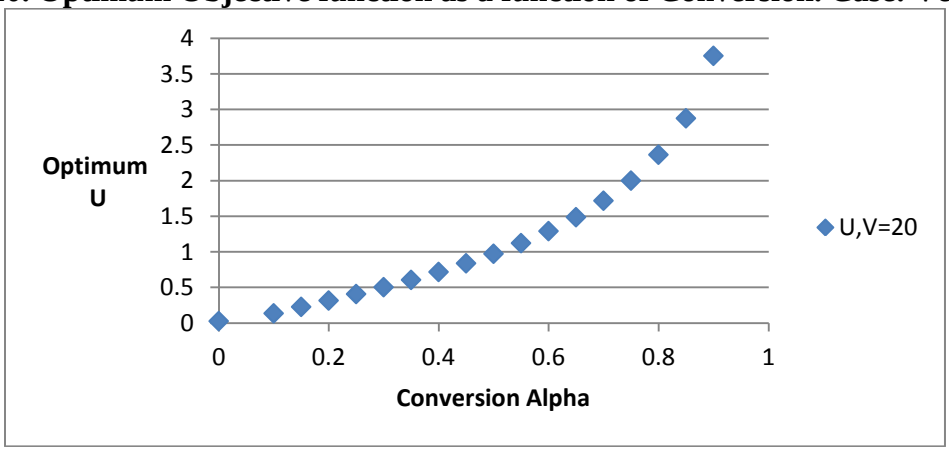

Figure 3-11 Optimum dimensionless length a function of conversion. Case: Velocity =20

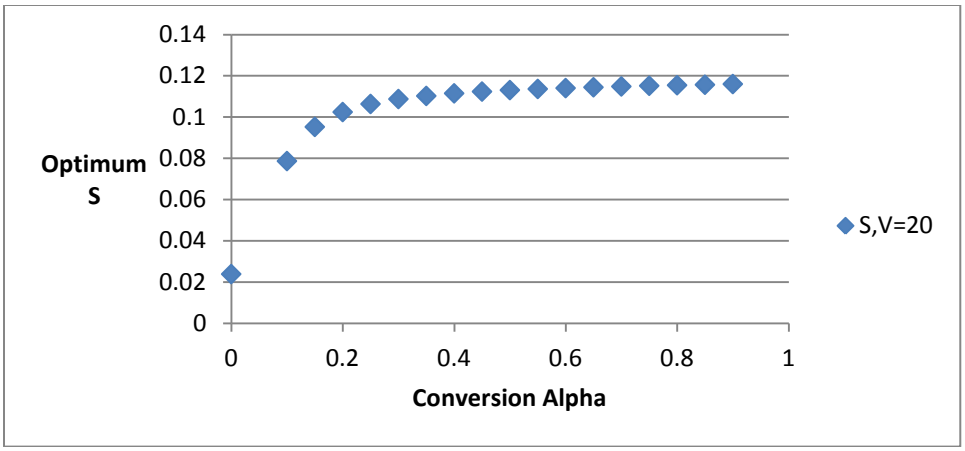

Figure 3-12. Optimum dimensionless height as a function of conversion. Case: Velocity =20

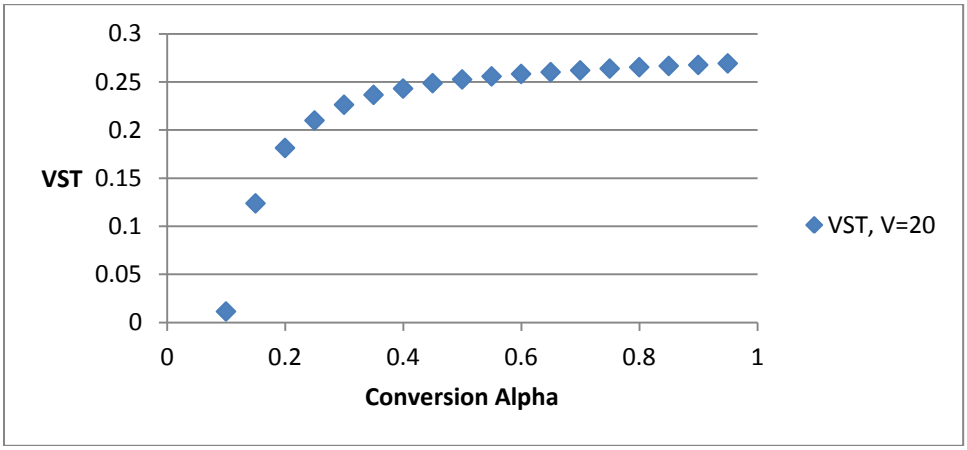

Figure 3-13. Optimum dimensionless VST as a function of conversion. Case: Velocity =20

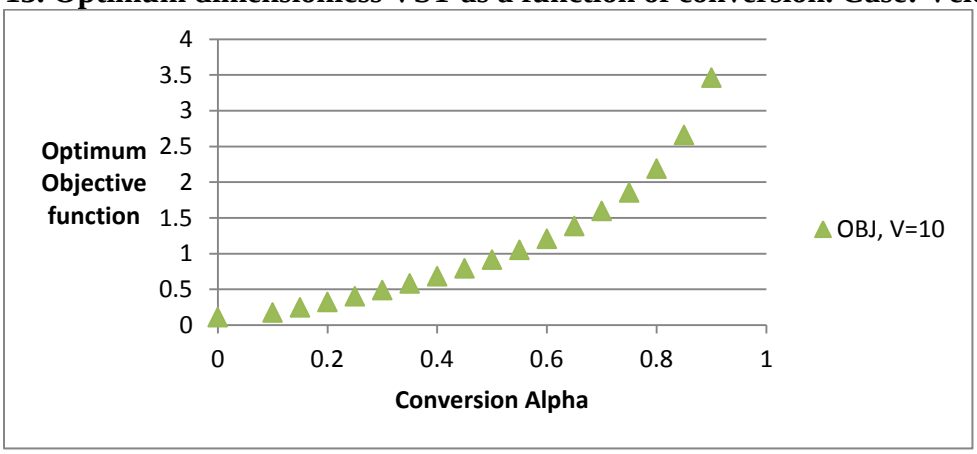

Figure 3-14. Optimum Objective function as a function of Conversion. Case: Velocity =10

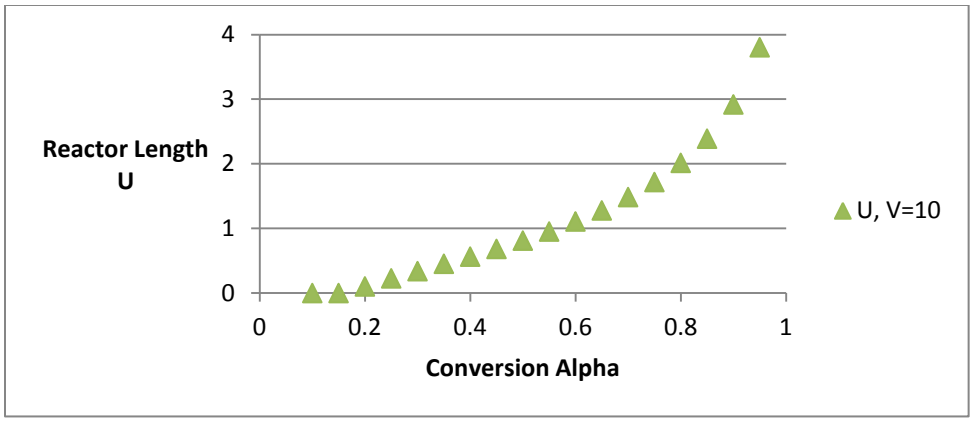

Figure 3-15. Optimum dimensionless length as a function of conversion. Case: Velocity =10

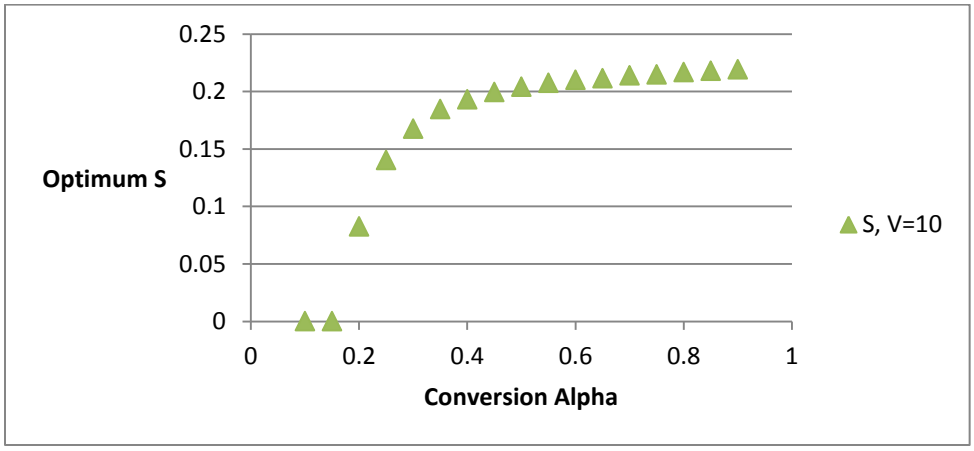

Figure 3-16. Optimum dimensionless height as a function of conversion. Case: Velocity =10

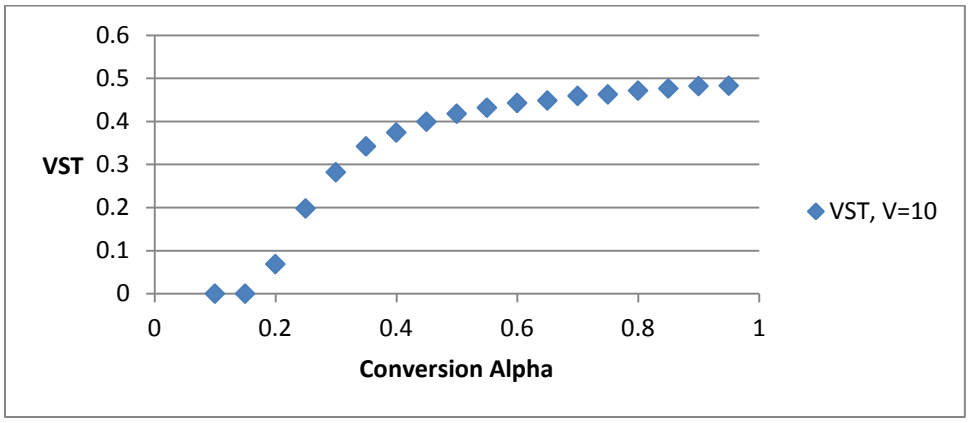

Figure 3-17. Optimum dimensionless VST as a function of conversion. Case: Velocity =10

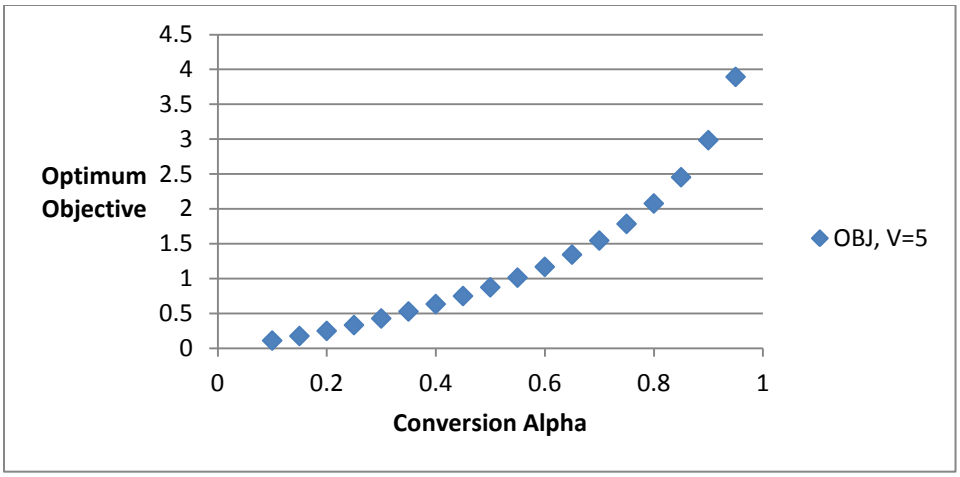

Figure 3-18. Optimum Objective function as a function of Conversion. Case: Velocity =5

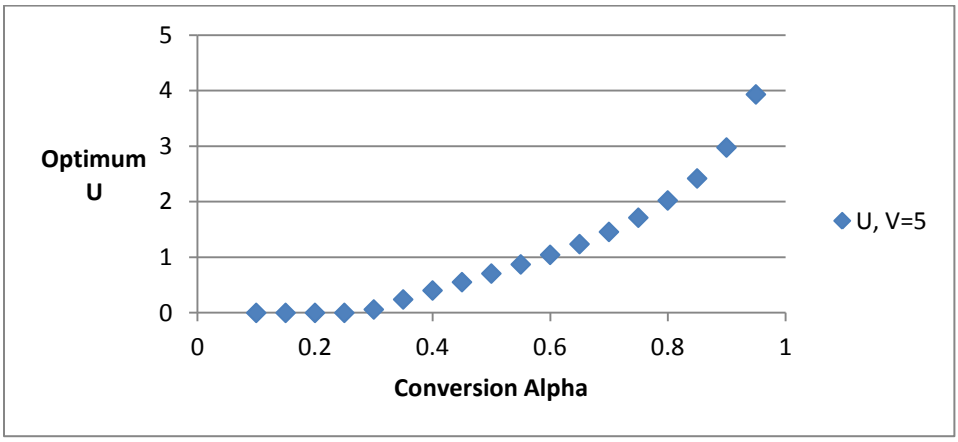

Figure 3-19. Optimum dimensionless length as a function of conversion. Case: Velocity =5

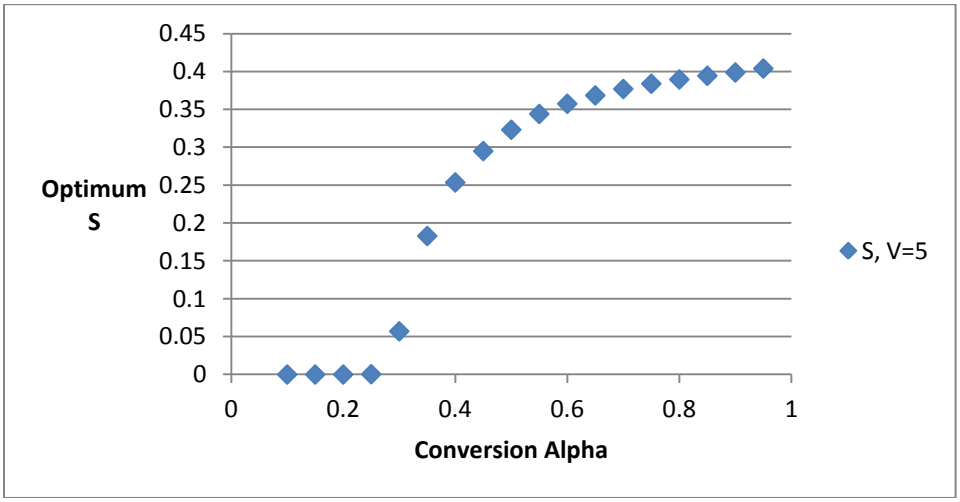

Figure 3-20. Optimum dimensionless height as a function of conversion. Case: Velocity =5

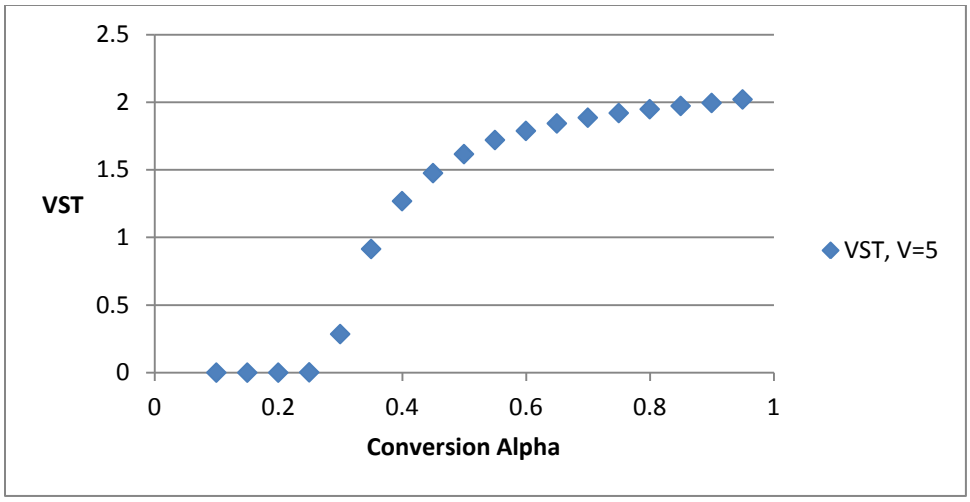

Figure 3-21. Optimum dimensionless VST as a function of conversion. Case: Velocity =5

Acknowledgements

Financial support from the U.S. National Science Foundation under grant # CTS-0829211, and Saudi Aramco Oil Company R&D is gratefully acknowledged.

3.5 References

A. Cybulski, JA Moulijn." *Structured Catalysts and Reactors"* 2nd Editon, (2006).

Parmaliana, A., et al. "A kinetic study of the hydrogenation of benzene over monolithic-supported platinum catalyst." *Applied Catalysis* 7.2 (1983): 221-232.

Parmaliana, A., et al. "A kinetic study of low temperature hydrogenation of benzene over monolithic-supported platinum catalyst." *Applied catalysis* 12.1 (1984): 49-57.

Klinghoffer, Alec A., Ramon L. Cerro, and Martin A. Abraham. "Influence of flow properties on the performance of the monolith froth reactor for catalytic wet oxidation of acetic acid." *Industrial & engineering chemistry research* 37.4 (1998): 1203-1210.

Nicolella, Crisliano, and Mauro Rovatti. "Mathematical modeling of monolith reactors for photocatalytic oxidation of air contaminants." *Chemical Engineering Journal* 69.2 (1998): 119-126.

Soni, D. S., and B. L. Crynes. "A comparison of the hydrodesulfurization and hydrodenitrogenation activities of monolith alumina impregnated with cobalt and molybdenum and a commercial catalyst." *ACS Symp. Ser*. Vol. 156. 1981.

Zabar, E., and M. Sheintuch. "OPTIMIZATION OF AN AUTOTHERMAL MONOLITHIC REACTOR-HEAT EXCHANGER FOR SO2 OXIDATION OVER PLATINUM." *Chemical Engineering Communications* 16.1-6 (1982): 313-323.

Sughrue, E. L., and C. H. Bartholomew. "Kinetics of carbon monoxide methanation on nickel monolithic catalysts." *Applied Catalysis* 2.4 (1982): 239-256.

Tucci, E. R., and W. J. Thomson. "Monolith catalyst favored for methanation." *Hydrocarbon Processing* 58 (1979): 123-126.

Groppi, G., et al. "A comparison of lumped and distributed models of monolith catalytic combustors." *Chemical Engineering Science* 50.17 (1995): 2705-2715.

Groppi, Gianpiero, and Enrico Tronconi. "Theoretical analysis of mass and heat transfer in monolith catalysts with triangular channels." *Chemical engineering science* 52.20 (1997): 3521-3526.

Groppi, Gianpiero, and Enrico Tronconi. "Simulation of structured catalytic reactors with enhanced thermal conductivity for selective oxidation reactions." *Catalysis today* 69.1 (2001): 63-73.

Groppi, Gianpiero, and Enrico Tronconi. "Honeycomb supports with high thermal conductivity for gas/solid chemical processes." *Catalysis today* 105.3 (2005): 297-304.

Veser, G., and J. Frauhammer. "Modelling steady state and ignition during catalytic methane oxidation in a monolith reactor." *Chemical Engineering Science* 55.12 (2000): 2271-2286.

Jarvi, G. A., K. B. Mayo, and C. H. Bartholomew. "Monolithic-supported nickel catalysts: I. Methanation activity relative to pellet catalysts." *Chemical Engineering Communications* 4.1-3 (1980): 325-341.

Koltsakis, G. C., P. A. Konstantinidis, and A. M. Stamatelos. "Development and application range of mathematical models for 3-way catalytic converters." *Applied Catalysis B: Environmental* 12.2 (1997): 161-191.

Pontikakis, G. N., G. S. Konstantas, and A. M. Stamatelos. "Three-way catalytic converter modeling as a modern engineering design tool." *Journal of Engineering for Gas Turbines and Power(Transactions of the ASME)* 126.4 (2004): 906-923.

MEI, Hong, et al. "Simulation of catalytic combustion of methane in a monolith honeycomb reactor." *Chinese Journal of Chemical Engineering* 14.1 (2006): 56-64.

Lachman, I. M., and R. N. McNally. "Monolithic honeycomb supports for catalysis." *Chem. Eng. Prog* 81 (1985).

Scinta, J., and S. W. Weller. "Catalytic hydrodesulfurization and liquefaction of coal: Batch autoclave studies." *Fuel Processing Technology* 1.4 (1978): 279-286.

S. T. Kolaczkowski and Hayes, R. E. "A study of Nusselt and Sherwood numbers in a monolith reactor." *Catalysis Today* 47.1 (1999): 295-303.

Kolaczkowski, Stan T. "Modelling catalytic combustion in monolith reactors–challenges faced." *Catalysis Today* 47.1 (1999): 209-218.

Young, LARRY C., and BRUCE A. Finlayson. "Mathematical modeling of the monolith converter." *Advances in Chemistry Series* 13 (1974): 629-643.

Crynes, Lawrence L., Ramon L. Cerro, and Martin A. Abraham. "Monolith froth reactor: Development of a novel three-phase catalytic system." *AIChE Journal* 41.2 (1995): 337-345.

Johnson, L. L., W. C. Johnson, and D. L. O'Brien. "The Use of Structural Ceramics in Automobile Exhaust Converters." *Chem. Eng. Progr. Symp. Ser*. Vol. 35. 1961.

Kreutzer, Michiel T., et al. "The pressure drop experiment to determine slug lengths in multiphase monoliths." *Catalysis today* 105.3 (2005): 667-672.

Ferguson, Noble B., and Bruce A. Finlayson. "Transient modeling of a catalytic converter to reduce nitric oxide in automobile exhaust." *AIChE Journal* 20.3 (1974): 539-550.

Canu, P., and S. Vecchi. "CFD simulation of reactive flows: catalytic combustion in a monolith." *AIChE journal* 48.12 (2002): 2921-2935.

Marín, Pablo, et al. "Combustion of methane lean mixtures in reverse flow reactors: Comparison between packed and structured catalyst beds." *Catalysis Today* 105.3 (2005): 701-708.

Parkinson, G. "Battelle maps ways to pare ethanol costs." *Chem. Eng* 88 (1981): 11-29.

Jahn, Robert, et al. "3-D modeling of monolith reactors." *Catalysis Today* 38.1 (1997): 39-46.

Edvinsson Albers, R., et al. "Development of a monolith-based process for H< sub> 2</sub> O< sub> 2</sub> production: from idea to large-scale implementation." *Catalysis today* 69.1 (2001): 247-252.

Hayes, R. E., et al. "The effect of washcoat geometry on mass transfer in monolith reactors." *Chemical Engineering Science* 59.15 (2004): 3169-3181.

Hayes, R. E., et al. "Three-way catalytic converter modelling with detailed kinetics and washcoat diffusion." *Topics in catalysis* 30.1-4 (2004): 411-415.

Hayes, R. E., et al. "The effect of washcoat geometry on mass transfer in monolith reactors." *Chemical Engineering Science* 59.15 (2004): 3169-3181.

Hayes, Robert E., et al. "Transient experiments and modeling of the catalytic combustion of methane in a monolith reactor." *Industrial & engineering chemistry research* 35.2 (1996): 406-414.

Heck, Roland H., James Wei, and James R. Katzer. "Mathematical modeling of monolithic catalysts." *AIChE Journal* 22.3 (1976): 477-484.

Edvinsson, Rolf K., Anna M. Holmgren, and Said Irandoust. "Liquid-phase hydrogenation of acetylene in a monolithic catalyst reactor." *Industrial & engineering chemistry research* 34.1 (1995): 94-100.

Edvinsson, Rolf, and Said Irandoust. "Hydrodesulfurization of dibenzothiophene in a monolithic catalyst reactor." *Industrial & engineering chemistry research*32.2 (1993): 391-395.

Heck, Ronald M., Suresh Gulati, and Robert J. Farrauto. "The application of monoliths for gas phase catalytic reactions." *Chemical Engineering Journal* 82.1 (2001): 149-156.

Irandoust, Said, and Bengt Andersson. "Monolithic catalysts for nonautomobile applications." *Catalysis Reviews Science and Engineering* 30.3 (1988): 341-392.

Tischer, Steffen, and Olaf Deutschmann. "Recent advances in numerical modeling of catalytic monolith reactors." *Catalysis Today* 105.3 (2005): 407-413.

Boger, Thorsten, and Monica Menegola. "Monolithic catalysts with high thermal conductivity for improved operation and economics in the production of phthalic anhydride." *Industrial & engineering chemistry research* 44.1 (2005): 30-40.

Nijhuis, T. A., et al. "Monolithic catalysts as more efficient three-phase reactors." *Catalysis Today* 66.2 (2001): 157-165.

Nijhuis, T. A., et al. "Water removal by reactive stripping for a solid-acid catalyzed esterification in a monolithic reactor." *Chemical engineering science*57.9 (2002): 1627-1632.T.A.

Patrick, Trent A., and Martin A. Abraham. "Evaluation of a monolith-supported Pt/Al2O3 catalyst for wet oxidation of carbohydrate-containing waste streams."*Environmental science & technology* 34.16 (2000): 3480-3488.

Tomašić, Vesna. "Application of the monoliths in DeNO< sub> x</sub> catalysis." *Catalysis today* 119.1 (2007): 106-113.

Tucci, E. R. "Use catalytic combustion for LHV gases." *Hydrocarbon Process.;(United States)* 61.3 (1982).

Hatziantoniou, Vasilios, and Bengt Andersson. "The segmented two-phase flow monolithic catalyst reactor. An alternative for liquid-phase hydrogenations."*Industrial & engineering chemistry fundamentals* 23.1 (1984): 82-88.

Hatziantoniou, Vasilios, Bengt Andersson, and Nils Herman Schoon. "Mass transfer and selectivity in liquid-phase hydrogenation of nitro compounds in a monolithic catalyst reactor with segmented gas-liquid flow." *Industrial & Engineering Chemistry Process Design and Development* 25.4 (1986): 964-970.

Sadykov, V. A., et al. "Oxidative dehydrogenation of propane over monoliths at short contact times." *Catalysis today* 61.1 (2000): 93-99.

Liu, Wei, et al. "Monolith reactor for the dehydrogenation of ethylbenzene to styrene." *Industrial & engineering chemistry research* 41.13 (2002): 3131-3138.

Xiaoding, Xu, et al. "Monolithic catalysts for selective hydrogenation of benzaldehyde." *Catalysis today* 30.1 (1996): 91-97.

3.6 Appendix A.3: Derivatives and Limits

Derivatives

$$\left\{\theta_n \tan\theta_n - S = 0, \quad n\pi \le \theta_n \le n\pi + \frac{\pi}{2} \;\; n = 0,\infty\right\} \Rightarrow$$

$$\left\{\frac{d\left(\theta_n \tan\theta_n - S\right)}{dS} = 0, \quad n\pi \le \theta_n \le n\pi + \frac{\pi}{2} \;\; n = 0,\infty\right\} \Leftrightarrow$$

$$\left\{\frac{d\theta_n}{dS}\tan\theta_n + \theta_n \frac{d\left(\tan\theta_n\right)}{dS} - 1 = 0, \quad n\pi \le \theta_n \le n\pi + \frac{\pi}{2} \;\; n = 0,\infty\right\} \Leftrightarrow$$

$$\left\{\frac{d\theta_n}{dS}\tan\theta_n + \theta_n \frac{1}{\left(\cos\theta_n\right)^2}\frac{d\theta_n}{dS} - 1 = 0, \quad n\pi \le \theta_n \le n\pi + \frac{\pi}{2} \;\; n = 0,\infty\right\} \Leftrightarrow$$

$$\left\{\frac{d\theta_n}{dS} = \frac{1}{\tan\theta_n + \theta_n \dfrac{1}{\left(\cos\theta_n\right)^2}}, \quad n\pi \le \theta_n \le n\pi + \frac{\pi}{2} \;\; n = 0,\infty\right\} \Leftrightarrow$$

$$\left\{\frac{d\theta_n}{dS} = \frac{\theta_n}{{\theta_n}^2 + S^2 + S}, \quad n\pi \le \theta_n \le n\pi + \frac{\pi}{2} \;\; n = 0,\infty\right\}. \text{ Similarly}$$

$$\left\{\frac{d\phi_m}{dT} = \frac{\phi_m}{{\phi_m}^2 + T^2 + T}, \quad m\pi \le \phi_m \le m\pi + \frac{\pi}{2} \;\; m = 0,\infty\right\}. \text{ Then}$$

$$\frac{\partial\left[\dfrac{1}{{\theta_n}^2\left({\theta_n}^2 + S^2 + S\right)}\right]}{\partial S} = \frac{-\left[2\theta_n \dfrac{\theta_n}{{\theta_n}^2 + S^2 + S}\left({\theta_n}^2 + S^2 + S\right) + {\theta_n}^2\left(2\theta_n \dfrac{\theta_n}{{\theta_n}^2 + S^2 + S} + 2S + 1\right)\right]}{\left[{\theta_n}^2\left({\theta_n}^2 + S^2 + S\right)\right]^2} \Leftrightarrow$$

$$\frac{\partial\left[\dfrac{1}{{\theta_n}^2\left({\theta_n}^2 + S^2 + S\right)}\right]}{\partial S} = \frac{-\left[\dfrac{2{\theta_n}^2}{{\theta_n}^2 + S^2 + S} + 2S + 3\right]}{\left[\theta_n\left({\theta_n}^2 + S^2 + S\right)\right]^2}. \text{ Similarly}$$

$$\frac{\partial\left[\frac{1}{\phi_m{}^2\left(\phi_m{}^2+T^2+T\right)}\right]}{\partial T}=\frac{-\left[\frac{2\phi_m{}^2}{\phi_m{}^2+T^2+T}+2T+3\right]}{\left[\phi_m\left(\phi_m{}^2+T^2+T\right)\right]^2}$$

$$\boxed{\frac{\partial\rho_{1,n.m}}{\partial U}=\frac{\rho_{1,n.m}}{U}},\boxed{\frac{\partial\left(\rho_{1,n.m}/U\right)}{\partial U}=0};\ \boxed{\frac{\partial\rho_{2,n.m}}{\partial U}=\frac{\rho_{2,n.m}}{U}},\boxed{\frac{\partial\left(\rho_{2,n.m}/U\right)}{\partial U}=0}$$

$$\frac{\partial\rho_{1,n.m}}{\partial V}=U\frac{\partial\left[\frac{V}{2}-\sqrt{\left(\frac{V}{2}\right)^2+\left(K+\frac{\phi_m{}^2}{T^2}+\frac{\theta_n{}^2}{S^2}\right)}\right]}{\partial V}=$$

$$=U\left[\left(\frac{1}{2}\right)-\left(\frac{1}{2}\right)\frac{\frac{2V}{4}}{\sqrt{\left(\frac{V}{2}\right)^2+\left(K+\frac{\phi_m{}^2}{T^2}+\frac{\theta_n{}^2}{S^2}\right)}}\right]=$$

$$=\frac{U}{2}\left[1-\frac{1}{2}\frac{V}{\sqrt{\left(\frac{V}{2}\right)^2+\left(K+\frac{\phi_m{}^2}{T^2}+\frac{\theta_n{}^2}{S^2}\right)}}\right]\Rightarrow$$

$$\boxed{\frac{\partial\rho_{1,n.m}}{\partial V}=U\frac{\rho_{1,n.m}}{2\rho_{1,n.m}-UV}=U\frac{\rho_{2,n.m}-VU}{2\rho_{2,n.m}-VU}=-U\frac{\rho_{1,n.m}}{\rho_{2,n.m}-\rho_{1,n.m}}}.\ \text{Similarly,}$$

$$\boxed{\frac{\partial\rho_{2,n.m}}{\partial V}=U\frac{VU-\rho_{1,n.m}}{VU-2\rho_{1,n.m}}=U\frac{\rho_{2,n.m}}{2\rho_{2,n.m}-VU}=U\frac{\rho_{2,n.m}}{\rho_{2,n.m}-\rho_{1,n.m}}}$$

$$\frac{\partial\rho_{1,n.m}}{\partial S}=U\frac{\partial\left[\frac{V}{2}-\sqrt{\left(\frac{V}{2}\right)^2+\left(K+\frac{\phi_m{}^2}{T^2}+\frac{\theta_n{}^2}{S^2}\right)}\right]}{\partial S}\Leftrightarrow$$

$$\frac{\partial \rho_{1,n.m}}{\partial S} = -U \frac{1}{2\sqrt{\left(\frac{V}{2}\right)^2 + \left(K + \frac{\phi_m{}^2}{T^2} + \frac{\theta_n{}^2}{S^2}\right)}} \left(\frac{\partial \left(\frac{\theta_n{}^2}{S^2} \right)}{\partial S} \right) \Leftrightarrow$$

$$\frac{\partial \rho_{1,n.m}}{\partial S} = -U \frac{1}{2\sqrt{\left(\frac{V}{2}\right)^2 + \left(K + \frac{\phi_m{}^2}{T^2} + \frac{\theta_n{}^2}{S^2}\right)}} \left(\frac{\left(\frac{2\theta_n{}^2}{\theta_n{}^2 + S^2 + S} \right) S^2 - 2S\theta_n{}^2}{S^4} \right) \Leftrightarrow$$

$$\frac{\partial \rho_{1,n.m}}{\partial S} = U \frac{\theta_n{}^2 \left(\left(\frac{\theta_n{}^2 + S^2}{\theta_n{}^2 + S^2 + S} \right) \right)}{S^3 \sqrt{\left(\frac{V}{2}\right)^2 + \left(K + \frac{\phi_m{}^2}{T^2} + \frac{\theta_n{}^2}{S^2}\right)}}. \text{ Similarly,}$$

$$\frac{\partial \rho_{2,n.m}}{\partial S} = -U \frac{\theta_n{}^2 \left(\left(\frac{\theta_n{}^2 + S^2}{\theta_n{}^2 + S^2 + S} \right) \right)}{S^3 \sqrt{\left(\frac{V}{2}\right)^2 + \left(K + \frac{\phi_m{}^2}{T^2} + \frac{\theta_n{}^2}{S^2}\right)}} = -\frac{\partial \rho_{1,n.m}}{\partial S}$$

$$\frac{\partial \rho_{1,n.m}}{\partial T} = U \frac{\phi_m{}^2 \left(\left(\frac{\phi_m{}^2 + T^2}{\phi_m{}^2 + T^2 + T} \right) \right)}{T^3 \sqrt{\left(\frac{V}{2}\right)^2 + \left(K + \frac{\phi_m{}^2}{T^2} + \frac{\theta_n{}^2}{S^2}\right)}} = -\frac{\partial \rho_{2,n.m}}{\partial T}. \text{ In addition,}$$

$$\frac{\partial \left[\frac{\left(\rho_{2,n,m}\right)^2 e^{-\rho_{1,n,m}} - \left(\rho_{1,n,m}\right)^2 e^{-\rho_{2,n,m}}}{\left(\rho_{2,n,m} - \rho_{1,n,m}\right)} \right]}{\partial S} = \frac{\left[\begin{array}{l} 2\rho_{2,n,m} \frac{\partial \rho_{2,n.m}}{\partial S} e^{-\rho_{1,n,m}} + \\ \left(\rho_{2,n,m}\right)^2 e^{-\rho_{1,n,m}} \left(-\frac{\partial \rho_{1,n.m}}{\partial S} \right) - \\ 2\left(\rho_{1,n,m}\right) \frac{\partial \rho_{1,n.m}}{\partial S} e^{-\rho_{2,n,m}} - \\ \left(\rho_{1,n,m}\right)^2 e^{-\rho_{2,n,m}} \left(-\frac{\partial \rho_{2,n.m}}{\partial S} \right) \end{array} \right] \left(\rho_{2,n,m} - \rho_{1,n,m}\right) - \left[\begin{array}{l} \left(\rho_{2,n,m}\right)^2 e^{-\rho_{1,n,m}} - \\ \left(\rho_{1,n,m}\right)^2 e^{-\rho_{2,n,m}} \end{array} \right] \left(\begin{array}{l} \frac{\partial \rho_{2,n.m}}{\partial S} - \\ \frac{\partial \rho_{1,n.m}}{\partial S} \end{array} \right)}{\left(\rho_{2,n,m} - \rho_{1,n,m}\right)^2} =$$

$$= \frac{\partial \rho_{2,n,m}}{\partial S} \frac{\begin{bmatrix} 2\rho_{2,n,m} e^{-\rho_{1,n,m}} + \\ \left(\rho_{2,n,m}\right)^2 e^{-\rho_{1,n,m}} + \\ 2\left(\rho_{1,n,m}\right) e^{-\rho_{2,n,m}} + \\ \left(\rho_{1,n,m}\right)^2 e^{-\rho_{2,n,m}} \end{bmatrix} \left(\rho_{2,n,m} - \rho_{1,n,m}\right) - 2\left[\left(\rho_{2,n,m}\right)^2 e^{-\rho_{1,n,m}} - \left(\rho_{1,n,m}\right)^2 e^{-\rho_{2,n,m}}\right]}{\left(\rho_{2,n,m} - \rho_{1,n,m}\right)^2} \Leftrightarrow$$

$$\boxed{\frac{\partial\left[\frac{\left(\rho_{2,n,m}\right)^2 e^{-\rho_{1,n,m}} - \left(\rho_{1,n,m}\right)^2 e^{-\rho_{2,n,m}}}{\left(\rho_{2,n,m} - \rho_{1,n,m}\right)}\right]}{\partial S} = -U \frac{\theta_n{}^2 \left(\frac{\theta_n{}^2 + S^2}{\theta_n{}^2 + S^2 + S}\right)}{S^3 \sqrt{\left(\frac{V}{2}\right)^2 + \left(K + \frac{\phi_m{}^2}{T^2} + \frac{\theta_n{}^2}{S^2}\right)}} \left[\begin{array}{l} \frac{\left[\left(\rho_{2,n,m}\right)^2 e^{-\rho_{1,n,m}} + \left(\rho_{1,n,m}\right)^2 e^{-\rho_{2,n,m}}\right]}{\left(\rho_{2,n,m} - \rho_{1,n,m}\right)} + \\ +2\rho_{1,n,m}\rho_{2,n,m} \frac{\left[e^{-\rho_{2,n,m}} - e^{-\rho_{1,n,m}}\right]}{\left(\rho_{2,n,m} - \rho_{1,n,m}\right)^2} \end{array}\right]}.$$

Similarly

$$\boxed{\frac{\partial\left[\frac{\left(\rho_{2,n,m}\right)^2 e^{-\rho_{1,n,m}} - \left(\rho_{1,n,m}\right)^2 e^{-\rho_{2,n,m}}}{\left(\rho_{2,n,m} - \rho_{1,n,m}\right)}\right]}{\partial T} = -U \frac{\phi_m{}^2 \left(\left(\frac{\phi_m{}^2 + T^2}{\phi_m{}^2 + T^2 + T}\right)\right)}{T^3 \sqrt{\left(\frac{V}{2}\right)^2 + \left(K + \frac{\phi_m{}^2}{T^2} + \frac{\theta_n{}^2}{S^2}\right)}} \left[\begin{array}{l} \frac{\left[\left(\rho_{2,n,m}\right)^2 e^{-\rho_{1,n,m}} + \left(\rho_{1,n,m}\right)^2 e^{-\rho_{2,n,m}}\right]}{\left(\rho_{2,n,m} - \rho_{1,n,m}\right)} + \\ +2\rho_{1,n,m}\rho_{2,n,m} \frac{\left[e^{-\rho_{2,n,m}} - e^{-\rho_{1,n,m}}\right]}{\left(\rho_{2,n,m} - \rho_{1,n,m}\right)^2} \end{array}\right]}$$

$$\frac{\partial\left[\frac{\left(\rho_{2,n,m}\right)^2 e^{-\rho_{1,n,m}} - \left(\rho_{1,n,m}\right)^2 e^{-\rho_{2,n,m}}}{\left(\rho_{2,n,m} - \rho_{1,n,m}\right)}\right]}{\partial U} = \frac{\left[\begin{array}{l} \frac{\partial\left[\left(\rho_{2,n,m}\right)^2 e^{-\rho_{1,n,m}} - \left(\rho_{1,n,m}\right)^2 e^{-\rho_{2,n,m}}\right]}{\partial U}\left(\rho_{2,n,m} - \rho_{1,n,m}\right) - \\ \left[\left(\rho_{2,n,m}\right)^2 e^{-\rho_{1,n,m}} - \left(\rho_{1,n,m}\right)^2 e^{-\rho_{2,n,m}}\right] \frac{\partial\left(\rho_{2,n,m} - \rho_{1,n,m}\right)}{\partial U} \end{array}\right]}{\left(\rho_{2,n,m} - \rho_{1,n,m}\right)^2} =$$

$$= \frac{\left[\begin{array}{l} \left[\begin{array}{l} 2\rho_{2,n,m} \frac{\partial \rho_{2,n,m}}{\partial U} e^{-\rho_{1,n,m}} + \left(\rho_{2,n,m}\right)^2 e^{-\rho_{1,n,m}} \frac{\partial\left(-\rho_{1,n,m}\right)}{\partial U} - \\ 2\rho_{1,n,m} \frac{\partial \rho_{1,n,m}}{\partial U} e^{-\rho_{2,n,m}} - \left(\rho_{1,n,m}\right)^2 e^{-\rho_{2,n,m}} \frac{\partial\left(-\rho_{2,n,m}\right)}{\partial U} \end{array}\right]\left(\rho_{2,n,m} - \rho_{1,n,m}\right) - \\ \left[\left(\rho_{2,n,m}\right)^2 e^{-\rho_{1,n,m}} - \left(\rho_{1,n,m}\right)^2 e^{-\rho_{2,n,m}}\right]\left(\frac{\partial \rho_{2,n,m}}{\partial U} - \frac{\partial \rho_{1,n,m}}{\partial U}\right) \end{array}\right]}{\left(\rho_{2,n,m} - \rho_{1,n,m}\right)^2} =$$

$$= \frac{\left[\begin{array}{l}\left[\begin{array}{l} 2\rho_{2,n,m}\dfrac{\rho_{2,n.m}}{U}e^{-\rho_{1,n,m}}+\left(\rho_{2,n,m}\right)^2 e^{-\rho_{1,n,m}}\dfrac{\left(-\rho_{1,n,m}\right)}{U}- \\ 2\rho_{1,n,m}\dfrac{\rho_{1,n,m}}{U}e^{-\rho_{2,n,m}}-\left(\rho_{1,n,m}\right)^2 e^{-\rho_{2,n,m}}\dfrac{\left(-\rho_{2,n,m}\right)}{U} \end{array}\right]\left(\rho_{2,n,m}-\rho_{1,n,m}\right)- \\ \left[\left(\rho_{2,n,m}\right)^2 e^{-\rho_{1,n,m}}-\left(\rho_{1,n,m}\right)^2 e^{-\rho_{2,n,m}}\right]\left(\dfrac{\rho_{2,n.m}}{U}-\dfrac{\rho_{1,n.m}}{U}\right) \end{array}\right]}{\left(\rho_{2,n,m}-\rho_{1,n,m}\right)^2} =$$

$$= \frac{1}{U}\frac{\left[\begin{array}{l}\left[\begin{array}{l} 2\left(\rho_{2,n,m}\right)^2 e^{-\rho_{1,n,m}}+\left(\rho_{2,n,m}\right)^2 e^{-\rho_{1,n,m}}\left(-\rho_{1,n,m}\right)- \\ 2\left(\rho_{1,n,m}\right)^2 e^{-\rho_{2,n,m}}-\left(\rho_{1,n,m}\right)^2 e^{-\rho_{2,n,m}}\left(-\rho_{2,n,m}\right) \end{array}\right]\left(\rho_{2,n,m}-\rho_{1,n,m}\right)- \\ \left[\left(\rho_{2,n,m}\right)^2 e^{-\rho_{1,n,m}}-\left(\rho_{1,n,m}\right)^2 e^{-\rho_{2,n,m}}\right]\left(\rho_{2,n,m}-\rho_{1,n,m}\right) \end{array}\right]}{\left(\rho_{2,n,m}-\rho_{1,n,m}\right)^2} \Leftrightarrow$$

$$\boxed{\frac{\partial\left[\dfrac{\left(\rho_{2,n,m}\right)^2 e^{-\rho_{1,n,m}}-\left(\rho_{1,n,m}\right)^2 e^{-\rho_{2,n,m}}}{\left(\rho_{2,n,m}-\rho_{1,n,m}\right)}\right]}{\partial U} = \frac{1}{U}\frac{\left[\left(\rho_{2,n,m}\right)^2 e^{-\rho_{1,n,m}}\left(1-\rho_{1,n,m}\right)-\left(\rho_{1,n,m}\right)^2 e^{-\rho_{2,n,m}}\left(1-\rho_{2,n,m}\right)\right]}{\left(\rho_{2,n,m}-\rho_{1,n,m}\right)}}$$

$$\frac{\partial\left[\dfrac{\left(\rho_{2,n,m}\right)^2 e^{-\rho_{1,n,m}}-\left(\rho_{1,n,m}\right)^2 e^{-\rho_{2,n,m}}}{\left(\rho_{2,n,m}-\rho_{1,n,m}\right)}\right]}{\partial V} = \frac{\left[\begin{array}{l}\dfrac{\partial\left[\left(\rho_{2,n,m}\right)^2 e^{-\rho_{1,n,m}}-\left(\rho_{1,n,m}\right)^2 e^{-\rho_{2,n,m}}\right]}{\partial V}\left(\rho_{2,n,m}-\rho_{1,n,m}\right)- \\ \left[\left(\rho_{2,n,m}\right)^2 e^{-\rho_{1,n,m}}-\left(\rho_{1,n,m}\right)^2 e^{-\rho_{2,n,m}}\right]\dfrac{\partial\left(\rho_{2,n,m}-\rho_{1,n,m}\right)}{\partial V} \end{array}\right]}{\left(\rho_{2,n,m}-\rho_{1,n,m}\right)^2} =$$

$$= \frac{\left[\begin{array}{l}\left[\begin{array}{l} 2\rho_{2,n,m}U\dfrac{\rho_{2,n.m}}{\rho_{2,n.m}-\rho_{1,n.m}}e^{-\rho_{1,n,m}}+\left(\rho_{2,n,m}\right)^2 e^{-\rho_{1,n,m}}U\dfrac{\rho_{1,n.m}}{\rho_{2,n.m}-\rho_{1,n.m}}+ \\ 2\rho_{1,n,m}U\dfrac{\rho_{1,n.m}}{\rho_{2,n.m}-\rho_{1,n.m}}e^{-\rho_{2,n,m}}+\left(\rho_{1,n,m}\right)^2 e^{-\rho_{2,n,m}}U\dfrac{\rho_{2,n.m}}{\rho_{2,n.m}-\rho_{1,n.m}} \end{array}\right]\left(\rho_{2,n,m}-\rho_{1,n,m}\right)- \\ \left[\left(\rho_{2,n,m}\right)^2 e^{-\rho_{1,n,m}}-\left(\rho_{1,n,m}\right)^2 e^{-\rho_{2,n,m}}\right]\left(U\dfrac{\rho_{2,n.m}}{\rho_{2,n.m}-\rho_{1,n.m}}+U\dfrac{\rho_{1,n.m}}{\rho_{2,n.m}-\rho_{1,n.m}}\right) \end{array}\right]}{\left(\rho_{2,n,m}-\rho_{1,n,m}\right)^2} =$$

$$= U\frac{\left[\begin{array}{l}\left[\begin{array}{l}2\left(\rho_{2,n,m}\right)^2 e^{-\rho_{1,n,m}}+\left(\rho_{2,n,m}\right)^2 e^{-\rho_{1,n,m}}\rho_{1,n.m}+\\ 2\left(\rho_{1,n,m}\right)^2 e^{-\rho_{2,n,m}}+\left(\rho_{1,n,m}\right)^2 e^{-\rho_{2,n,m}}\rho_{2,n.m}\end{array}\right]-\\ \left[\left(\rho_{2,n,m}\right)^2 e^{-\rho_{1,n,m}}-\left(\rho_{1,n,m}\right)^2 e^{-\rho_{2,n,m}}\right]\left(\frac{UV}{\rho_{2,n.m}-\rho_{1,n.m}}\right)\end{array}\right]}{\left(\rho_{2,n,m}-\rho_{1,n,m}\right)^2}\Leftrightarrow$$

$$\boxed{\frac{\partial\left[\frac{\left(\rho_{2,n,m}\right)^2 e^{-\rho_{1,n,m}}-\left(\rho_{1,n,m}\right)^2 e^{-\rho_{2,n,m}}}{\left(\rho_{2,n,m}-\rho_{1,n,m}\right)}\right]}{\partial V}=U\frac{\left[\begin{array}{l}\left[\left(\rho_{2,n,m}\right)^2 e^{-\rho_{1,n,m}}\left(2+\rho_{1,n.m}\right)+\left(\rho_{1,n,m}\right)^2 e^{-\rho_{2,n,m}}\left(2+\rho_{2,n.m}\right)\right]-\\ \left[\left(\rho_{2,n,m}\right)^2 e^{-\rho_{1,n,m}}-\left(\rho_{1,n,m}\right)^2 e^{-\rho_{2,n,m}}\right]\left(\frac{UV}{\rho_{2,n.m}-\rho_{1,n.m}}\right)\end{array}\right]}{\left(\rho_{2,n,m}-\rho_{1,n,m}\right)^2}}$$

Now we evaluate $\frac{\partial C_A^{out^*}}{\partial S},\frac{\partial C_A^{out^*}}{\partial T},\frac{\partial C_A^{out^*}}{\partial U},\frac{\partial C_A^{out^*}}{\partial V}$

$$\frac{\partial C_A^{out^*}}{\partial S}=\frac{\partial\left[4UVS^2T^2\sum_{n=0}^{\infty}\sum_{m=0}^{\infty}\left\{\frac{\left[\frac{1}{\theta_n^{\,2}\left(\theta_n^{\,2}+S^2+S\right)}\right]\left[\frac{1}{\phi_m^{\,2}\left(\phi_m^{\,2}+T^2+T\right)}\right]}{\left[\frac{\left(\rho_{2,n,m}\right)^2 e^{-\rho_{1,n,m}}-\left(\rho_{1,n,m}\right)^2 e^{-\rho_{2,n,m}}}{\left(\rho_{2,n,m}-\rho_{1,n,m}\right)}\right]}\right\}\right]}{\partial S}\Leftrightarrow$$

$$\frac{\partial C_A^{out^*}}{\partial S}=4UVT^2\left(\begin{array}{l}2S\sum_{n=0}^{\infty}\sum_{m=0}^{\infty}\left\{\frac{\left[\frac{1}{\theta_n^{\,2}\left(\theta_n^{\,2}+S^2+S\right)}\right]\left[\frac{1}{\phi_m^{\,2}\left(\phi_m^{\,2}+T^2+T\right)}\right]}{\left[\frac{\left(\rho_{2,n,m}\right)^2 e^{-\rho_{1,n,m}}-\left(\rho_{1,n,m}\right)^2 e^{-\rho_{2,n,m}}}{\left(\rho_{2,n,m}-\rho_{1,n,m}\right)}\right]}\right\}+\\ +S^2\sum_{n=0}^{\infty}\sum_{m=0}^{\infty}\left[\frac{1}{\phi_m^{\,2}\left(\phi_m^{\,2}+T^2+T\right)}\right]\frac{\partial\left\{\frac{\left[\frac{1}{\theta_n^{\,2}\left(\theta_n^{\,2}+S^2+S\right)}\right]}{\left[\frac{\left(\rho_{2,n,m}\right)^2 e^{-\rho_{1,n,m}}-\left(\rho_{1,n,m}\right)^2 e^{-\rho_{2,n,m}}}{\left(\rho_{2,n,m}-\rho_{1,n,m}\right)}\right]}\right\}}{\partial S}\end{array}\right)\Leftrightarrow$$

$$\frac{\partial C_A^{out^*}}{\partial S} = \frac{2C_A^{out^*}}{S} + 4UVS^2T^2 \left(\sum_{n=0}^{\infty}\sum_{m=0}^{\infty}\left[\frac{1}{\phi_m^{\,2}\left(\phi_m^{\,2}+T^2+T\right)}\right] \frac{\partial\left\{\dfrac{\left[\dfrac{1}{\theta_n^{\,2}\left(\theta_n^{\,2}+S^2+S\right)}\right]}{\left[\dfrac{\left(\rho_{2,n,m}\right)^2 e^{-\rho_{1,n,m}} - \left(\rho_{1,n,m}\right)^2 e^{-\rho_{2,n,m}}}{\left(\rho_{2,n,m}-\rho_{1,n,m}\right)}\right]}\right\}}{\partial S} \right) \Leftrightarrow$$

$$\frac{\partial C_A^{out^*}}{\partial S} = \frac{2C_A^{out^*}}{S} + 4UVS^2T^2 \left(\sum_{n=0}^{\infty}\sum_{m=0}^{\infty} \frac{\left[-\dfrac{\left[\dfrac{2\theta_n^{\,2}\left(\theta_n^{\,2}+S^2+S\right)}{\theta_n^{\,2}+S^2+S} + \theta_n^{\,2}\left(\dfrac{2\theta_n^{\,2}}{\theta_n^{\,2}+S^2+S}+2S+1\right)\right]}{\left[\theta_n^{\,2}\left(\theta_n^{\,2}+S^2+S\right)\right]^2}\right]\left[\dfrac{\left(\rho_{2,n,m}\right)^2 e^{-\rho_{1,n,m}} - \left(\rho_{1,n,m}\right)^2 e^{-\rho_{2,n,m}}}{\left(\rho_{2,n,m}-\rho_{1,n,m}\right)}\right] - \left[\dfrac{1}{\theta_n^{\,2}\left(\theta_n^{\,2}+S^2+S\right)}\right]\dfrac{\partial\left[\dfrac{\left(\rho_{2,n,m}\right)^2 e^{-\rho_{1,n,m}} - \left(\rho_{1,n,m}\right)^2 e^{-\rho_{2,n,m}}}{\left(\rho_{2,n,m}-\rho_{1,n,m}\right)}\right]}{\partial S}}{\left[\phi_m^{\,2}\left(\phi_m^{\,2}+T^2+T\right)\right]\left[\dfrac{\left(\rho_{2,n,m}\right)^2 e^{-\rho_{1,n,m}} - \left(\rho_{1,n,m}\right)^2 e^{-\rho_{2,n,m}}}{\left(\rho_{2,n,m}-\rho_{1,n,m}\right)}\right]^2} \right) \Leftrightarrow$$

$$\frac{\partial C_A^{out^*}}{\partial S} = \frac{2C_A^{out^*}}{S} - 4UVS^2T^2 \left(\sum_{n=0}^{\infty}\sum_{m=0}^{\infty} \frac{\left[\begin{array}{l} \left(\dfrac{2\theta_n^{\,2}}{\theta_n^{\,2}+S^2+S} + 2S + 3 \right) \left[\dfrac{\left(\rho_{2,n,m}\right)^2 e^{-\rho_{1,n,m}} - \left(\rho_{1,n,m}\right)^2 e^{-\rho_{2,n,m}}}{\left(\rho_{2,n,m}-\rho_{1,n,m}\right)} \right] + \\ \dfrac{\partial \rho_{2,n.m}}{\partial S} \dfrac{\left[\begin{array}{l} \left[\begin{array}{l} 2\left(\rho_{2,n,m}\right)e^{-\rho_{1,n,m}} + \left(\rho_{2,n,m}\right)^2 e^{-\rho_{1,n,m}} + \\ +2\left(\rho_{1,n,m}\right)e^{-\rho_{2,n,m}} + \left(\rho_{1,n,m}\right)^2 e^{-\rho_{2,n,m}} \end{array} \right] \left(\rho_{2,n,m}-\rho_{1,n,m}\right) - \\ 2\left[\left(\rho_{2,n,m}\right)^2 e^{-\rho_{1,n,m}} - \left(\rho_{1,n,m}\right)^2 e^{-\rho_{2,n,m}} \right] \end{array} \right]}{\left(\rho_{2,n,m}-\rho_{1,n,m}\right)^2} \end{array} \right]}{\left[\theta_n^{\,2}\left(\theta_n^{\,2}+S^2+S\right)\right]\left[\phi_m^{\,2}\left(\phi_m^{\,2}+T^2+T\right)\right]\left[\dfrac{\left(\rho_{2,n,m}\right)^2 e^{-\rho_{1,n,m}} - \left(\rho_{1,n,m}\right)^2 e^{-\rho_{2,n,m}}}{\left(\rho_{2,n,m}-\rho_{1,n,m}\right)} \right]^2} \right) \Leftrightarrow$$

$$\frac{\partial C_A^{out^*}}{\partial S} = \frac{2C_A^{out^*}}{S} - 4UVS^2T^2 \left(\sum_{n=0}^{\infty}\sum_{m=0}^{\infty} \frac{\left[\begin{array}{l} \left[\dfrac{2\theta_n^{\,2}}{\theta_n^{\,2}+S^2+S} + 2S + 3 \right] \left[\dfrac{\left(\rho_{2,n,m}\right)^2 e^{-\rho_{1,n,m}} - \left(\rho_{1,n,m}\right)^2 e^{-\rho_{2,n,m}}}{\left(\rho_{2,n,m}-\rho_{1,n,m}\right)} \right] + \\ \dfrac{\partial \rho_{2,n.m}}{\partial S} \left[\begin{array}{l} \dfrac{\left[\left(\rho_{2,n,m}\right)^2 e^{-\rho_{1,n,m}} + \left(\rho_{1,n,m}\right)^2 e^{-\rho_{2,n,m}} \right]}{\left(\rho_{2,n,m}-\rho_{1,n,m}\right)} + \\ +2\rho_{1,n,m}\rho_{2,n,m} \dfrac{\left[e^{-\rho_{2,n,m}} - e^{-\rho_{1,n,m}} \right]}{\left(\rho_{2,n,m}-\rho_{1,n,m}\right)^2} \end{array} \right] \end{array} \right]}{\left[\theta_n^{\,2}\left(\theta_n^{\,2}+S^2+S\right)\right]\left[\phi_m^{\,2}\left(\phi_m^{\,2}+T^2+T\right)\right]\left[\dfrac{\left(\rho_{2,n,m}\right)^2 e^{-\rho_{1,n,m}} - \left(\rho_{1,n,m}\right)^2 e^{-\rho_{2,n,m}}}{\left(\rho_{2,n,m}-\rho_{1,n,m}\right)} \right]^2} \right) \Leftrightarrow$$

$$\frac{\partial C_{A}^{out^{*}}}{\partial S}=\frac{2C_{A}^{out^{*}}}{S}-4UVS^{2}T^{2}\left(\sum_{n=0}^{\infty}\sum_{m=0}^{\infty}\frac{\left[\frac{\left[\frac{2\theta_n^{2}}{\theta_n^{2}+S^{2}+S}+2S+3\right]}{\left[\theta_n^{2}+S^{2}+S\right]}\left[\frac{\left(\rho_{2,n,m}\right)^{2}e^{-\rho_{1,n,m}}-\left(\rho_{1,n,m}\right)^{2}e^{-\rho_{2,n,m}}}{\left(\rho_{2,n,m}-\rho_{1,n,m}\right)}\right]-\right.}{\left[\theta_n^{2}\left(\theta_n^{2}+S^{2}+S\right)\right]\left[\phi_m^{2}\left(\phi_m^{2}+T^{2}+T\right)\right]\left[\frac{\left(\rho_{2,n,m}\right)^{2}e^{-\rho_{1,n,m}}-\left(\rho_{1,n,m}\right)^{2}e^{-\rho_{2,n,m}}}{\left(\rho_{2,n,m}-\rho_{1,n,m}\right)}\right]^{2}}\right.$$
$$\left.\left.U\frac{\theta_n^{2}\left(\frac{\theta_n^{2}+S^{2}}{\theta_n^{2}+S^{2}+S}\right)}{S^{3}\sqrt{\left(\frac{V}{2}\right)^{2}+\left(K+\frac{\phi_m^{2}}{T^{2}}+\frac{\theta_n^{2}}{S^{2}}\right)}}\left[\frac{\left[\left(\rho_{2,n,m}\right)^{2}e^{-\rho_{1,n,m}}+\left(\rho_{1,n,m}\right)^{2}e^{-\rho_{2,n,m}}\right]}{\left(\rho_{2,n,m}-\rho_{1,n,m}\right)}+\right.\right.$$
$$\left.\left.+2\rho_{1,n,m}\rho_{2,n,m}\frac{\left[e^{-\rho_{2,n,m}}-e^{-\rho_{1,n,m}}\right]}{\left(\rho_{2,n,m}-\rho_{1,n,m}\right)^{2}}\right]\right]$$

Similarly

$$\frac{\partial C_{A}^{out^{*}}}{\partial T}=\frac{2C_{A}^{out^{*}}}{T}-4UVS^{2}T^{2}\left(\sum_{n=0}^{\infty}\sum_{m=0}^{\infty}\frac{\left[\frac{\left[\frac{2\phi_m^{2}}{\phi_m^{2}+T^{2}+T}+2T+3\right]}{\left[\phi_m^{2}+T^{2}+T\right]}\left[\frac{\left(\rho_{2,n,m}\right)^{2}e^{-\rho_{1,n,m}}-\left(\rho_{1,n,m}\right)^{2}e^{-\rho_{2,n,m}}}{\left(\rho_{2,n,m}-\rho_{1,n,m}\right)}\right]-\right.}{\left[\theta_n^{2}\left(\theta_n^{2}+S^{2}+S\right)\right]\left[\phi_m^{2}\left(\phi_m^{2}+T^{2}+T\right)\right]\left[\frac{\left(\rho_{2,n,m}\right)^{2}e^{-\rho_{1,n,m}}-\left(\rho_{1,n,m}\right)^{2}e^{-\rho_{2,n,m}}}{\left(\rho_{2,n,m}-\rho_{1,n,m}\right)}\right]^{2}}\right.$$
$$\left.\left.U\frac{\phi_m^{2}\left(\frac{\phi_m^{2}+T^{2}}{\phi_m^{2}+T^{2}+T}\right)}{T^{3}\sqrt{\left(\frac{V}{2}\right)^{2}+\left(K+\frac{\phi_m^{2}}{T^{2}}+\frac{\theta_n^{2}}{S^{2}}\right)}}\left[\frac{\left[\left(\rho_{2,n,m}\right)^{2}e^{-\rho_{1,n,m}}+\left(\rho_{1,n,m}\right)^{2}e^{-\rho_{2,n,m}}\right]}{\left(\rho_{2,n,m}-\rho_{1,n,m}\right)}+\right.\right.$$
$$\left.\left.+2\rho_{1,n,m}\rho_{2,n,m}\frac{\left[e^{-\rho_{2,n,m}}-e^{-\rho_{1,n,m}}\right]}{\left(\rho_{2,n,m}-\rho_{1,n,m}\right)^{2}}\right]\right]$$

$$\frac{\partial C_{A}^{out^{*}}}{\partial T}=\frac{2C_{A}^{out^{*}}}{T}-4UVS^{2}T^{2}\left(\sum_{n=0}^{\infty}\sum_{m=0}^{\infty}\frac{\left[\frac{\left[\frac{2\phi_m^{\,2}}{\phi_m^{\,2}+T^2+T}+2T+3\right]}{\left[\phi_m^{\,2}+T^2+T\right]}\left[\frac{\left(\rho_{2,n,m}\right)^2 e^{-\rho_{1,n,m}}-\left(\rho_{1,n,m}\right)^2 e^{-\rho_{2,n,m}}}{\left(\rho_{2,n,m}-\rho_{1,n,m}\right)}\right]-U\frac{\phi_m^{\,2}\left(\frac{\phi_m^{\,2}+T^2}{\phi_m^{\,2}+T^2+T}\right)}{T^3\sqrt{\left(\frac{V}{2}\right)^2+\left(K+\frac{\phi_m^{\,2}}{T^2}+\frac{\theta_n^{\,2}}{S^2}\right)}}\left[\frac{\left[\left(\rho_{2,n,m}\right)^2 e^{-\rho_{1,n,m}}+\left(\rho_{1,n,m}\right)^2 e^{-\rho_{2,n,m}}\right]}{\left(\rho_{2,n,m}-\rho_{1,n,m}\right)}+2\rho_{1,n,m}\rho_{2,n,m}\frac{\left[e^{-\rho_{2,n,m}}-e^{-\rho_{1,n,m}}\right]}{\left(\rho_{2,n,m}-\rho_{1,n,m}\right)^2}\right]\right]}{\left[\theta_n^{\,2}\left(\theta_n^{\,2}+S^2+S\right)\right]\left[\phi_m^{\,2}\left(\phi_m^{\,2}+T^2+T\right)\right]\left[\frac{\left(\rho_{2,n,m}\right)^2 e^{-\rho_{1,n,m}}-\left(\rho_{1,n,m}\right)^2 e^{-\rho_{2,n,m}}}{\left(\rho_{2,n,m}-\rho_{1,n,m}\right)}\right]^2}\right)$$

$$\frac{\partial C_{A}^{out^{*}}}{\partial U}=\frac{\partial\left[4UVS^{2}T^{2}\sum_{n=0}^{\infty}\sum_{m=0}^{\infty}\left\{\frac{\left[\frac{1}{\theta_n^{\,2}\left(\theta_n^{\,2}+S^2+S\right)}\right]\left[\frac{1}{\phi_m^{\,2}\left(\phi_m^{\,2}+T^2+T\right)}\right]}{\left[\frac{\left(\rho_{2,n,m}\right)^2 e^{-\rho_{1,n,m}}-\left(\rho_{1,n,m}\right)^2 e^{-\rho_{2,n,m}}}{\left(\rho_{2,n,m}-\rho_{1,n,m}\right)}\right]}\right\}\right]}{\partial U}=$$

$$=\frac{C_{A}^{out^{*}}}{U}+4UVS^{2}T^{2}\sum_{n=0}^{\infty}\sum_{m=0}^{\infty}\left\{\frac{1}{\left[\theta_n^{\,2}\left(\theta_n^{\,2}+S^2+S\right)\right]\left[\phi_m^{\,2}\left(\phi_m^{\,2}+T^2+T\right)\right]}\frac{\partial\left[\frac{1}{\left[\frac{\left(\rho_{2,n,m}\right)^2 e^{-\rho_{1,n,m}}-\left(\rho_{1,n,m}\right)^2 e^{-\rho_{2,n,m}}}{\left(\rho_{2,n,m}-\rho_{1,n,m}\right)}\right]}\right]}{\partial U}\right\}=$$

$$=\frac{C_{A}^{out^{*}}}{U}-4VS^{2}T^{2}\sum_{n=0}^{\infty}\sum_{m=0}^{\infty}\left\{\frac{\frac{\left[\left(\rho_{2,n,m}\right)^2 e^{-\rho_{1,n,m}}\left(1-\rho_{1,n,m}\right)-\left(\rho_{1,n,m}\right)^2 e^{-\rho_{2,n,m}}\left(1-\rho_{2,n,m}\right)\right]}{\left(\rho_{2,n,m}-\rho_{1,n,m}\right)}}{\left[\theta_n^{\,2}\left(\theta_n^{\,2}+S^2+S\right)\right]\left[\phi_m^{\,2}\left(\phi_m^{\,2}+T^2+T\right)\right]\left[\frac{\left(\rho_{2,n,m}\right)^2 e^{-\rho_{1,n,m}}-\left(\rho_{1,n,m}\right)^2 e^{-\rho_{2,n,m}}}{\left(\rho_{2,n,m}-\rho_{1,n,m}\right)}\right]^2}\right\}\Leftrightarrow$$

$$\frac{\partial C_A^{out^*}}{\partial U}=\frac{C_A^{out^*}}{U}-4VS^2T^2\sum_{n=0}^{\infty}\sum_{m=0}^{\infty}\left\{\frac{\left[\left(\rho_{2,n,m}\right)^2 e^{-\rho_{1,n,m}}\left(1-\rho_{1,n,m}\right)-\left(\rho_{1,n,m}\right)^2 e^{-\rho_{2,n,m}}\left(1-\rho_{2,n,m}\right)\right]\left(\rho_{2,n,m}-\rho_{1,n,m}\right)}{\left[\theta_n^{\,2}\left(\theta_n^{\,2}+S^2+S\right)\right]\left[\phi_m^{\,2}\left(\phi_m^{\,2}+T^2+T\right)\right]\left[\left(\rho_{2,n,m}\right)^2 e^{-\rho_{1,n,m}}-\left(\rho_{1,n,m}\right)^2 e^{-\rho_{2,n,m}}\right]^2}\right\}$$

$$\frac{\partial C_A^{out^*}}{\partial V}=\frac{\partial\left[4UVS^2T^2\sum_{n=0}^{\infty}\sum_{m=0}^{\infty}\left\{\frac{\left[\frac{1}{\theta_n^{\,2}\left(\theta_n^{\,2}+S^2+S\right)}\right]\left[\frac{1}{\phi_m^{\,2}\left(\phi_m^{\,2}+T^2+T\right)}\right]}{\left[\frac{\left(\rho_{2,n,m}\right)^2 e^{-\rho_{1,n,m}}-\left(\rho_{1,n,m}\right)^2 e^{-\rho_{2,n,m}}}{\left(\rho_{2,n,m}-\rho_{1,n,m}\right)}\right]}\right\}\right]}{\partial V}=$$

$$=\frac{C_A^{out^*}}{V}+4UVS^2T^2\sum_{n=0}^{\infty}\sum_{m=0}^{\infty}\left\{\frac{1}{\left[\theta_n^{\,2}\left(\theta_n^{\,2}+S^2+S\right)\right]\left[\phi_m^{\,2}\left(\phi_m^{\,2}+T^2+T\right)\right]}\frac{\partial\left[\frac{1}{\left[\frac{\left(\rho_{2,n,m}\right)^2 e^{-\rho_{1,n,m}}-\left(\rho_{1,n,m}\right)^2 e^{-\rho_{2,n,m}}}{\left(\rho_{2,n,m}-\rho_{1,n,m}\right)}\right]}\right]}{\partial V}\right\}=$$

$$=\frac{C_A^{out^*}}{V}+4UVS^2T^2\sum_{n=0}^{\infty}\sum_{m=0}^{\infty}\left\{\frac{-U\frac{\left[\left[\left(\rho_{2,n,m}\right)^2 e^{-\rho_{1,n,m}}\left(2+\rho_{1,n.m}\right)+\left(\rho_{1,n,m}\right)^2 e^{-\rho_{2,n,m}}\left(2+\rho_{2,n.m}\right)\right]-\right.}{\left.\left[\left(\rho_{2,n,m}\right)^2 e^{-\rho_{1,n,m}}-\left(\rho_{1,n,m}\right)^2 e^{-\rho_{2,n,m}}\right]\left(\frac{UV}{\rho_{2,n.m}-\rho_{1,n.m}}\right)\right]}{\left(\rho_{2,n,m}-\rho_{1,n,m}\right)^2}}{\left[\theta_n^{\,2}\left(\theta_n^{\,2}+S^2+S\right)\right]\left[\phi_m^{\,2}\left(\phi_m^{\,2}+T^2+T\right)\right]\left[\frac{\left(\rho_{2,n,m}\right)^2 e^{-\rho_{1,n,m}}-\left(\rho_{1,n,m}\right)^2 e^{-\rho_{2,n,m}}}{\left(\rho_{2,n,m}-\rho_{1,n,m}\right)}\right]^2}\right\}=$$

$$\frac{\partial C_A^{out^*}}{\partial V}=\frac{C_A^{out^*}}{V}-4U^2VS^2T^2\sum_{n=0}^{\infty}\sum_{m=0}^{\infty}\left\{\frac{\left[\left[\left(\rho_{2,n,m}\right)^2 e^{-\rho_{1,n,m}}\left(2+\rho_{1,n.m}\right)+\left(\rho_{1,n,m}\right)^2 e^{-\rho_{2,n,m}}\left(2+\rho_{2,n.m}\right)\right]-\right.}{\left.\left[\left(\rho_{2,n,m}\right)^2 e^{-\rho_{1,n,m}}-\left(\rho_{1,n,m}\right)^2 e^{-\rho_{2,n,m}}\right]\left(\frac{UV}{\rho_{2,n.m}-\rho_{1,n.m}}\right)\right]}{\left[\theta_n^{\,2}\left(\theta_n^{\,2}+S^2+S\right)\right]\left[\phi_m^{\,2}\left(\phi_m^{\,2}+T^2+T\right)\right]\left[\left(\rho_{2,n,m}\right)^2 e^{-\rho_{1,n,m}}-\left(\rho_{1,n,m}\right)^2 e^{-\rho_{2,n,m}}\right]^2}\right\}$$

Limits

$$C_A^{out^*} = 4UVS^2T^2\sum_{n=0}^{\infty}\sum_{m=0}^{\infty}\left\{\frac{\left(\rho_{2,n,m}-\rho_{1,n,m}\right)}{\left[\theta_n^{\,2}\left(\theta_n^{\,2}+S^2+S\right)\right]\left[\phi_m^{\,2}\left(\phi_m^{\,2}+T^2+T\right)\right]\left[\left(\rho_{2,n,m}\right)^2 e^{-\rho_{1,n,m}}-\left(\rho_{1,n,m}\right)^2 e^{-\rho_{2,n,m}}\right]}\right\} \Leftrightarrow$$

$$C_A^{out^*} = 4VS^2T^2\sum_{n=0}^{\infty}\sum_{m=0}^{\infty}\left\{\frac{\left(\frac{\rho_{2,n,m}}{U}-\frac{\rho_{1,n,m}}{U}\right)}{\left[\left(\frac{\rho_{2,n,m}}{U}\right)^2 e^{-\rho_{1,n,m}}-\left(\frac{\rho_{1,n,m}}{U}\right)^2 e^{-\rho_{2,n,m}}\right]\left[\theta_n^{\,2}\left(\theta_n^{\,2}+S^2+S\right)\right]\left[\phi_m^{\,2}\left(\phi_m^{\,2}+T^2+T\right)\right]}\right\}$$

$$\lim_{U\to+\infty} C_A^{out^*} = 4VS^2T^2\sum_{n=0}^{\infty}\sum_{m=0}^{\infty}\left\{\frac{\left(\frac{\rho_{2,n,m}}{U}-\frac{\rho_{1,n,m}}{U}\right)}{\left[\left(\frac{\rho_{2,n,m}}{U}\right)^2 \lim_{U\to+\infty}\left(e^{-\rho_{1,n,m}}\right)-\left(\frac{\rho_{1,n,m}}{U}\right)^2 \lim_{U\to+\infty}\left(e^{-\rho_{2,n,m}}\right)\right]\left[\theta_n^{\,2}\left(\theta_n^{\,2}+S^2+S\right)\right]\left[\phi_m^{\,2}\left(\phi_m^{\,2}+T^2+T\right)\right]}\right\} \Leftrightarrow$$

$$\lim_{U\to+\infty} C_A^{out^*} = 4VS^2T^2\sum_{n=0}^{\infty}\sum_{m=0}^{\infty}\left\{\frac{\left(\frac{\rho_{2,n,m}}{U}-\frac{\rho_{1,n,m}}{U}\right)}{\left[\left(\frac{\rho_{2,n,m}}{U}\right)^2 (+\infty)-\left(\frac{\rho_{1,n,m}}{U}\right)^2 (0)\right]\left[\theta_n^{\,2}\left(\theta_n^{\,2}+S^2+S\right)\right]\left[\phi_m^{\,2}\left(\phi_m^{\,2}+T^2+T\right)\right]}\right\} \Leftrightarrow$$

$$\boxed{\lim_{U\to+\infty} C_A^{out^*} = 0}$$

and

$$\lim_{U\to 0^+} C_A^{out^*} = 4VS^2T^2\sum_{n=0}^{\infty}\sum_{m=0}^{\infty}\left\{\frac{\left(\frac{\rho_{2,n,m}}{U}-\frac{\rho_{1,n,m}}{U}\right)}{\left[\left(\frac{\rho_{2,n,m}}{U}\right)^2\lim_{U\to 0^+}\left(e^{-\rho_{1,n,m}}\right)-\left(\frac{\rho_{1,n,m}}{U}\right)^2\lim_{U\to 0^+}\left(e^{-\rho_{2,n,m}}\right)\right]\left[\theta_n{}^2\left(\theta_n{}^2+S^2+S\right)\right]\left[\phi_m{}^2\left(\phi_m{}^2+T^2+T\right)\right]}\right\}\Leftrightarrow$$

$$\lim_{U\to 0^+} C_A^{out^*} = 4VS^2T^2\sum_{n=0}^{\infty}\sum_{m=0}^{\infty}\left\{\frac{\left(\frac{\rho_{2,n,m}}{U}-\frac{\rho_{1,n,m}}{U}\right)}{\left[\left(\frac{\rho_{2,n,m}}{U}\right)^2(1)-\left(\frac{\rho_{1,n,m}}{U}\right)^2(1)\right]\left[\theta_n{}^2\left(\theta_n{}^2+S^2+S\right)\right]\left[\phi_m{}^2\left(\phi_m{}^2+T^2+T\right)\right]}\right\}\Leftrightarrow$$

$$\boxed{\lim_{U\to 0^+} C_A^{out^*} = 4S^2T^2\sum_{n=0}^{\infty}\sum_{m=0}^{\infty}\left\{\frac{1}{\left[\theta_n{}^2\left(\theta_n{}^2+S^2+S\right)\right]\left[\phi_m{}^2\left(\phi_m{}^2+T^2+T\right)\right]}\right\}}$$

Chapter 4

4 Method To Estimate Rate Constants By Identifying Reaction Invariants For Complex Kinetic Models

Abstract

In this work, we present a novel method for determining reaction kinetics using the reaction invariant reduction method for any set of complex chemical reactions. This work is an effective way for reducing the dimension of chemical reaction mechanisms and to predict the kinetics from a given set of data. This new method will be developed based on a convex formulation of the associated optimization problem. A case study on the Trambouze reaction scheme carried out in a plug flow reactor (PFR) will be used to illustrate the proposed methodology.

4.1 Introduction

Many chemical processes involve reaction mechanisms with hundreds of reactions and thousands of species [1−4] as can be seen in petroleum refining [5], fuel combustion [6], and atmospheric chemistry [7]. These reaction mechanisms are often developed based on the consideration of elementary reactions, whose kinetic rates are determined based on mass action kinetics. However, numerical computations using such detailed reaction kinetic mechanisms are challenging due to the significant computational burden associated with their use. To make their use more practical often times reduced mechanisms are sought which utilize a reduced number of species and/or reactions, [8]. In addition to the former features, the reduced/simplified (also called “skeletal”) model needs to provide quantitative information regarding the mechanism parameters as well as qualitative sensitivity of the mechanism kinetics [1].

From [1−4], three typical methods to reduce reaction mechanisms are: skeletal reduction, lumping, and time-scale analysis. In skeletal reduction, some reactions and/or species are

eliminated as they are found not to be critical in the detailed mechanism. For lumping, chemical species and reactions are lumped together creating fictitious species that represent global reaction steps calculated from the elementary reaction rates. Finally, in time-scale analysis, reactions are divided into “fast/minor” reactions and “slow/major” reactions where the fast/minor reactions are removed from the detailed mechanism.

According to [8], the following techniques produce reduced models for detailed mechanisms, but they lack control over accuracy: lumping (Weekman, 1979), sensitivity analysis (Tilden, Costanza, McRae & Seinfeld, 1981; Rabitz, Kramer & Dacol, 1983; Edelson & Flamm, 1984), comparison of reaction rates (Frenklach, 1987, 1991), concomitant parameter estimation and model reduction (Maria, 1989), ridge regression analysis (Maria & Muntean, 1987), functional group analysis (Graedel, 1977), target factor analysis (Bonvin & Rippin, 1990), and singular perturbation theory (van Breusegem & Bastin, 1991) [11-20].

In recent years, computational singular perturbation (CSP) has been widely used in the realm of fuel combustion such, as hydrocarbons [1−3] and ethanol [4]. CSP outputs families of reduced models, which then need to be tested for accuracy. Also, it is important to note that [1] developed an algorithm which simplifies reaction mechanisms based on CSP. Another approach was described by (Conner and Manousiouthakis, 2011) [10], who described a globally optimal method of determining parameters from experimental data for systems described by ordinary differential equations. The method they proposed is guaranteed to identify the global optimum of the non-linear regression problem and is also able to deliver ranges for the model parameters for which the proposed model describes the available data within a predetermined level of accuracy.

The problem considered in this work is the identification of chemical reaction mechanism kinetic rate constants, based on PFR experimental data obtained for several (not necessarily all)

species participating in the reaction mechanism. The proposed methodology employs the concept of reaction invariants, and involves the formulation and subsequent global solution of convex optimization problems. The aforementioned global solutions yield both the globally optimum values of the kinetic rate constants and can be used to calculate the associated concentration profiles for the mechanism's participating species.

The remainder of this work first reviews dimensionality reduction for chemical reaction mechanisms based on the concept of reaction invariants. Then the proposed kinetic rate constant identification methodology using convex optimization techniques is described. The proposed methodology is then illustrated on a case study involving the Trambouze reaction scheme carried out in a plug flow reactor (PFR). Finally, conclusions are drawn.

4.2 Reaction Invariant based Dimensionality Reduction

Consider a reaction system involving n species and m reactions described by: $\sum_{i=1}^{n} \nu_{ij} A_i = 0 \quad \forall j = 1,..,m$, where $\{A_i\}_1^n$ is the species vector, and ν_{ij} is the stoichiometric coefficient of the i^{th} species in the j^{th} reaction, with $\nu_{ij} > 0$ ($\nu_{ij} < 0$) if the i^{th} species is a product (reactant) in the j^{th} reaction. Let $\vec{C} = [C_1\ C_2 \cdots C_n]^T \in \mathbb{R}^n$ denote the species concentration vector; $R_i \ \forall i = 1,...,n$ the volumetric generation rate of the i^{th} species; and $r_j \ \forall j = 1,...,m$ the volumetric reaction rate of the j^{th} reaction. Then $R_i = \sum_{j=1}^{m} \nu_{ij} r_j \ \forall i = 1,...,n$, and since mass is conserved, $\sum_{i=1}^{n} M_i R_i = \sum_{i=1}^{n} \sum_{j=1}^{m} M_i \nu_{ij} r_j = 0$.

Let $\mathbb{Q}$ be the vector space of all continuous functions mapping from $\mathbb{R}^n$ to $\mathbb{R}^1$ and thus $r_j \in \mathbb{Q} \quad \forall j = 1,...,m$, and also $R_i = \sum_{j=1}^{m} v_{ij} r_j \in \mathbb{Q} \quad \forall i = 1,...,n$. Then the sets $S = \{r_j,\ j = 1,....,m\}$ and $H = \{R_i,\ i = 1,....,n\}$ are both subsets of $\mathbb{Q}$, and $[S] \triangleq span(S) \triangleq \left\{ s \in \mathbb{Q} : s = \sum_{j=1}^{m} \eta_j r_j,\ \eta_j \in \mathbb{R}\ \forall j = 1,m \right\}$ and $[H] \triangleq span(H) \triangleq \left\{ h \in \mathbb{Q} : h = \sum_{i=1}^{n} \eta_i R_i,\ \eta_i \in \mathbb{R}\ \forall i = 1,n \right\}$ are both subspaces of $\mathbb{Q}$ that contain all linear combinations of elements in S and H respectively. It then holds $R_i = \sum_{j=1}^{m} v_{ij} r_j \in [S] \subset \mathbb{Q} \quad \forall i = 1,...,n$, $H \subset [S] \subset \mathbb{Q}$, and $[H] \subset [S] \subset \mathbb{Q}$.

To introduce the concept of a basis for the above defined subspaces, the concept of linear independence is first defined. Let $\{\varphi_1, \varphi_2, \cdots \varphi_x\} \triangleq S_x \subset [S]$ have a finite number of elements x, and $r_x \in [S]$. Then r_x is linearly dependent (independent) upon S_x iff $r_x \in [S_x] \triangleq span(S_x) \triangleq \left\{ \varphi \in \mathbb{Q} : \varphi = \sum_{i=1}^{x} \eta_i \varphi_i,\ \eta_i \in \mathbb{R}\ \forall i = 1,x \right\} (r_x \notin [S_x])$, i.e. iff r_x can (cannot) be expressed as a linear combination of the elements of S_x. Equivalently, r_x is linearly dependent (independent) upon S_x iff $\exists \{\eta_1, \eta_2, \cdots \eta_x\} \in \mathbb{R}^x : r_x = \sum_{i=1}^{x} \eta_i \varphi_i$ ($\nexists \{\eta_1, \eta_2, \cdots \eta_x\} \in \mathbb{R}^x : r_x = \sum_{i=1}^{x} \eta_i \varphi_i$). S_x is a linearly independent set iff each element of S_x is linearly independent of the remaining vectors in S_x, or equivalently S_x is a linearly independent set iff $\sum_{i=1}^{x} \eta_i \varphi_i = 0 \Rightarrow \{\eta_1, \eta_2, \cdots \eta_x\} = \{0, 0, \cdots 0\} \in \mathbb{R}^x$. A set $\{\varphi_1, \varphi_2, \cdots \varphi_x\} \triangleq S_x \subset [S]$ is a basis

for $[S]$ iff $[S_x]=[S] \wedge \left\{ \sum_{i=1}^{x} \eta_i \varphi_i = 0 \Rightarrow \{\eta_1, \eta_2, \cdots \eta_x\} = \{0,0,\cdots 0\} \in \mathbb{R}^x \right\}$, i.e. $S_x \subset [S]$ is a basis for $[S]$ iff S_x is a linearly independent set and $[S_x]=[S]$.

The following proposition is then valid, [9].

Proposition 1: Let $m_B(n_B)$ be the number of elements of a basis of subspace $[S]([H])$. Then, $m_B \le m(n_B \le n-1)$. In addition, $[H] \subseteq [S]$ *and* $n_B \le m_B$.

Zhou and Manousiouthakis, [9], established the following proposition for a PFR:

Proposition 2: Consider a constant density, isothermal plug flow reactor, with inlet and outlet species concentrations C_i^{in}, C_i^{out} $i=1,n$ respectively. Let the reaction scheme $\sum_{i=1}^{n} \nu_{ij} A_i = 0 \ \ \forall j = 1,..,m$, be carried out in this PFR, with volumetric reaction rates in $S = \{r_j,\ j=1,....,m\}$ and associated volumetric species generation rates in $H = \{R_i,\ i=1,....,n\}$.

If $\exists \{\eta_1, \eta_2, \cdots \eta_n\} \neq \{0,0,\cdots 0\} \in \mathbb{R}^n : \sum_{i=1}^{n} \eta_i R_i = 0$, then $\sum_{i=1}^{n} \eta_i \left(C_i^{out} - C_i^{in} \right) = 0$.

This proposition helps identify the concept of reaction invariants. Indeed if one identifies a basis B for $[H]$ with number of elements equal to n_B , then there $n - n_B$ linearly independent reaction invariants. If one is able to construct a basis B with elements that belong to H, then the construction of linearly independent reaction invariants becomes a simple linear algebra exercise. After reviewing the theory of dimensionality reduction, the next section presents the mathematical formulation of the proposed kinetic parameter identification methodology.

4.3 Mathematical Formulation of Kinetic Constant Parameter Estimation

A constant density fluid PFR can be modeled using a system of ordinary differential equations:

$\frac{dC_i(\tau)}{d\tau} = f_i\left(\left\{k_p\right\}_{p=1}^{q}, \left\{C_j(\tau)\right\}_{j=1}^{n}, \tau\right),\ C_i(\tau_0) = C_{i,0} \quad \forall i = 1,n;\ \forall \tau \in \left[0, t_f\right]$, where, C_i is the i^{th} species concentration, C_{i0} is the i^{th} species initial concentration, and k is a vector of kinetic parameters. Consider that measurements $\hat{C}_i(\tau_j)\ \ i \in \Lambda \subset \{1,\cdots,n\}\ \ j = 1,N$ are available on some of the species (quantified by the index set Λ) participating in the reaction scheme at the times $\tau_j \in \left[0, t_f\right];\ \tau_j > \tau_{j-1};\ \tau_0 = 0;\ \forall j = 1,N$.

The kinetic constant parameter identification problem is an infinite dimensional optimization problem over the Hilbert space of squared integrable functions defined over $\left[0, t_f\right]$, that can be written in penalty form as follows:

$$\mu(\varepsilon) \hat{=} \inf_{\substack{\{k_p\}_{p=1}^{q} \\ \{C_i(\cdot)\}_{i=1}^{n}}} \left[\begin{array}{l} \sum_{i=1}^{n}\sum_{j=1}^{N}\left[W_i(\tau_j)\left(C_i(\tau_j) - \hat{C}_i(\tau_j)\right)^2\right] + \\ +\varepsilon\sum_{i=1}^{n}\int_0^{t_f}\left[\dot{C}_i(\tau) - f_i\left(\left\{k_p\right\}_{p=1}^{q}, \left\{C_j(\tau)\right\}_{j=1}^{n}, \tau\right)\right]^2 d\tau \end{array} \right] \qquad (1)$$

$$s.t. \qquad C_i(\tau_0) = C_{i,0}$$

where $W_i(\tau_j) = 0\ \ \forall i \notin \Lambda\ \ \forall j = 1,N$.

The infinite dimensional nature of the above optimization problem suggests that an approximation procedure must be employed for computations to become feasible. To this end, it is assumed that $C_j(\cdot)$ belongs to the M+1 dimensional subspace of M[th] degree polynomials, $\forall j = 1,n$, i.e. $C_j(\cdot): \left[0, t_f\right] \to \mathbb{R}^+;\ C_j(\cdot): \tau \to C_j(\tau) \hat{=} \sum_{l=0}^{M} \Delta_l^j \tau^l \quad \forall j = 1,n$.

Then $\dot{C}_j(\cdot):\left[0,t_f\right]\to\mathbb{R}^+;\ \dot{C}_j(\cdot):\tau\to\dot{C}_j(\tau)\triangleq\sum_{l=1}^{M}l\Delta_l^j\tau^{l-1}\quad\forall j=1,n.$ The resulting approximate optimization problem then becomes:

$$\mu_M(\varepsilon)\triangleq\inf_{\substack{\{k_p\}_{p=1}^q\\ \left\{\{\Delta_l^j\}_{l=0}^M\right\}_{j=1}^n}}\left[\begin{array}{l}\displaystyle\sum_{i=1}^{n}\sum_{j=1}^{N}\left[W_i(\tau_j)\left(\sum_{l=0}^{M}\Delta_l^i\tau^l-\hat{C}_i(\tau_j)\right)^2\right]+\\ \displaystyle+\varepsilon\sum_{i=1}^{n}\int_0^{t_f}\left[\sum_{l=1}^{M}l\Delta_l^i\tau^{l-1}-f_i\left(\{k_p\}_{p=1}^q,\left\{\sum_{l=0}^{M}\Delta_l^j\tau^l\right\}_{j=1}^n,\tau\right)\right]^2d\tau\end{array}\right]\qquad(2)$$

$$s.t.\quad C_i(\tau_0)=C_{i,0}$$

Which is finite dimensional, but also nonconvex. Thus its global solution is difficult to attain. Instead, a sequential optimization procedure is proposed, each step of which is a convex finite dimensional problem. In carrying out the procedure, it is assumed that the sum of the cardinality of the aforementioned index set Λ with the number of linearly independent reaction invariants of the underlying reaction scheme is greater than or equal to the total number of species n.

The proposed sequential optimization procedure is:

1. Solve $\mu_M(0)$. This is accomplished through solution of a finite number (equal to the cardinality of the index set Λ) of strictly convex problems for strictly positive weights.

2. Fix $\left\{\{\Delta_l^j\}_{l=0}^M\right\}_{j\in\Lambda}$ to their optimal values for $\mu_M(0)$, and use them to identify $\left\{\{\Delta_l^j\}_{l=0}^M\right\}_{j\in\{1,\cdots,n\}-\Lambda}$ (possibly in a least square sense).

3. Use the $\left\{\{\Delta_l^j\}_{l=0}^M\right\}_{j\in\{1,\cdots,n\}}$ values identified in steps 1, 2, and calculate the integrals $\displaystyle\int_0^{t_f}\left[\sum_{l=1}^{M}l\Delta_l^i\tau^{l-1}-f_i\left(\{k_p\}_{p=1}^q,\left\{\sum_{l=1}^{M}\Delta_l^j\tau^l\right\}_{j=1}^n,\tau\right)\right]^2d\tau$ as functions of $\{k_p\}_{p=1}^q$.

4. Solve the following convex optimization problem

$$\inf_{\{k_p\}_{p=1}^q} \sum_{i=1}^{n} \int_0^{t_f} \left[\sum_{l=1}^{M} l\Delta_l^i \tau^{l-1} - f_i\left(\left\{k_p\right\}_{p=1}^q, \left\{ \sum_{l=0}^{M} \Delta_l^j \tau^l \right\}_{j=1}^n, \tau \right) \right]^2 d\tau .$$

The ordinary differential equations

$$\dot{C}_i(\tau) \triangleq \frac{dC_i(\tau)}{d\tau} = f_i\left(\left\{k_p\right\}_{p=1}^q, \left\{C_j(\tau)\right\}_{j=1}^n, \tau \right), \; C_i(\tau_0) = C_{i,0} \quad \forall i = 1,n; \; \forall \tau \in \left[0, t_f\right] \tag{3}$$

are equivalent to the following:

$$\sum_{i=1}^{n} \int_0^{t_f} \left[\dot{C}_i(\tau) - f_i\left(\left\{k_p\right\}_{p=1}^q, \left\{C_j(\tau)\right\}_{j=1}^n, \tau \right) \right]^2 d\tau = 0 \tag{4}$$

Let the functions $f_i(\cdot,\cdot,\cdot) \; \forall i = 1,n$ be quadratic multinomials in $\left\{C_j(\cdot)\right\}_{j=1}^n$ of the form:

$$f_i(\cdot,\cdot,\cdot) : \mathbb{R}^q \times \mathbb{R}^n \times \mathbb{R} \to \mathbb{R} \; \forall i = 1,n$$

$$f_i(\cdot,\cdot,\cdot) : \left(\left\{k_p\right\}_{p=1}^q, \left\{C_j(\tau)\right\}_{j=1}^n, \tau \right) \to f_i\left(\left\{k_p\right\}_{p=1}^q, \left\{C_j(\tau)\right\}_{j=1}^n, \tau \right) \triangleq$$

$$\triangleq \mathrm{A}^i + \left[\mathrm{B}^i\right]^{\mathrm{T}} \left[C(\tau)\right] + \left[C(\tau)\right]^{\mathrm{T}} \left[\Gamma^i\right] \left[C(\tau)\right] = \tag{5}$$

$$= \mathrm{A}^i + \sum_{j=1}^{n} \mathrm{B}_j^i C_j(\tau) + \sum_{k=1}^{n} \sum_{j=1}^{n} \Gamma_{jk}^i C_j(\tau) C_k(\tau) \quad \forall i = 1,n$$

where $\mathrm{B}^i \triangleq \left[\mathrm{B}_1^i \quad \cdots \quad \mathrm{B}_n^i \right]^{\mathrm{T}} \; \forall i = 1,n$; $\Gamma^i \triangleq \begin{bmatrix} \Gamma_{11}^i & \cdots & \Gamma_{1n}^i \\ \vdots & \ddots & \vdots \\ \Gamma_{n1}^i & \cdots & \Gamma_{nn}^i \end{bmatrix} \; \forall i = 1,n .$

Then the above integral equation can be written as:

$$\sum_{i=1}^{n} \int_0^{t_f} \left[\dot{C}_i(\tau) - \mathrm{A}^i - \sum_{j=1}^{n} \mathrm{B}_j^i C_j(\tau) - \sum_{k=1}^{n} \sum_{j=1}^{n} \Gamma_{jk}^i C_j(\tau) C_k(\tau) \right]^2 d\tau = 0 \tag{6}$$

Now, let us consider that $C_j(\tau) \triangleq \sum_{l=0}^{M} \Delta_l^j \tau^l \quad \forall j = 1,n$

i.e. $C_j(\cdot):\left[0,t_f\right]\to\mathbb{R}^+ \quad \forall j=1,n$ belongs to the M+1 dimensional subspace of Mth degree polynomial functions defined over $\left[0,t_f\right]$. Then, $\dot{C}_j(\tau)\triangleq\sum_{l=1}^{M} l\Delta_l^j\tau^{l-1}$, and the above integral equation becomes:

$$\sum_{i=1}^{n}\int_0^{t_f}\left[\sum_{l=1}^{M} l\Delta_l^i\tau^{l-1}-\mathrm{A}^i-\sum_{j=1}^{n}\mathrm{B}_j^i\sum_{l=1}^{M}\Delta_l^j\tau^l-\sum_{k=1}^{n}\sum_{j=1}^{n}\Gamma^i_{jk}\sum_{l=1}^{M}\Delta_l^j\tau^l\sum_{m=1}^{M}\Delta_m^k\tau^m\right]^2 d\tau=0\Leftrightarrow \tag{7}$$

$$\sum_{i=1}^{n}\int_0^{t_f}\left[\sum_{l=1}^{M} l\Delta_l^i\tau^{l-1}-\mathrm{A}^i-\sum_{j=1}^{n}\sum_{l=1}^{M}\mathrm{B}_j^i\Delta_l^j\tau^l-\sum_{k=1}^{n}\sum_{j=1}^{n}\sum_{l=1}^{M}\sum_{m=1}^{M}\Gamma^i_{jk}\Delta_l^j\Delta_m^k\tau^{l+m}\right]^2 d\tau=0\Leftrightarrow \tag{8}$$

$$\sum_{i=1}^{n}\int_0^{t_f}\left\{\begin{array}{l}\left[\sum_{l=1}^{M} l\Delta_l^i\tau^{l-1}-\mathrm{A}^i-\sum_{j=1}^{n}\sum_{l=1}^{M}\mathrm{B}_j^i\Delta_l^j\tau^l-\sum_{k=1}^{n}\sum_{j=1}^{n}\sum_{l=1}^{M}\sum_{m=1}^{M}\Gamma^i_{jk}\Delta_l^j\Delta_m^k\tau^{l+m}\right]\cdot\\ \left[\sum_{l'=1}^{M} l'\Delta_{l'}^i\tau^{l'-1}-\mathrm{A}^i-\sum_{j'=1}^{n}\sum_{l'=1}^{M}\mathrm{B}_{j'}^i\Delta_{l'}^{j'}\tau^{l'}-\sum_{k'=1}^{n}\sum_{j'=1}^{n}\sum_{l'=1}^{M}\sum_{m'=1}^{M}\Gamma^i_{j'k'}\Delta_{l'}^{j'}\Delta_{m'}^{k'}\tau^{l'+m'}\right]\end{array}\right\}d\tau=0\Leftrightarrow \tag{9}$$

$$\sum_{i=1}^{n}\int_0^{t_f}\left\{\begin{array}{l}\left[\begin{array}{l}\left(\sum_{l=1}^{M} l\Delta_l^i\tau^{l-1}\right)\left(\sum_{l'=1}^{M} l'\Delta_{l'}^i\tau^{l'-1}\right)-\left(\sum_{l=1}^{M} l\Delta_l^i\tau^{l-1}\right)\mathrm{A}^i+\\ +\left(-\sum_{l=1}^{M} l\Delta_l^i\tau^{l-1}\right)\left(\sum_{j'=1}^{n}\sum_{l'=1}^{M}\mathrm{B}_{j'}^i\Delta_{l'}^{j'}\tau^{l'}\right)-\left(\sum_{l=1}^{M} l\Delta_l^i\tau^{l-1}\right)\left(\sum_{k'=1}^{n}\sum_{j'=1}^{n}\sum_{l'=1}^{M}\sum_{m'=1}^{M}\Gamma^i_{j'k'}\Delta_{l'}^{j'}\Delta_{m'}^{k'}\tau^{l'+m'}\right)\end{array}\right]+\\ +\left[-\mathrm{A}^i\sum_{l'=1}^{M} l'\Delta_{l'}^i\tau^{l'-1}+\mathrm{A}^i\mathrm{A}^i+\mathrm{A}^i\sum_{j'=1}^{n}\sum_{l'=1}^{M}\mathrm{B}_{j'}^i\Delta_{l'}^{j'}\tau^{l'}+\mathrm{A}^i\sum_{k'=1}^{n}\sum_{j'=1}^{n}\sum_{l'=1}^{M}\sum_{m'=1}^{M}\Gamma^i_{j'k'}\Delta_{l'}^{j'}\Delta_{m'}^{k'}\tau^{l'+m'}\right]\\ +\left[\begin{array}{l}-\left(\sum_{j=1}^{n}\sum_{l=1}^{M}\mathrm{B}_j^i\Delta_l^j\tau^l\right)\left(\sum_{l'=1}^{M} l'\Delta_{l'}^i\tau^{l'-1}\right)+\left(\sum_{j=1}^{n}\sum_{l=1}^{M}\mathrm{B}_j^i\Delta_l^j\tau^l\right)\mathrm{A}^i+\\ +\left(\sum_{j=1}^{n}\sum_{l=1}^{M}\mathrm{B}_j^i\Delta_l^j\tau^l\right)\left(\sum_{j'=1}^{n}\sum_{l'=1}^{M}\mathrm{B}_{j'}^i\Delta_{l'}^{j'}\tau^{l'}\right)+\left(\sum_{j=1}^{n}\sum_{l=1}^{M}\mathrm{B}_j^i\Delta_l^j\tau^l\right)\left(\sum_{k'=1}^{n}\sum_{j'=1}^{n}\sum_{l'=1}^{M}\sum_{m'=1}^{M}\Gamma^i_{j'k'}\Delta_{l'}^{j'}\Delta_{m'}^{k'}\tau^{l'+m'}\right)\end{array}\right]\\ +\left[\begin{array}{l}-\left(\sum_{k=1}^{n}\sum_{j=1}^{n}\sum_{l=1}^{M}\sum_{m=1}^{M}\Gamma^i_{jk}\Delta_l^j\Delta_m^k\tau^{l+m}\right)\left(\sum_{l'=1}^{M} l'\Delta_{l'}^i\tau^{l'-1}\right)+\left(\sum_{k=1}^{n}\sum_{j=1}^{n}\sum_{l=1}^{M}\sum_{m=1}^{M}\Gamma^i_{jk}\Delta_l^j\Delta_m^k\tau^{l+m}\right)\mathrm{A}^i+\\ +\left(\sum_{k=1}^{n}\sum_{j=1}^{n}\sum_{l=1}^{M}\sum_{m=1}^{M}\Gamma^i_{jk}\Delta_l^j\Delta_m^k\tau^{l+m}\right)\left(\sum_{j'=1}^{n}\sum_{l'=1}^{M}\mathrm{B}_{j'}^i\Delta_{l'}^{j'}\tau^{l'}\right)+\\ +\left(\sum_{k=1}^{n}\sum_{j=1}^{n}\sum_{l=1}^{M}\sum_{m=1}^{M}\Gamma^i_{jk}\Delta_l^j\Delta_m^k\tau^{l+m}\right)\left(\sum_{k'=1}^{n}\sum_{j'=1}^{n}\sum_{l'=1}^{M}\sum_{m'=1}^{M}\Gamma^i_{j'k'}\Delta_{l'}^{j'}\Delta_{m'}^{k'}\tau^{l'+m'}\right)\end{array}\right]\end{array}\right\}d\tau=0\Leftrightarrow$$

(10)

$$\sum_{i=1}^{n}\int_{0}^{t_f}\left\{\left[\begin{array}{l}\left(\sum_{l=1}^{M} l\Delta_l^i\tau^{l-1}\right)\sum_{l'=1}^{M} l'\Delta_{l'}^i\tau^{l'-1}-\left(\sum_{l=1}^{M} l\Delta_l^i\tau^{l-1}\right)\mathrm{A}^i+\\ +\left(-\sum_{l=1}^{M} l\Delta_l^i\tau^{l-1}\right)\sum_{j'=1}^{n}\sum_{l'=1}^{M}\mathrm{B}_{j'}^i\Delta_{l'}^{j'}\tau^{l'}-\left(\sum_{l=1}^{M} l\Delta_l^i\tau^{l-1}\right)\sum_{k'=1}^{n}\sum_{j'=1}^{n}\sum_{l'=1}^{M}\sum_{m'=1}^{M}\Gamma_{j'k'}^i\Delta_{l'}^{j'}\Delta_{m'}^{k'}\tau^{l'+m'}\end{array}\right]\right\}d\tau+$$

$$+\sum_{i=1}^{n}\int_{0}^{t_f}\left\{\left[-\mathrm{A}^i\sum_{l'=1}^{M} l'\Delta_{l'}^i\tau^{l'-1}+\mathrm{A}^i\mathrm{A}^i+\mathrm{A}^i\sum_{j'=1}^{n}\sum_{l'=1}^{M}\mathrm{B}_{j'}^i\Delta_{l'}^{j'}\tau^{l'}+\mathrm{A}^i\sum_{k'=1}^{n}\sum_{j'=1}^{n}\sum_{l'=1}^{M}\sum_{m'=1}^{M}\Gamma_{j'k'}^i\Delta_{l'}^{j'}\Delta_{m'}^{k'}\tau^{l'+m'}\right]\right\}d\tau+$$

$$+\sum_{i=1}^{n}\int_{0}^{t_f}\left\{\left[\begin{array}{l}-\left(\sum_{j=1}^{n}\sum_{l=1}^{M}\mathrm{B}_j^i\Delta_l^j\tau^l\right)\sum_{l'=1}^{M} l'\Delta_{l'}^i\tau^{l'-1}+\left(\sum_{j=1}^{n}\sum_{l=1}^{M}\mathrm{B}_j^i\Delta_l^j\tau^l\right)\mathrm{A}^i+\\ +\left(\sum_{j=1}^{n}\sum_{l=1}^{M}\mathrm{B}_j^i\Delta_l^j\tau^l\right)\sum_{j'=1}^{n}\sum_{l'=1}^{M}\mathrm{B}_{j'}^i\Delta_{l'}^{j'}\tau^{l'}+\left(\sum_{j=1}^{n}\sum_{l=1}^{M}\mathrm{B}_j^i\Delta_l^j\tau^l\right)\sum_{k'=1}^{n}\sum_{j'=1}^{n}\sum_{l'=1}^{M}\sum_{m'=1}^{M}\Gamma_{j'k'}^i\Delta_{l'}^{j'}\Delta_{m'}^{k'}\tau^{l'+m'}\end{array}\right]\right\}d\tau+$$

$$\sum_{i=1}^{n}\int_{0}^{t_f}\left\{\left[\begin{array}{l}-\left(\sum_{k=1}^{n}\sum_{j=1}^{n}\sum_{l=1}^{M}\sum_{m=1}^{M}\Gamma_{jk}^i\Delta_l^j\Delta_m^k\tau^{l+m}\right)\sum_{l'=1}^{M} l'\Delta_{l'}^i\tau^{l'-1}+\left(\sum_{k=1}^{n}\sum_{j=1}^{n}\sum_{l=1}^{M}\sum_{m=1}^{M}\Gamma_{jk}^i\Delta_l^j\Delta_m^k\tau^{l+m}\right)\mathrm{A}^i+\\ +\left(\sum_{k=1}^{n}\sum_{j=1}^{n}\sum_{l=1}^{M}\sum_{m=1}^{M}\Gamma_{jk}^i\Delta_l^j\Delta_m^k\tau^{l+m}\right)\sum_{j'=1}^{n}\sum_{l'=1}^{M}\mathrm{B}_{j'}^i\Delta_{l'}^{j'}\tau^{l'}+\\ +\left(\sum_{k=1}^{n}\sum_{j=1}^{n}\sum_{l=1}^{M}\sum_{m=1}^{M}\Gamma_{jk}^i\Delta_l^j\Delta_m^k\tau^{l+m}\right)\sum_{k'=1}^{n}\sum_{j'=1}^{n}\sum_{l'=1}^{M}\sum_{m'=1}^{M}\Gamma_{j'k'}^i\Delta_{l'}^{j'}\Delta_{m'}^{k'}\tau^{l'+m'}\end{array}\right]\right\}d\tau=0\Leftrightarrow$$

(11)

$$\sum_{i=1}^{n}\int_{0}^{t_f}\left\{\left[\begin{array}{l}\left(\sum_{l=1}^{M}\sum_{l'=1}^{M} l'\Delta_{l'}^{i} l\Delta_{l}^{i}\tau^{l'+l-2}\right)-\mathrm{A}^{i}\left(\sum_{l=1}^{M} l\Delta_{l}^{i}\tau^{l-1}\right)+\\ +\left(-\sum_{l=1}^{M}\sum_{j'=1}^{n}\sum_{l'=1}^{M}\mathrm{B}_{j'}^{i}\Delta_{l'}^{j'} l\Delta_{l}^{i}\tau^{l'+l-1}\right)-\left(\sum_{l=1}^{M}\sum_{k'=1}^{n}\sum_{j'=1}^{n}\sum_{l'=1}^{M}\sum_{m'=1}^{M}\Gamma_{j'k'}^{i}\Delta_{l'}^{j'}\Delta_{m'}^{k'} l\Delta_{l}^{i}\tau^{l'+m'+l-1}\right)\end{array}\right]\right\}d\tau+$$

$$+\sum_{i=1}^{n}\left[-\mathrm{A}^{i}\sum_{l'=1}^{M} l'\Delta_{l'}^{i}\frac{t_f^{\,l'}}{l'}+\mathrm{A}^{i}\mathrm{A}^{i}t_f+\mathrm{A}^{i}\sum_{j'=1}^{n}\sum_{l'=1}^{M}\mathrm{B}_{j'}^{i}\Delta_{l'}^{j'}\frac{t_f^{\,l'+1}}{l'+1}+\mathrm{A}^{i}\sum_{k'=1}^{n}\sum_{j'=1}^{n}\sum_{l'=1}^{M}\sum_{m'=1}^{M}\Gamma_{j'k'}^{i}\Delta_{l'}^{j'}\Delta_{m'}^{k'}\frac{t_f^{\,l'+m'+1}}{l'+m'+1}\right]+$$

$$+\sum_{i=1}^{n}\int_{0}^{t_f}\left\{\left[\begin{array}{l}-\left(\sum_{j=1}^{n}\sum_{l=1}^{M}\sum_{l'=1}^{M} l'\Delta_{l'}^{i}\mathrm{B}_{j}^{i}\Delta_{l}^{j}\tau^{l+l'-1}\right)+\mathrm{A}^{i}\left(\sum_{j=1}^{n}\sum_{l=1}^{M}\mathrm{B}_{j}^{i}\Delta_{l}^{j}\tau^{l}\right)+\\ +\left(\sum_{j=1}^{n}\sum_{l=1}^{M}\sum_{j'=1}^{n}\sum_{l'=1}^{M}\mathrm{B}_{j'}^{i}\Delta_{l'}^{j'}\mathrm{B}_{j}^{i}\Delta_{l}^{j}\tau^{l+l'}\right)+\left(\sum_{j=1}^{n}\sum_{l=1}^{M}\sum_{k'=1}^{n}\sum_{j'=1}^{n}\sum_{l'=1}^{M}\sum_{m'=1}^{M}\Gamma_{j'k'}^{i}\Delta_{l'}^{j'}\Delta_{m'}^{k'}\mathrm{B}_{j}^{i}\Delta_{l}^{j}\tau^{l+l'+m'}\right)\end{array}\right]\right\}d\tau+$$

$$+\sum_{i=1}^{n}\int_{0}^{t_f}\left\{\left[\begin{array}{l}-\left(\sum_{k=1}^{n}\sum_{j=1}^{n}\sum_{l=1}^{M}\sum_{m=1}^{M}\sum_{l'=1}^{M} l'\Delta_{l'}^{i}\Gamma_{jk}^{i}\Delta_{l}^{j}\Delta_{m}^{k}\tau^{l+m+l'-1}\right)+\mathrm{A}^{i}\left(\sum_{k=1}^{n}\sum_{j=1}^{n}\sum_{l=1}^{M}\sum_{m=1}^{M}\Gamma_{jk}^{i}\Delta_{l}^{j}\Delta_{m}^{k}\tau^{l+m}\right)+\\ +\left(\sum_{k=1}^{n}\sum_{j=1}^{n}\sum_{l=1}^{M}\sum_{m=1}^{M}\sum_{j'=1}^{n}\sum_{l'=1}^{M}\mathrm{B}_{j'}^{i}\Delta_{l'}^{j'}\Gamma_{jk}^{i}\Delta_{l}^{j}\Delta_{m}^{k}\tau^{l'+l+m}\right)+\\ +\left(\sum_{k=1}^{n}\sum_{j=1}^{n}\sum_{l=1}^{M}\sum_{m=1}^{M}\sum_{k'=1}^{n}\sum_{j'=1}^{n}\sum_{l'=1}^{M}\sum_{m'=1}^{M}\Gamma_{j'k'}^{i}\Delta_{l'}^{j'}\Delta_{m'}^{k'}\Gamma_{jk}^{i}\Delta_{l}^{j}\Delta_{m}^{k}\tau^{l'+m'+l+m}\right)\end{array}\right]\right\}d\tau=0\Leftrightarrow$$

(12)

$$\sum_{i=1}^{n}\left[\begin{array}{l}\left(\sum_{l=1}^{M}\sum_{l'=1}^{M} l'\Delta^i_{l'} l\Delta^i_l \frac{t_f^{\,l'+l-1}}{l'+l-1}\right)-\mathrm{A}^i\left(\sum_{l=1}^{M} l\Delta^i_l \frac{t_f^{\,l}}{l}\right)+\\ +\left(-\sum_{l=1}^{M}\sum_{j'=1}^{n}\sum_{l'=1}^{M}\mathrm{B}^i_{j'}\Delta^{j'}_{l'} l\Delta^i_l \frac{t_f^{\,l'+l}}{l'+l}\right)-\left(\sum_{l=1}^{M}\sum_{k'=1}^{n}\sum_{j'=1}^{n}\sum_{l'=1}^{M}\sum_{m'=1}^{M}\Gamma^i_{j'k'}\Delta^{j'}_{l'}\Delta^{k'}_{m'} l\Delta^i_l \frac{t_f^{\,l'+m'+l}}{l'+m'+l}\right)\end{array}\right]+$$

$$+\sum_{i=1}^{n}\left[-\mathrm{A}^i\sum_{l'=1}^{M} l'\Delta^i_{l'}\frac{t_f^{\,l'}}{l'}+\mathrm{A}^i\mathrm{A}^i t_f+\mathrm{A}^i\sum_{j'=1}^{n}\sum_{l'=1}^{M}\mathrm{B}^i_{j'}\Delta^{j'}_{l'}\frac{t_f^{\,l'+1}}{l'+1}+\mathrm{A}^i\sum_{k'=1}^{n}\sum_{j'=1}^{n}\sum_{l'=1}^{M}\sum_{m'=1}^{M}\Gamma^i_{j'k'}\Delta^{j'}_{l'}\Delta^{k'}_{m'}\frac{t_f^{\,l'+m'+1}}{l'+m'+1}\right]+$$

$$+\sum_{i=1}^{n}\left[\begin{array}{l}-\left(\sum_{j=1}^{n}\sum_{l=1}^{M}\sum_{l'=1}^{M} l'\Delta^i_{l'}\mathrm{B}^i_j\Delta^j_l \frac{t_f^{\,l+l'}}{l+l'}\right)+\mathrm{A}^i\left(\sum_{j=1}^{n}\sum_{l=1}^{M}\mathrm{B}^i_j\Delta^j_l\frac{t_f^{\,l+1}}{l+1}\right)+\\ +\left(\sum_{j=1}^{n}\sum_{l=1}^{M}\sum_{j'=1}^{n}\sum_{l'=1}^{M}\mathrm{B}^i_{j'}\Delta^{j'}_{l'}\mathrm{B}^i_j\Delta^j_l\frac{t_f^{\,l+l'+1}}{l+l'+1}\right)+\left(\sum_{j=1}^{n}\sum_{l=1}^{M}\sum_{k'=1}^{n}\sum_{j'=1}^{n}\sum_{l'=1}^{M}\sum_{m'=1}^{M}\Gamma^i_{j'k'}\Delta^{j'}_{l'}\Delta^{k'}_{m'}\mathrm{B}^i_j\Delta^j_l\frac{t_f^{\,l+l'+m'+1}}{l+l'+m'+1}\right)\end{array}\right]+$$

$$+\sum_{i=1}^{n}\left[\begin{array}{l}-\left(\sum_{k=1}^{n}\sum_{j=1}^{n}\sum_{l=1}^{M}\sum_{m=1}^{M}\sum_{l'=1}^{M} l'\Delta^i_{l'}\Gamma^i_{jk}\Delta^j_l\Delta^k_m\frac{t_f^{\,l'+l+m}}{l'+l+m}\right)+\mathrm{A}^i\left(\sum_{k=1}^{n}\sum_{j=1}^{n}\sum_{l=1}^{M}\sum_{m=1}^{M}\Gamma^i_{jk}\Delta^j_l\Delta^k_m\frac{t_f^{\,l+m+1}}{l+m+1}\right)+\\ +\left(\sum_{k=1}^{n}\sum_{j=1}^{n}\sum_{l=1}^{M}\sum_{m=1}^{M}\sum_{j'=1}^{n}\sum_{l'=1}^{M}\mathrm{B}^i_{j'}\Delta^{j'}_{l'}\Gamma^i_{jk}\Delta^j_l\Delta^k_m\frac{t_f^{\,l'+l+m+1}}{l'+l+m+1}\right)+\\ +\left(\sum_{k=1}^{n}\sum_{j=1}^{n}\sum_{l=1}^{M}\sum_{m=1}^{M}\sum_{k'=1}^{n}\sum_{j'=1}^{n}\sum_{l'=1}^{M}\sum_{m'=1}^{M}\Gamma^i_{j'k'}\Delta^{j'}_{l'}\Delta^{k'}_{m'}\Gamma^i_{jk}\Delta^j_l\Delta^k_m\frac{t_f^{\,l'+m'+l+m+1}}{l'+m'+l+m+1}\right)\end{array}\right]=0$$

(13)

In the next section we apply the proposed kinetic parameter estimation procedure to a case study.

4.4 Case Study

The Trambouze reaction scheme shown below, is carried out in a PFR.

$$\left(\begin{array}{l}A\xrightarrow{k_1}B\ ,\ k_1=0.025\frac{kmol}{m^3\cdot s}\\ A\xrightarrow{k_2}C\ ,\ k_2=0.2\frac{1}{s}\\ A\xrightarrow{k_3}D\ ,\ k_3=0.4\frac{m^3}{kmol\cdot s}\qquad k_2{}^2=4k_1k_3;\quad \alpha=\frac{k_2}{2k_3}=0.25>0\end{array}\right)\tag{14}$$

The resulting set of differential equations describing the PFR behavior is:

$$\begin{pmatrix} \dot{C}_A = R_A = -k_1 - k_2 C_A - k_3 {C_A}^2 \\ \dot{C}_B = R_B = k_1 \\ \dot{C}_C = R_C = k_2 C_A \\ \dot{C}_D = R_D = k_3 {C_A}^2 \end{pmatrix} \tag{15}$$

For the above kinetic parameter values, the PFR modeling equations are analytically solvable with solutions:

$$\begin{aligned} &C_A(t) = -\alpha + \frac{1}{k_3 t + \frac{1}{C_A^{in} + \alpha}} \\ &C_B(t) = C_B^{in} + k_1 t \\ &C_C(t) = C_C^{in} - 2\alpha^2 k_3 t + 2\alpha \ln\left(k_3 t\left(C_A^{in} + \alpha\right) + 1\right) \\ &C_D(t) = C_D^{in} + k_3\left[\alpha^2 t - \frac{2\alpha}{k_3}\ln\left(\left(C_A^{in} + \alpha\right)k_3 t + 1\right) + \frac{\left(C_A^{in} + \alpha\right)^2 t}{k_3 t\left(C_A^{in} + \alpha\right) + 1}\right] \end{aligned} \tag{16}$$

It is easy to verify that this reaction scheme possesses one reaction invariant. It is:

$$\begin{aligned} &C_A(t) + C_B(t) + C_C(t) + C_D(t) = \\ &-\alpha + \frac{1}{k_3 t + \frac{1}{C_A^{in} + \alpha}} + C_B^{in} + k_1 t + \\ &+C_C^{in} - 2\alpha^2 k_3 t + 2\alpha \ln\left(k_3 t\left(C_A^{in} + \alpha\right) + 1\right) + \\ &+C_D^{in} + k_3\left[\alpha^2 t - \frac{2\alpha}{k_3}\ln\left(\left(C_A^{in} + \alpha\right)k_3 t + 1\right) + \frac{\left(C_A^{in} + \alpha\right)^2 t}{k_3 t\left(C_A^{in} + \alpha\right) + 1}\right] = \end{aligned} \tag{17}$$

$$= -\alpha + C_B^{in} + C_C^{in} + C_D^{in} + \frac{1}{k_3 t + \frac{1}{C_A^{in} + \alpha}} + k_1 t - \alpha^2 k_3 t + k_3 \frac{\left(C_A^{in} + \alpha\right)^2 t}{k_3 t\left(C_A^{in} + \alpha\right) + 1} =$$

$$= -\alpha + C_B^{in} + C_C^{in} + C_D^{in} + + k_1 t - \alpha^2 k_3 t + \left(C_A^{in} + \alpha\right) =$$

$= C_A^{in} + C_B^{in} + C_C^{in} + C_D^{in} + \left(k_1 - \alpha^2 k_3\right)t \overset{\alpha^2 \triangleq k_1/k_3}{=}$. Thus

$$\boxed{C_A(t) + C_B(t) + C_C(t) + C_D(t) = C_A^{in} + C_B^{in} + C_C^{in} + C_D^{in}} \tag{18}$$

We now consider that the above listed kinetic parameters are not known, and that simply the experimental data $\hat{C}_B(\tau_j), \hat{C}_C(\tau_j), \hat{C}_D(\tau_j) \quad j = 1, N$ are available for only the species B, C, D. These are listed in the Table Appendix A:

We first solve the convex problem:

$$\mu_M(0) \triangleq \inf_{\left\{\Delta_n^k\right\}_{k=0,n=1,4}^{M}} \left[\sum_{j=1}^{N} \left[\begin{array}{l} W_B(\tau_j)\left(\sum_{k=0}^{M} \Delta_B^k (\tau_j)^k - \hat{C}_B(\tau_j) \right)^2 + W_C(\tau_j)\left(\sum_{k=0}^{M} \Delta_C^k (\tau_j)^k - \hat{C}_C(\tau_j) \right)^2 + \\ + W_D(\tau_j)\left(\sum_{k=0}^{M} \Delta_D^k (\tau_j)^k - \hat{C}_D(\tau_j) \right)^2 \end{array} \right] \right] \tag{19}$$

$$s.t. \qquad C_A(0) = C_A^{in},\ C_B(0) = C_B^{in},\ C_C(0) = C_C^{in},\ C_D(0) = C_D^{in}$$

The identified globally optimal $\Delta_B^k, \Delta_C^k, \Delta_D^k \quad k = 0, M$, are listed in columns 3, 4, 5 of the Table below. Using the above identified reaction invariant, $\Delta_A^k \quad k = 0, M$ are then readily identified and listed belowin column 2 of the Table below.

K	ΔA	ΔC	ΔB	ΔD
0	1	0	0	0
1	-4.782938618	1.590503629	0.199992239	3.007847499
2	14.8973597	-3.646866274	0	-11.45612904
3	-31.53668803	6.651681028	0	25.80124738
4	40.17724515	-8.337125561	0	-33.64831737
5	-27.32980546	5.81807013	0	23.14577428
6	7.576873585	-1.672287483	0	-6.456918637

Table 4-1. $\Delta_A^k, \Delta_B^k, \Delta_C^k, \Delta_D^k \quad k = 0, M$

The resulting concentration profiles obtained from the above fits are compared to the experimental data in the figure below.

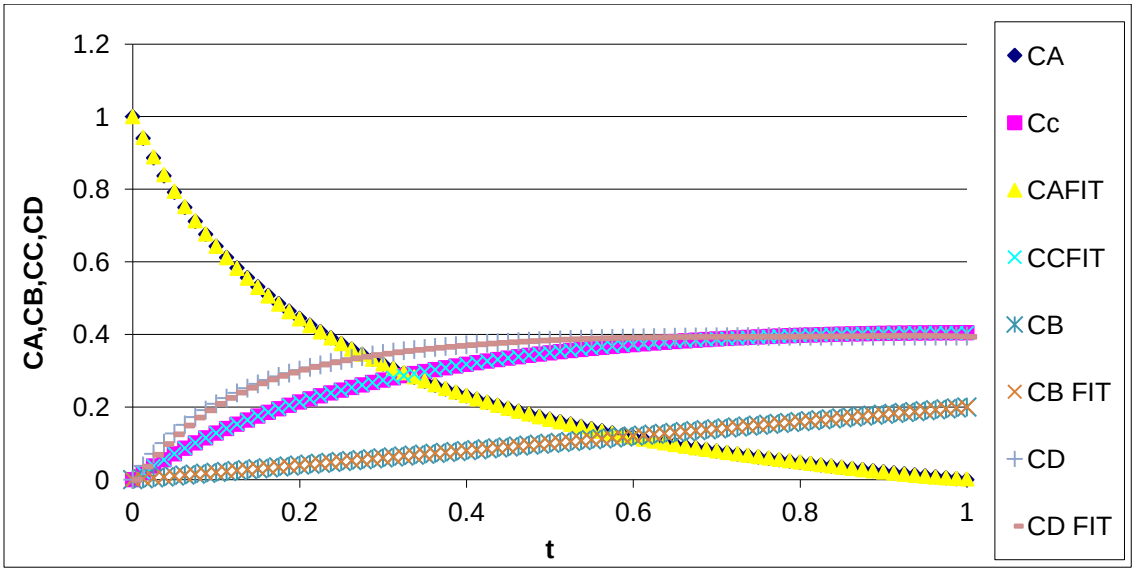

Figure 4-1 Concentration profiles

We then proceed to solve the following convex optimization problem:

$$\left(\begin{array}{l} \nu \triangleq \inf\limits_{\{k_i\}_{i=1}^{3}} \left[\begin{array}{l} \int_0^1 \left[\sum_{k=1}^{M}\Delta_A^k k\tau^{k-1} + k_1 + k_2\sum_{k=0}^{M}\Delta_A^k\tau^k + k_3\left[\sum_{k=0}^{M}\Delta_A^k\tau^k\right]^2\right]^2 d\tau + \int_0^1\left[\sum_{k=1}^{M}\Delta_B^k k\tau^{k-1} - k_1\right]^2 d\tau + \\ + \int_0^1\left[\sum_{k=1}^{M}\Delta_C^k k\tau^{k-1} - k_2\sum_{k=0}^{M}\Delta_A^k\tau^k\right]^2 d\tau + \int_0^1\left[\sum_{k=1}^{M}\Delta_D^k k\tau^{k-1} - k_3\left(\sum_{k=0}^{M}\Delta_A^k\tau^k\right)^2\right]^2 d\tau \end{array}\right] \\ \quad s.t. \qquad C_A(0) = C_A^{in},\ C_B(0) = C_B^{in},\ C_C(0) = C_C^{in},\ C_D(0) = C_D^{in} \end{array}\right) \tag{20}$$

To this end, the evaluation of the integrals forming the objective function is carried out below:

$$\int_0^1\left[\sum_{k=1}^{M}\Delta_C^k k\tau^{k-1} - k_2\sum_{k=0}^{M}\Delta_A^k\tau^k\right]^2 d\tau =$$

$$\int_0^1\left[\left(\sum_{k=1}^{M}\Delta_C^k k\tau^{k-1}\right)^2 - 2\left(\sum_{k=1}^{M}\Delta_C^k k\tau^{k-1}\right)\left(k_2\sum_{k=0}^{M}\Delta_A^k\tau^k\right) + \left(k_2\sum_{k=0}^{M}\Delta_A^k\tau^k\right)^2\right]d\tau =$$

$$\int_0^1\left(\sum_{k=1}^{M}\Delta_C^k k\tau^{k-1}\right)^2 d\tau + k_2^2\int_0^1\left(\sum_{k=0}^{M}\Delta_A^k\tau^k\right)^2 d\tau - 2k_2\int_0^1\left(\sum_{k=1}^{M}\Delta_C^k k\tau^{k-1}\right)\left(\sum_{k=0}^{M}\Delta_A^k\tau^k\right)d\tau =$$

$$\int_0^1\left(\sum_{k=1}^{M}\sum_{l=1}^{M}\Delta_C^k\Delta_C^l kl\tau^{k+l-2}\right)d\tau + k_2^2\int_0^1\left(\sum_{k=0}^{M}\sum_{l=0}^{M}\Delta_A^k\Delta_A^l\tau^{k+l}\right)d\tau - 2k_2\int_0^1\left(\sum_{k=1}^{M}\sum_{l=0}^{M}\Delta_C^k\Delta_A^l k\tau^{k+l-1}\right)d\tau =$$

$$\left(\sum_{k=1}^{M}\sum_{l=1}^{M}\Delta_C^k\Delta_C^l kl\int_0^1\tau^{k+l-2}d\tau\right)+{k_2}^2\left(\sum_{k=0}^{M}\sum_{l=0}^{M}\Delta_A^k\Delta_A^l\int_0^1\tau^{k+l}d\tau\right)-2k_2\left(\sum_{k=1}^{M}\sum_{l=0}^{M}\Delta_A^l\Delta_C^k k\int_0^1\tau^{k+l-1}d\tau\right)=$$

$$\left[\sum_{k=1}^{M}\sum_{l=1}^{M}\Delta_C^k\Delta_C^l kl\frac{\tau^{k+l-1}}{k+l-1}+{k_2}^2\left(\sum_{k=0}^{M}\sum_{l=0}^{M}\Delta_A^k\Delta_A^l\frac{\tau^{k+l+1}}{k+l+1}\right)-2k_2\left(\sum_{k=1}^{M}\sum_{l=0}^{M}\Delta_A^l\Delta_C^k k\frac{\tau^{k+l}}{k+l}\right)\right]_0^1=$$

$${k_2}^2\left(\sum_{k=0}^{M}\sum_{l=0}^{M}\Delta_A^k\Delta_A^l\frac{1}{k+l+1}\right)-2k_2\left(\sum_{k=1}^{M}\sum_{l=0}^{M}\Delta_A^l\Delta_C^k\frac{k}{k+l}\right)+\sum_{k=1}^{M}\sum_{l=1}^{M}\Delta_C^k\Delta_C^l\frac{kl}{k+l-1}\Rightarrow$$

$$\boxed{\begin{aligned}&\int_0^1\left[\sum_{k=1}^{M}\Delta_C^k k\tau^{k-1}-k_2\sum_{k=0}^{M}\Delta_A^k\tau^k\right]^2 d\tau=\\&{k_2}^2\left(\sum_{k=0}^{M}\sum_{l=0}^{M}\Delta_A^k\Delta_A^l\frac{1}{k+l+1}\right)-2k_2\left(\sum_{k=1}^{M}\sum_{l=0}^{M}\Delta_A^l\Delta_C^k\frac{k}{k+l}\right)+\sum_{k=1}^{M}\sum_{l=1}^{M}\Delta_C^k\Delta_C^l\frac{kl}{k+l-1}\end{aligned}} \qquad (21)$$

$$\int_0^1\left[\sum_{k=1}^{M}\Delta_A^k k\tau^{k-1}+k_1+k_2\sum_{k=0}^{M}\Delta_A^k\tau^k+k_3\left[\sum_{k=0}^{M}\Delta_A^k\tau^k\right]\left[\sum_{k=0}^{M}\Delta_A^k\tau^k\right]\right]^2 d\tau=$$

$$\int_0^1\left[\sum_{k=1}^{M}\Delta_A^k k\tau^{k-1}+k_1+k_2\sum_{k=0}^{M}\Delta_A^k\tau^k+k_3\left[\sum_{k=0}^{M}\sum_{l=0}^{M}\Delta_A^k\Delta_A^l\tau^{k+l}\right]\right]^2 d\tau=$$

$$\int_0^1\left[\begin{aligned}&\left(\sum_{k=1}^{M}\Delta_A^k k\tau^{k-1}\right)^2+{k_1}^2+\left(k_2\sum_{k=0}^{M}\Delta_A^k\tau^k\right)^2+\left[k_3\left[\sum_{k=0}^{M}\sum_{l=0}^{M}\Delta_A^k\Delta_A^l\tau^{k+l}\right]\right]^2+2k_1\sum_{k=1}^{M}\Delta_A^k k\tau^{k-1}+\\&+2\left(\sum_{k=1}^{M}\Delta_A^k k\tau^{k-1}\right)\left(k_2\sum_{k=0}^{M}\Delta_A^k\tau^k\right)+2k_3\left(\sum_{k=1}^{M}\Delta_A^k k\tau^{k-1}\right)\left[\sum_{k=0}^{M}\sum_{l=0}^{M}\Delta_A^k\Delta_A^l\tau^{k+l}\right]+2k_1k_2\sum_{k=0}^{M}\Delta_A^k\tau^k+\\&+2k_1k_3\left[\sum_{k=0}^{M}\sum_{l=0}^{M}\Delta_A^k\Delta_A^l\tau^{k+l}\right]+2k_2k_3\left(\sum_{k=0}^{M}\Delta_A^k\tau^k\right)\left[\sum_{k=0}^{M}\sum_{l=0}^{M}\Delta_A^k\Delta_A^l\tau^{k+l}\right]\end{aligned}\right]d\tau=$$

$$\int_0^1\left[\begin{aligned}&\left(\sum_{k=1}^{M}\sum_{l=1}^{M}\Delta_A^k\Delta_A^l kl\tau^{k+l-2}\right)+{k_1}^2+\left({k_2}^2\sum_{k=0}^{M}\sum_{l=0}^{M}\Delta_A^k\Delta_A^l\tau^{k+l}\right)+{k_3}^2\left[\sum_{k=0}^{M}\sum_{l=0}^{M}\sum_{p=0}^{M}\sum_{s=0}^{M}\Delta_A^p\Delta_A^s\Delta_A^k\Delta_A^l\tau^{k+l+p+s}\right]+\\&+2k_1\sum_{k=1}^{M}\Delta_A^k k\tau^{k-1}+2k_2\left(\sum_{k=1}^{M}\sum_{l=0}^{M}\Delta_A^l\Delta_A^k k\tau^{k+l-1}\right)+2k_3\left[\sum_{k=0}^{M}\sum_{l=0}^{M}\sum_{p=1}^{M}\Delta_A^p\Delta_A^k\Delta_A^l p\tau^{k+l+p-1}\right]+2k_1k_2\sum_{k=0}^{M}\Delta_A^k\tau^k+\\&+2k_1k_3\left[\sum_{k=0}^{M}\sum_{l=0}^{M}\Delta_A^k\Delta_A^l\tau^{k+l}\right]+2k_2k_3\left[\sum_{k=0}^{M}\sum_{l=0}^{M}\sum_{p=0}^{M}\Delta_A^p\Delta_A^k\Delta_A^l\tau^{k+l+p}\right]\end{aligned}\right]d\tau=$$

$$\left[\left(\sum_{k=1}^{M}\sum_{l=1}^{M}\Delta_A^k\Delta_A^l kl\frac{\tau^{k+l-1}}{k+l-1}\right)+k_1{}^2\tau+k_2{}^2\left(\sum_{k=0}^{M}\sum_{l=0}^{M}\Delta_A^k\Delta_A^l\frac{\tau^{k+l+1}}{k+l+1}\right)+k_3{}^2\sum_{k=0}^{M}\sum_{l=0}^{M}\sum_{p=0}^{M}\sum_{s=0}^{M}\Delta_A^p\Delta_A^s\Delta_A^k\Delta_A^l\frac{\tau^{k+l+p+s+1}}{k+l+p+s+1}+\right.$$
$$+2k_1\sum_{k=1}^{M}\Delta_A^k k\frac{\tau^k}{k}+2k_2\sum_{k=1}^{M}\sum_{l=0}^{M}\Delta_A^l\Delta_A^k k\frac{\tau^{k+l}}{k+l}+2k_3\sum_{k=0}^{M}\sum_{l=0}^{M}\sum_{p=1}^{M}\Delta_A^p\Delta_A^k\Delta_A^l p\frac{\tau^{k+l+p}}{k+l+p}+2k_1k_2\sum_{k=0}^{M}\Delta_A^k\frac{\tau^{k+1}}{k+1}+$$
$$\left.+2k_1k_3\sum_{k=0}^{M}\sum_{l=0}^{M}\Delta_A^k\Delta_A^l\frac{\tau^{k+l+1}}{k+l+1}+2k_2k_3\sum_{k=0}^{M}\sum_{l=0}^{M}\sum_{p=0}^{M}\Delta_A^p\Delta_A^k\Delta_A^l\frac{\tau^{k+l+p+1}}{k+l+p+1}\right]_0^1=$$

$$\left[\left(\sum_{k=1}^{M}\sum_{l=1}^{M}\Delta_A^k\Delta_A^l kl\frac{1}{k+l-1}\right)+k_1{}^2+k_2{}^2\left(\sum_{k=0}^{M}\sum_{l=0}^{M}\Delta_A^k\Delta_A^l\frac{1}{k+l+1}\right)+k_3{}^2\sum_{k=0}^{M}\sum_{l=0}^{M}\sum_{p=0}^{M}\sum_{s=0}^{M}\Delta_A^p\Delta_A^s\Delta_A^k\Delta_A^l\frac{1}{k+l+p+s+1}+\right.$$
$$+2k_1\sum_{k=1}^{M}\Delta_A^k+2k_2\sum_{k=1}^{M}\sum_{l=0}^{M}\Delta_A^l\Delta_A^k k\frac{1}{k+l}+2k_3\sum_{k=0}^{M}\sum_{l=0}^{M}\sum_{p=1}^{M}\Delta_A^p\Delta_A^k\Delta_A^l p\frac{1}{k+l+p}+2k_1k_2\sum_{k=0}^{M}\Delta_A^k\frac{1}{k+1}+\Rightarrow$$
$$\left.+2k_1k_3\sum_{k=0}^{M}\sum_{l=0}^{M}\Delta_A^k\Delta_A^l\frac{1}{k+l+1}+2k_2k_3\sum_{k=0}^{M}\sum_{l=0}^{M}\sum_{p=0}^{M}\Delta_A^p\Delta_A^k\Delta_A^l\frac{1}{k+l+p+1}\right]$$

$$\boxed{\begin{aligned}&\int_0^1\left[\sum_{k=1}^{M}\Delta_A^k k\tau^{k-1}+k_1+k_2\sum_{k=0}^{M}\Delta_A^k\tau^k+k_3\left[\sum_{k=0}^{M}\Delta_A^k\tau^k\right]\left[\sum_{k=0}^{M}\Delta_A^k\tau^k\right]\right]^2 d\tau=\\&\left[\left(\sum_{k=1}^{M}\sum_{l=1}^{M}\Delta_A^k\Delta_A^l kl\frac{1}{k+l-1}\right)+k_1{}^2+k_2{}^2\left(\sum_{k=0}^{M}\sum_{l=0}^{M}\Delta_A^k\Delta_A^l\frac{1}{k+l+1}\right)+k_3{}^2\sum_{k=0}^{M}\sum_{l=0}^{M}\sum_{p=0}^{M}\sum_{s=0}^{M}\Delta_A^p\Delta_A^s\Delta_A^k\Delta_A^l\frac{1}{k+l+p+s+1}+\right.\\&+2k_1\sum_{k=1}^{M}\Delta_A^k+2k_2\sum_{k=1}^{M}\sum_{l=0}^{M}\Delta_A^l\Delta_A^k k\frac{1}{k+l}+2k_3\sum_{k=0}^{M}\sum_{l=0}^{M}\sum_{p=1}^{M}\Delta_A^p\Delta_A^k\Delta_A^l p\frac{1}{k+l+p}+2k_1k_2\sum_{k=0}^{M}\Delta_A^k\frac{1}{k+1}+\\&\left.+2k_1k_3\sum_{k=0}^{M}\sum_{l=0}^{M}\Delta_A^k\Delta_A^l\frac{1}{k+l+1}+2k_2k_3\sum_{k=0}^{M}\sum_{l=0}^{M}\sum_{p=0}^{M}\Delta_A^p\Delta_A^k\Delta_A^l\frac{1}{k+l+p+1}\right]\end{aligned}}\quad(22)$$

$$\int_0^1\left[\sum_{k=1}^{M}\Delta_B^k k\tau^{k-1}-k_1\right]^2 d\tau=\int_0^1\left[\left(\sum_{k=1}^{M}\Delta_B^k k\tau^{k-1}\right)^2-2k_1\left(\sum_{k=1}^{M}\Delta_B^k k\tau^{k-1}\right)+k_1{}^2\right]d\tau=$$
$$=\int_0^1\left[\left(\sum_{k=1}^{M}\sum_{l=1}^{M}\Delta_B^k\Delta_B^l kl\tau^{k+l-2}\right)-2k_1\left(\sum_{k=1}^{M}\Delta_B^k k\tau^{k-1}\right)+k_1{}^2\right]d\tau=$$
$$\left[\left(\sum_{k=1}^{M}\sum_{l=1}^{M}\Delta_B^k\Delta_B^l kl\frac{\tau^{k+l-1}}{k+l-1}\right)-2k_1\sum_{k=1}^{M}\Delta_B^k\tau^k+k_1{}^2\tau\right]_0^1=$$
$$=\left[\left(\sum_{k=1}^{M}\sum_{l=1}^{M}\Delta_B^k\Delta_B^l kl\frac{1}{k+l-1}\right)-2k_1\sum_{k=1}^{M}\Delta_B^k+k_1{}^2\right]\Rightarrow$$

$$\boxed{\int_0^1\left[\sum_{k=1}^{M}\Delta_B^k k\tau^{k-1}-k_1\right]^2 d\tau=\left[\left(\sum_{k=1}^{M}\sum_{l=1}^{M}\Delta_B^k\Delta_B^l kl\frac{1}{k+l-1}\right)-2k_1\sum_{k=1}^{M}\Delta_B^k+k_1{}^2\right]}\quad(23)$$

$$\int_0^1\left[\sum_{k=1}^{M}\Delta_D^k k\tau^{k-1}-k_3\left(\sum_{k=0}^{M}\Delta_A^k\tau^k\right)^2\right]^2 d\tau=\int_0^1\left[\sum_{k=1}^{M}\Delta_D^k k\tau^{k-1}-k_3\left(\sum_{k=0}^{M}\sum_{l=0}^{M}\Delta_A^k\Delta_A^l\tau^{k+l}\right)\right]^2 d\tau=$$
$$=\int_0^1\left[\left(\sum_{k=1}^{M}\Delta_D^k k\tau^{k-1}\right)^2-2k_3\left(\sum_{k=1}^{M}\Delta_D^k k\tau^{k-1}\right)\left(\sum_{k=0}^{M}\sum_{l=0}^{M}\Delta_A^k\Delta_A^l\tau^{k+l}\right)+k_3{}^2\left(\sum_{k=0}^{M}\sum_{l=0}^{M}\Delta_A^k\Delta_A^l\tau^{k+l}\right)^2\right]d\tau=$$

$$= \int_0^1 \left[\left(\sum_{k=1}^{M} \sum_{l=1}^{M} \Delta_D^k \Delta_D^l kl \tau^{k+l-2} \right) - 2k_3 \sum_{k=0}^{M} \sum_{l=0}^{M} \sum_{p=1}^{M} \Delta_D^p \Delta_A^k \Delta_A^l p \tau^{k+l+p-1} + k_3^2 \sum_{k=0}^{M} \sum_{l=0}^{M} \sum_{p=0}^{M} \sum_{s=0}^{M} \Delta_A^p \Delta_A^s \Delta_A^k \Delta_A^l \tau^{k+l+p+s} \right] d\tau =$$

$$\left[\left(\sum_{k=1}^{M} \sum_{l=1}^{M} \Delta_D^k \Delta_D^l kl \frac{\tau^{k+l-1}}{k+l-1} \right) - 2k_3 \sum_{k=0}^{M} \sum_{l=0}^{M} \sum_{p=1}^{M} \Delta_D^p \Delta_A^k \Delta_A^l p \frac{\tau^{k+l+p}}{k+l+p} + k_3^2 \sum_{k=0}^{M} \sum_{l=0}^{M} \sum_{p=0}^{M} \sum_{s=0}^{M} \Delta_A^p \Delta_A^s \Delta_A^k \Delta_A^l \frac{\tau^{k+l+p+s+1}}{k+l+p+s+1} \right]_0^1 =$$

$$\left[\left(\sum_{k=1}^{M} \sum_{l=1}^{M} \Delta_D^k \Delta_D^l \frac{kl}{k+l-1} \right) - 2k_3 \sum_{k=0}^{M} \sum_{l=0}^{M} \sum_{p=1}^{M} \Delta_D^p \Delta_A^k \Delta_A^l p \frac{1}{k+l+p} + k_3^2 \sum_{k=0}^{M} \sum_{l=0}^{M} \sum_{p=0}^{M} \sum_{s=0}^{M} \Delta_A^p \Delta_A^s \Delta_A^k \Delta_A^l \frac{1}{k+l+p+s+1} \right] \Rightarrow$$

$$\int_0^1 \left[\sum_{k=1}^{M} \Delta_D^k k \tau^{k-1} - k_3 \left(\sum_{k=0}^{M} \Delta_A^k \tau^k \right)^2 \right]^2 d\tau =$$

$$\left[\left(\sum_{k=1}^{M} \sum_{l=1}^{M} \Delta_D^k \Delta_D^l \frac{kl}{k+l-1} \right) - 2k_3 \sum_{k=0}^{M} \sum_{l=0}^{M} \sum_{p=1}^{M} \Delta_D^p \Delta_A^k \Delta_A^l p \frac{1}{k+l+p} + k_3^2 \sum_{k=0}^{M} \sum_{l=0}^{M} \sum_{p=0}^{M} \sum_{s=0}^{M} \Delta_A^p \Delta_A^s \Delta_A^k \Delta_A^l \frac{1}{k+l+p+s+1} \right] \tag{24}$$

The solution of the above convex optimization problem yields the following optimum kinetic parameter values and associated optimum objective function value:

$$k_1 = 0.19993 \frac{kmol}{m^3 \cdot s}$$
$$k_2 = 1.6036 \frac{1}{s} \tag{25}$$
$$k_3 = 3.17083 \frac{m^3}{kmol \cdot s}$$
$$objective\ function = 0.00183$$

The identified kinetic parameter values are close to the original kinetic parameter values, $k_1 = 0.2 \frac{kmol}{m^3 \cdot s}, k_2 = 1.6 \frac{1}{s}, k_3 = 3.17 \frac{m^3}{kmol \cdot s}$, used to generate the "experimental" data. Once the k values are found, they are used to simulate the PFR ODE's. The resulting concentration profiles are shown below and are indistinguishable from the analytic solutions presented earlier for the original kinetic parameter values.

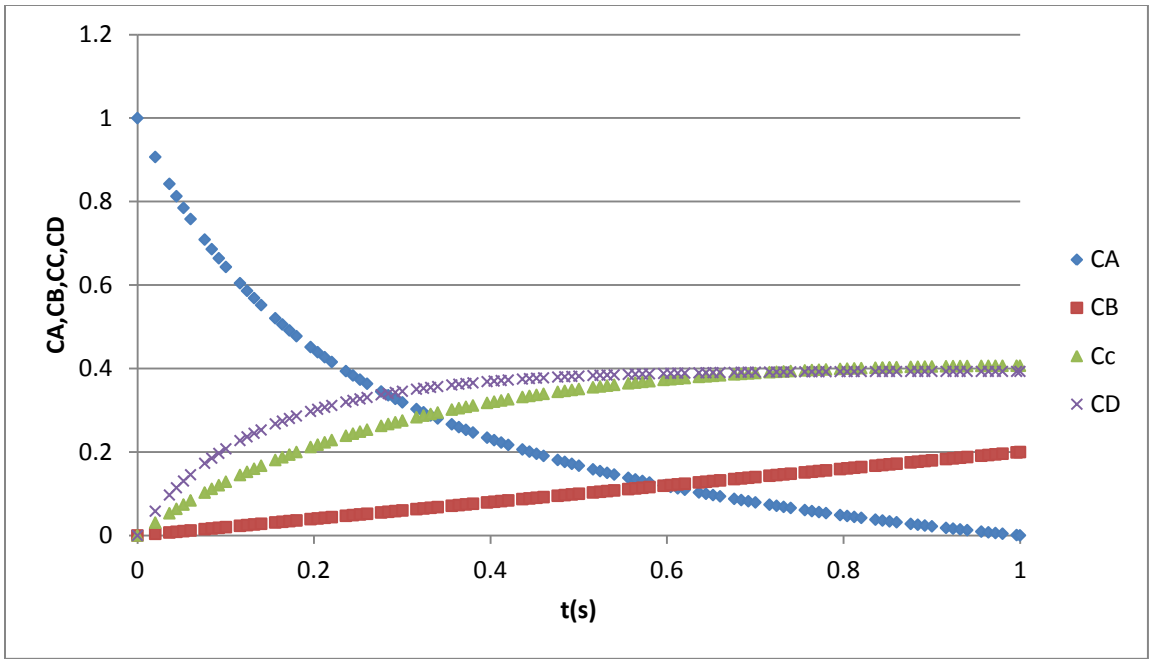

Figure 4-2. Concentration Profiles for identified kinetic parameters

4.5 Appendix A.4

τ (s)	$\hat{C}_A(\tau_j)$	$\hat{C}_B(\tau_j)$	$\hat{C}_C(\tau_j)$	$\hat{C}_D(\tau_j)$	W
0	1	0	0	0	1
0.0125	0.940476	0.0025	0.019395	0.037629	1
0.025	0.886364	0.005	0.037655	0.070981	1
0.0375	0.836957	0.0075	0.054881	0.100663	1
0.05	0.791667	0.01	0.071161	0.127173	1
0.0625	0.75	0.0125	0.086572	0.150928	1
0.075	0.711538	0.015	0.101182	0.172279	1
0.0875	0.675926	0.0175	0.115052	0.191522	1
0.1	0.642857	0.02	0.128236	0.208907	1
0.1125	0.612069	0.0225	0.140782	0.224649	1
0.125	0.583333	0.025	0.152733	0.238934	1
0.1375	0.556452	0.0275	0.164127	0.251921	1
0.15	0.53125	0.03	0.175002	0.263748	1
0.1625	0.507576	0.0325	0.185388	0.274537	1
0.175	0.485294	0.035	0.195314	0.284392	1
0.1875	0.464286	0.0375	0.204808	0.293406	1
0.2	0.444444	0.04	0.213893	0.301662	1
0.2125	0.425676	0.0425	0.222593	0.309232	1
0.225	0.407895	0.045	0.230927	0.316178	1
0.2375	0.391026	0.0475	0.238915	0.32256	1
0.25	0.375	0.05	0.246574	0.328426	1
0.2625	0.359756	0.0525	0.25392	0.333824	1
0.275	0.345238	0.055	0.260969	0.338793	1
0.2875	0.331395	0.0575	0.267734	0.343371	1
0.3	0.318182	0.06	0.274229	0.34759	1
0.3125	0.305556	0.0625	0.280465	0.351479	1
0.325	0.293478	0.065	0.286455	0.355067	1
0.3375	0.281915	0.0675	0.292208	0.358377	1
0.35	0.270833	0.07	0.297734	0.361432	1
0.3625	0.260204	0.0725	0.303044	0.364252	1
0.375	0.25	0.075	0.308145	0.366855	1
0.3875	0.240196	0.0775	0.313047	0.369257	1
0.4	0.230769	0.08	0.317756	0.371475	1
0.4125	0.221698	0.0825	0.32228	0.373522	1
0.425	0.212963	0.085	0.326626	0.375411	1
0.4375	0.204545	0.0875	0.3308	0.377154	1
0.45	0.196429	0.09	0.33481	0.378762	1
0.4625	0.188596	0.0925	0.338659	0.380244	1
0.475	0.181034	0.095	0.342355	0.38161	1
0.4875	0.173729	0.0975	0.345903	0.382869	1
0.5	0.166667	0.1	0.349306	0.384027	1

0.5125	0.159836	0.1025	0.352571	0.385093	1
0.525	0.153226	0.105	0.355701	0.386073	1
0.5375	0.146825	0.1075	0.358701	0.386973	1
0.55	0.140625	0.11	0.361575	0.3878	1
0.5625	0.134615	0.1125	0.364327	0.388557	1
0.575	0.128788	0.115	0.366961	0.389251	1
0.5875	0.123134	0.1175	0.36948	0.389885	1
0.6	0.117647	0.12	0.371888	0.390465	1
0.6125	0.112319	0.1225	0.374187	0.390994	1
0.625	0.107143	0.125	0.376381	0.391476	1
0.6375	0.102113	0.1275	0.378474	0.391914	1
0.65	0.097222	0.13	0.380467	0.392311	1
0.6625	0.092466	0.1325	0.382364	0.392671	1
0.675	0.087838	0.135	0.384166	0.392996	1
0.6875	0.083333	0.1375	0.385878	0.393289	1
0.7	0.078947	0.14	0.387501	0.393552	1
0.7125	0.074675	0.1425	0.389037	0.393788	1
0.725	0.070513	0.145	0.390488	0.393999	1
0.7375	0.066456	0.1475	0.391858	0.394187	1
0.75	0.0625	0.15	0.393147	0.394353	1
0.7625	0.058642	0.1525	0.394358	0.3945	1
0.775	0.054878	0.155	0.395493	0.394628	1
0.7875	0.051205	0.1575	0.396554	0.394741	1
0.8	0.047619	0.16	0.397542	0.394839	1
0.8125	0.044118	0.1625	0.398459	0.394923	1
0.825	0.040698	0.165	0.399308	0.394995	1
0.8375	0.037356	0.1675	0.400088	0.395056	1
0.85	0.034091	0.17	0.400802	0.395107	1
0.8625	0.030899	0.1725	0.401452	0.395149	1
0.875	0.027778	0.175	0.402039	0.395184	1
0.8875	0.024725	0.1775	0.402564	0.395211	1
0.9	0.021739	0.18	0.403028	0.395233	1
0.9125	0.018817	0.1825	0.403434	0.395249	1
0.925	0.015957	0.185	0.403781	0.395261	1
0.9375	0.013158	0.1875	0.404072	0.39527	1
0.95	0.010417	0.19	0.404308	0.395275	1
0.9625	0.007732	0.1925	0.404489	0.395279	1
0.975	0.005102	0.195	0.404618	0.39528	1
0.9875	0.002525	0.1975	0.404694	0.395281	1
1	0	0.2	0.404719	0.395281	1

4.6 References

[1] Valorani, M., Creta, F., Goussis, D. A., Lee, J. C., & Najm, H. N. (2006). An automatic procedure for the simplification of chemical kinetic mechanisms based on CSP. Combustion and Flame, 146, 29-51.

[2] Pepiot-Desjardins, & P., Pitsch, H. (2008). An efficient error-propagation-based reduction method for large chemical kinetic mechanisms. Combustion and Flame, 154, 67-81.

[3] Salvato, L., Viggiano, A., Valorani, M., & Magi, V. (2013). On the simplification of kinetic reaction mechanisms of air-ethanol under high pressure conditions. Fuel, 104, 488-499.

[4] Prager, J., Najm, H. N., Valorani, M., & Goussis, D. A. (2009). Skeletal mechanism generation with CSP and validation for premixed n-heptane flames. Proceedings of the Combustion Institute, 32, 509-517.

[5] Sapre, A. V. (1991). Kinetic modeling at Mobil: an historical perspective. Chemical Reactions in Complex Mixtures: The Mobil Workshop. In Van Nostrand Reinhold (pp. 222-253).

[6] Frenklach, M. (1990). Reduction of chemical reaction models. Numerical approaches to combustion modeling. American Institute of Aeronautics and Astronautics. Washington, DC.

[7] Leone, J. A., & Seinfeld, J. H. (1985). Comparative analysis of chemical reaction mechanisms for photochemical smog. Atmospheric Environment, 19(3), 437-464.

[8] Edwards, K., Edgar, T. F., & Manousiouthakis, V. I. (2000). Reaction mechanism simplification using mixed-integer nonlinear programming. Computers and Chemical Engineering, 24, 67-79.

[9] Zhou, W., & Manousiouthakis, V. I. (2008). On dimensionality of attainable region construction for isothermal reactor networks. Computers & Chemical Engineering, 32(3), 439-450.

[10] Conner, J. & Manousiouthakis, V.I. (2011). ODE Model Parameter Identification Via Global Optimization Techniques. AIChE Annual Meeting (679d).

[11] Weekman, V. W. (1979). Lumps, models, and kinetics in practice. American Institute of Chemical Engineers.

[12] Tilden, J. W., Costanza, V., McRae, G. J., & Seinfeld, J. H. (1981). Sensivity Analysis of Chemically Reacting Systems. In Modelling of Chemical Reaction Systems (pp. 69-91). Springer Berlin Heidelberg.

[13] Rabitz, H., Kramer, M., & Dacol, D. (1983). Sensitivity analysis in chemical kinetics. Annual review of physical chemistry, 34(1), 419-461.

[14] Edelson, D., & Flamm, D. L. (1984). Computer simulation of a CF< inf> 4</inf> plasma etching silicon. Journal of applied physics, 56(5), 1522-1531.

[15] Frenklach, M., & Wang, H. (1991, December). Detailed modeling of soot particle nucleation and growth. In Symposium (International) on Combustion(Vol. 23, No. 1, pp. 1559-1566). lsevier.

[16] Frenklach, M., & Harris, S. J. (1987). Aerosol dynamics modeling using the method of moments. Journal of colloid and interface science, 118(1), 252-261.

[16] Maria, G. (1989). An adaptive strategy for solving kinetic model concomitant estimation—reduction problems. The Canadian Journal of Chemical Engineering, 67(5), 825-832.

[17] Maria, G., & Muntean, O. (1987). Model reduction and kinetic parameters identification for the methanol conversion to olefins. Chemical engineering science, 42(6), 1451-1460.

[18] Graedel, T. E. (1977). Functional group analysis of large chemical kinetic systems. The Journal of Physical Chemistry, 81(25), 2372-2374.

[19] Bonvin, D., & Rippin, D. W. T. (1990). Target factor analysis for the identification of stoichiometric models. Chemical Engineering Science, 45(12), 3417-3426.

[20] Van Breusegem, V., & Bastin, G. (1991, December). Reduced order dynamical modelling of reaction systems: a singular perturbation approach. In Decision and Control, 1991., Proceedings of the 30th IEEE Conference on (pp. 1049-1054). IEEE.